Rivista Italiana di Paleontologia e Stratigrafia
(*Research in Paleontology and Stratigraphy*)
vol. 132(2): 431-512. **July 2026**
DOI: https://doi.org/10.54103/2039-4942/30814

LATE EOCENE FISHES FROM THE TUPELO BAY FORMATION OF SOUTH CAROLINA, USA

DAVID J. CICIMURRI[1*], JUN A. EBERSOLE[2] & ANDREW R. BOWMAN[3]

[1]Geological Investigations, Geological Survey of Alabama, 420 Hackberry Lane, Tuscaloosa, AL 35486, USA.
E-mail: dcicimurri@gsa.state.al.us, zoobank.org:author: F0155EA1-F5D6-49E4-B578-7A14DBB7B902
[2]McWane Science Center, 200 19th Street North, Birmingham, AL 35203, USA.
E-mail: jebersole@mcwane.org, zoobank.org:author: D48E2AF-EC92-4C32-9F2A-2D39716C459E
[3]Groundwater Assessment Program, Geological Survey of Alabama, 420 Hackberry Lane, Tuscaloosa, AL 35486, USA.
E-mail: abowman@gsa.state.al.us, zoobank.org:author: 042F5C79-F2EC-4F35-9860-D75791DDE5D1
*Corresponding author.

Associate Editor: Giorgio Carnevale.

To cite this article: Cicimurri D.J., Ebersole J.A. & Bowman A.R. (2026) - Late Eocene fishes from the Tupelo Bay Formation of South Carolina, USA. *Rivista Italiana di Paleontologia e Stratigrafia*, vol. 132(2): 431-512.

Keywords: Eocene; Chondrichthyes; Osteichthyes; South Carolina; Atlantic Coastal Plain.

Abstract: The Tupelo Bay Formation is an Eocene carbonate unit occurring in the outer Atlantic Coastal Plain of South Carolina, USA. This formation has yielded a rather diverse assemblage of late Eocene fishes that is dominated by sharks (squalomorph and galeomorph) but contains a lesser number of batoid and teleost fishes. Of the six orders of sharks represented, Carcharhiniformes is the most diverse, with teeth of 12 taxa identified, including *Pachyscyllium* sp., *Premontreia* (*Oxyscyllium*) *gilberti*, *Hemipristis curvatus*, *Pseudabdounia claibornensis*, *Abdounia enniskilleni*, *A. minutissima*, *Carcharhinus* sp., *Negaprion gilmorei*, *Physogaleus* aff. *contortus*, *P.* aff. *secundus*, *Galeocerdo clarkensis*, and a new species, *Galeorhinus semiserratus*. Lamniformes are less diverse and represented by *Otodus* (*Carcharocles*) *sokolowi*?, *Anomotodon novus*, *Striatolamia macrota*, *Brachycarcharias twiggsensis*, Carchariidae indet., *Macrorhizodus praecursor*, *Isurolamna inflata*, and *Alopias* cf. *alabamensis*. Other, less diverse, orders include Hexanchiformes (*Hexanchus agassizi*), Squatiniformes (*Squatina* sp.), Heterodontiformes (*Heterodontus* aff. *vincenti*), and Orectolobiformes (*Nebrius thielensi*, *Eostegostoma angustum*, Ginglymostomatidae indet.). Five batoids are represented by isolated teeth and rostral spines, including *Pristis* sp., *Propristis schweinfurthi*, "*Aetomylaeus*" sp., "*Myliobatis*" sp., and "*Rhinoptera*" sp. Eleven bony fish taxa, *Egertonia isodonta*, *Albula oweni*, *Sphyraena* sp., *Xiphiorhynchus* sp., *Trichiurides sagittidens*, *Scomberomorus* sp., *Sphyraenodus* sp., Ostraciidae indet., *Lobodus pedemontanus*, *Progymnodon hilgendorfi*, and *Cylindracanthus rectus*, were identified based on teeth, jaws, dermal armor and other elements. Teeth of *E. angustum*, *I. inflata*, *Sphyraenodus* sp., and *L. pedemontanus* represent rare records of these taxa in North America. The apparently depauperate batoid and teleost components of the assemblage may reflect taphonomic processes and/or a collecting bias towards larger specimens. Nonetheless, this assemblage increases our knowledge of the paleoenvironmental and paleobiogeographic distributions of the species represented.

urn:lsid:zoobank.org:pub:B0E76192-FE9A-4DE0-96D9-CD3358F9B771

Received: February 2, 2026; accepted: June 5, 2026

Introduction

Numerous Eocene lithostratigraphic units in the South Carolina Atlantic Coastal Plain, USA, represent marine deposition, but relatively little is known about the vertebrate assemblages they may contain. Although marine tetrapods have been reported from several of these units, including chelonioid turtles (Weems & Brown 2017), dugongid sirenians (Domning et al. 1982), and protocetid cetaceans (Albright 1996; Uhen & Gingerich 2001; Geisler et al. 2005), the only reasonably well-documented fish assemblage includes that of the Priabonian Dry Branch Formation of the Barnwell Group (i.e., Zullo & Kite 1985; Cicimurri & Ebersole 2015; Cicimurri & Knight 2019). Kite (1982) collected several elasmobranch teeth and caudal spines from the middle Eocene (Lutetian) Huber Formation in Aiken County that were later taxonomically identified by Cicimurri & Knight (2019). Case et al. (2015) recovered a small elasmobranch assemblage from Berkeley County that was thought to have been sourced from the lower Eocene (Ypresian) Fishburne Formation, but it has since been demonstrated (Cicimurri et al. 2016) that the specimens in question were derived from the upper Paleocene (Thanetian) Chicora Member of the Williamsburg Formation.

The upper Eocene Tupelo Bay Formation is a marine limestone occurring in the outer coastal plain of South Carolina. Based on scattered accounts, this unit has yielded an array of marine vertebrates, including a dugongid sirenian (Doming et al. 1982), a dermochelyid turtle (Weems & Brown 2017), and the protocetid whales *Carolinacetus gingerichi* Geisler et al., 2005 and *Tupelocetus palmeri* Gibson et al., 2018. A partial rostrum and associated spines of the sawfish *Pristis* were described by Cicimurri (2007), but other fishes occurring in the Tupelo Bay Formation are poorly known. Herein, we provide the results of our evaluation of nearly 600 fish fossils from the Tupelo Bay Formation, including taxonomic identifications, updates on morphology and heterodonty and on the temporal and paleobiogeographic distributions of the species, and we comment on the paleoecological implications of the assemblage.

Geologic Setting and Age

The specimens described herein were recovered from three active quarries in South Carolina, USA, including two in Dorchester County and one in Orangeburg County. All three quarries are located along the north-south roadway that is SC 453, north or south of US I-26, with the Giant Portland Cement (formerly Carolina Cement and Lime Co.; 33.23727, -80.44323) and Argos (formerly Blue Circle Cement and Lafarge; 33.22580, -80.45118) quarries being in Dorchester County and Holcim Holly Hill Cement (formerly Santee Portland Cement and Holnam; 33.27673, -80.43457) in Orangeburg County (Fig. 1C). These quarries commercially target limestones that are the source for the fossils documented herein.

The Giant Portland Cement quarry has a long history of geological investigation, and a summary of that work is provided herein. Cooke and MacNeil (1952) identified the exposed Eocene gray limestones as Castle Hayne Limestone and Pooser (1965) and Banks (1977) later referred to these beds as the Santee Limestone (Lutetian-Bartonian). Ward et al. (1979) subdivided the Santee Limestone into the Moultrie Member and superjacent Cross Member, and the exposures at the Giant Porland Cement quarry were ascribed to the latter unit. Baum et al. (1980) subsequently elevated the Cross Member to formation status and designated the Giant Portland Cement quarry as an auxiliary reference section. Zullo & Harris (1987) correlated the Cross Formation with the Eocene (Bartonian, NP17) Gosport Sand and Moodys Branch Formation of the Gulf Coastal Plain of the USA, and the Clinchfield Formation of Georgia, USA. Campbell (1995) noted the discrepancies in naming convention used to identify the limestones in Berkeley, Orangeburg, and Dorchester counties in South Carolina, but ultimately identified the limestone beds at the Giant Portland Cement quarry as the Cross Formation.

In their evaluation of the USGS-Pregnall No. 1 Core (DOR-208), Edwards et al. (1997) identified roughly 50 m of section as Moultrie and Cross strata, and both units were recognized as members of the Santee Limestone. Geisler et al. (2005) utilized the DOR-208 core, which was recovered roughly 6 km south of the Giant Portland Cement quarry, and the conclusions drawn by Edwards et al. (1997) to formalize the Tupelo Bay Formation as a replacement name for the limestones exposed at Giant Portland Cement. Geisler et al. (2005) redesignated the 21 m-thick "Moultrie" portion of the DOR-208 core (*sensu* Edwards et al. 1997) as the Cross Member and the remaining 30 m "Cross" portion as the

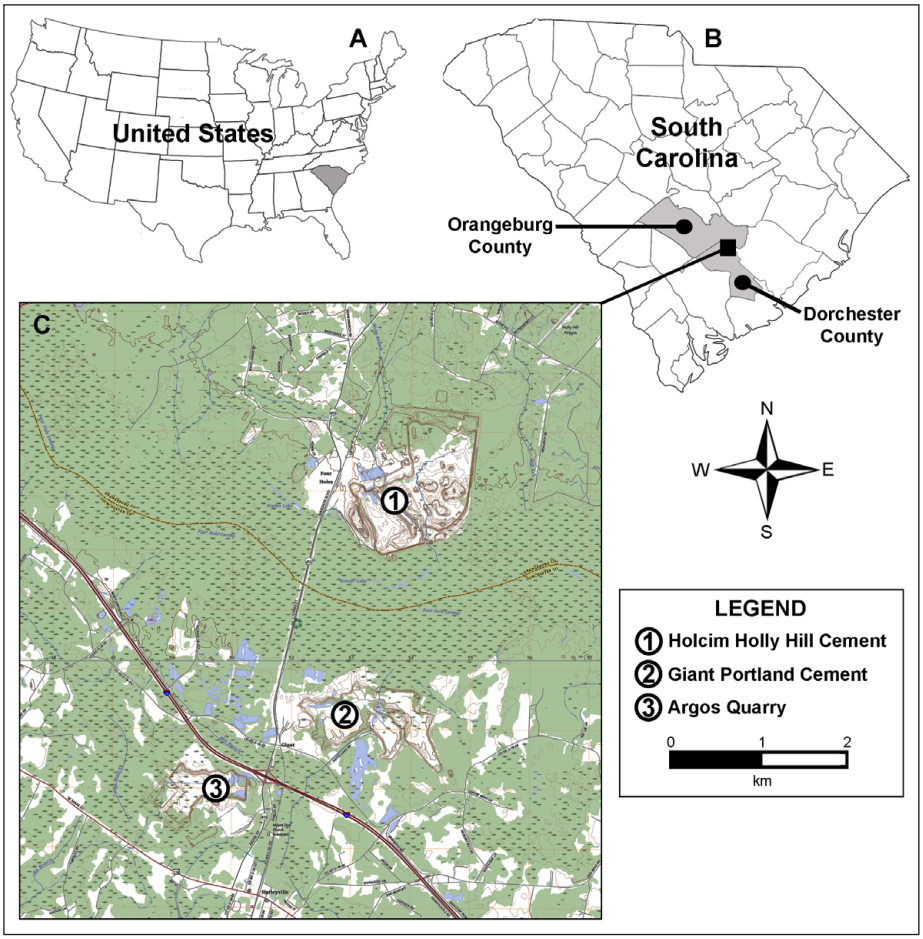

Fig. 1 - Geographic maps showing the locations of the collection areas. A, Outline map of the United States showing the location of South Carolina (gray). B, County map of South Carolina showing the location of Dorchester and Orangeburg counties. C, Map of Dorchester and Orangeburg counties showing locations of the Holcim quarry (1), Giant Portland Cement quarry (2), and Argos quarry (3). Bodies of water are indicated by blue. C is modified from the USGS Holly Hill and Harleyville 1:24,000 topographic maps, version 1/1/2024.

Pregnall Member, with these units comprising the lower and upper parts (respectively) of the Tupelo Bay Formation (Fig. 2). The terms Cross Member and Pregnall Member, in the context of the Tupelo Bay Formation, have thus far largely been recognized in paleontological investigations (i.e., Geisler et al. 2005; Cicimurri 2007; Frantescu et al. 2010; Gibson et al. 2018), and we utilize these terms herein following those accounts and that of Weems et al. (2016).

The Pregnall Member occurs at the Holcim, Giant Portland Cement, and Argos quarries, and post-Tupelo Bay Formation deposits at these sites have been variously referred to as the Cooper Marl, Cooper Formation, or Harleyville Formation (i.e., Pooser 1965; Banks 1977; Geisler et al. 2005). However, Weems et al. (2016) showed that at the Giant Portland Cement quarry the Parkers Ferry Formation unconformably overlies the Tupelo Bay Formation, and the Eocene section is capped by the Harleyville Formation. The Parkers Ferry Formation is apparently absent from the DOR-208 core and the Harleyville Formation disconformably overlies the Tupelo Bay Formation. The Parkers Ferry and Harleyville formations, along with the lower Oligocene (Rupelian) Ashley Formation, are part of the Cooper Group. At each of the collecting sites a conspicuous unconformity separates the Tupelo Bay Formation from the Parkers Ferry Formation, and the contact zone of the Tupelo Bay Formation is phosphatized. Banks (1977: fig. 12) noted this phenomenon at the Giant Portland Cement quarry but stated that the surface was horizontal, although one of us (DJC) has observed highly irregular surfaces with meter-scale relief (see also Weems et al. 2016: fig. 3). This erosional surface may represent current scouring related to the Gulf Trough, but a recent discovery by Ganis et al. (2025) presents a plausible explanation that the Tupelo Bay Formation was scoured by a massive tsunami related to the Chesapeake Bay Bolide Impact.

The deposits of the Pregnall Member of the Tupelo Bay Formation differ slightly, as has been observed by previous researchers. Cooke & MacNeil (1952) described the lower part of the section at the Giant Portland Cement quarry as "soft, fine-grained, granular" and the upper part "tough to hard, crumbly" (p. 26). Banks (1977) later subdi-

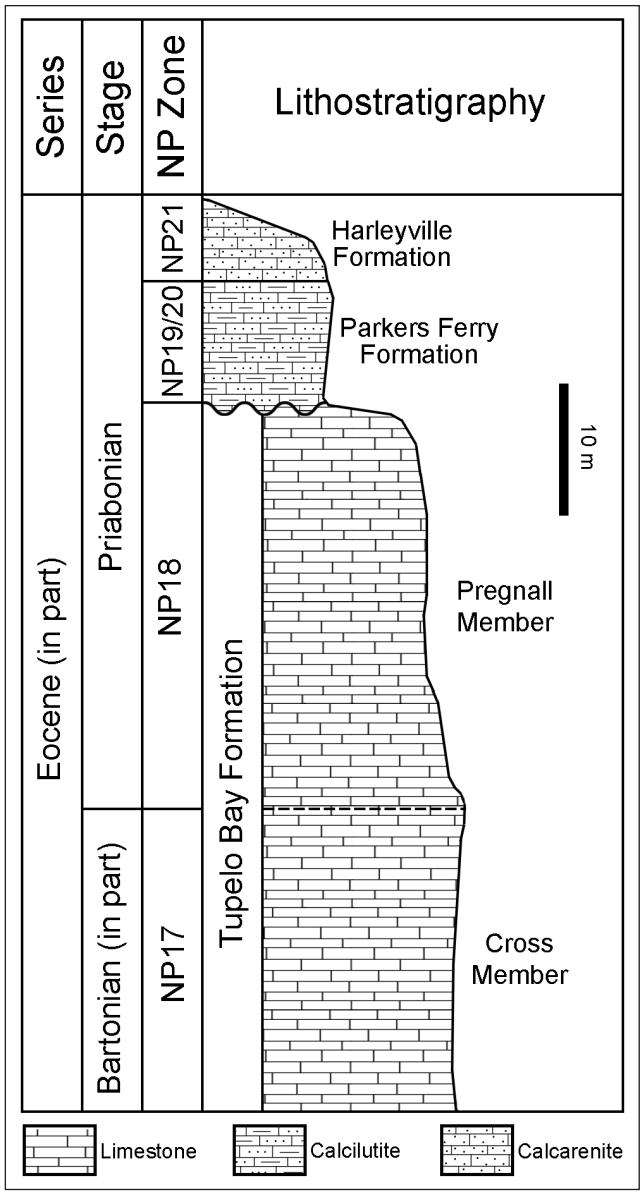

Fig. 2 - Generalized stratigraphic section of some Eocene units occurring in Dorchester and Orangeburg counties, South Carolina, USA, based on exposures observed at the Giant Portland Cement quarry and interpretations of part of the USGS Pregnall #1 (DOR-208) core (Edwards et al. 1997; Geisler et al. 2005).

vided the Eocene limestones in Berkeley, Dorchester, and Orangeburg counties into several informal "Lithozones," with those at Holcim and Giant Portland Cement being referred to Lithozone IV and being comprised of biomicrite, biomicrudite, and biosparrudite. Banks (1977) further subdivided these lithozones, with the lower 4-6 m of the Pregnall Member at both quarries being assigned to Lithozone IVa, which was described as a peloid-rich foraminiferal biomicrite, fine- to medium-grained arenite (p. 111, 147). Ward et al. (1979) identified the limestones at the Giant Portland Cement quarry as calcarenite and biomicrudite, and Edwards et al. (1997) recognized the lower two-thirds of the Pregnall Member (their Cross Member within the DOR-208 core) as a peloid-foram-bivalve-serpulid packstone and the upper one-third as a peloid-foram-bivalve grainstone and packstone. The lower portion of the Pregnall Member is the source of most of the fossils we examined, but some fossils were recovered from the uppermost 1 m of the unit at the Giant Portland Cement quarry. A few specimens appear to have been derived from the Tupelo Bay/Parkers Ferry formational contact zone, and their exact provenience is uncertain (see Albright et al. 2019: 107).

Pooser (1965) determined a Claibornian age (Lutetian-Bartonian) for the Giant Portland Cement quarry limestones, but Banks (1977) later assigned them a Jacksonian age (late Bartonian-Priabonian). We examined two matrix samples associated with pectinid bivalves that were collected from the Giant Portland Cement quarry. One matrix block includes an isolated valve of what appears to be *Chlamys* (*Aequipecten*) sp. as identified by Campell (1995: pl. 1, fig. 2), who considered this taxon as conspecific with *C. deshayesii* as identified by Cooke & MacNeil (1952). Banks (1977) tentatively reported *C. deshayesii* (Lea, 1833) and a "broad ribbed" *Chlamys* (p. 147) from his Lithozone IVd that may also be conspecific. According to Banks (1977), this lithozone is a 3 m-thick interval occurring between 3.5–6.5 m below the phosphatised upper formational contact. Matrix was also recovered from the internal surfaces of isolated valves of ?*Chlamys ducenticostatus* (Campbell, 1995; see more recent determination by Waller 2006) that were collected from the uppermost 1 m of the Tupelo Bay Formation at Giant Portland Cement. The taxon was originally described from this quarry but has also been observed at the Argos quarry to the south (by DJC). Campbell (1995) considered *Chlamys* n. sp. of Cooke & MacNeil (1952) to be conspecific with ?*C. ducenticostatus*, and the "fine ribbed" *Chlamys* reported by Banks (1977) is likely the same species. All these authors noted that this scallop occurs in the upper part of the formation (i.e., Lithozone IVe of Banks 1977).

Edwards et al. (1997) determined from the DOR-208 core that the Cross Member of the Tupelo Bay Formation is of NP17 age and the Pregnall Member represents zone NP18. Our biostrati-

graphic analysis of calcareous nannofossils from matrix associated with pectinid valves (collected from the Giant Portland Cement quarry by DJC) confined the Tupelo Bay Formation to uppermost NP17 to intra-NP18. This age range is determined by the frequent/consistent occurrence of *Reticulofenestra stavensis* (Levin & Joerger, 1967) (FO *R. stavensis* [consistent] = uppermost NP17) and the absence of *Isthmolithus recurvus* Deflandre *in* Deflandre & Fert, 1954 (FO *I. recurvus* = NP18/NP19). Although *R. stavensis* is often rare and sporadic throughout the lower part of its range within NP16-NP17, the first occurrence (FO) of *R. stavensis* [consistent] demonstrates a more frequent and consistent occurrence in uppermost NP17, very close to the NP17/NP18 boundary. The absence of *I. recurvus* in the sample supports the age assignment of intra NP18, as FO *I. recurvus* defines the NP18/NP19 boundary. However, considering the calcareous nannofossil data of Edwards et al. (1997) and the stratigraphic position from which one scallop matrix sample was collected in the Tupelo Bay Formation (within the upper 1 m), the age of the sample may be restricted to NP18. The NP17 Cross Member therefore closely correlates to the Clinchfield Formation of Georgia (see Albright et al. 2019) and the Bartonian Gosport Sand/Cockfield Formation and Moodys Branch Formation in the Gulf Coastal Plain, whereas the Pregnall Member is correlative to the Priabonian Yazoo Clay (North Twistwood Creek Clay Member and/or Cocoa Sand) in the Gulf region.

Material and Methods

The fossils discussed herein were collected from three quarries located in the adjacent Dorchester and Orangeburg counties in South Carolina, USA (Fig. 1). All three quarries are active, and quarrying methods involve removal of limestone via large excavators that break up the rock. Fossils are loosened from the rock both during quarrying and through natural erosional processes. Although multiple bedding surfaces have been observed (as erosional surfaces seen in weathered high walls), no concentrations of vertebrate fossils (i.e., lags) have been identified. With the permission of quarry personnel, fossils were collected from these quarries over the course of several decades (1990s to 2020s). Specimens were predominantly recovered from within the lower 5 m of the exposed portion of the Tupelo Bay Formation, and collection was facilitated by the sloping (versus vertical) surfaces created during quarrying operations. Much of the material was recovered as float, but a *Pristis* sp. rostrum was excavated *in situ* from the Argos quarry (Cicimurri 2007). Interestingly, microscopic evaluation of the concentrates from the approximately 100 kg of matrix surrounding this specimen and two dugongid skulls yielded a total of three teeth. Several xiphiid rostra were collected as float from the Giant Portland Cement quarry, mostly from the contact zone between the Tupelo Bay Formation and suprajacent Parkers Ferry Formation. Adhering matrix demonstrates that some of the rostra originated from the Tupelo Bay Formation, but it is difficult to say if more weathered specimens lived within the Tupelo Bay or Parkers Ferry paleoenvironment. They are included here for completeness (more below in Systematic Paleontology section). All specimens discussed herein are housed at the South Carolina State Museum (**SC**) in Columbia, USA.

To further aid our study of the Tupelo Bay Formation ichthyofauna, we examined extensive collections of fossils from the middle Eocene (Bartonian) Clinchfield Formation of central Georgia (Fig. 2) that are contained within accessions SC2004.34 and SC2013.44. We also utilized specimens from the middle Eocene (Lutetian) Piney Point Formation of Virginia (SC2020.43) and the lower Eocene (Ypresian) Bashi Formation of Mississippi (SC2012.28). With respect to the Clinchfield Formation, the shark and otolith-based teleost taxa have been described (Parmley & Cicimurri 2003 and Stringer et al. 2022, respectively) but the batoids and other teleost elements have heretofore not been reported. Thus, the information we include herein provides further insight into the Clinchfield Formation paleofauna. Skeletal collections of extant elasmobranch and teleost species at SC and McWane Science Center (**MSC**) in Birmingham, Alabama, USA, helped us evaluate the fossil species we discuss herein. Lastly, photographs of White's (1956) hypodigm of *Alopias latidens alabamensis* provided by the Natural History Museum UK (**NHMUK**) helped to elucidate the identity of Tupelo Bay Formation *Alopias* specimens.

The taxonomic hierarchy utilized herein largely follows that of Nelson et al. (2016; higher level), Wiley & Johnson (2010; ordinal placement), and

Van der Laan et al. (2024; family-level). Tooth group terminology follows Siverson (1999) and Cicimurri et al. (2020), and our assignment of teeth to specific files is largely based on examination of jaws of extant shark and ray taxa at MSC and SC. Terminology and abbreviations describing features of xiphiid rostra follows Fierstine & Stringer (2007). We provided a brief synonymy listing for taxa that have been previously reported from lithostratigraphic units within the Atlantic and Gulf Coastal plains, USA, especially if the species identification differs from our attribution.

Figured specimens were photographed at MSC, and fossils exceeding 5.0 mm in greatest dimension were photographed with a Nikon D-80 camera with Tamron macro-lens. Specimens smaller than 5.0 mm in greatest dimension were photographed with a Wild Photomakroskop M400 microscope with mounted Canon Eos R50 camera. To account for depth of field, specimens were photographed from several focal lengths, and the resulting photographs were stacked and merged in Helicon Focus 8 software. Final figures were produced in Adobe Photoshop v. 22.5.9.

Systematic Paleontology

Class CHONDRICHTHYES Huxley, 1880
Subclass EUSELACHII Hay, 1902
Infraclass ELASMOBRANCHII Bonaparte, 1838
Division **Selachii** Cope, 1871
Superorder **Squalomorphii** Compagno, 1973
Order **Hexanchiformes** Buen, 1926
Family Hexanchidae Gray, 1851
Genus *Hexanchus* Rafinesque, 1810

Hexanchus agassizi Cappetta, 1976

Fig. 3A–G

Material: 16 teeth, including SC2015.59.1, SC2018.7.7 (Fig. 3E), SC2018.7.8 (Fig. 3F–G), SC2018.7.71, SC2018.7.72, SC2018.7.73, SC2022.27.1 (Fig. 3A–B), SC2022.27.2, SC2022.27.3, SC2022.27.4 (Fig. 3C–D), SC2022.27.5, SC2022.27.6, SC2022.27.7, SC2022.27.8, SC2022.27.9, SC2022.27.10.

Description. Upper anterior teeth consist of a distally curved main cusp and simple undivided root. In mesial view, the cusp may be sinuous. The labial and lingual faces are smooth and convex (the lingual face more so). The cutting edges, if present, are smooth and restricted to the upper one-half of the cusp. The root is somewhat rectangular, and the lingual face bears a conspicuous shelf-like boss that lacks a nutritive groove. Teeth from more lateral files are wider and more complex than those from anterior positions. These lateral teeth consist of a large main cusp and two much smaller distal cusplets. The main cusp is rather narrow, and the labial and lingual faces are smooth. The labial face is weakly convex, and the lingual face is very convex. The mesial cutting edge is rather straight and smooth except for a few serrations at the base. The distal cutting edge is smooth and sharp but may not reach the cusp base. The accessory cusplets are sharply pointed and distally inclined, well-separated from each other and the main cusp, bear smooth cutting edges, and decrease in size distally. The root is sub-rectangular and thickest at the shelf-like lingual boss below the crown. The area below the boss appears concave.

The largest well-preserved lower teeth measure up to 15 mm in mesio-distal width. The main cusp (acrocone) is smaller than that of the upper teeth, and it is succeeded by up to ten cusps that decrease in size distally. The mesial cutting edge of the acrocone is straight to weakly convex and serrated along the basal one-half to two-thirds. The apical portion of the mesial edge is smooth, as are the distal cutting edge and the edges of the accessory cusps. The root is rectangular and very thin labio-lingually.

Remarks. *Hexanchus agassizi* dentitions exhibit various forms of heterodonty, with crowns varying in width and height from the symphysis to the commissure (monognathic heterodonty), and upper teeth are morphologically distinct from the lowers (dignathic heterodonty). With respect to monognathic heterodonty, specimen SC2022.27.1 has a rather conical crown, no distal cusplets, and a very simple root, indicating it is an upper first anterior tooth (Fig. 3A–B), and the distal crown inclination demonstrates it originated from the right side. Specimen SC2022.27.4 (Fig. 3C–D) exhibits fine serrae on the lower part of the mesial cutting edge, and there is a single distal cusplet, indicating the tooth was in approximately the third file of the left palatoquadrate. Specimens SC2018.7.7 and SC2018.7.8 are both lower teeth, and the slight mesial projection of the crown foot indicates they were in the region of the second through sixth jaw files. Speci-

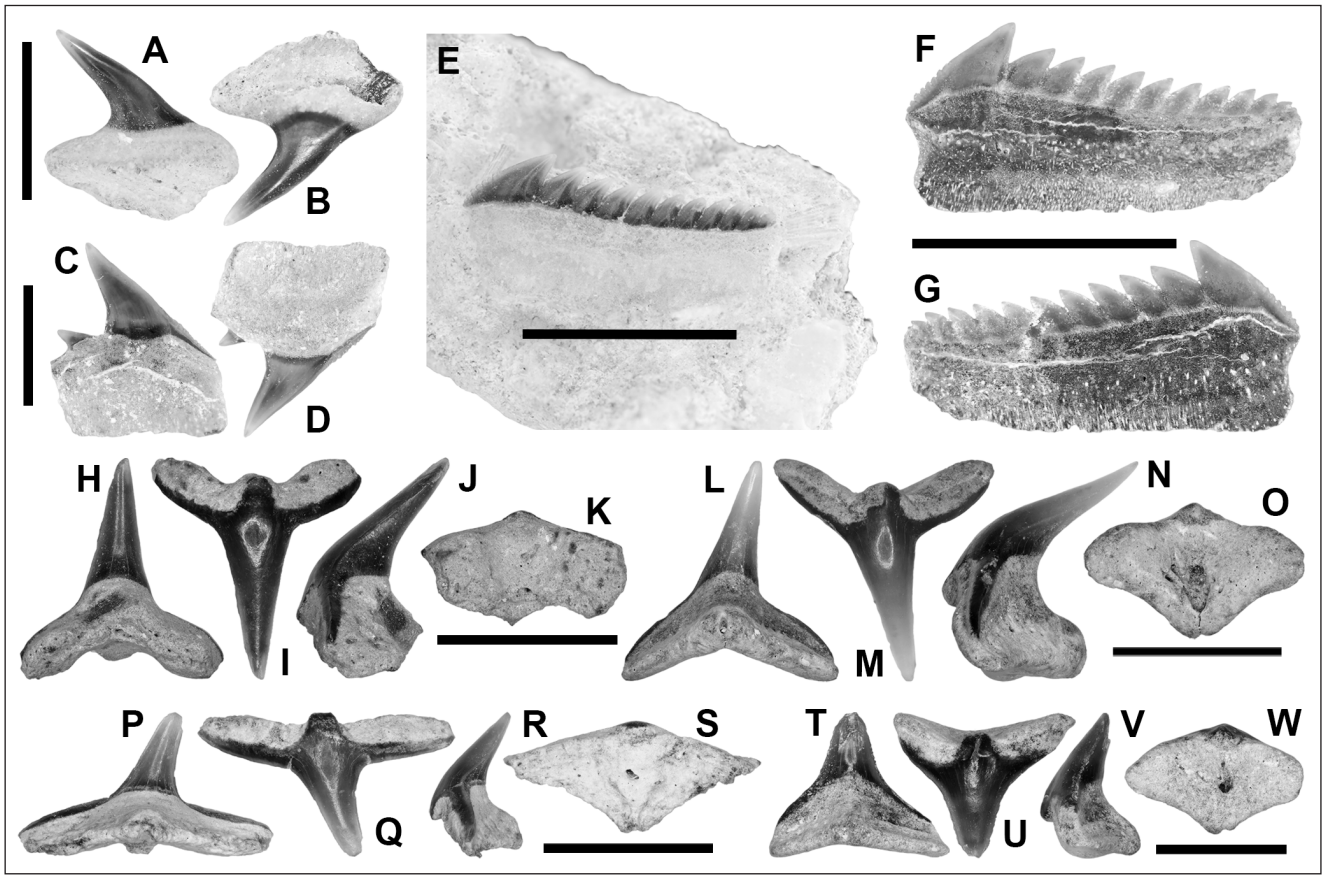

Fig. 3 - Sharks from the Tupelo Bay Formation. A-G) *Hexanchus agassizi*, upper right first anterior tooth (A-B), SC2024.27.1, in lingual (A), and labial (B) views; upper left anterior tooth (C-D), SC2022.27.4, in labial (C), and lingual (D) views; lower left lateral tooth (E), SC2018.7.7, in labial view; lower right tooth (F-G), SC2018.7.8 in lingual (F), and labial (G) views. H-W) *Squatina prima*, upper? anterior tooth (H-K), SC2022.27.11 in lingual (H), labial (I), mesial (J), and basal (K) views; anterolateral tooth (L-O), SC2022.27.17 In lingual (L), labial (M), mesial (N), and basal (O) views; lateral tooth (P-S), SC2022.27.15, in lingual (P), labial (Q), mesial (R), and basal (S) views; lower? anterior tooth (T-W), SC2022.27.16, in lingual (T), labial (U), distal (V), and basal (W) views. Scale bars: 5 mm in A-D & H-W, 1 cm in E-G.

men SC2018.7.7 (Fig. 3E) is from the left jaw, and its shorter and more distally inclined acrocone indicates it was located closer to the commissure compared to SC2018.7.8 (Fig. 3F–G).

Hexanchus agassizi will not be confused with other selachians occurring in the Tupelo Bay Formation. However, *Notorynchus* sp. occurs within the overlying (Priabonian) Parkers Ferry and Harleyville formations (SC86.59.4 and SC86.59.5), and the genus was reported from the Priabonian Dry Branch Formation by Cicimurri & Knight (2019). However, *Hexanchus* has a much straighter crown, more numerous distal cusplets, and finer mesial serrations when compared to *Notorynchus*.

The Tupelo Bay Formation specimens are like *H. agassizi* teeth reported by Cappetta (1976) and are identified as such herein. Adnet (2006a) synonymized *Hexanchus collinsonae* Ward, 1979 and *H. hookeri* Ward, 1979 with *H. agassizi* based on morphometric analyses of extant hexanchid sharks. Thus, *H. agassizi* has been reported from lower-to-middle Eocene strata of Europe (i.e., Cappetta 1976; Bor 1985; Van den Eekhaut & DeSchutter 2009) and various disparate locations like Egypt (i.e., Underwood et al. 2011; Zalmout et al. 2012; Zalat et al. 2017), Argentina (Charnelli et al. 2023), and Japan (Tanaka & Kohno 2025). *Hexanchus* is virtually unknown from the Eocene of the Atlantic and Gulf coastal plains, but specimens comparable to *H. agassizi* have been reported from the Ypresian Nanjemoy Formation of Virginia (Kent 1999).

Order **Squatiniformes** Buen, 1926
Family Squatinidae Bonaparte, 1838
Genus *Squatina* Dumeril, 1806

Squatina prima (Winkler, 1874)
Fig. 3H–W

Material: 10 teeth, including SC2022.27.11 (Fig. 3H–K), SC2022.27.12, SC2022.27.13, SC2022.27.14, SC2022.27.15 (Fig. 3 P–S), SC2022.27.16 (Fig. 3T–W), SC2022.27.17 (Fig. 3L–O), SC2022.27.18, SC2022.27.19, SC2022.27.20.

Description. The teeth can attain sizes of 7 mm in mesio-distal width and 5 mm in apico-basal height. The crown of each tooth consists of a needle-like cusp that is flanked by low lateral shoulders. The cusp is somewhat conical, as it has convex labial and lingual faces. In labial view, the cusp is erect to distally inclined, and the cusp is lingually curved in profile view. The mesial and distal cutting edges on the cusp are indistinct, but they extend onto the lateral shoulders. The shoulders are oblique to perpendicular to cusp height, and they may be straight or weakly convex. There is a narrow basal labial projection that extends below the level of the root. The root is very low and may be flat to arched in labial/lingual view. In basal view the attachment surface is sub-triangular and perforated by a large nutritive foramen. In profile view the root is shelf-like and extends well beyond the crown foot. Numerous foramina occur on the upper surface of the root below the line formed by the lateral shoulders.

Remarks. Based on the jaws of a *Squatina nebulosa* Regan, 1906 that we examined (SC2020.53.5), teeth from anterior and lateral files are represented (monognathic heterodonty). Anterior teeth have a rather symmetrical appearance in labial view, and the root is highly arched with the lateral crown shoulders being oblique to cusp height (Fig. 3H–I). On lateral teeth the cusp is distally inclined (Fig. 3L–M), and the inclination increases towards the jaw commissure. The root also becomes flatter such that the lateral crown shoulders are more perpendicular to the main cusp (Fig. 3P–Q). There are noticeable differences in cusp width among the Tupelo Bay Formation teeth that may represent dignathic heterodonty. Specimens having a relatively narrow cusp were from the upper dentition and those with wider cusps from the lower dentition (compare Fig. 3I to 3U).

Based on previous reports, *Squatina prima* has a very long temporal range (late Paleocene to late Eocene) and had a wide geographic range during that time (see Cappetta 2012). However, as Rodríguez et al. (2023) have pointed out, there is some morphological variation among the specimens referred to this species, and it may have become a "wastebasket" taxon consisting of several different species having a conservative tooth morphology. The Tupelo Bay Formation specimens are more similar to middle Eocene (Lutetian) *S. prima* from Belgium (Van den Eeckhaut & De Schutter 2009) and Russia (Popov et al. 2025) rather than to a somewhat more robust morphology reported from the Paleocene of Chile (Rodríguez et al. 2023). Comparable teeth were reported from the Clinchfield and Dry Branch formations of Georgia (Parmley & Cicimurri 2003 and Case 1981, respectively). The Clinchfield Formation has been assigned an NP18 age and correlated with the Pregnall Member of the Tupelo Bay Formation (Albright et al. 2019), but Stringer et al. (2022) more recently stated an NP17 (possibly earliest NP18) age and correlated the Clinchfield Formation with the Gosport Sand and Moodys Branch Formation of the Gulf Coastal Plain. Huddlestun & Hetrick (1979) reported benthic foraminifera from the Riggins Mill Member of the Clinchfield Formation that also occur in the Cockfield/Moodys Branch formational contact zone of Louisiana (Treadwell 1954), indicating an upper NP17 age.

Superorder **Galeomorphi** Compagno, 1973
Order **Heterodontiformes** Berg, 1940
Family Heterodontidae Gray, 1851
Genus *Heterodontus* de Blainville, 1816

Heterodontus aff. ***vincenti*** (Leriche, 1905)
Fig. 4

2003 *Heterodontus* sp. – Parmley & Cicimurri, p. 158–159, fig. 3 B.

Material: 10 teeth, including SC2022.27.21 (Fig. 4A–D), SC2022.27.22 (Fig. 4N–O), SC2022.27.23, SC2022.27.24, SC2022.27.25 (Fig. 4H–J), SC2022.27.26 (Fig. 4K–M), SC2022.27.27 (Fig. 4Q–S), SC2022.27.28 (Fig. 4T–V), SC2022.27.29, SC2022.27.30 (Fig. 4E–G).

Description. Specimen SC2022.27.21 is a small tooth measuring 2 mm in crown width and approximately 2 mm in height. The crown is massive and bears a single large main cusp flanked by a single pair of large lateral cusplets. The main cusp is broad-based, somewhat conical, and divided into strongly convex labial and lingual faces by thick and smooth lateral cutting edges. The main cusp as well as the lateral cusplets are both lingually and distally inclined. The bases of the lateral cusplets occur at

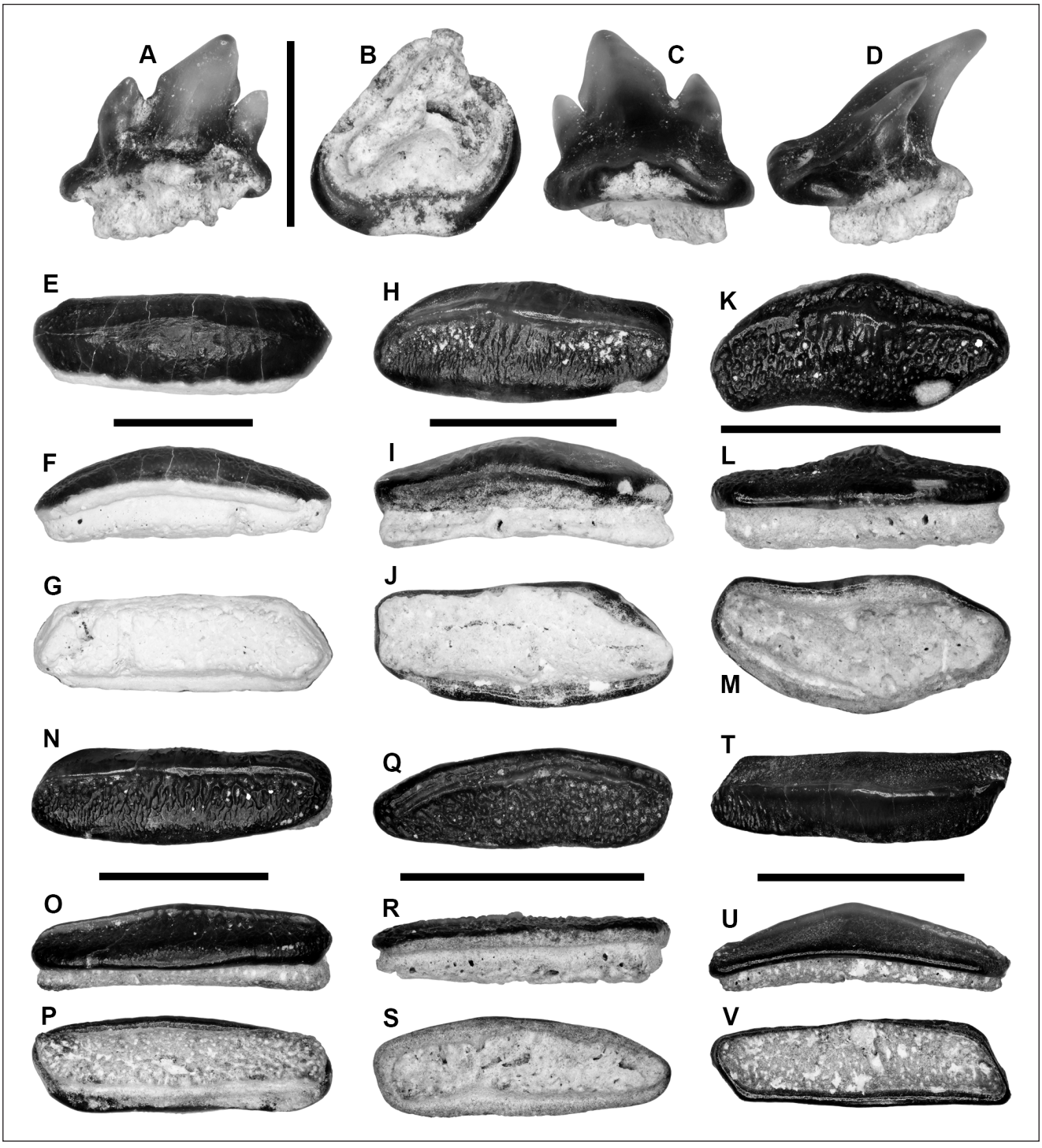

Fig. 4 - *Heterodontus* aff. *vincenti* from the Tupelo Bay Formation. A-D) anterior tooth, SC2022.27.21, in lingual (A), basal (B), labial (C), and mesial (D) views; lateral tooth (E-G), SC2022.27.30, in occlusal (E), labial (F), and basal (G) views; lateral tooth (H-J), SC2022.27.25, in occlusal (H), labial (I), and basal (J) views; lateral tooth (K-M), SC2022.27.26, in occlusal (K), labial (L), and basal (M) views; lateral tooth (N-O), SC2022.27.22, in occlusal (N), labial (O), and basal (P) views; lateral tooth (Q-S), SC2022.27.27, in occlusal (Q), labial (R), and basal (S) views; lateral tooth (T-V), SC2022.27.28, in occlusal (T), labial (U) and basal (V) views. Scale bars: 5 mm.

roughly one-half the crown's height. Both cusplets are triangular (the mesial one is wider than the distal one), pointed apically, roughly conical (with weak lateral cutting edges), and separated from the main cusp by a deep notch. The crown enameloid is smooth. In profile and occlusal views, the crown base flares labially and laterally, and a lingual protuberance extends over the root. The labial crown foot is thickened and forms a ridge-like structure that extends between the outer margins of the lat-

eral cusplets. In basal view, the crown overhangs the root in all directions (particularly labially). The root is ablated, but in basal view it is V-shaped with very thin lobes that converge to form a prominent lingual boss. The mesial root lobe is much longer than the distal one, and a distinctive foramen occurs at the apex of the boss.

The remaining teeth in the sample are mesio-distally wide, labio-lingually narrow, and apico-basally short. The maximum mesio-distal crown width measures almost 9 mm and the crown height is less than 4 mm. In occlusal view, teeth have an oval or sub-rectangular appearance, but several much wider specimens have sinuous labial and lingual margins. The mesial and distal margin may be rounded or squared. The crown is divided into labial and lingual faces by a transverse crest, the position of which varies such that it is (usually) medially located but can be situated closer to the labial or lingual margin. The labial face ranges from flat to weakly convex, whereas the lingual face may be moderately to strongly convex. The transverse crest varies from weak to robust and may not reach the mesial or distal margins. The crown enameloid is heavily ornamented on the labial and lingual faces. The enameloid of the labial face often consists of coarse bifurcating and anastomosing longitudinal ridges that emanate from the transverse crest and transition into a more reticulated network closer to the labial margin. On some teeth the reticulated network is more extensive, and still other specimens have a more rugose appearance. The lingual face often bears robust (larger than those on the labial face) bifurcating ridges that do not extend to the crown foot. The crown overhangs the root in all directions. The root is very low and anaulocorhize but highly vascularized.

Remarks. As the name implies, *Heterodontus* dentitions exhibit considerable morphological variation that reflects monognathic, dignathic, and ontogenetic heterodonty. Observations of extant *Heterodontus zebra* (Gray, 1831) and *H. portusjacksoni* (Meyer, 1793) jaws at SC (SC2020.53.6 and SC2020.53.7, respectively) indicate that the Tupelo Bay Formation teeth represent adult individuals, with SC2022.27.21 being from an anterolateral file (Fig. 4A–D), SC2022.27.22 and SC2022.27.28 being from lateral files (Figs. 4N–O & 4T–V, respectively), and flat-crowned teeth like SC2022.27.25 (Fig. 4H–J) were derived from a more posterior file. Specimen SC2022.27.26 (Fig. 4K-M) likely occupied a file between SC2022.27.21 and SC2022.27.22.

Unfortunately, most of the nominal fossil species of *Heterodontus* are based on relatively few isolated teeth. Hovestadt (2018) evaluated the dentitions of all extant *Heterodontus* species and grouped them into one of two "lineages" based on tooth morphology. He also conducted an overview of the fossil record and largely rejected the species names assigned to most of the fossil taxa, preferring instead to group teeth into one of two morphotypes (Morphotype 1 or Morphotype 2). Following Hovestadt (2018), the Tupelo Bay Formation *Heterodontus* teeth can be assigned to his Morphotype 2 because the crown ornamentation consists of coarse longitudinal ridges on the lingual crown face, and the longitudinal ridges on the labial face transition to a finer reticulated network. We note here that grouping species based on Hovestadt's (2018) morphotypes does not necessarily imply close phylogenetic relationships, as Slater et al. (2020) showed that extant *H. galeatus* (Günther, 1870) and *H. portusjacksoni* are more closely related to each other than *H. zebra* is to *H. portusjacksoni*. Per Hovestadt (2018) the latter two taxa display Morphotype 1 dentitions and *H. galeatus* Morphotype 2.

With respect to Eocene *Heterodontus* species that have been named, lateral teeth of *H. sowasheense* Case, 1994 (Ypresian Bashi Formation of Mississippi) have much reduced to absent crown ornamentation (based on our evaluation of a larger sample size recovered from Case's (1994) type locality; see SC2013.28) compared to the Tupelo Bay Formation teeth. The proposed hypodigm of *H. pineti* Case, 1981 from the upper Eocene Dry Branch Formation of Georgia and *H. elongatus* Case & Borodin, 2000b from the middle Eocene Castle Hayne Limestone of North Carolina both include only a single lateral tooth. That of *H. pineti* differs from the Tupelo Bay Formation specimens in that it is very convex and has a more dimpled appearance. The taxon *H. elongatus* includes high-crowned teeth that, in our opinion, may not belong to a chondrichthyan fish, let alone *Heterodontus*, and the lateral tooth attributed to *H. elongatus* is not dissimilar from the two teeth of *Cestracion* (= *Heterodontus*) *vincenti* Leriche, 1905 from the Eocene of Belgium. These *H. vincenti* lateral teeth are very wide but rather low and have ornamentation of coarse lingual longitudinal ridges and finer labial ridges, which are features consistent

with the Tupelo Bay Formation specimens. Case et al. (1996) reported very similar lateral teeth from the White Mountain Formation of Uzbekistan, and the species was recently reported in the middle Eocene Osinovaya Formation in Russia (Popov et al. 2025). With respect to teeth from more anterior tooth positions, those reported for *H. sowasheense* appear to have cusplets occurring higher on the crown compared to specimen SC2022.27.21. Anterior teeth of Eocene *H. wardensis* (Casier, 1966) have two pairs of lateral cusplets, and cusplets on Ypresian *H. woodwardi* (Casier, 1946) teeth are much reduced or absent. It is difficult to compare these species if the teeth described do not all represent the same jaw position and/or ontogenetic stage (i.e., Hovestadt 2018).

Heterodontus appears to have been an uncommon component of middle and late Eocene fish faunas of the Atlantic and Gulf coastal plains, as evidenced by the reports cited above. Additionally, only a single tooth was reported from the Clinchfield Formation of Georgia (Parmley & Cicimurri 2003), and seven teeth were identified among the tens of thousands of specimens from three different formations of the Claiborne Group (upper Ypresian to middle Bartonian) in Alabama (Ebersole et al. 2019). Ebersole & Cicimurri (2025) examined roughly 5,000 chondrichthyan and osteichthyan specimens from Cretaceous through Pleistocene units in Louisiana and encountered only a single *Heterodontus* tooth. The cuspidate (possibly juvenile) lateral tooth, derived from the middle Eocene Moodys Branch Formation (NP17), was first reported as *H. pineti* by Manning & Standhardt (1986) but later simply referred to *Heterodontus* sp. by Ebersole & Cicimurri (2025: fig. 6.10).

The *H. pineti* teeth reported by Case (1981) were recovered from the Dry Branch Formation (Twiggs Clay facies) of Georgia, but this taxon was not documented in the Dry Branch Formation (Irwinton Sand facies) in South Carolina (Cicimurri & Knight, 2019).

Order **Orectolobiformes** Applegate, 1972
Superfamily Hemiscylloidea Naylor et al., 2012
Family Ginglymostomatidae Gill, 1862
Genus *Nebrius* Rüppell, 1837

Nebrius thielensi (Winkler, 1874)
Figs. 5A–R

1874 *Plicodus thielensis* – Winkler, p. 301, pl. 7, fig. 5.
1877 *Acrodobatus obliquus* – Leidy, p. 250, pl. 34, fig. 14.
1981 *Ginglymostoma obliquum* (Leidy, 1877) – Case, p. 61., pl. 4, fig.1
2000a *Nebrius thielensis* (Winkler, 1874) – Case & Borodin, p. 8, pl. 1, figs. 1-2.
2000b *Nebrius thielensis* (Winkler, 1874) – Case & Borodin, p. 22, pl. 3, figs. 29-30.
2003 *N. thielensis* – Parmley & Cicimurri, p. 159 fig. 3 C.
2016 *Nebrius obliquus* (Leidy, 1877) – Cappetta & Case, p. 48, pl. 2, figs. 1-4.

Material: 11 teeth, including SC2015.59.40, SC2022.27.31, SC2022.27.32 (Fig. 5A–D), SC2022.27.33 (Fig. 5F–J), SC2022.27.34, SC2022.27.35, SC2022.27.36, SC2022.27.37 (Fig. 5O–R), SC2022.27.38, SC2022.27.39, SC2022.27.40 (Fig. 5K–N).

Description. Teeth can attain sizes up to 12 mm in mesio-distal width and 8 mm in apico-basal height. In labial view, the crown is low with a triangular appearance. There is a short, triangular main cusp that is flanked by up to seven pairs of much smaller lateral cusplets, although cusplets are more numerous on the mesial side. The cutting edge is smooth across the main cusp and lateral cusplets. The labial crown foot is highly convex and there is a large medial protuberance that extends basally below the root surface. The lingual crown face bears a lingually directed boss that extends onto the upper root surface. In profile view, the lingual face is rather vertical, but the labial face is oblique and may be sinuous. The crown enameloid is smooth but there may be crenulations on the labial crown protuberance, particularly on large specimens. In profile view, the root is low but in basal view, the root is sub-triangular and may be flat or weakly convex, and it is perforated by a large nutritive foramen. Several smaller foramina are located on the upper root surface, adjacent to the lingual crown protuberance, and a single foramen occurs at the lingualmost margin of the root.

Remarks. Monognathic heterodonty is evident in our sample, as teeth from more anterior files are rather symmetrical and have a similar number of cusplets on the mesial and distal sides of the crown (Fig. 5C–D). Teeth from lateral positions have a more elongated and convex mesial edge, and a greater number of cusplets occur on the mesial edge than on the distal edge, and the main cusp is offset distally (Fig. 5H–I). Additionally, the cusp becomes more distally inclined the closer a tooth was located to the commissure. Furthermore, the labial crown protuberance is more elongated and easily distinguished from the crown itself (Fig. 5Q). Ontogenetic heterodonty also appears to be represented,

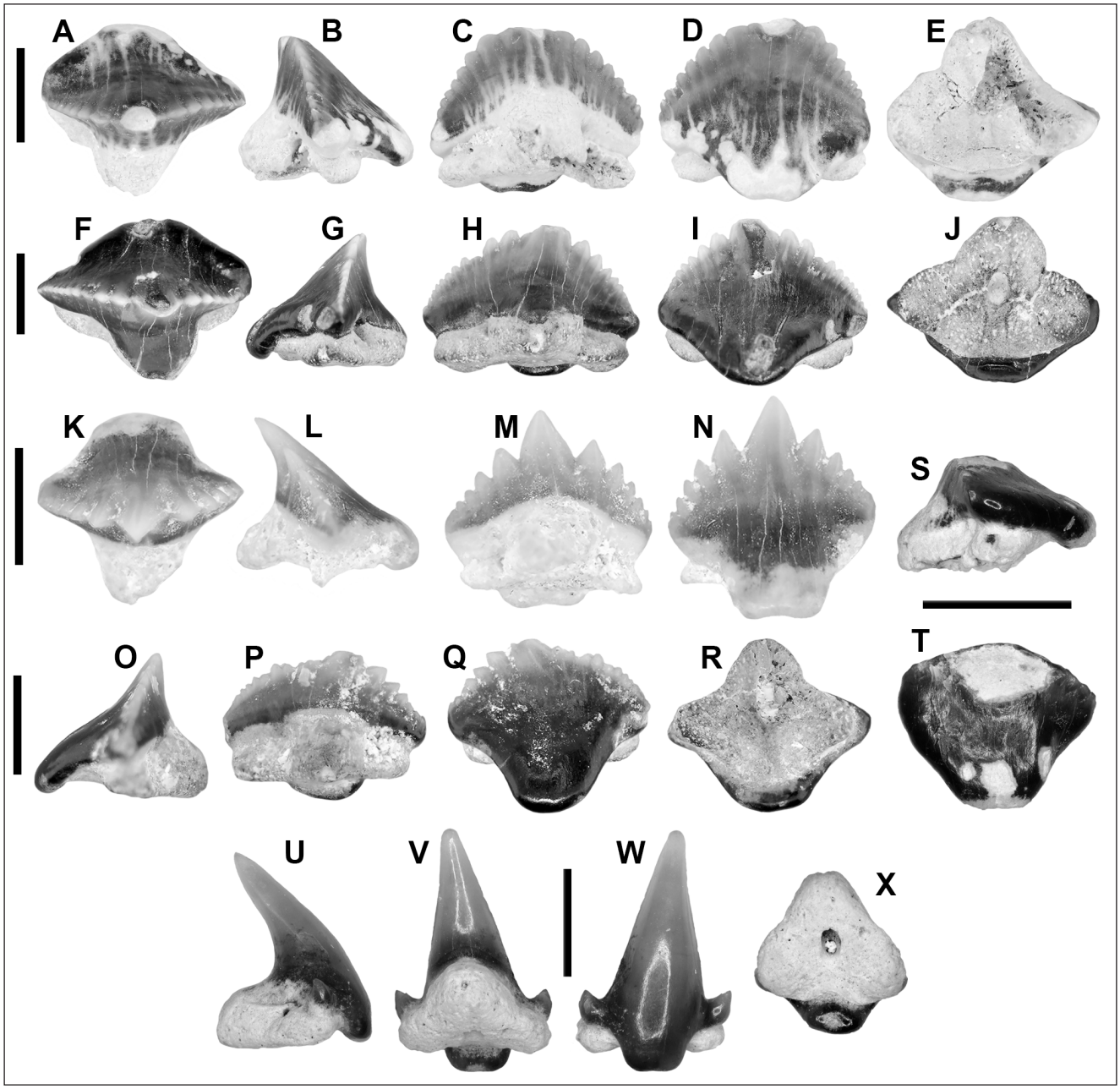

Fig. 5 - Orectolobiform sharks from the Tupelo Bay Formation. A-R) *Nebrius thielensi*, anterolateral tooth (A-E), SC2022.27.32, in occlusal (A), mesial (B), lingual (C), labial (D), and basal (E) views; lateral tooth (F-J), SC2022.27.33, in occlusal (F), mesial (G), lingual (H), labial (I), and basal (J) views; juvenile anterior tooth (K-N), SC2022.27.40, in occlusal (K), mesial (L), lingual (M), and labial (N) views; lateral tooth (O-R), SC2022.27.37, in mesial (O), lingual (P), labial (Q), and basal (R) views. S-T) Ginglymostomatidae tooth, SC2018.2.74, in mesial (S), and labial (T) views. U-X) *Eostegostoma angustum*, anterolateral tooth, SC2021.26.1, in mesial (U), lingual (V), labial (W), and basal (X) views. Scale bars: 2 mm in U-X, 5 mm in A-J & O-T.

as smaller teeth have fewer cusplets compared to large specimens (i.e., four vs. seven or more) from the equivalent file, and the cusplets are larger with respect to overall crown size (compare Fig. 5K–N to 5A–D).

Other regional occurrences of *Nebrius thielensi* include the Lutetian Castle Hayne Formation of North Carolina (Case & Borodin 2000b), Clinchfield and Dry Branch formations of Georgia (Parmley & Cicimurri 2003, Case 1981, and Case & Borodin 2000a, respectively) and the Dry Branch Formation of South Carolina (Cicimurri & Knight 2019). The taxon is also present in the middle Eocene (Lutetian-Bartonian) Lisbon Formation and Bartonian Gosport Sand of Alabama (Ebersole et al. 2019) and the Bartonian (NP17) Moodys Branch Formation of Louisiana (Ebersole & Cicimurri 2025).

Ginglymostomatidae
gen. et sp. indet.
Fig. 5S–T

Material: One tooth, SC2018.7.74.

Description. The tooth measures 5 mm in mesio-distal width, but its total height is unknown due to apical crown loss through *in vivo* use. In profile view, the crown is divided into labial and lingual faces by a transverse crest. The lingual face is rather narrow except for a medial elongation that extends onto the root. The labial face is expansive, with the thickened and very convex crown foot overhanging the root. Although much of the apical part of the crown is not preserved, the labial face has a weakly sinuous profile. The crown enameloid is smooth. In labial view, two very weak cusplets are visible on the mesial side of the transverse crest, whereas three slightly larger cusplets occur on the distal side. The labial crown foot is drawn out into a very convex apron.

Remarks. The crown and root of the specimen are incompletely preserved, the former apparently through *in vivo* wear (Fig. 5T) and the latter due to postmortem ablation (Fig. 5S), hampering our ability to accurately identify the tooth. However, it is comparable in size to a tooth of *N. thielensi* (see above) that bears five distinct pairs of lateral cusplets. It is possible that specimen SC2018.7.74 represents a very poorly preserved *N. thielensi* tooth, but it could be attributed to *Ginglymostoma* based on the lesser number and smaller size of observable lateral cusplets. Additional specimens are necessary to confirm the presence of the latter taxon in the Tupelo Bay Formation.

Family Brachaeluridae Applegate, 1972
Genus *Eostegostoma* Herman, 1977

Eostegostoma angustum (Nolf & Taverne in Herman, 1977)
Fig. 5U–X

1996 *Palaeorhincodon wardi* Herman, 1977 – Case et al., pl. 11, figs. 204–208.

Material: One tooth, SC2021.26.1.

Description. This tooth measures slightly over 4.5 mm in apico-basal height. The crown of this narrow tooth consists of a tall and triangular main cusp that is flanked by a single pair of small lateral cusplets (Fig. 5W). The main cusp appears conical due to convex labial and lingual faces, although a weak cutting edge divides the cusp into a rather thin labial face and much more extensive lingual face (Fig. 5U). In profile view, the cusp is lingually curved. The cusplets are roughly conical and located very low on the main cusp. There is a conspicuous labial crown protuberance that extends below the base of the root. In profile view, the root is low but in basal view it has a sub-triangular outline and is perforated by a large centrally located nutritive foramen (Fig. 5X). Additional foramina are located on the upper root surface behind the cusplets, and a single foramen occurs at the lingual-most margin of the root (Fig. 5V).

Remarks. The Tupelo Bay Formation *Eostegostoma* tooth is easily separated from those of *Nebrius thielensi* by being mesio-distally compressed, having only a single pair of lateral cusplets occurring very low on the main cusp, and having a much narrower labial crown projection. These features also clearly distinguish *Eostegostoma* from the Ginglymostomatidae indet. tooth described above.

Eostegostoma angustum has been reported (although not always illustrated) from the middle Eocene of Europe, including Belgium (Herman 1977; Taverne & Nolf 1978; Van den Eeckhaut & De Schutter 2009), the Netherlands (Bor 1985), France (Adnet 2006b; Adnet et al. 2008) and England (Ward 1980; Kemp et al. 1990; Bone et al. 1991), and the genus has been identified in the middle Eocene of Egypt (see Underwood et al. 2011). The species also occurs in middle Eocene deposits of Uzbekistan, where it was identified by Case et al. (1996) as *Palaeorhincodon wardi* Herman, 1977.

Specimen SC2021.26.1 represents only the second record of the genus in North America, where it is unknown from Eocene strata elsewhere in the Atlantic Coastal Plain, like the Castle Hayne Limestone (Lutetian) of North Carolina (Case & Borodin 2000b) and Clinchfield Formation (Bartonian) of Georgia (Parmley & Cicimurri 2003). Interestingly, Ebersole et al. (2024) provided the first North American record of *Eostegostoma* sp. based on a tooth from the basal Oligocene (early Rupelian) of Alabama. That specimen was recovered from the Red Bluff Clay, a lithostratigraphic unit that immediately overlies the upper Eocene (Priabonian)

Yazoo Clay, and both units are temporally younger than those that have previously yielded *Eostegostoma* teeth (see Cappetta 2012). Elsewhere in the Gulf Coastal Plain, the species is unknown from the well-documented middle Eocene elasmobranch assemblages in the Tallahatta and Lisbon formations and Gosport Sand of Alabama (Cappetta & Case 2016; Ebersole et al. 2019; Maisch et al. 2014) and was not encountered in Louisiana in temporally equivalent deposits like the Cook Mountain, Cockfield, and Moodys Branch formations (Cicimurri & Ebersole 2021; Ebersole & Cicimurri 2025).

Order **Lamniformes** Berg, 1958
Family Otodontidae Glickman, 1964
Genus *Otodus* Agassiz, 1843

Otodus* (*Carcharocles*) *sokolowi? (Jaekel, 1895)
Figs. 6A–Q

1895 *Carcharodon sokolowi* – Jaekel, p. 8, pl. 8, figs. 1–5.
1981 *Procarcharodon auriculatus* (Blainville, 1818) – Case, p. 56-57, pl. 2, figs. 1–2.
1942 *Carcharodon auriculatus* var. *sokolowi* (Jaekel, 1895) – Leriche, p. 46–47, pl. 3, figs. 1–4
1986 *Carcharodon auriculatus* (Blainville, 1818) – Manning & Standhardt, p. 143, fig. 2.4; Dockery & Manning, pls. 1–2.
2003 *Carcharocles angustidens* (Agassiz, 1843) – Parmley & Cicimurri, p. 165–166, fig. 4C.

Material: 8 teeth, including SC86.56.1, SC86.59.3 (Fig. 6F–H), SC2018.7.1 (Fig. 6D–E), SC2018.7.150 (Fig. 6I–K), SC2018.7.152 (Fig. 6A–C), SC2022.27.41, SC2022.27.42 (Fig. 6L–N), SC2022.27.43 (Fig. 6O–Q).

Description. The teeth consist of a broadly triangular crown and massive bilobed root. The crown is comprised of the main cusp and a single pair of lateral cusplets. Of the available specimens, the crown of each is distally inclined albeit to varying degrees. The labial faces are flat to weakly convex, whereas the lingual faces are highly convex. The crown enameloid is smooth. The lateral cusplets are generally triangular but they can be broad-based or narrow, high or low, and well-separated from, or closely connected to, the main cusp. The cutting edges are coarsely serrated and continuous across the cusplets and main cusp. The serration density and complexity varies, even along the same cutting edge. The serrations on the cusplets are often compound and can be large enough to resemble additional lateral cusplets. The bilobate root includes moderately elongated, diverging lobes that have rounded basal margins. There is a robust lingual boss that may be perforated by one or more nutritive foramina. The interlobe area is U-shaped.

Remarks. We believe that our small sample of eight teeth reflects monognathic and dignathic heterodonty within a single taxon. Specimen SC2018.7.150, for example, is an upper left anterior tooth based on its broad-based crown and symmetrical appearance (Fig. 6I–J). Specimen SC2018.7.152 is a tooth with a broad-based and distally inclined crown that represents an upper left lateral file (Fig. 6B–C). Tooth SC2022.27.42 is a small postero-lateral tooth (Fig. 6L–M), and the narrowness of the crown indicates it is from a lower jaw file. Specimen SC2022.27.43 is an unusual tooth in that it is very small, has a simple but broadly triangular crown with a pair of diminutive lateral cusplets, and an asymmetrical root (i.e., the distal lobe is more elongated than the mesial one). This tooth morphology (Fig. 6O–Q) may represent a distal upper right posterior tooth (see also Case 1981; pl. 1, fig. 4).

Accurate identification of *Otodus* (*Carcharocles*) teeth is hampered by the numerous nominal species that have been named (see Applegate & Espinosa-Arrubarrena 1996), which are often based on a limited sample size that may not capture the full range of intraspecific variation. Within *Otodus* (*Carcharocles*), two middle-to-upper Eocene species are most often reported in the literature, including *O.* (*C.*) *auriculatus* (Blainville, 1818) and *O.* (*C.*) *sokolowi* Jaekel, 1895. A third species, *O.* (*C.*) *poseidoni* Zhelezko & Kozlov, 1999, has been named but does not seem to be widely recognized. Several chronological subspecies were named by Zhelezko & Kozlov (1999) to account for the morphological variation they observed among the three species, and ancestor-descendent relationships were suggested, from *O.* (*C.*) *auriculatus* (Lutetian) to *O.* (*C.*) *poseidoni* (Bartonian) to *O.* (*C.*) *sokolowi* (Priabonian) (see also Applegate & Espinosa-Arrubarrena, 1996). However, Dockery & Manning (1986) believed that *O.* (*C.*) *sokolowi* and the Oligocene taxon, *O.* (*C.*) *angustidens*, were conspecific with *O.* (*C.*) *auriculatus*. Although typically stratigraphically/temporally separated, *O.* (*C.*) *auriculatus* and *O.* (*C.*) *sokolowi* have been reported as coeval (i.e., Diedrich 2013; Popov et al. 2025), indicating that two contemporaneous very large shark taxa with similar dentitions were competing for similar resources. Alternatively, the apparent contemporaneous occurrence reinforces the phenomenon

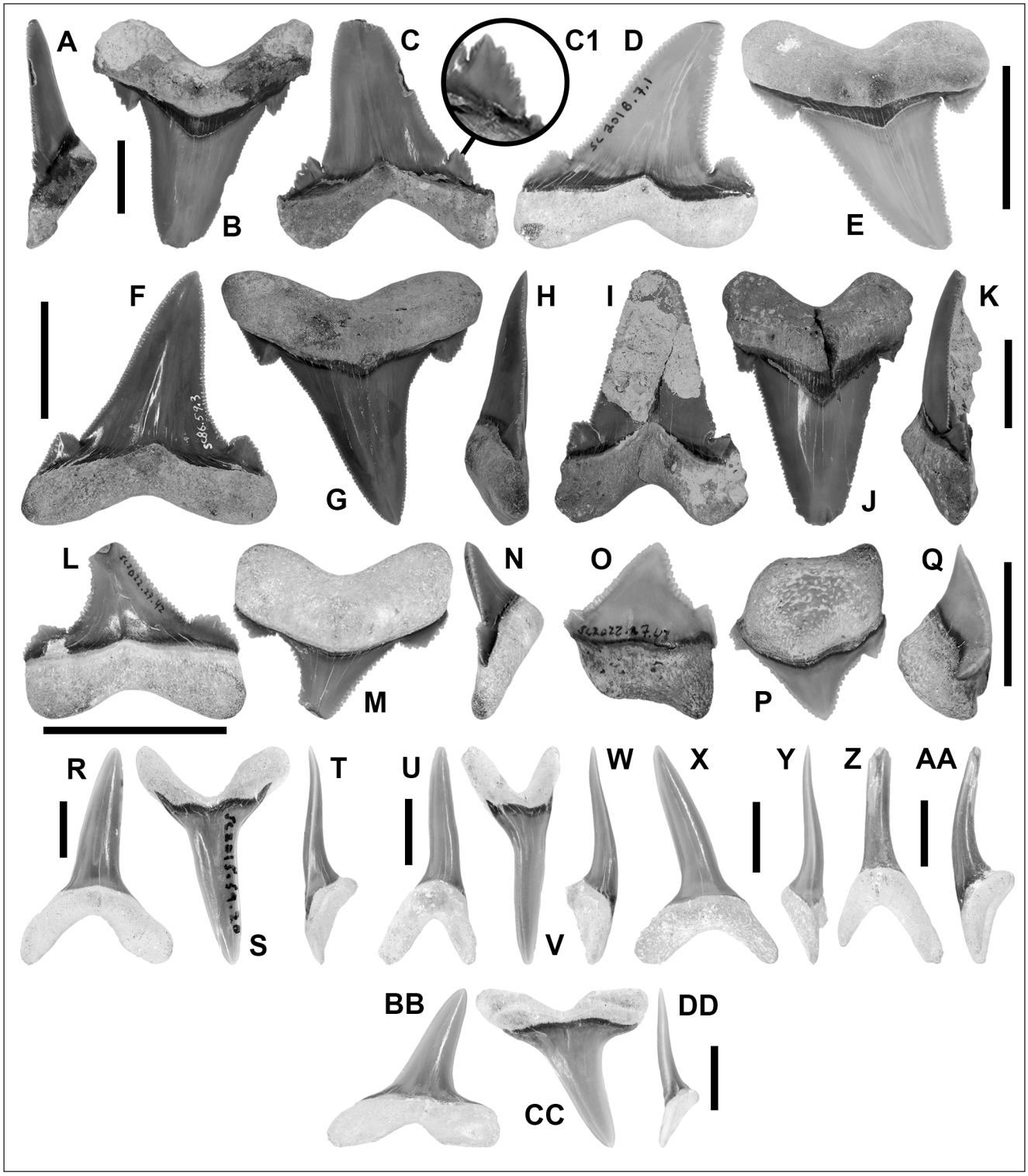

Fig. 6 - Lamniform sharks from the Tupelo Bay Formation. A-Q) *Otodus* (*Carcharocles*) *sokolowi*?, tooth (A-C), SC2018.7.152, in mesial (A), lingual (B), and labial (C) views; lateral tooth (D-E), SC2018.7.1, in labial (D), and lingual (E) views; lateral tooth, SC86.59.3 (F-H), in labial (F), lingual (G), and mesial (H) views; anterior tooth (I-K), SC2018.7.150, in labial (I), lingual (J), and mesial (K) views; postero-lateral tooth (L-N), SC2020.27.42, in labial (L), lingual (M), and mesial (N) views; posterior(?) tooth (O-Q), SC2022.27.43, in labial (O), lingual (P), and mesial (Q) views. R-DD) *Anomotodon novus,* lower right fourth anterior tooth (R-T), SC2015.59.20, in lingual (R), labial (S), and mesial (T) views; lower left third anterior tooth (U-W), SC2018.7.86, in lingual (U), labial (V), and mesial (W) views; upper third anterior tooth (X-Y), SC2018.7.88, in lingual (X), and mesial (Y) views; juvenile lower anterior tooth (Z-AA), SC2018.7.92, in lingual (Z), and mesial (AA) views; upper left lateral tooth (BB-DD), SC2022.27.90, in lingual (BB), labial (CC), and mesial (DD) views. Scale bars: 5 mm in R-DD, 1 cm in O-Q, 2 cm in A-L.

that it is very difficult to distinguish biological species based on the morphological variation of their teeth.

The various species and purported subspecies are recognized based largely on serration complexity, along with the narrowness of the main cusp apex and size and fusion of the cusplets to the main cusp (i.e., Zhelezko & Kozlov 1999: 154-155). Although the serration size of the Tupelo Bay Formation specimens appears to be smaller, the serration density is greater compared to teeth identified as *O.* (*C.*) *auriculatus* from the Lutetian of Kazakhstan (Zhelezko & Kozlov 1999) and Lede Sand of Belgium (NP15) (Herman et al. 2000; Van den Eeckhaut & De Schutter 2009) and similar to Lutetian material from Russia (Popov et al. 2025). Specimens from the "lower" Lisbon Formation (NP15) of Alabama (Ehret & Ebersole 2014; Ebersole et al. 2019) are comparable to those from the Lede Sand.

On the Tupelo Bay Formation teeth, serrations can be narrow and have closely spaced apices, broad-based with widely separated apices, or combinations of the two. This variation occurs not only among the eight teeth (compare Fig. 6G to 6M) but also between the mesial and distal sides of the same crown (i.e., Fig. 6C) and even along the same cutting edge (i.e., Fig. 6D). Although the apices of most of the Tupelo Bay Formation teeth are damaged, this area appears to be rather broad and the cutting edges convex (i.e., Fig. 6B & 6E), comparable to Zhelezko & Kozlov's (1999: 154-155) concept of *O.* (*C.*) *sokolowi*. However, one specimen has a narrower main cusp apex with less convex edges (i.e., Fig. 6 G), more in line with their *O.* (*C.*) *poseidoni*. The serration patterns and lateral cusplet morphology of the Tupelo Bay Formation specimens are more consistent with *O.* (*C.*) *sokolowi* as outlined by Zhelezko & Kozlov (1999), and we tentatively assign the South Carolina material to this species.

In addition to the occurrence in Kazakhstan (Zhelezko & Kozlov 1999), other global records attributed to *O.* (*C.*) *sokolowi* include Ukraine (Jaekel, 1895), Uzbekistan (Case et al. 1996; Malyshkina & Ward 2016), Jordan (Mustafa & Zalmout 2002), Europe (i.e., Trif et al. 2021; Popov et al. 2025), and northern Africa (i.e., Case & Cappetta 1990; Adnet et al. 2010; Underwood et al. 2011; Zalat et al. 2017; Zouhri et al. 2021). The species is an uncommon component of the Clinchfield Formation paleofauna of Georgia (Parmley & Cicimurri 2003), and of two Clinchfield Formation teeth we examined, one is a massive upper anterior tooth with diminutive lateral cusplets and serrations that are unevenly developed (SC2004.34.7). The serrae are generally well differentiated, although serration size varies from rather small to very large within the span of one centimeter of length, and the larger serrations are often incompletely subdivided into smaller serrations. However, the other specimen (SC2004.34.8) is an upper right lateral tooth with rather evenly and regularly serrated cutting edges, and the main cusp apex is rather wide and biconvex. The tooth is comparable to Tupelo Bay Formation teeth shown in Figure 6D–E and 6F–H, including the serration size and density on the lateral cusplets. The Clinchfield Formation teeth are perhaps slightly older than those from the Tupelo Bay Formation, but the morphologies appear to be conspecific.

Freile et al. (2001) reported *O.* (*C.*) *auriculatus* from Georgia, but they confusingly cited the stratigraphic provenience as the Riggins Mill Member of the Twiggs Clay Formation. However, the Riggins Mill Member is part of the Clinchfield Formation, and the Twiggs Clay Member is part of the superjacent Dry Branch Formation. Based on geographic provenience, the fossils in question were derived from the Clinchfield Formation, as this unit immediately underlies unfossiliferous sand of the Dry Branch Formation (DJC personal observation). Freile et al. (2001) identified an upper left lateral tooth (fig. 1 C) as *O.* (*C.*) *auriculatus* that was purportedly collected from the Santee Limestone of South Carolina. This tooth is comparable to SC2018.7.152 (Fig. 6A–C), and it is possible that the former specimen was collected from strata now recognized as the Tupelo Bay Formation (the geographic provenience of the fossil is unclear). Case (1981) identified specimens from the Ocala Limestone and Dry Branch Formation of Georgia as *O.* (*C.*) *auriculatus*, but the material was later identified as *O.* (*C.*) *sokolowi* by Cappetta & Case (1990). Cicimurri & Knight (2019) did not recover teeth of the subgenus from coastal sands of the Dry Branch Formation in South Carolina.

Teeth like those from the Tupelo Bay Formation were reported from the Yazoo Clay (Priabonian) of Alabama (Leriche 1942; Ehret & Ebersole 2014), Mississippi (Dockery & Manning 1986), and Louisiana (Manning & Standhardt 1986). Similar specimens have also been documented from the Moodys

Branch Formation (late Bartonian) of Alabama and Mississippi (Dockery & Manning 1986; Ebersole & Cicimurri 2025), and additional teeth were noted in the Gosport Sand (Bartonian) of Alabama (Ebersole et al. 2019). Unfortunately, these records are often based on relatively few, sometimes incompletely preserved specimens, and additional investigations into the units yielding the fossils are necessary to help elucidate the species they represent.

Family Mitsukurinidae Jordan, 1888
Genus *Anomotodon* Arambourg, 1952

Anomotodon novus (Winkler, 1874)
Fig. 5R–DD

Material: 31 teeth, including: SC2001.109.2, SC2015.59.20 (Fig. 6R–T), SC2015.59.21 (4 specimens), SC2015.59.22, SC2015.59.23, SC2015.59.24 (2 specimens), SC2018.7.5, SC2018.7.6, SC2018.7.85, SC2018.7.86 (Fig. 6U–W), SC2018.7.87, SC2018.7.88 (Fig. 6X–Y), SC2018.7.89, SC2018.7.90, SC2018.7.91, SC2018.7.92 (Fig. 6Z–AA), SC2018.7.93, SC2018.7.94, SC2018.7.95, SC2018.7.96, SC2022.27.90 (Fig. 6BB–DD), SC2022.27.91, SC2022.27.92, SC2022.27.93, SC2022.27.94, SC2022.27.95, SC2022.27.96.

Description. Teeth are variable in shape, but all generally consist of a triangular crown and root. The crown ranges from very narrow and tall to broadly triangular, with development of lateral shoulders that extend onto the root lobes. The cutting edges are smooth and continuous across the main cusp, and they extend basally onto the lateral shoulders. The lingual face is moderately to strongly convex and ranges from smooth to ornamented with fine vertical ridges. In contrast, the labial face varies from smooth and flat to weakly convex. The root is bilobate, with lobes ranging from narrow and elongated to short and sub-rectangular. The lobes are separated by a V-shaped or U-shaped interlobe area, and there is a distinctive lingual nutritive groove.

Remarks. This goblin shark species exhibits monognathic heterodonty, with anterior teeth having a relatively narrow and sinuous main cusp (i.e., Fig. 6R–S), and lateral teeth a broader, flatter main cusp with elongated lateral shoulders (Fig. 6BB–DD). The anterior teeth have elongated and rather narrowly spaced root lobes (i.e., Fig. 6–V), whereas lateral teeth have shorter, somewhat rectangular, and strongly diverging lobes (Fig. 6CC). Additionally, the cusp inclination increases but overall height decreases towards the commissure. Dignathic heterodonty appears to be expressed in the form of distally inclined upper lateral teeth but rather erect lower lateral teeth. Additionally, upper anterior teeth have shorter but more diverging lobes compared to lower anterior teeth (compare Fig. 6R to 6U). Ontogenetic heterodonty appears to be expressed as a difference in overall tooth size and robustness within tooth files, as juvenile teeth are essentially smaller and more gracile versions of adult teeth (compare Fig. 6Z–AA to 6U–W). Specimen SC2001.109.2 was recovered from matrix surrounding a partial rostrum of *Pristis* sp. (SC2001.109.1).

Anomotodon novus is easily separated from all the other lamniform sharks in our sample by the combination of their gracile morphology, lack of serrated cutting edges and lateral cusplets, and presence of lingual crown ornamentation. *Anomotodon novus* differs from the Eocene *A. sheppeyensis* Casier, 1966 by its larger overall size, with the largest (upper) anterior tooth in our sample measuring over 2.5 cm in height. In addition, the crown ornamentation on the Tupelo Bay Formation specimens is very faint or lacking altogether and the root lobe extremities of lateral teeth are pointed. In contrast, the lobe extremities on *A. sheppeyensis* appear to be more rounded (Casier 1966; Cappetta 1976). Another Eocene taxon, *A. mulitidenticulatus* Long, 1992, exhibits conspicuous lateral cusplets, whereas the heels of *A. novus* lack these structures. It is possible that *A. sheppeyensis* and *A. novus* temporally overlapped, as the former was identified in the lower-to-middle Eocene of Denmark (Carlsen & Cuny 2014) and the latter in the middle Eocene of Belgium (Van den Eekhaut & DeSchutter 2009). Rodriguez et al. (2023) recently reported *A. novus* in upper Paleocene (Thanetian) deposits of Chile. Incomplete teeth from the Bartonian Gosport Sand of Alabama may represent *A. novus* (Ebersole et al. 2019).

Genus *Striatolamia* Glickman, 1964

Striatolamia macrota (Agassiz, 1843)
Fig. 7A–Q

1843 *Otodus macrotus* – Agassiz, p. 273, pls. 27–28.
1956 *Odontaspis macrota* – White, p. 147–148.
1968 *Striatolamia macrota* – Applegate, p. 32–36, pls. 1–3.

Material: 22 teeth, including: SC2015.59.15, SC2015.59.16 (2 specimens), SC2015.59.17 (Fig. 7A–B), SC2015.59.41, SC2015.59.42, SC2018.7.4, SC2018.7.75, SC2018.7.76, SC2018.7.78,

SC2018.7.148, SC2018.7.149, SC2022.27.97, SC2022.27.98 (Fig. 7C–E), SC2022.27.99 (Fig. 7F–H), SC2022.27.100, SC2022.27.101, SC2022.27.102, SC2022.27.103 (Fig. 7L–N), SC2022.27.104 (Fig. 7I–K), SC2022.27.105, SC2022.27.106 (Fig. 7O–Q).

Description. The largest anterior tooth in our sample reaches 5.5 cm in total height. Anterior teeth have a tall and very narrow main cusp that is erect to slightly distally curving. The labial face is smooth and rather flat, whereas the lingual face is very convex and ornamented with longitudinal ridges of varying robustness. These ridges can extend to three-fourths of the crown height. The cutting edges are smooth and sub-parallel and usually do not reach the base of the main cusp. Lateral cusplets may not be present, but generally there is a single diminutive pair that are sub-conical, diverging, and separated from the main cusp by an expanse of dentine. Distal lateral teeth have a larger pair of lateral cusplets with smooth cutting edges and bi-convex faces that are separated from the main cusp by a deep notch. The cusplets may be of equal size, but the distal cusplet is often larger than the mesial one. The bilobate root exhibits elongated and divergent lobes, with the mesial lobe being narrower and more elongated than the distal lobe. The interlobe area can be V-shaped or U-shaped, and a large lingual boss is bisected by a conspicuous nutritive groove.

Lateral teeth have a shorter, broader, and labio-lingually thinner main cusp compared to anterior teeth. Lingual ornamentation is also less robust. The crown may be erect or distally inclined, and the smooth cutting edges extend to the base of the lateral cusplets. The single pair of cusplets is separated from the main cusp by a deep notch. The cusplets are generally biconvex and have smooth cutting edges, and the distal cusplet is often larger than the mesial cusplet. Both cusplets are broader, lower, and less pointed than those on anterior teeth. The bilobate root has rather short, highly diverging, subrectangular lobes with rounded or pointed extremities. The interlobe area is shallow and V-shaped or U-shaped, and the lingual nutritive groove is narrow and elongated.

Remarks. *Striatolamia* exhibits monognathic and dignathic heterodonty, with the upper and lower dentitions bearing anterior and lateral tooth files. Anterior teeth are tall and narrow with incomplete cutting edges (i.e., Fig. 7I–K) and robust lingual ornamentation (Fig. 7M). A single pair of diminutive lateral cusplets is generally present but they may be lacking altogether (compare Fig. 7R to 7L). Additionally, the root lobes are narrow, elongated, and separated by a narrow interlobe area (i.e., Fig. 7J & 7M). In contrast, lateral teeth are broader (mesio-distally), flatter (labio-lingually), have reduced ornamentation, a single pair of large lateral cusplets, and shorter sub-rectangular root lobes that are highly diverging (Fig. 7F–G). Additionally, the cusp size decreases towards the commissure. The upper anterior teeth have shorter and more widely separated lobes compared to lower anterior teeth (compare Fig. 7C & 7P to 7J). The upper lateral teeth are distally inclined (Fig. 7F–G), whereas lower lateral teeth are more vertical. Upper lateral teeth become more distally inclined to curved towards the commissure. Ontogenetic heterodonty is also apparent, as smaller teeth from the various jaw positions are more gracile than their larger, presumably adult counterparts, and smaller anterior teeth often lack lateral cusplets (compare Fig. 7I–K and 7L–N).

Cunningham (2000) reconstructed the dentition of *Striatolamia macrota* based on that of the extant *Carcharias taurus* Rafinesque, 1810 and subsequently assigned *Striatolamia* to Odontaspididae. Prior to this work, Siverson (1995) hesitantly placed the genus into Mitsukurinidae, a ranking that was followed by Cappetta & Nolf (2005) and Ebersole et al. (2019) based on the apparent absence of intermediate tooth files. However, Malyshkina (2021) described a new species, *Striatolamia tchelkarnurensis*, and placed the genus in Carchariidae following Adolfssen & Ward (2013), who supported Cunningham's (2000) reconstructed dental similarity to *C. taurus* Rafinesque, 1810 (Carchariidae *sensu* Stone & Shimada, 2019). Malyshkina's (2021) reconstructed dentition for S. *tchelkarnurensis* is based on a partial associated dentition, which unfortunately does not preserve the tooth morphologies that would support her taxonomic assignment. Although the dentition of both *Mitsukurina* and *Carcharias taurus* possess three upper and four lower anterior files, a distinctive (upper) intermediate file is absent in the former (Mitsukurinidae) and usually present in the latter (Carchariidae). Ebersole et al. (2019) reported a sample of more than 2,100 *S. macrota* teeth from Alabama that did not include intermediate teeth. Additionally, other shark taxa possibly having intermediate teeth occur in the same deposit from which Cunningham's (2000) sample was obtained, and it is

possible that the teeth he included represent non-*Striatolamia* taxa. For the purposes of this report, we continue to place *Striatolamia* within Mitsukurinidae.

The species *Striatolamia tchelkarnurensis* is based on large teeth from the late Bartonian or early Priabonian (Late Eocene) of Kazakhstan. Although anterior teeth are like those from the Tupelo Bay Formation, the lateral teeth of S. *tchelkarnurensis* differ by having a much larger and often triangular distal cusplet, and there is a second, diminutive cusplet. *Striatolamia* teeth are easily distinguished from those of other large lamniform sharks in our Tupelo Bay Formation sample by their lack of serrated cutting edges, single pair of lateral cusplets (the distal one being larger than the mesial one), and conspicuous labial ornamentation (particularly on anterior teeth).

Kozlov (2001) named *Turania* based on specimens from the middle Eocene of Kazakhstan, but Cappetta (2012) questioned the validity of the taxon. If considered valid, teeth of *Turania* are comparable in size to those of juvenile *Striatolamia*, but they differ by having finer lingual crown ornamentation, larger lateral cusplets on anterior teeth, and lateral cusplets on lateral teeth are narrow and pointed.

Striatolamia macrota was globally widespread and has been reported from locations in Belgium (Van den Eeckhaut & De Schutter 2009), Romania (Trif et al. 2021), Antarctica (Welton & Zinsmeister 1980), Australia (Pledge 1967), Russia (i.e., Popov et al. 2025) and the USA. It is particularly abundant in the Lisbon Formation (NP15-16) and Gosport Sand (NP17) of Alabama (Ebersole et al. 2019) and occurs in the Cane River Formation (NP16), Cook Mountain Formation (NP17), and Yazoo Clay (NP17-NP21) of Louisiana (Ebersole & Cicimurri 2025). The taxon is poorly known from middle-to-upper Eocene deposits of Georgia, where it is apparently rare in the Clinchfield Formation (Parmley & Cicimurri 2003).

Family Odontaspididae Müller & Henle, 1839
Genus *Brachycarcharias* Cappetta & Nolf, 2005

Brachycarcharias twiggsensis (Case, 1981)

Fig. 7R–Z

1981 *Lamna twiggsensis* – Case, p. 58-59, pl. 3, figs. 4–8.
1990 *Cretolamna twiggsensis* (Case, 1981) – Case & Cappetta, p. 9–10, pl. 3, figs. 40–55.
2003 *Carcharias* aff. *koerti* (Stromer, 1910) – Parmley & Cicimurri, p. 162, fig. 3 G.
2011 *Brachycarcharias* aff. *twiggsensis* (Case, 1981) – Underwood et al., p. 52, fig. 4 K–M.
2019 *B. twiggsensis* (Case, 1981) – Ebersole et al., p. 43–45, fig. 14.
2016 *Tethylamna twiggsensis* (Case, 1981) – Cappetta & Case, p. 51.
2025 *T. twiggsensis* – Abd-Elhameed & Abd-Elhameed, p. 25.

Material: 13 teeth, including: SC2018.7.21, SC2018.7.23, SC2018.7.78, SC2022.27.67 (Fig. 7X–Z), SC2022.27.68 (Fig. 7R–T), SC2022.27.69, SC2022.27.70, SC2022.27.71, SC2022.27.72, SC2022.27.73 (Fig. 7U–W), SC2022.27.74, SC2022.27.75, SC2022.27.76.

Description. The teeth reach up to 3 cm in total height and consist of a massive crown and robust root. The triangular crown is variable and can be narrow but labio-lingually thick or broad-based but labio-lingually thin. The labial crown face is flat but the lingual crown face ranges from moderately to strongly convex. The crown enameloid is smooth. The crown is flanked by one or two pairs of lateral cusplets that are well-separated from the main cusp. Cusplets may be tall, narrow, sharply pointed, and medially curved, or broad-based and triangular. Many teeth exhibit a second pair of diminutive cusplets. The root is narrow and bilobate, but the elongated lobes vary in length and degree of divergence. There is a robust lingual boss that is bisected by a narrow nutritive groove.

Remarks. Monognathic heterodonty is evident in our sample. Anterior teeth have a somewhat narrow but thick crown that is flanked by a single pair of needle-like lateral cusplets (Fig. 7U–W), whereas lateral teeth have a broader crown, two pairs of broadly triangular lateral cusplets, and more divergent root lobes (Fig. 7X–Z). The crown height of lateral teeth decreases but cusp inclination increases towards the commissure. With respect to dignathic heterodonty, upper anterior teeth have shorter but wider root lobes, and upper lateral teeth are distally inclined compared to specimens from lower lateral files. Specimen SC2022.27.73 (Fig. 7U–W) is believed to be a lower right second anterior tooth due to the medially curved lateral cusplets and rather elongated root lobes of equal length, features we observed on *C. taurus* teeth in this jaw position. Specimen SC2022.27.67 has long but relatively narrow root lobes and a U-shaped interlobe area, and the main cusp is rather narrow and erect (although it is apically recurved), features consistent with lower lateral teeth of *C. taurus*. Specimen SC2022.27.68 (Fig. 7R–T) is unusual in that it has a very broad-based and erect crown and sub-rectangular root lobes with elongated extremities. As there are two

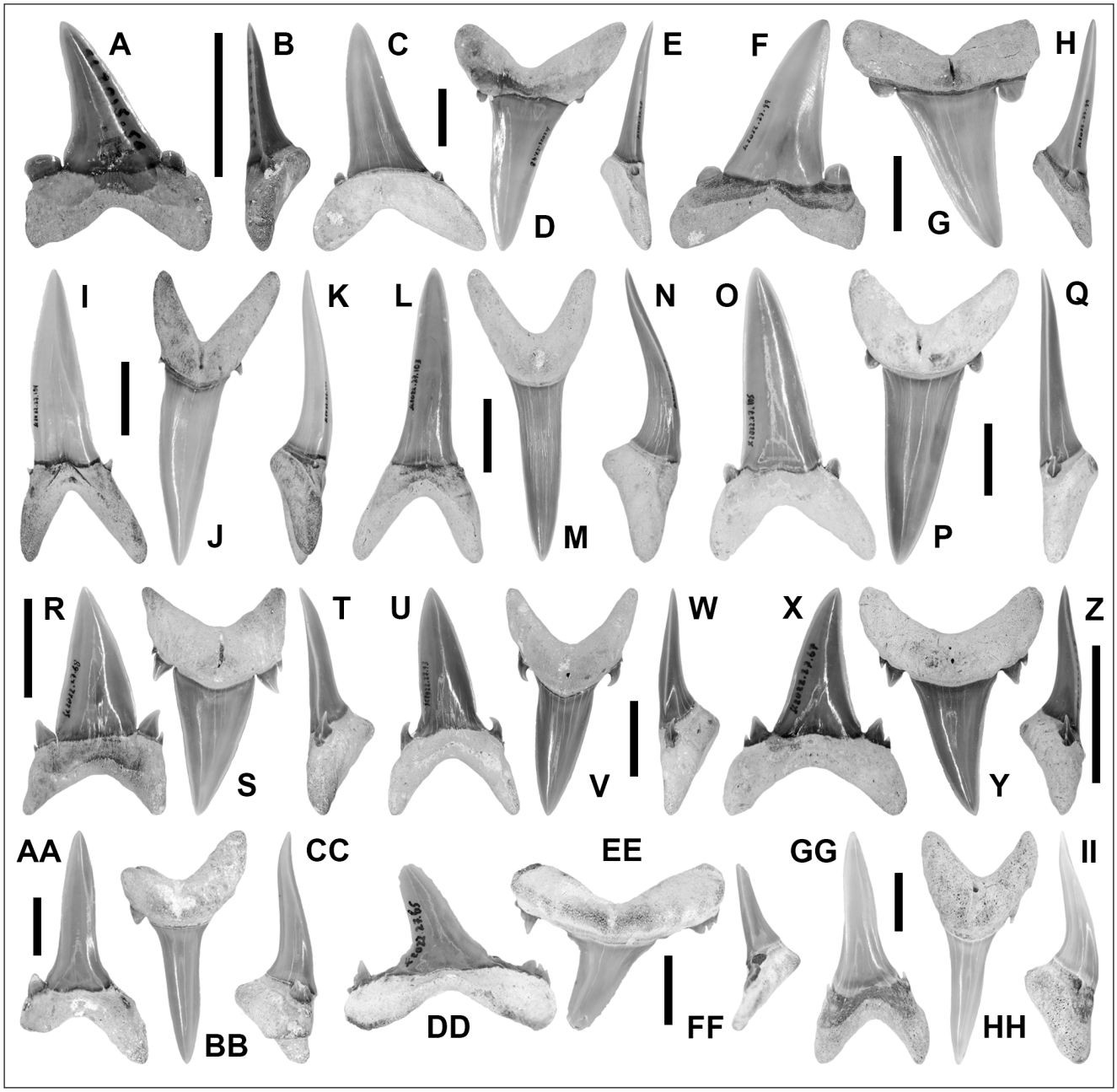

Fig. 7 - Lamniform sharks from the Tupelo Bay Formation. A-Q) *Striatolamia macrota*, juvenile upper left lateral tooth (A-B), SC2015.59.17, in labial (A), and mesial (B) views; upper left third anterior tooth (C-E), SC2022.27.98, in lingual (C), labial (D), and mesial (E) views; upper right lateral tooth (F-H), SC2022.27.99, in labial (F), lingual (G), and mesial (H) views; lower right anterior tooth (I-K), SC2022.27.104, in labial (I), lingual (J), and distal (K) views; juvenile lower left anterior tooth (L-N), SC2022.27.103, in labial (L), lingual (M), and mesial (N) views; upper left second anterior tooth (O-Q), SC2022.27.105, in labial (O), lingual (P), and mesial (Q) views. R-Z) *Brachycarcharias twiggsensis*, tooth (R-T), SC2022.27.68, in labial (R), lingual (S), and mesial (T) views; lower anterior tooth (U-W), SC2022.27.73, in labial (U), lingual (V), and mesial (W) views; upper right lateral tooth (X-Z), SC2022.27.67, in labial (X), lingual (Y), and mesial (Z) views. AA-II) Carchariidae, anterior tooth (AA-CC), SC2022.27.63, in labial (AA), lingual (BB), and mesial (CC) views; upper left lateral tooth (DD-FF), SC2022.27.65, in labial (DD), lingual (EE), and mesial (FF) views; anterior tooth (GG-II), SC2022.27.64, in labial (GG), lingual (HH), and mesial (II) views. Scale bar: 5 mm in AA-CC & GG-II, 1 cm in A-Z & DD-FF.

pairs of lateral cusplets, the main cusp is slightly distally inclined, and root lobes are pointed, it likely represents a lateral position, perhaps one that was located closer to the symphysis. The very large size of this tooth could also reflect an adult ontogenetic stage.

These teeth can be differentiated from those of other Tupelo Bay Formation lamnoid sharks by having a broad and robust main cusp (in all tooth positions), smooth labial and lingual crown faces, and one (anterior teeth) or two (lateral teeth) pairs of sharply pointed lateral cusplets. These features

contrast with the narrow, ornamented teeth of *Anomotodon*, which lack lateral cusplets. Additionally, the cutting edges of *Otodus* (*Carcharocles*) teeth are coarsely serrated. *Alopias* teeth are much smaller and lack lateral cusplets. *Striatolamia* teeth bear conspicuous lingual ornamentation and have smaller lateral cusplets compared to *B. twiggsensis*.

The generic assignment of the taxon has changed several times since it was originally named, first as *Lamna twiggsensis* Case, 1981, then as *Cretalamna twiggsensis* by Cappetta & Case (1990), and later tentatively as *Brachycarcharias twiggsensis* by Underwood et al. (2011). This latter assignment was likely proposed due to the close dental similarity to the type species of *Brachycarcharias* Cappetta & Nolf, 2005, *B. lerichei* (Casier, 1946). Cappetta & Case (2016) more recently placed this morphology into their new genus, *Tethylamna*, an assignment refuted by Ebersole et al. (2019) but supported by Abd-Elhameed & Abd-Elhameed (2025).

Abd-Elhameed & Abd-Elhameed (2025) utilized quantitative analyses to differentiate between three species that have been assigned to *Brachycharcharias*, including *B. atlasi* (Arambourg, 1952), *B. lerichei* (Casier, 1946), and *B. twiggsensis*. Abd-Elhameed & Abd-Elhameed (2025) concluded that the *Brachcarcharias twiggsensis* morphology is distinct from that of *B. atlasi* and *B. lerichei* based on larger overall tooth size and greater breadth. These authors further stated that the features distinguishing this morphology as a species also justified its inclusion in *Tethylamna*.

Ebersole et al. (2019) refuted assigning the *twiggsensis* morphology to *Tethylamna* based on their observations of teeth of the type species, *T. dunni* Cappetta & Case, 2016. These authors noted that, although *T. dunni* teeth have one or two pairs of lateral cusplets, the primary mesial and distal lateral cusplet are usually both distally directed. This feature was noted by Cappetta & Case (2016) and contrasts with the cusplet orientation of the *B. twiggsensis* morphology, which Case (1981) stated was "flaring out in opposite directions from the tooth blade" (p. 59). Furthermore, Ebersole et al. (2019) found that the distal primary cusplet of *T. dunni* lateral teeth is often conspicuously larger than the mesial one, a condition we also observed on *Striatolamia macrota* lateral teeth (see Fig. 7A & 7G). In contrast, the diverging primary lateral cusplets on the *B. twiggsensis* teeth do not appreciably differ in size. Of note is the nature of the lateral cusplets on some *B. lerichei* teeth identified by Cappetta and Nolf (2005: pl. 2), on which cusplets of both sides are distally directed (although they are roughly equal in size). One could therefore argue that the *B. lerichei* morphology be placed in *Tethylamna*, but Cappetta & Case (2016) indicated that the only other distinguishing feature of *Tethylamna* is the lack of crown ornamentation, which may or may not occur on teeth of *B. lerichei*. It is our experience that the presence or absence of ornamentation is variable among species (intraspecific) and within the dentition of a species (interspecific), and this phenomenon may not be taxonomically relevant. We maintain the *twiggsensis* morphology within *Brachycarcharias* following Ebersole et al. (2019), and the taxon is placed within Odontaspididae due to the occurrence of two cusplet pairs on lateral teeth.

Brachycarcharias twiggsensis occurs within the entirety of the NP18 portion of the Tupelo Bay Formation with specimens having been recovered from the deepest portions of the excavations to just below the overlying Parkers Ferry Formation (Priabonian, NP19/20). Preliminary investigation of post-Tupelo Bay Formation deposits at Giant Portland Cement and Argos (by DJC) revealed that the species also occurs in the Parkers Ferry Formation and erosional remnants that have been attributed to the Harleyville Formation (NP21; see Weems et al. 2016). Additional Atlantic Coastal Plain records include the Clinchfield Formation (Bartonian) and Dry Branch Formation (Priabonian) of Georgia (Case 1981; Case & Borodin 2000a; Parmley & Cicimurri 2003). Within the Gulf Coastal Plain, Ebersole et al. (2019) documented the taxon in the Gosport Sand (Bartonian) of Alabama and Ebersole & Cicimurri (2025) identified the species in the Moodys Branch Formation of Louisiana.

Interestingly, teeth that Case & Cappetta (1990) reported from the Qasr el-Sagha Formation (Priabonian) of Egypt conform to the *B. twiggsensis* morphology, all of which have diverging cusplets of equal size. At least one specimen that Underwood et al. (2011) tentatively referred to *B. twiggsensis* from Qasr el-Sagha Formation has both lateral cusplets distally directed, and the distal one is significantly larger (i.e., fig. 4K). Zouhri et al. (2021) identified *Tethylamna twiggsensis* from the Eocene of Morocco, including teeth that have both cusplets inclined distally and the distal cusplet larger than the mesial one

(i.e., fig. 3C-D). Although *Tethylamna* appears to occur in the Tethyan region, previous species attributions should be reevaluated.

Family Carchariidae Müller & Henle, 1838
gen. et sp. indet.
Fig. 7AA–II

Material: 5 teeth, including: SC2018.7.97, SC2022.27.63 (Fig. 7AA–CC), SC2022.27.64 (Fig. 7GG–II), SC2022.27.65 (Fig. 7DD–FF), SC2022.27.66.

Description. The teeth measure up to 2 cm in apico-basal height and slightly more than 2 mm in mesio-distal width. The teeth vary in shape, with some specimens having a very narrow main cusp that is flanked by a single pair of small to moderately sized lateral cusplets. The labial face of the main cusp is rather flat, but the lingual face is very convex, and the enameloid is smooth. The mesial and distal cutting edges are smooth and sub-parallel, and they do not reach the crown foot. The cusplets are located close to the main cusp but separated by a deep notch. The root is bilobate with short, narrow, slightly diverging lobes that are separated by a U-shaped interlobe area. A robust lingual boss bears a conspicuous nutritive groove.

One large tooth has a broad-based main cusp that is distally inclined and quickly narrows apically. The labial face is flat, but the lingual face is moderately convex and the enameloid is smooth. The cutting edge is smooth and continuous across the main cusp, but it is damaged apically and at the crown foot of both sides. One tall and sharply pointed lateral cusplet is preserved distally, but three cusplets occur mesially. The bilobate root exhibits rather short, sub-rectangular, highly diverging lobes separated by a somewhat V-shaped interlobe area. The mesial lobe is slightly more elongated and pointed at its extremity compared to the mesial lobe. There is a conspicuous lingual nutritive groove.

Remarks. Examination of extant *C. taurus* dentitions (SC86.62.2 and SC2000.120.6) indicates that anterior and lateral tooth files are represented in the Tupelo Bay Formation sample. Anterior teeth, like SC2022.27.63 and SC2022.27.64 have a very narrow, erect crown with a sinuous profile, and the cutting edges do not reach the base of the main cusp. Specimen SC2022.27.63 (Fig. 7AA–CC) is a lower anterior tooth based on its sinuous crown profile and flat labial crown foot, whereas SC2022.267.64 (Fig. 7GG–II) is an upper anterior tooth due to its straighter profile and convex labial face. An upper lateral tooth (Fig. 7DD–FF) has a wider and distally inclined main cusp, and more lateral cusplets compared to anterior teeth.

The five specimens available are easily differentiated from *Striatolamia macrota* (see above) by having smooth lingual crown enameloid. They also differ from *Brachycarcharias twiggsensis* (see above) by having teeth that are smaller in overall size and narrower main cusps, and the lateral cusplets are comparatively smaller. A less bulky root with nutritive groove separates these teeth from *Isurolamna* (see below). Our small sample size is not morphologically diverse enough to allow us to ascertain if the taxon represents a species of *Carcharias* or *Mennerotodus,* the latter genus having been reported from the middle Eocene Clinchfield Formation of Georgia, the Moodys Branch Formation of Arkansas and Louisiana, and Gosport Sand of Alabama (Cicimurri et al. 2020; Ebersole & Cicimurri 2025).

Family Lamnidae Müller & Henle, 1838
Genus *Macrorhizodus* Glickman, 1964

Macrorhizodus praecursor (Leriche, 1905)
Fig. 8A–U

1905 *Oxyrhina desori praecursor* – Leriche, p. 128.
1942 *O. praecursor americana* – Leriche, p. 45.
1976 *Macrorhizodus praecursor* (Leriche, 1905) – Zarkov et al., p. 132
1981 *Isurus oxyrhynchus* Rafinesque, 1810 – Case, p. 8–9, pl. 2, figs. 3–5.
2000a *I. praecursor* (Leriche, 1905) – Case & Borodin, p. 8, pl. 1, figs. 8–10.
2000b *I. praecursor* (Leriche, 1905) – Case & Borodin, p. 26, pl. 3, figs. 21–26.
2003 *I. praecursor* (Leriche, 1905) – Parmley & Cicimurri, p. 165, fig. 4 A–B.
2002 *Cosmopolitodus praecursor* (Leriche, 1905) – Mustafa & Zalmout, p. 82.
2019 *M. praecursor* (Leriche, 1905) – Ebersole et al., p. 56–58, fig. 20.

Material: 21 teeth, including: SC2015.59.18 (2 specimens), SC2015.59.19, SC2018.7.2, SC2018.7.3, SC2018.7.80, SC2018.7.81, SC2018.7.82, SC2018.7.83, SC2018.7.84 (2 specimens), SC2022.27.44 (Fig. 8A–C), SC2022.27.45 (Fig. 8D–F), SC2022.27.46 (Fig. 8J–L), SC2022.27.47 (Fig. 8G–I), SC2022.27.48 (Fig. 8P–R), SC2022.27.49, SC2022.27.50 (Fig. 8M–O), SC2022.27.51, SC2022.27.52, SC2022.27.53 (Fig. 8S–U).

Description. The teeth are large and attain sizes greater than 4 cm in apico-basal height. The crown is triangular and may be mesio-distally narrow or broad-based, depending on jaw location. Teeth with narrow crowns are labio-lingually thick, but

broad-based specimens are labio-lingually narrow. The cutting edges are sharp, smooth, and continuous across the crown. The labial crown face is flat, whereas the lingual face is moderately to strongly convex. The crown enameloid is smooth. The root is bilobate, with the lobes ranging in morphology from narrow, elongated and moderately diverging, to being very short, sub-rectangular and highly diverging. The interlobe area can be U-shaped or V-shaped. There is no lingual nutritive groove, but there are one or more medially located foramina on a low root boss.

Remarks. The morphological variation we observed in the Tupelo Bay Formation sample is attributed, at least in part, to monognathic heterodonty. Teeth from anterior files are relatively narrow (mesio-distally) and labio-lingually thick with elongated root lobes (i.e., Fig. 8A–C), whereas those from lateral files have a broader and labio-lingually thinner crown with elongated lateral shoulders, and root lobes are short and sub-rectangular (i.e., Fig. 8P–R). Within lateral files, the crown height decreases and cusp inclination increases towards the commissure (compare Fig. 8Q to 8T). Dignathic heterodonty is evident in anterior files, where upper teeth are broader and have shorter lobes compared to lower anteriors (compare Fig. 8H to 8B). Within lateral files, upper teeth are more distally inclined compared to their more vertical lower counterparts. The same patterns are evident in the jaws of extant *Isurus oxyrynchus* Rafinesque, 1810 (SC202.53.11 and MSC 42606) and *I. paucus* Guitart, 1966 (SC2020.53.27) that we examined. Furthermore, SC 2022.27.47 is an upper right first anterior tooth (Fig. 8J–L), whereas SC2022.27.46 is an upper left second anterior (Fig. 8G–I). The roughly equal crown height to root height ratio indicates that SC2022.27.53 is from a more posterior file (Fig. 8S–T). Based on the jaws of a juvenile *I. oxyrynchus* (SC86.186.2), ontogenetic heterodonty is also evident in the Tupelo Bay Formation sample, but small teeth (juvenile) are essentially smaller and more gracile versions of their presumed adult counterparts (compare Fig. 8A–C to 8D–F).

Macrorhizodus teeth are characterized by their large size and robust stature, smooth cutting edges, lack of lateral cusplets and crown ornamentation, and lack of a nutritive groove on the lingual root face. These features serve to separate this taxon from other lamnoid sharks occurring in the Tupelo Bay Formation. Leriche (1942) named the subspecies *I. praecursor americana* based on an unknown number of specimens that were apparently recovered from the Yazoo Clay (Priabonian) of Alabama and Ashley Formation (Oligocene, Rupelian) of South Carolina. The specimens he illustrated (pl. 3, figs. 6–13) are comparable to *M. praecursor* and in our opinion the minor differences Leriche (1942) noted among the mixed sample do not warrant recognition of a subspecies.

Teeth of *M. praecursor* occur in the Lutetian of North Carolina (Case & Borodin 2000b), the Bartonian to Priabonian of Georgia (Case 1981; Case & Borodin 2000a; Parmley & Cicimurri 2003), and middle-to-late Eocene of Alabama (Leriche 1942; Ebersole et al. 2019), and Louisiana (Manning & Standhardt 1986; McPherson & Manning 1986; Ebersole & Cicimurri 2025). The species has also been reported in numerous middle-to-upper Eocene deposits from widely separated geographic localities, as for example Belgium (Leriche 1905; Van den Eeckhaut & De Schutter 2009), Romania (Trif et al. 2019), Ukraine (Kovalchuk et al. 2023), Russia (Popov et al. 2025), Egypt (Case & Cappetta 1990; Underwood et al. 2011; Zalat et al. 2017), and Morocco (Adnet et al. 2010).

Genus *Isurolamna* Cappetta, 1976

Isurolamna inflata (Leriche, 1905)

Fig. 8V–JJ

Material: 9 teeth, including: SC2022.27.54 (Fig. 8EE–GG), SC2022.27.55 (Fig. 8V–X), SC2022.27.56 (Fig. 8HH–JJ), SC2022.27.57, SC2022.27.58, SC2022.27.59, SC2022.27.60 (Fig. 8BB–DD), SC2022.27.61, SC2022.27.62 (Fig. 8Y–AA).

Description. These moderately large teeth measure up to 2 cm in apico-basal height. The crown includes a triangular main cusp that is usually flanked by a single pair of lateral cusplets. The cusplets vary in size from diminutive to large with respect to main cusp height. In lingual view, the cusplets appear to be well separated from the main cusp, but in labial view the cusplets are united only to the base of the main cusp. One specimen exhibits two pairs of lateral cusplets, with the second and more distal pair being smaller than the primary medial pair. The labial face of the main cusp is flat, whereas the lingual face is convex to varying degrees, and the enameloid is smooth. In profile view,

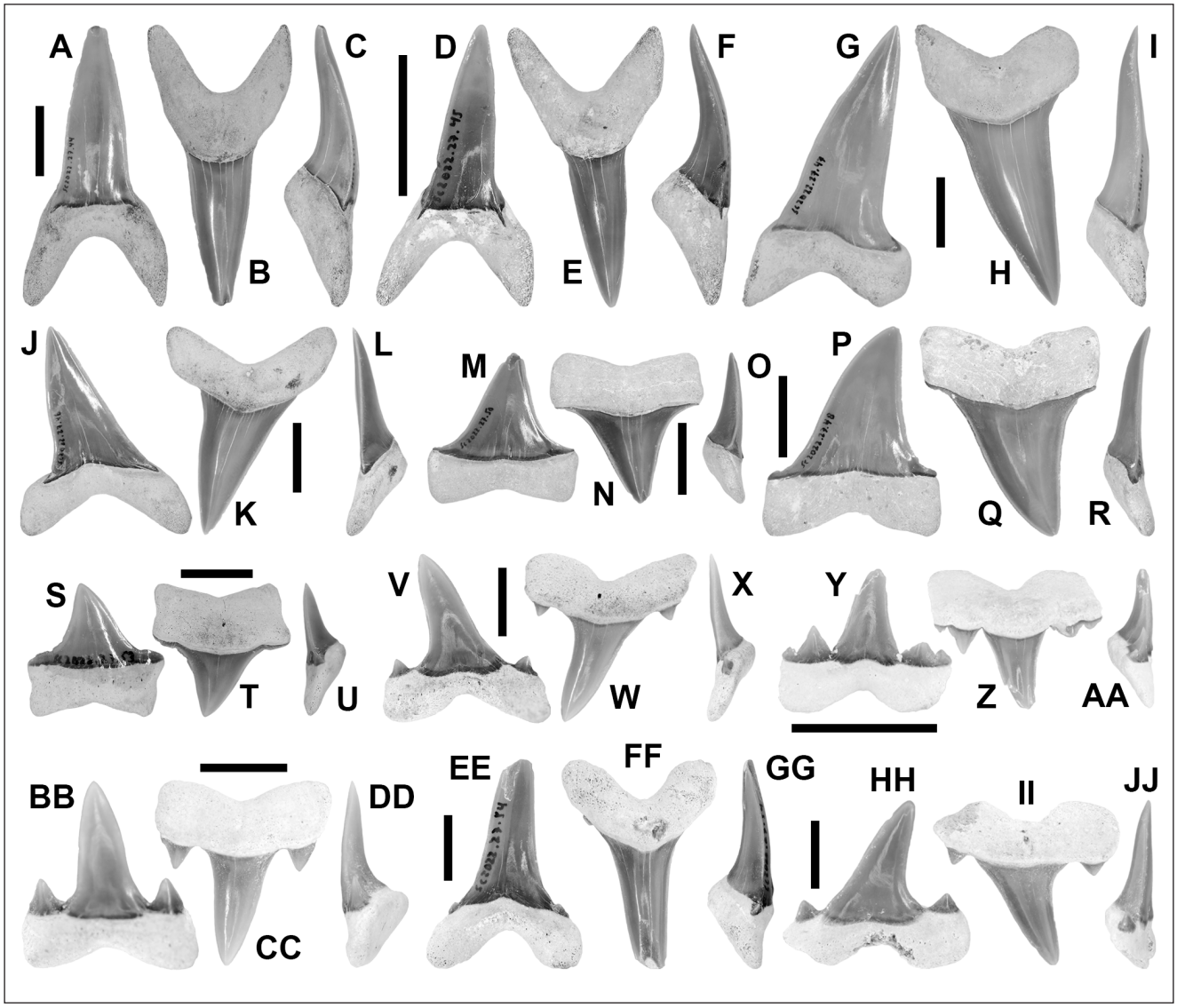

Fig. 8 - Lamniform sharks from the Tupelo Bay Formation. A-U) *Macrorhizodus praecursor*, lower anterior tooth (A-C), SC2022.27.44, in labial (A), lingual (B), and mesial (C) views; juvenile lower anterior tooth (D-F), SC2022.27.45, in labial (D), lingual (E), and mesial (F) views; adult upper right second anterior tooth (G-I), SC2022.27.47, in labial (G), lingual (H), and mesial (I) views; juvenile upper left first anterior tooth (J-L), SC2022.27.46, in labial (J), lingual (K), and mesial (L) views; lower left lateral tooth M-O, SC2022.27.50, in labial (M), lingual (N), and mesial (O) views; upper right lateral tooth (P-R), SC2022.27.48, in labial (P), lingual (Q), and mesial (R) views; posterolateral tooth (S-U), SC2022.27.53, in labial (S), lingual (T), and mesial (U) views. V-JJ) *Isurolamna inflata*, upper left lateral tooth (V-X), SC2022.27.55, in labial (V), lingual (W), and mesial (X) views; lower posterolateral tooth (Y-AA), SC2022.27.62, in labial (Y), lingual (Z), and mesial (AA) views; lower right lateral tooth (BB-DD), SC2022.27.60, in labial (BB), lingual (CC), and mesial (DD) views; anterior tooth (EE-GG), SC2022.27.54, in labial (EE), lingual (FF), and mesial (GG) views; upper right lateral tooth (HH-JJ), SC2022.27.56, in labial (HH), lingual (II), and mesial (JJ) views. Scale bars: 1 cm.

the crown is rather flat, and the smooth cutting edge is continuous along the main cusp. The lateral cusplets also bear smooth cutting edges and have smooth enameloid. The root is bilobate, with the lobes being rather short and widely diverging, and the extremities are rounded to somewhat pointed. A lingual boss bears at least one nutritive foramen. The interlobe area is broadly V-shaped or U-shaped.

Remarks. The Tupelo Bay Formation *Isurolamna* teeth can be differentiated from those of Carchariidae and *Brachycarcharias* by their rather massive appearance despite small stature and absence of a lingual nutritive groove. The teeth of *Macrorhizodus* lack lateral cusplets and those of *Otodus* (*Carcharocles*) are serrated. Several species of *Isurolamna* are generally reported from Eocene strata, including *I. affinis* (Casier, 1946), *I. bajarunasi* (Glickman & Zhelezko, 1985), and *I. inflata*. An Oligocene species, *I. gracilis* (Le Hon, 1871), has very small lateral cusplets compared to the Tupelo Bay

Formation species. Unfortunately, Leriche (1905) did not adequately describe the tooth morphology of his new taxon, which he identified as *Lamna vincenti* var. *inflata*. He also did not illustrate specimens, nor did he designate a type specimen. However, Casier (1946) later illustrated two lateral teeth that he at least tentatively assigned to the species (see pl. 2, figs. 4–5), and one of these was designated as a plesiotype (fig. 5). In the same report, Casier (1946) named the taxon *Odontaspis hopei* var. *affinis* based on an anterior tooth (pl. 2, fig. 11b–c), and Casier (1966) later assigned numerous anterior teeth and some lateral teeth to this species (pl. 5, figs.7–14). This species was ultimately assigned to the genus *Isurolamna* by Cappetta (1976).

Cappetta (1976) erected the genus *Isurolamna* and considered it to be monospecific, including only *I. affinis* (Casier, 1946). Although Cappetta (1976) did not discuss the *I. inflata* morphology, two teeth that he regarded as upper laterals of *I. affinis* (pl. 2, figs. 3–4) are comparable to the *L. inflata* teeth shown by Casier (1946: pl. 2, figs. 4–5). Cappetta (1976) also showed anterior teeth (pl. 2, figs. 5–6) that are consistent with the specimen identified as *O. h.* aff. *affinis* by Casier (1946; pl. 2, fig. 11). Two additional specimens Cappetta (1976: pl. 2, figs. 7–8) identified as lower lateral teeth have a rather broad main cusp and broad cusplets in comparison to the "upper" teeth. Both morphologies are contained within the Tupleo Bay sample, and this variation is consistent with the range of *I. affinis* teeth presented by Van den Eeckhaut & Deschutter (2009: pl. 3). Interestingly, Casier (1966) assigned lateral teeth to *L. affinis* (pl. 5, figs. 12 & 14) that are similar to teeth he identified in 1946 as *L. inflata*.

Because Leriche (1905) never designated a type specimen and did not illustrate any specimens of his *L. inflata* species, one could argue that the taxon is a *nomen dubium*. However, if one considers the specimens discussed by Casier (1946), and assumes that those specimens are congruent with Leriche's (1905) concept of the species, Casier's (1946) designation of a plesiotype could validate the species. Furthermore, it is entirely possible that the anterior tooth of Casier's (1946) *O. h. affinis* morphology is conspecific with the lateral morphologies he ascribes to the *L. inflata* species, which is supported by the material documented by Cappetta (1976), Van den Eeckhaut & Deschutter (2009), and by the Tupelo Bay Formation sample. The senior name would therefore be *I. inflata* (Leriche, 1905) and is utilized herein.

With respect to *I. bajarunasi*, the Tupelo Bay Formation specimens generally compare well to the species as illustrated by Popov et al. (2025: fig. 6A–C). For example, a lower lateral tooth (fig. 6C) is virtually identical to the specimen we show in our Figure 8Y–Z, and an upper lateral tooth (fig. 6B) differs from the Tupelo Bay Formation specimen shown in Figure 8V–X only in that the lateral cusplets are larger and more closely connected to the main cusp. One significant difference concerns the anterior teeth, as the Tupleo Bay Formation specimen (Fig. 8EE–GG) has diminutive cusplets that are closely united to the base of the main cusp, whereas *I. bajarunasi* shown by Popov et al. (2025: fig. 6A) has conspicuously larger and conical cusplets that are well-separated from the main cusp. Lateral cusplets are poorly developed or absent altogether on *I. inflata* anterior teeth (see references noted above) and the phenomenon is regarded as a distinguishing feature of this species.

As noted above, *Isurolamna inflata* exhibits monognathic and dignathic heterodonty, with teeth varying in shape along a functional row (monognathic) and between the upper and lower jaws (dignathic). Specimen SC2022.27.54 is regarded as an anterior tooth (Fig. 8EE–GG) based on its erect and mesio-distally narrow crown, and the lateral cusplets are diminutive. Lateral teeth have a broader and labio-lingually thinner crown compared to anterior teeth. Upper lateral teeth are distinguished from lowers by their more inclined versus erect main cusp (compare Figs. 8V & 8HH to 8BB). Although both upper and lower lateral teeth can have two pairs of lateral cusplets (see Van den Eeckhaut & De Schutter 2009; Cappetta 2012), specimen SC2022.27.62 is regarded as a lower anterior tooth due to its erect main cusp (Fig. 8Y–AA). The species was geographically widely distributed during the middle Eocene and is known from numerous localities in Europe, including Belgium (Van den Eeckhaut & De Schutter 2009), Denmark (Carlsen & Cuny 2014) and England (Cappetta, 1976). This taxon is also known from Uzbekistan in Asia (Malyshkina & Ward 2016). Although the species has been reported from the middle Eocene of Ukraine (Kovalchuck et al. 2023), the specimens shown (fig. 5 M-S) are more like *Anomotodon*. To our knowledge, the only other North American record of *I. inflata* is from the "lower" Lisbon Formation (Lutetian, NP15) of Alabama (Cappetta & Case 2016).

Family Alopiidae Bonaparte, 1838
Genus *Alopias* Rafinesque, 1810

Alopias cf. ***alabamensis*** (White, 1956)
Fig. 9

Material examined: 15 teeth, including: SC2018.7.79 (Fig. 9V–X), SC2022.27.77 (Fig. 9S–U), SC2022.27.78 (Fig. 9A–C), SC2022.27.79 (Fig. 9G-H), SC2022.27.80 (Fig. 9J–L), SC2022.27.81 (Fig. 9M–O), SC2022.27.82, SC2022.27.83 (Fig. 9P-R), SC2022.27.84 (Fig. 9D–F), SC2022.27.85 (Fig. 9BB–DD), SC2022.27.86 (Fig. 9Y–AA), SC2024.17.1, SC2024.17.2, SC2024.17.3, SC2024.17.4.

Description. The teeth measure up to 1.5 cm in apico-basal height and 1.5 cm in mesio-distal width and consist of a triangular crown and bilobate root. The crown ranges from relatively narrow and erect (and nearly symmetrical) to broad-based and distally recurved, and it is divided into labial and lingual parts by mesial and distal cutting edges. Both crown faces are smooth, but the labial face is virtually flat, and the lingual face is very convex. The cutting edges are smooth, continuous, and may be formed basally into elongated heels. On some teeth the cutting edges are convex and of equal length, but more often the mesial edge is convex and elongated, whereas the distal edge is shorter and weakly to highly convex. The bilobed root is thick, particularly on the lingual side below the crown where an indistinct nutritive groove is located. Root lobes are moderately elongated, generally rounded at their distal extremities, and separated by a wide and deep U-shaped interlobe area.

Remarks. Several Eocene species of *Alopias* have been named, including *A. leeensis* Ward, 1978 that has a much lower main cusp with rounded apex, and more elongated root lobes compared to the Tupelo Bay Formation taxon. Teeth of *A. crochardi* Ward, 1978 differ by their smaller overall size, narrower crown with convex mesial cutting edge, narrower root lobes, and presence of a deep lingual nutritive groove. *Alopias denticulatus* Cappetta, 1981 teeth have a much narrower and more erect main cusp, elongated lateral crown shoulders bearing minute cusplets, more elongated root lobes, and a lingual nutritive groove. Teeth of *A. hermani* Zhelezko & Kozlov, 1999 from the Priabonian of Kazakhstan are distinguished from the Tupelo Bay Formation specimens by their narrower but taller crown (particularly on lateral teeth), more deeply concave distal margin, and higher distal heel.

White (1956) named the subspecies *Alopias latidens alabamensis* based on teeth from Jacksonian deposits of Alabama. His site information and the preservation of the specimens he examined indicate that the fossils were derived from the Priabonian Yazoo Clay (although it is unclear from which member). The subspecies was later elevated to species status by Case & Cappetta (1990) when they tentatively referred their Egyptian alopiid teeth to *A. alabamensis*, despite pointing out the insufficient differential diagnosis and low-quality illustrations provided by White (1956). More recent reports of *A. alabamensis* from Egypt and Morocco appear to have followed Case & Cappetta (1990) (i.e., Adnet et al. 2010; Underwood et al. 2011; Zalmout et al. 2012; Asan et al. 2022).

White's (1956) hypodigm of *A. alabamensis* includes nine specimens, all of which were figured as line drawings (figs. 28–32) but only two are shown in photographs (pl. 11, figs. 5–6), including the holotype NHMUK P30853-1. Although White's (1956) specimens are etched by plant roots-, photographs provided by the NHMUK show that most are comparable to the South Carolina material in terms of overall size, crown width and height, length and shape of the mesial cutting edge, and transition from distal cutting edge to distal heel. Slight differences include the lingual nutritive groove being more conspicuous on the Alabama specimens, and the cusp width of the South Carolina specimens appearing to be greater. One tooth shown by White (1956; fig. 32) is an upper lateral tooth of *Negaprion gilmorei* and not *Alopias*.

The overall tooth morphology and apparent dental heterodonty of the Tupelo Bay Formation *Alopias* are comparable to the condition of the extant Common Thresher Shark, *A. vulpinus* (Bonnaterre, 1788), as we observed with SC2015.30.1. Based on that specimen, the Eocene dentition included anterior and lateral positions, with anterior teeth (i.e., Fig. 9A, 9D, 9M) being narrower and more erect than lateral teeth. Within lateral files, the tooth crowns have a very elongated, sinuous to convex mesial edge and a conspicuous distal heel (i.e., Fig. 9G, 9J, 9BB). Crown height appears to decrease but crown width increases towards the commissure. Additionally, the root lobes of anterior teeth are less diverging than those on lateral teeth (compare Fig. 9B to 9K). We measured the crown width and height of the Tupelo Bay Formation

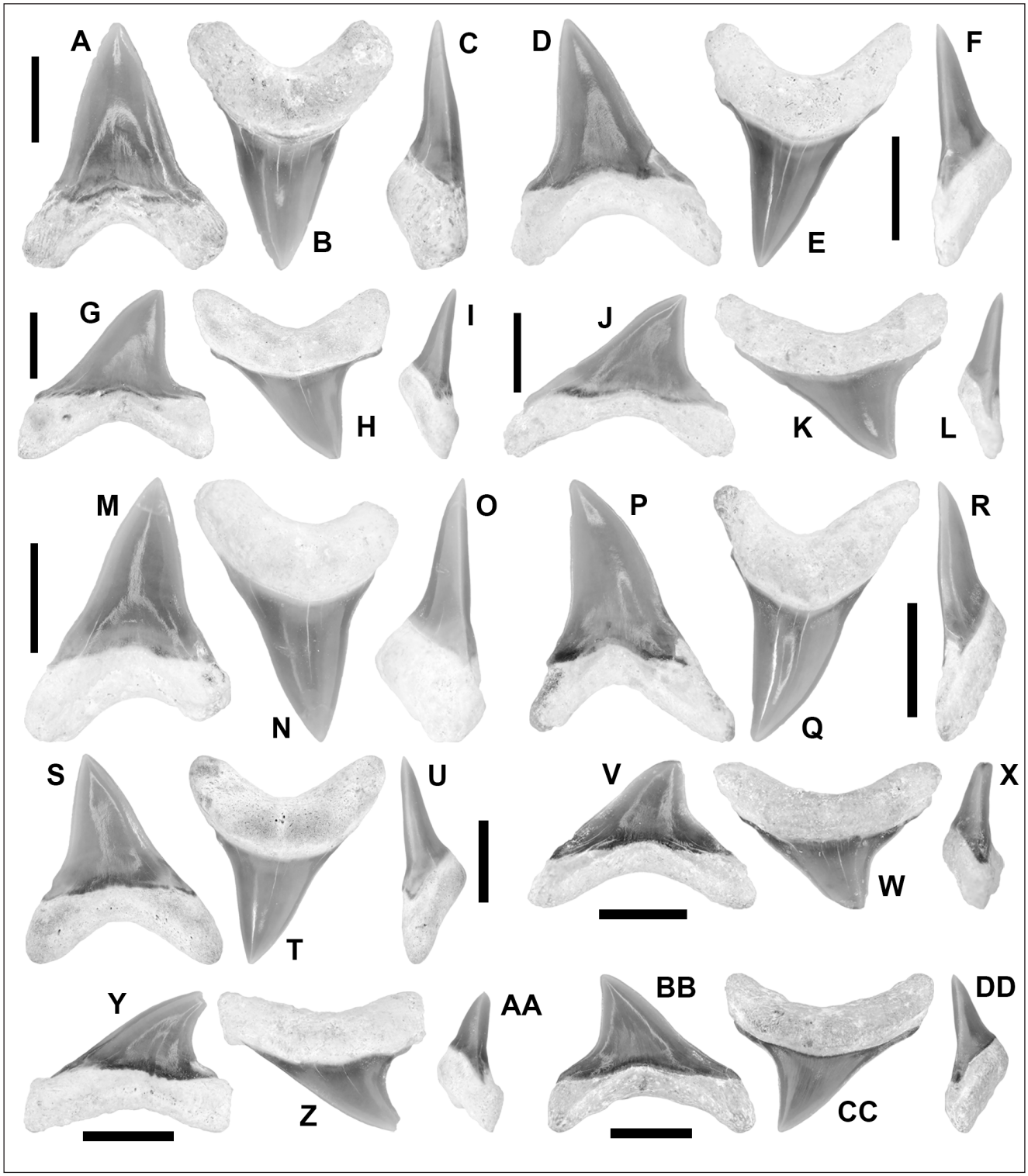

Fig. 9 - *Alopias* cf. *alabamensis* from the Tupelo Bay Formation. A-C) upper left anterior tooth, SC2022.27.78, in labial (A), lingual (B), and distal (C) views; lower? right lateral tooth (D-F), SC2022.27.84, in labial (D), lingual (E), and mesial (F) views; upper right lateral tooth (G-I), SC2022.27.79, in labial (G), lingual (H), and mesial (I) views; upper right posterolateral tooth (J-L), SC2022.27.80, in labial (J), lingual (K), and mesial (L) views. M-O) upper right anterior tooth, SC2022.27.81, in labial (M), lingual (N), and mesial (O) views; lower? right anterior tooth (P-R), SC2022.27.83, in labial (P), lingual (Q), and mesial (R) views; upper lateral tooth (S-U), SC2022.27.77, in labial (S), lingual (T), and mesial (U) views; upper posterolateral tooth (V-X); SC2018.7.79, in labial (V), lingual (W), and mesial (X) views; lower? posterolateral tooth (Y-AA), SC2022.27.86, in labial (Y), lingual (Z), and mesial (AA) views; lower(?) posterior tooth (BB-DD), SC2022.27.85, in labial (BB), lingual (CC), and mesial (CC) views. Scale bars: 5 mm.

teeth and found that they cluster together based on tooth position, with anterior teeth clearly separated from lateral teeth. White's (1956) Alabama material clusters within the range of the South Carolina specimens and can also be distinguished by tooth position. Although there appear to be minor differences between the limited samples of Alabama and South Carolina teeth, there is not a clear enough distinction between them to rule out heterodonty in a single species. We therefore tentatively identify the South Carolina specimens as *A. alabamensis* until larger samples of *Alopias* teeth from the Yazoo Clay of Alabama are available for study.

The Egyptian *Alopias* teeth reported by Case & Cappetta (1990), Underwood et al. (2011), Zalmout et al. (2012), and Asan et al. (2022) generally conform to White's (1956) concept of the *A. alabamensis* morphology, although there is variation among the specimens. Differences in tooth shapes have been interpreted as dignathic (Case & Cappetta 1990) or gynandric (Underwood et al. 2011) heterodonty within a single taxon. The anterior teeth in our sample vary in width and cutting edge convexity (compare Fig. 9A to 9P), although it is unclear whether this reflects dignathic heterodonty or gynandric heterodonty, a phenomenon documented in extant *Alopias* species (Cigala-Fulgosi, 1983). The North American *A. alabamensis* sample thus far does not exhibit such extreme variation in crown width as shown by Underwood et al. (2011: fig. 5X–Y). González Barba (2003) identified Priabonian alopiid teeth from Baja California, Mexico as *A. alabamensis* that are comparable to the Alabama and South Carolina specimens.

Order **Carcharhiniformes** Compagno, 1973
Family Triakidae Gray, 1851

Genus *Galeorhinus* Blainville, 1816

Type species: *Squalus galeus* Linnaeus, 1758

Galeorhinus semiserratus sp. nov.
Figs 10 & 11

urn:lsid:zoobank.org:act:35ACB9E0-953E-44B2-A548-C3AC411108B5

Hypodigm: holotype SC2022.27.187 (Fig. 10J–L), paratype SC2022.27.174 (Fig. 10A–B), paratype SC2022.27.176 (Fig. 10W–X), paratype SC2022.27.179 (Fig. 10E–F).

Diagnosis: Teeth attaining large size for the genus, reaching just over 9 mm in mesio-distal width. Labial crown foot overhangs the root and bears short longitudinal ridges that may coalesce into a transverse ridge. Lower one-half to two-thirds of mesial cutting edge with weak to very coarse serrations. Distal heel bearing up to nine denticles that decrease in size distally.

Etymology: The species name is based on the development of coarse, simple serrations along the lower one-half to two-thirds of the mesial cutting edge.

Referred material: 66 teeth, including SC2006.30.2, SC2015.59.6, SC2015.59.7, SC2015.59.8 (3 specimens), SC2022.27.118 (Fig. 10P–R), SC2022.27.162, SC2022.27.163 (Fig. 10S–T), SC2022.27.164 (Fig. 10U–V), SC2022.27.165 (Fig. 10Y–Z), SC2022.27.166, SC2022.27.167 (Fig. 10AA–BB), SC2022.27.168 (Fig. 10EE–FF), SC2022.27.169, SC2022.27.170 (Fig. 10GG–HH), SC2022.27.171 (Fig. 11A–B), SC2022.27.172 (Fig. 11G–H), SC2022.27.173, SC2022.27.175 (Fig. 11L), SC2022.27.177 (Fig. 10II–KK), SC2022.27.178 (Fig.10C–D), SC2022.27.180 (3 specimens), SC2022.27.181 (3 specimens), SC2022.27.182 (Fig. 10CC–DD), SC2022.27.183, SC2022.27.184 (Fig. 10G–I), SC2022.27.185 (Fig. 11I–K), SC2022.27.186 (Fig. 11M–N), SC2022.27.188 (2 specimens), SC2022.27.189 (Fig. 11R–S), SC2022.27.190 (8 specimens), SC2022.27.191 (Fig. 11O–Q), SC2022.27.192 (Fig. 10M–O), SC2022.27.193 (Fig. 11E–F), SC2022.27.194 (Fig. 11C–D), SC2022.27.195 (4 specimens), SC2022.27.196 (Fig. 11Y–Z), SC2022.27.197 (3 specimens), SC2022.27.198 (Fig. 11W–X), SC2022.27.199 (2 specimens), SC2022.27.200 (Fig. 11T–V), SC2024.17.9, SC2024.17.10, SC2024.17.11 (3 specimens), SC2024.17.12, SC2024.17.13 (2 specimens), SC2024.17.14.

Type horizon: Pregnall Member, Tupelo Bay Formation; Eocene, Priabonian Stage/Age, calcareous nannoplankton Zone NP18; approximately 10 m below contact with the overlying Parkers Ferry Formation.

Type locality: Giant Portland Cement quarry, east side of SC 453, approximately 1.6 km north of US I-26, Dorchester County, South Carolina, USA (note this is an active quarry, with portions being mined and others being reclaimed).

Description. The largest teeth in the sample measure just over 9 mm in mesio-distal width and less than 7 mm in apico-basal height. The teeth can be generally described as mesio-distally wide, with a rather short but distally inclined cusp, elongated mesial cutting edge, short distal cutting edge, and distal heel bearing numerous denticles. The labial crown face is rather flat, and the crown foot is a thin shelf-like projection that overhangs the root. The lingual crown face is convex. The crown enameloid is smooth except for short vertical ridges occurring on the labial crown foot. The elongated mesial cutting edge may be uniformly convex, straight, or weakly concave. The portion forming the main cusp is smooth, but the remainder of the mesial edge generally bears serrations that range from weak to very coarse. The distal edge is always smooth and usually weakly convex. The distal heel is oblique to tooth height and bears between two to nine robust denticles that decrease in size distally. The bilobate

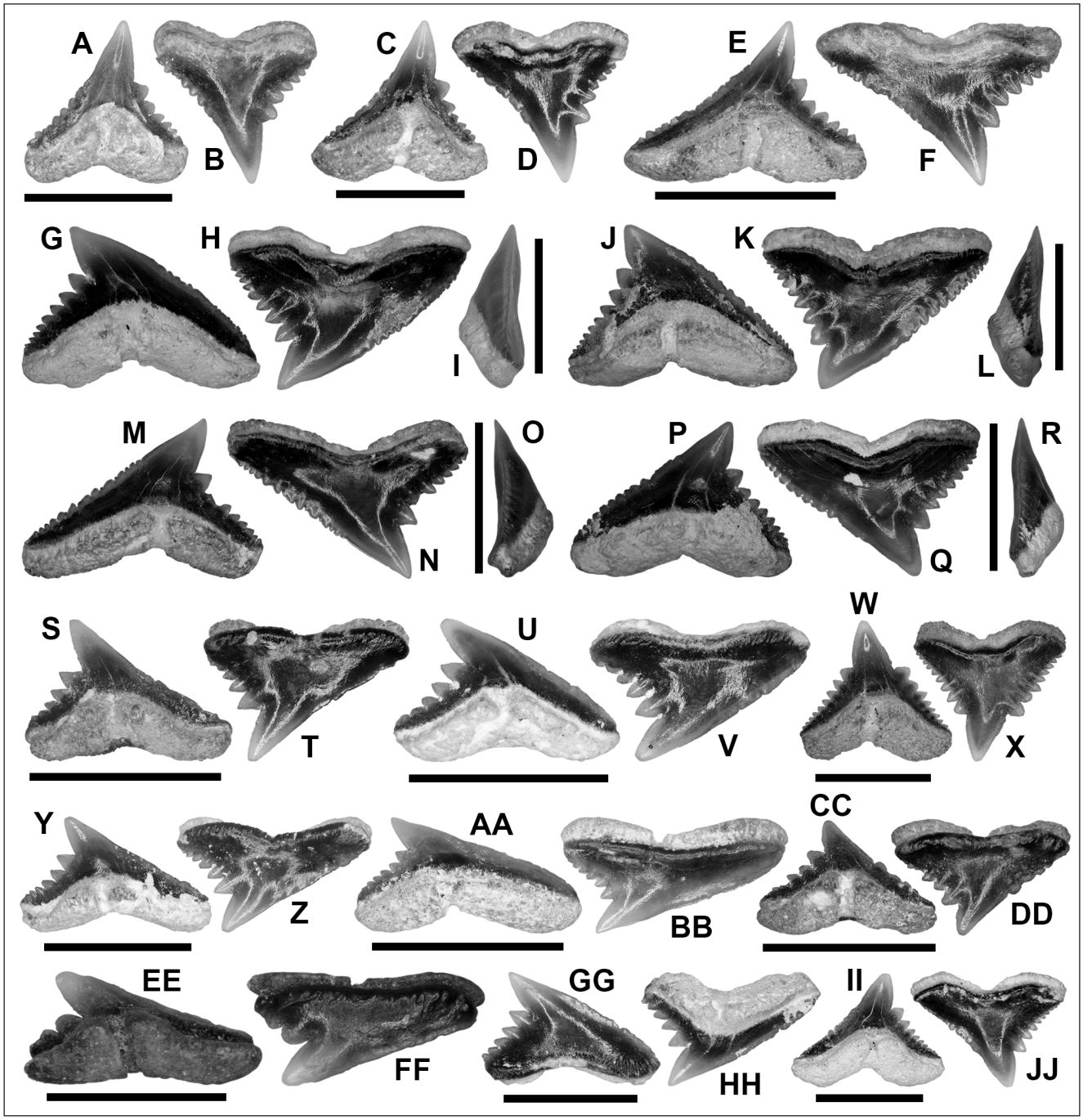

Fig. 10 - *Galeorhinus semiserratus* sp. nov. from the Tupelo Bay Formation. A-B) lower right anterior tooth, SC2022.27.174 (paratype), in lingual (A) and labial (B) views; lower right anterior tooth (C-D), SC2022.27.178, in lingual (C) and labial (D) views; lower right lateral tooth (E-F), SC2022.27.179 (paratype), in lingual (E) and labial (F) views; upper right lateral tooth (G-I), SC2022.27.184, in lingual (G), labial (H), and mesial (I) views; upper right lateral tooth (J-L), SC2022.27.187 (holotype), in lingual (J), labial (K), and mesial (L) views; lateral tooth (M-O), SC2022.27.192, in lingual (M), labial (N), and mesial (O) views; upper left lateral tooth (P-R), SC2022.27.118, in lingual (P), labial (Q), and mesial (R) views; juvenile lower left lateral tooth (S-T), SC2022.27.163, in lingual (S) and labial (T) views; juvenile upper right lateral tooth (U-V), SC2022.27.164, in lingual (U) and labial (V) views; upper right anterior tooth (W-X), SC2022.27.176 (paratype), in lingual (W) and labial (X) views; juvenile lateral tooth (Y-Z), SC2022.27.165, in lingual (Y) and labial (Z) views; posterolateral tooth (AA-BB), SC2022.27.167, in lingual (AA) and labial (BB) views; juvenile lower left anterior tooth (CC-DD), SC2022.27.182, in lingual (CC) and labial (DD) views; posterior tooth (EE-FF), SC2022.27.168, in lingual (EE) and labial (FF) views; upper left lateral tooth (GG-HH), SC2022.27.170, in labial (GG) and lingual (HH) views; lower right anterior tooth (II-JJ), SC2022.27.177, in lingual (II) and labial (JJ) views. Scale bars: 3 mm in Y-JJ, 5 mm in A-X.

root has somewhat elongated, widely separated lobes that are oval to reniform in lingual view, and the mesial lobe is often longer than the distal one. The lobes are separated by a wide and deep nutritive groove and the interlobe area ranges from shallow to deep, and V-shaped to U-shaped.

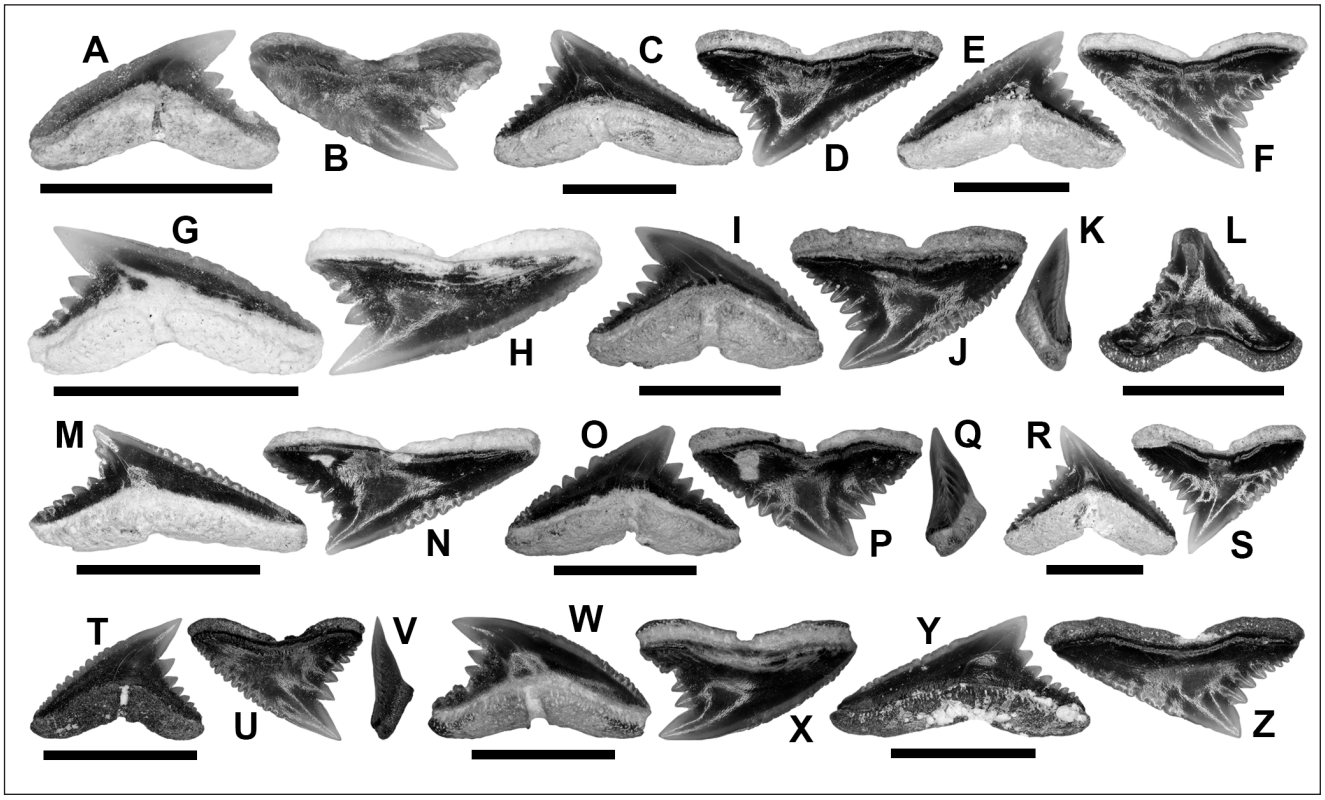

Fig. 11 - *Galeorhinus semiserratus* sp. nov. from the Tupelo Bay Formation. A-B) posterolateral tooth, SC2022.27.171, in lingual (A) and labial (B) views; posterolateral tooth (C-D), SC2022.27.194, in lingual (C) and labial (D) views; upper left lateral tooth (E-F), SC2022.27.1943, in lingual (E) and labial (F) views; posterolateral tooth (G-H), SC2022.27.172, in lingual (G) and labial (H) views; upper right lateral tooth (I-K), SC2022.27.185, in lingual (I), labial (J), and mesial (K) views; lower right anterior tooth (L), SC2022.27.175, in labial view; posterolateral tooth (M-N), SC2022.27.186, in lingual (M) and labial (N) views; lateral tooth (O-Q), SC2022.27.191, in lingual (O), labial (P), and mesial (Q) views; upper right anterolateral tooth (R-S), SC2022.27.189, in lingual (R) and labial (S) views; juvenile upper left lateral tooth (T-V), SC2022.27.200, in lingual (T), labial (U), and mesial (V) views; juvenile lateral tooth (W-X), SC2022.27.198, in lingual (W) and labial (X) views; posterolateral tooth (Y-Z), SC2022.27.196, in lingual (Y) and labial (Z) views. Scale bars: 5 mm.

Remarks. Three different size classes and sub-morphologies have been identified within our *Galeorhinus* sample. Some teeth are 2–3 mm in mesio-distal width (i.e., Fig. 10EE–FF) but most are between 4–8 mm wide, and some specimens are slightly greater than 9 mm (i.e., Fig. 10G-I). The teeth can have a roughly symmetrical triangular outline with only slight distal cusp inclination but more often they are asymmetrical with a distally inclined cusp (compare Figs. 10A and 11I). The cusp height is variable, as is the degree of distal inclination (compare Figs. 10J, 11E and 11G). The mesial cutting edge is highly variable and may be straight, uniformly convex, slightly sinuous, or moderately concave. Additionally, its complexity ranges from virtually smooth, crenulated (Fig. 10H), moderately serrated (Fig. 11F), to coarsely serrated (Fig. 11P) along the basal one-half to three-quarters of crown height. The distal heel is weakly to strongly oblique to crown height, and although five to six denticles appear to be common, as few as two (Fig. 10EE) and as many as nine (Fig. 10W–X) have been observed.

Despite these variations we believe the teeth represent a single species based on the shared presence of mesial serrations and ornamentation at the labial crown foot. With respect to monognathic heterodonty, we believe that rather symmetrical teeth in the sample reflect parasymphyseal and anterior tooth files, whereas wider teeth with distally inclined cusps represent lateral files. Within a tooth row, the crown height decreases, but cusp inclination increases towards the commissure. Regarding dignathic heterodonty, teeth with a relatively wide main cusp and convex mesial edge likely represent upper teeth, whereas those with a narrower, "upturned" main cusp and concave mesial edge are from lower tooth files. This interpretation is consistent with the illustrations of upper and lower teeth of extant *G. galeus* (Linnaeus, 1758) and *Hypogaleus hyugaensis* (Mi-

yosi, 1939) provided by Herman et al. (1988; pl. 13 and 14, respectively). Herman et al. (1988) and Fanti et al. (2016) indicated that, although dignathic heterodonty is weak in fossil and extant species, gynandric heterodonty is not developed in *Galeorhinus*.

The shape and complexity of the mesial cutting edge is not unique to any singular tooth size class, as small, medium, and large teeth could have a convex mesial cutting edge with coarse basal serrations or a straight and smooth edge. This phenomenon indicates that these features are not growth dependent (ontogenetic). However, ontogenetic heterodonty may be reflected in the labial crown ornamentation, as it is nearly obsolete on large teeth of presumably adult individuals but more complex on smaller teeth of probable juveniles. On the smallest teeth, ornamentation consists of numerous short longitudinal ridges that often coalesce to form an irregular transverse ridge along the labial crown foot. Moderately sized teeth are often ornamented with closely spaced but separate longitudinal ridges along the width of the tooth. Ornamentation is less extensive on larger teeth and generally consists of indistinct ridges that are limited to the mesial and distal sides of the crown.

The teeth in our sample are often larger than the size typically ascribed to *Galeorhinus* (10 mm vs < 8 mm in width; Cappetta 2012), and they could be mistaken for those of the co-occurring *Galeocerdo*. However, these genera are easily differentiated by the lack of serrations on the upper one-half of the mesial edge and entirety of the distal cutting edge on the main cusp of *Galeorhinus* teeth. Although some *Galeorhinus* teeth are superficially similar to those of *Pseudabdounia claibornensis* (White, 1956), the former can be identified by the ornamented and thickened labial crown foot that overhangs the root.

Galeorhinus semiserratus sp. nov. teeth differ from those of other Eocene species, including *G. minutissimus* (Arambourg, 1935), *G. ypresiensis* (Casier, 1946), *G. mesetaensis* Noubhani & Cappetta, 1997, *G. duchaussoisi* Adnet & Cappetta, 2008, *G. louisi* Adnet & Cappetta, 2008, and *G. cuvieri* (Agassiz, 1835), as well as younger fossil species and extant *G. galeus* (Linnaeus, 1758) by the combination of larger maximum size, common occurrence of weak to coarse mesial serrations that extend up to two-thirds of the crown height, greater maximum number of denticles on the distal heel (up to nine), and less or more crown ornamentation (depending on the species). Case (1981) named *G. huberensis* based on late Eocene teeth from the Dry Branch Formation of Georgia, which are of similar size (ca. 10 mm) to those from the Tupelo Bay Formation. However, the Georgia specimens lack a conspicuously convex labial crown foot that overhangs the root. Instead, the labial face is flat and flush with the root, a feature that is more consistent with *Physogaleus*. A small *Galeorhinus*-like tooth, identified as *G. galeus* (Linnaeus, 1758), was reported by Case (1981) from the Dry Branch Formation of Georgia, and it differs from *G. semiserratus* sp. nov. by being smaller in size, having fewer distal heel denticles, and possessing a completely smooth mesial cutting edge.

SC2006.30.2 was associated with a skull and post-cranial elements of the dugongid sirenian, *Eotheroides* sp. (SC2006.30.1) The right limb of this animal exhibits several cut marks that appear to have been made by a serrated cutting edge. One plausible interpretation is that the *Galeorhinus* tooth was shed while an individual fed on the sirenian, but we cannot rule out the possibility that the marks are the result of impact by a *Galeocerdo* tooth.

Family Scyliorhinidae Gill, 1862
Genus *Pachyscyllium* Reinecke, Moths, Grant & Breitkreuz, 2005

Pachyscyllium sp.
Fig. 12A–X

Material: 11 teeth, including: SC2016.47.2, SC2022.27.140 (Fig. 12A–D), SC2022.27.141 (Fig. 12E–H), SC2022.27.142, SC2022.27.143 (Fig. 12I–L), SC2022.27.144, SC2022.27.152 (Fig. 12Q–T), SC2022.27.154 (Fig. 12U–X), SC2022.27.155 (Fig. 12M–P), SC2022.27.156, SC2022.27.157.

Description. The teeth are small, only slightly exceeding 6 mm in apico-basal height and measuring up to 5 mm in mesio-distal width. The tooth crown consists of a rather narrow main cusp that is flanked by up to two pairs of lateral cusplets. The labial face of the main cusp is weakly convex, but the lingual face is very convex, and a smooth cutting edge extends from the apex to the base. The lateral cusplets are generally robust but of variable height and width and slightly diverging. A mesial cusplet is always well-developed, but a distal cusplet can be much reduced to nearly absent. The cusplets may be separated from the main cusp by a deep angular notch or a U-shaped embayment. Well-developed

cusplets are rather conical but do possess cutting edges, but poorly developed cusplets are largely denoted by a sinuous cutting edge. One tooth has two pairs of lateral cusplets, with the second pair being smaller than the primary pair, and yet another specimen has inconspicuous cusplets. The crown enameloid is smooth on all specimens. The labial crown foot of each specimen is thickened, is medially embayed, and overhangs the root. The root is bilobate with very short and highly diverging lobes. The lingual root face is thick and bisected by a long and narrow nutritive groove. The basal attachment surface is flat and relatively narrow. In labial view the extremities of the root lobes extend slightly beyond the crown margin.

Remarks. Although the 11 specimens available are rather variable, we believe they reflect heterodonty within a single species. Of the specimens, one tooth has a single pair of well-developed cusplets (Fig. 12R–S), whereas one specimen virtually lacks cusplets (SC2022.27.157 not figured). These two teeth appear to represent extremes in variation of the cusplet shape, as most of the teeth in the sample have a well-developed mesial cusplet but poorly developed distal cusplet (i.e., Fig. 12G & 12W). One additional outlier has a relatively broad-based main cusp and two pairs of lateral cusplets (Fig. 12J-K). However, the variation is consistent with that observed on teeth of *Pachyscyllium braashi* Reinecke et al., 2005, where the mesial cusplet can be smaller than the distal one, and both cusplets can be relatively small. We believe that the Tupelo Bay Formation *Pachysyllium* sp. sample reflects at least monognathic heterodonty, as rather narrow and symmetrical specimens were likely located in more anterior jaw positions (Fig. 12S), whereas more broad-based teeth are from lateral files (Fig. 12V). Of lateral teeth, those with a distally directed crown could be from upper files (Fig.12N–O), whereas specimen SC2022.27.143 has a vertical main cusp that is flanked by two pairs of lateral cusplets and could be interpreted as a lower lateral tooth (Fig. 12J).

The teeth referred to *Pachyscyllium* sp. differ from those we assign to *Premontreia* (see below) by lacking crown ornament, having larger lateral cusplets, and possessing a thickened and medially concave labial crown foot that significantly overhangs the root. The root is also oblique to crown height, whereas it is nearly perpendicular on *Premontreia*. With respect to *Abdounia minutissima* (see above), the lateral cusplets of *Pachyscyllium* sp. are more conical and the labial crown foot of *Abdounia* is rather flat and does not overhang the root.

The specimens we assign to *Pachyscyllium* sp. are similar to teeth identified as *Foumtizia* sp. by Cicimurri & Knight (2019) occurring in the upper Eocene (Priabonian) Dry Branch Formation of south-central South Carolina. The Dry Branch Formation specimens are smaller than the Tupelo Bay Formation specimens (4 mm in heigh versus slightly over 5 mm), and closer in size to *Foumtizia*. However, the Tupelo Bay Formation specimens are very well preserved, but the Dry Branch Formation teeth are ablated, broken, and lack enameloid. The crowns of teeth from both formations are very similar and we consider the fossils to represent the same taxon, which we herein refer to *Pachyscyllium*.

Genus *Premontreia* Cappetta, 1992
Subgenus *Oxyscyllium* Noubhani & Cappetta, 1997

Premontreia* (*Oxyscyllium*) *gilberti (Casier, 1946)
Fig. 12Y–ZZ

1946 *Scyliorhinus gilberti* – Casier, p. 58–60, pl. 1. fig. 14.
1999 *S. gilberti* Casier, 1946 – Kent, p. 22–23.
2003 *S. gilberti* Casier, 1946 – Parmley & Cicimurri, p. 166–167, fig. 5 D.

Material: 23 teeth, including: SC2016.47.4, SC2022.27.145 (Fig. 12OO–RR), SC2022.27.146 (Fig. 12WW–ZZ), SC2022.27.147 (Fig. 12CC–FF), SC2022.27.148 (Fig. 12GG–JJ), SC2022.27.149, SC2022.27.150 (Fig. 12KK–NN), SC2022.27.151, SC2022.27.153 (Fig. 12 SS-VV), SC2022.27.155, SC2022.27.156 (6 teeth), SC2022.27.158, SC2022.27.159, SC2022.27.160 (Fig. 12Y–BB), SC2022.27.161 (2 teeth), SC2022.27.162 (2 teeth).

Description. Small teeth measuring slightly over 5 mm in apico-basal height and close to 5 mm in mesio-distal width. The tooth crown consists of a tall, rather narrow, triangular main cusp flanked by one or two sets of lateral cusplets. The labial face of the main cusp is weakly to moderately convex, whereas the lingual face is very convex. The lower one-fifth of the labial crown face generally bears coarse vertical ridges, but this ornamentation can be very reduced and occur as very short ridges at the crown foot, often only below the lateral cusplets. The labial crown foot is thickened and slightly bulges beyond the root, but its basal margin is relatively straight. With respect to the lateral cusplets, each tooth possesses at least one pair, but many have a diminutive second pair or a second diminutive

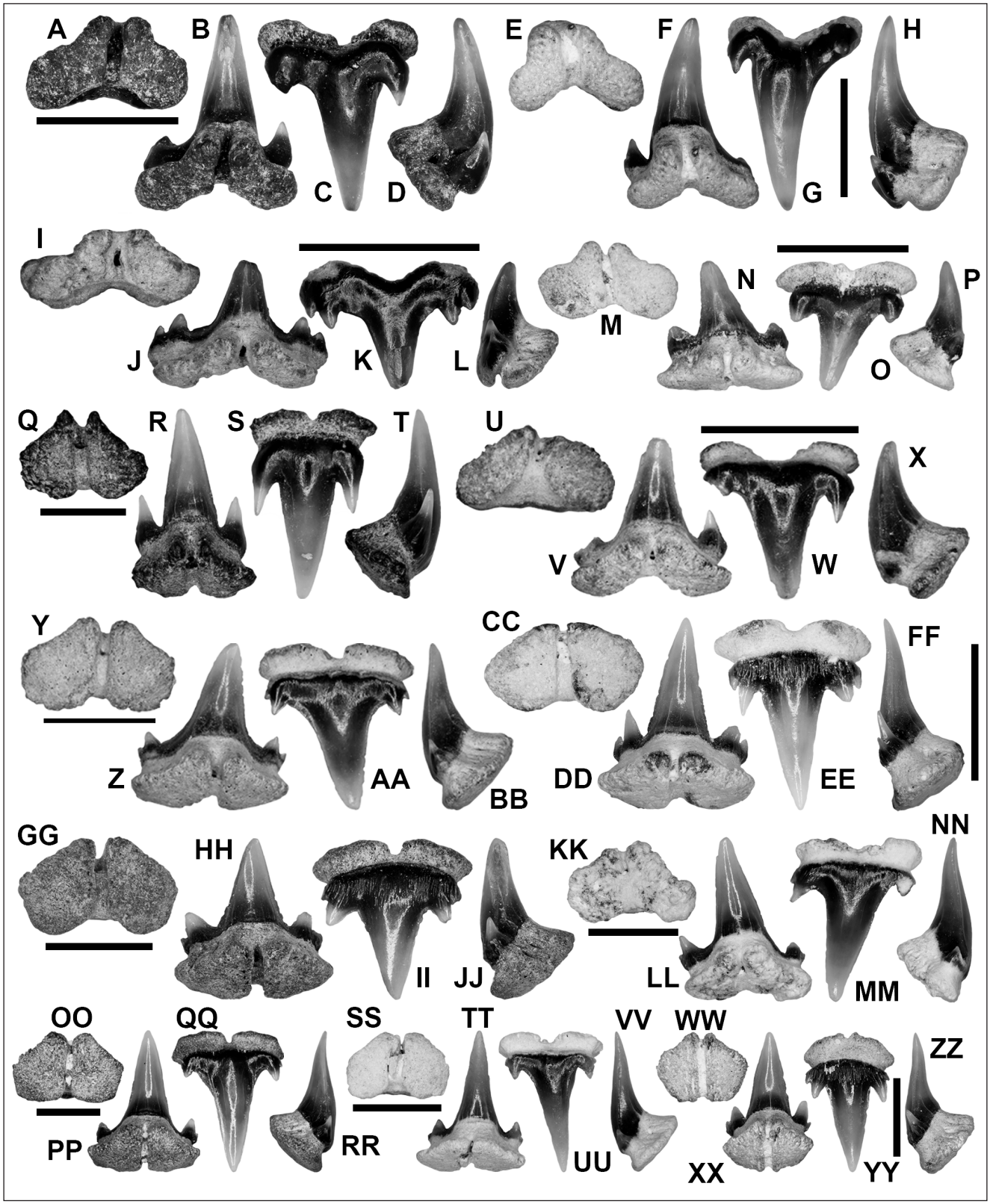

Fig. 12 - Scyliorhinid sharks from the Tupelo Bay Formation. A-X) *Pachyscyllium* sp., tooth (A-D), SC2022.27.140, in basal (A), lingual (B), labial (C), and distal (D) views; tooth (E-H), SC2022.27.141, in basal (E), lingual (F), labial (G), and distal (H) views; lower lateral(?) tooth (I-L), SC2022.27.143, in basal (I), lingual (J), labial (K), and mesial (L) views; lateral tooth (M-P), SC2022.27.155, in basal (M), lingual (N), labial (O), and mesial (P) views; anterior tooth (Q-T), SC2022.27.152, in basal (Q), lingual (R), labial (S), and mesial (T) views; anterolateral tooth (U-X), SC2022.27.154, in basal (U), lingual (V), labial (W), and mesial (X) views. Y-ZZ) *Premontreia* (*Oxyscyllium*) *gilberti*, lateral tooth (Y-BB), SC2022.27.160, in basal (Y), lingual (Z), labial (AA), and mesial (BB) views; anterior tooth (CC-FF), SC2022.27.147, in basal (CC), lingual (DD), labial (EE), and mesial (FF) views; lateral tooth (GG-JJ), SC2022.27.148, in basal (GG), lingual (HH), labial (II), and mesial (JJ) views; lateral tooth (KK-NN), SC2022.27.150, in basal (KK), lingual (LL), labial (MM), and mesial (NNN) views; anterior tooth (OO-RR), SC2022.27.145, in basal (OO), lingual (PP), labial (QQ), and mesial (RR) views; anterior tooth (SS-VV), SC2022.27.153, in basal (SS), lingual (TT), labial (UU), and distal (VV) views; anterior tooth (WW-ZZ), SC2022.27.146, in basal (WW), lingual (XX), labial (YY), and profile (ZZ) views. Scale bars: 2 mm.

cusplet only on the distal side. The primary cusplets can be relatively tall or short compared to main cusp height, and they can be separated from the main cusp by a V-shaped or U-shaped embayment. In the latter case, the smooth cutting edge extends from the main cusp apex and across the cusplets in a curved unbroken line (as opposed to having an angular notch). The primary cusplets are sub-conical (with smooth cutting edges), and although generally divergent both can be distally directed. The labial face of the primary cusplets can be smooth or bear coarse vertical ridges to the apex. The lingual crown face is usually smooth but fainter ridges can occur on the lateral cusplets. The bilobate root has very short, very divergent, and high lobes that have a reniform appearance in lingual view. There is a long, narrow and deep nutritive groove, and the expansive attachment surface is flat and oblique to the nearly perpendicular to cusp height. The root lobes are rounded and extend beyond the mesial and distal crown margin.

Remarks. The *Premontreia* (*Oxyscyllium*) *gilberti* sample includes teeth that have robust longitudinal ridges on the labial face (Fig. 12EE & 12II) and teeth that are nearly (Fig. 12MM) to completely smooth (Fig. 12QQ). The material is considered conspecific because the of the shared gross morphology of the main cusp, overlapping morphologies of the primary pair of lateral cusplets, and shared presence of a diminutive second lateral cusplet. This variation is indicated by the type suite of teeth shown by Casier (1946: pl. 1) and can be attributed to heterodonty within a single taxon. Many of the teeth in our sample are rather narrow and symmetrical, and we consider these to represent anterior files (i.e., Fig. 12PP), whereas teeth that have a broadly triangular and distally inclined main cusp (Fig. 12Z) are believed to be from lateral files (monognathic heterodonty). Casier (1946) showed an upper lateral tooth (pl. 1, fig. 14j–k) that has both lateral cusplets inclined distally, like some of the Tupelo Bay Formation specimens. Specimens that are roughly symmetrical but with more elongated mesial and distal root lobes (Fig. 12V) are thought to represent lower lateral teeth (dignathic heterodonty). It is also possible that, within anterior files, upper teeth have a wider main cusp compared to lower teeth (compare Fig. 12DD & 12PP to 12TT).

Noubhani & Cappetta (1997) split *Premontreia* into two subgenera, *P.* (*Oxyscyllium*) and *P.* (*Premontreia*), that are distinguished by the nature of the lateral cusplets. In the former subgenus, lateral cusplets are relatively large and may be present in two pairs, whereas on the latter subgenus they are comparatively small or absent altogether. The combination of small size, development of labial (and sometimes lingual) crown ornamentation, and presence of a second diminutive lateral cusplet are more consistent with *P.* (*O.*) *gilberti* teeth described by Casier (1946) than to either *P.* (*O.*) *subulidens* (Arambourg, 1952) or *P.* (*O.*) *peypouqueti* Noubhani & Cappetta, 1997.

These teeth are distinguished from all other similar shark teeth occurring in the Tupelo Bay Formation by the combination of small size, presence of robust labial crown ridges, thickened labial crown foot that is straight and slightly overhangs the root, and presence of a second diminutive lateral cusplet. With respect to North American Eocene occurrences, the species has been identified based on relatively few specimens from the Ypresian Nanjemoy Formation of Virginia (Kent 1994) and Bashi Formation of Mississippi (Case 1994). From younger deposits, the species is uncommon but occurs in the Bartonian Clinchfield Formation of Georgia (Parmley & Cicimurri 2003). The taxon was tentatively identified in the upper Eocene Dry Branch Formation of South Carolina (Cicimurri & Knight 2019), and similar teeth from the Yazoo Clay of Louisiana were identified as *P.* (*O.*) *distans* (Manning & Standhardt 1986; Ebersole & Cicimurri 2025). The species is widely reported from lower-to-middle Eocene strata of Belgium, England, France and the Netherlands (Casier 1946, 1966; Cappetta 1976; Bor 1985; Adnet 2006b; Adnet et al. 2008).

Family Hemigaleidae Hasse, 1879
Genus *Hemipristis* Agassiz, 1843

Hemipristis curvatus Dames, 1883

Fig. 13

1956 *Hemipristis wyattdurhami* White, p. 134.
1981 *H. wyattdurhami* White, 1956 – Case, p. 63, pl. 5, figs. 1–4.
1986 *H. wyattdurhami* White, 1956 – Manning & Standhardt, p. 144, fig.2.8.
1987 *H. curvatus* Dames, 1883 – Cappetta, p. 120
2000a *H. curvatus* Dames, 1883 – Case & Borodin, p. 10, pl. 3, figs. 20–23.
2003 *H. curvatus* Dames, 1883 – Parmley & Cicimurri, p. 169–170, fig. 6 A.
2019 *H. curvatus* Dames, 1883 – Ebersole et al., p. 66–67, fig. 24.

Material: 14 teeth, including: SC2018.7.105, SC2018.7.106, SC2018.7.107, SC2018.7.108, SC2022.27.256 (Fig. 13C–D), SC2022.27.257 (Fig. 13E–F), SC2022.27.258, SC2022.27.259, SC2022.27.260, SC2022.27.261, SC2022.27.262 (Fig. 13A–B), SC2022.27.263, SC2022.27.264, SC2022.27.265 (Fig. 13G–H).

Description. The largest specimens available measure 1.5 cm in apico-basal height and 1.5 cm in mesio-distal width. The teeth consist of a crown and bilobate root. The crown varies in height, width, and degree of distal inclination. In general, the crown is triangular, the labial face is relatively flat, the lingual face is convex, and the enameloid is smooth on both crown faces. The labial and lingual crown edges are denticulated, and the individual denticles vary in number, size, and degree of development. The mesial edge may be completely smooth, weakly crenulated, bear several well-developed denticles, or exhibit a combination of the latter two. Crenulation/denticulation does not extend beyond one-half the crown height, and denticles decrease in size basally. Denticles nearly always occur on the distal crown margin, typically between two and nine, and they decrease in size basally. Denticles may be narrow or broad-based. The non-denticulated portion of the crown is developed into a cusp that varies in size (depending on how high denticles extend on the crown). All cutting edges are smooth. The labial crown foot is thickened and extends slightly beyond the root. The bilobate root has lobes that may be somewhat elongated and narrow or wide, sub-rectangular, and highly diverging. The interlobe area can be U-shaped or V-shaped. A lingual boss is bisected by a very conspicuous nutritive groove.

Remarks. Using extant *Hemipristis elongata* (Klunzinger, 1871) as a model (SC84.177.1, SC86.53.1), *H. curvatus* exhibits monognathic and dignathic heterodonty, with tooth shape changing from the symphysis to the commissure, and between upper and lower dentitions. Upper anterior teeth are triangular, rather erect (but may be distally inclined), have a flat labial face, and several denticles occur on the distal edge (Fig. 13C–D). The upper lateral teeth are much broader, have a convex mesial edge, a distally inclined cusp, more numerous distal denticles, and the root lobes are shorter but wider (Fig. 13E–F). The crown height decreases but cusp inclination increases towards the commissure. Lower anterior teeth are very mesio-distally compressed, the labial face is very convex to only moderately so, and denticles are usually absent (Fig. 13A–B). Lower lateral teeth are similar in appearance to the upper anterior teeth, but the lowers have a maximum of two narrow denticles (Fig. 13G–H).

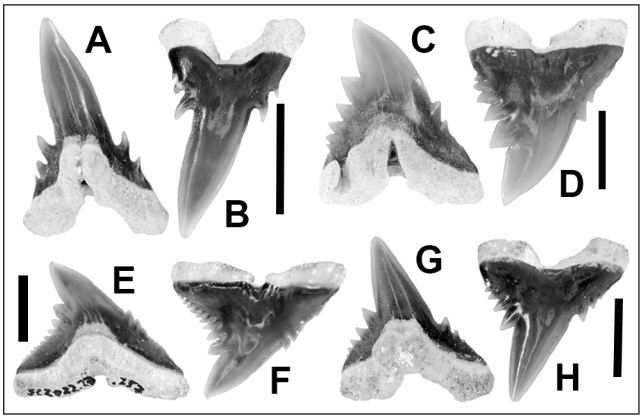

Fig. 13 - *Hemipristis curvatus* from the Tupelo Bay Formation. A-B) lower left anterior tooth, SC2022.27.262, in lingual (A) and labial (B) views; upper right anterior tooth (C-D), SC2022.27.256, in lingual (C) and labial (D) views; upper right lateral tooth (E-F), SC2022.27.757, in lingual (E) and labial (F) views; lower left lateral tooth (G-H), SC2022.27.265, in lingual (G) and labial (H) views. Scale bars: 5 mm.

Hemipristis teeth are unlikely to be confused with other Tupelo Bay Formation carcharhiniform taxa due to the size of the teeth, gross morphology, lack of labial crown ornamentation, and development of denticulation. Some anterior teeth of *Galeocerdo clarkensis* White, 1956 are superficially similar but cutting edges of this taxon have distinctive compound serrations (see below).

White (1956) named *Hemipristis wyattdurhami* based on Eocene specimens from Alabama, and Cappetta (1987) later synonymized this species with *H. curvatus*. The taxon is common in the Clinchfield Formation of Georgia (Parmley & Cicimurri 2003) and occurs in the Dry Branch Formation of Georgia (Case 1981; Case & Borodin 2000a) and South Carolina (Cicimurri & Knight 2019). Gulf Coastal Plain records include the Bartonian Gosport Sand of Alabama (Ebersole et al. 2019), Bartonian Moodys Branch Formation and Priabonian Yazoo Clay of Louisiana (Manning & Standhardt 1986; McPherson & Manning 1986; Ebersole & Cicimurri 2025), and Westgate (1984) identified material from Arkansas that may have been derived from the middle-to-upper Eocene Moodys Branch Formation. In Africa, the species has been documented from the middle-to-upper Eocene deposits of Egypt (Dames 1883; Case & Cappetta 1990; Underwood et al. 2011; Asan et al. 2022), Morocco (Zouhri et

al., 2021), and Tunisia (Adnet et al. 2020), and it occurs in Asia (Jordan; see Mustafa & Zalmout 2002). Interestingly, the species was not documented from the middle Eocene (Lutetian) Castle Hayne Formation of North Carolina (Case & Borodin 2000b) or Piney Point Formation of Virginia (Müller 1999). Adnet et al. (2020) commented that *H. curvatus* occurred in "all tropical seas" during the middle and late Eocene, and this potentially explains the apparent absence of the species in the central Atlantic Coastal Plain.

Family Carcharhinidae Jordan & Evermann, 1896
Genus *Abdounia* Cappetta, 1980

Abdounia enniskilleni (White, 1956)

Fig. 14A–E

1956 *Scyliorhinus enniskilleni* White, p. 128.
1980 *Abdounia enniskilleni* (White, 1956) – Cappetta, p. 37.
1981 *S. enniskilleni* White, 1956 – Case, p. 62, pl. 4, figs. 4–6.
1986 *S. enniskilleni* White, 1956 – Manning & Standhardt, p. 141, fig. 1.3.
2000a *Abdounia enniskilleni* (White, 1956) – Case & Borodin, p.28, pl. 5, figs. 40–44.
2000b *Abdounia enniskilleni* (White, 1956) – Case & Borodin, p.10, pl. 4, figs. 31–34.
2003 *A. enniskilleni* (White, 1956) – Parmley & Cicimurri, p. 172–173, fig. 7 A.

Material: 29 teeth, including: SC2015.59.12, SC2015.59.13, SC2015.59.14; SC2018.7.15, SC2018.7.113, SC2018.7.114 (Fig. 14C–D), SC2018.7.115 (Fig. 14A–B), SC2018.7.116, SC2018.7.117, SC2018.7.118 (5 teeth), SC2018.7.119 (5 teeth), SC2022.27.120, SC2022.27.121, SC2022.27.122, SC2022.27.123, SC2022.27.124 (Fig. 14E), SC2022.27.125, SC2022.27.126, SC2022.27.127, SC2022.27.128, SC2022.27.129.

Description. The teeth are rather small and measure less than 15 mm in apico-basal height. Some teeth have a tall and rather narrow main cusp consisting of a flat labial face and convex lingual face. The lingual face often bears fine longitudinal ridges that extend halfway to the apex. The cutting edges of the main cusp are continuous and smooth, and the main cusp is separated from a single pair of tall lateral cusplets by a deep notch. The root is robust, with a lingual boss that is bisected by a deep nutritive groove, and the attachment surface is flat. Very short, diverging root lobes are separated by a shallow U-shaped interlobe area.

Other teeth have a comparably wider main cusp that varies in overall height and degree of distal inclination. Typically, there is a single pair of broad but low lateral cusplets, and a few teeth exhibit a second distal cusplet. Additionally, the mesial cusplet may be absent from teeth such that the mesial edge is roughly continuous apico-basally. The root has a more shelf-like lingual boss, a deep nutritive groove, relatively narrow but flat attachment surface, and very short and highly diverging lobes.

Remarks. The dentition of this species certainly possessed monognathic heterodonty, with teeth from presumed anterior jaw files having a more symmetrical appearance and single pair of large lateral cusplets (Fig. 14E). Lateral teeth have a wider, lower, and distally inclined main cusp that can be flanked by two pairs of lateral cusplets. It appears that cusp inclination increased and cusp height decreased towards the jaw commissure (compare Fig. 14C to 14A). Teeth from more posterior files lack or have greatly reduced mesial cusplets.

Abdouina enniskilleni differs from *A. minutissima* (Winkler, 1874) (see below) by attaining a larger overall height (14 mm versus 3 mm) and often having vertical ridges on the lingual crown face. *Pseudabdounia claibornensis* teeth lack ornamentation but have more numerous lateral cusplets. Although teeth of *Premontreia* can have similar crown ornamentation to *A. enniskilleni*, the cusplet and root morphologies between the two genera are quite different (see above).

Additional *A. enniskilleni* records from the Atlantic Coastal Plain include the Lutetian Castle Hayne Formation of North Carolina (Case & Borodin 2000b), Piney Point Formation of Virginia (Müller 1999), Priabonian Dry Branch Formation of South Carolina (Cicimurri & Knight 2019), and the Clinchfield and Dry Branch formations of Georgia (Case 1981; Case & Borodin 2000a; Parmley & Cicimurri 2003). This species was reported from the Gosport Sand of Alabama (White 1956; Ebersole et al. 2019), middle-to-upper Eocene Moodys Branch Formation of Arkansas (Westgate 1984), and the Cook Mountain Formation, Moodys Branch Formation, and Yazoo Clay of Louisiana (Manning & Standhardt 1986; Ebersole & Cicimurri 2025).

Abdounia minutissima (Winkler, 1874)

Fig. 14F–Q

1874 *Otodus minutissimus* Winkler, p. 110, pl. 7, fig. 2.
1980 *Abdounia minutissima* (Winkler, 1874) – Cappetta, p. 37.
2014 *Scyliorhinus* sp. – Maisch et al., p. 192, fig. 3, 17–19.
2019 *A. minutissim*a (Winkler, 1874) – Ebersole et al., p. 86–87, fig. 31P–GG.

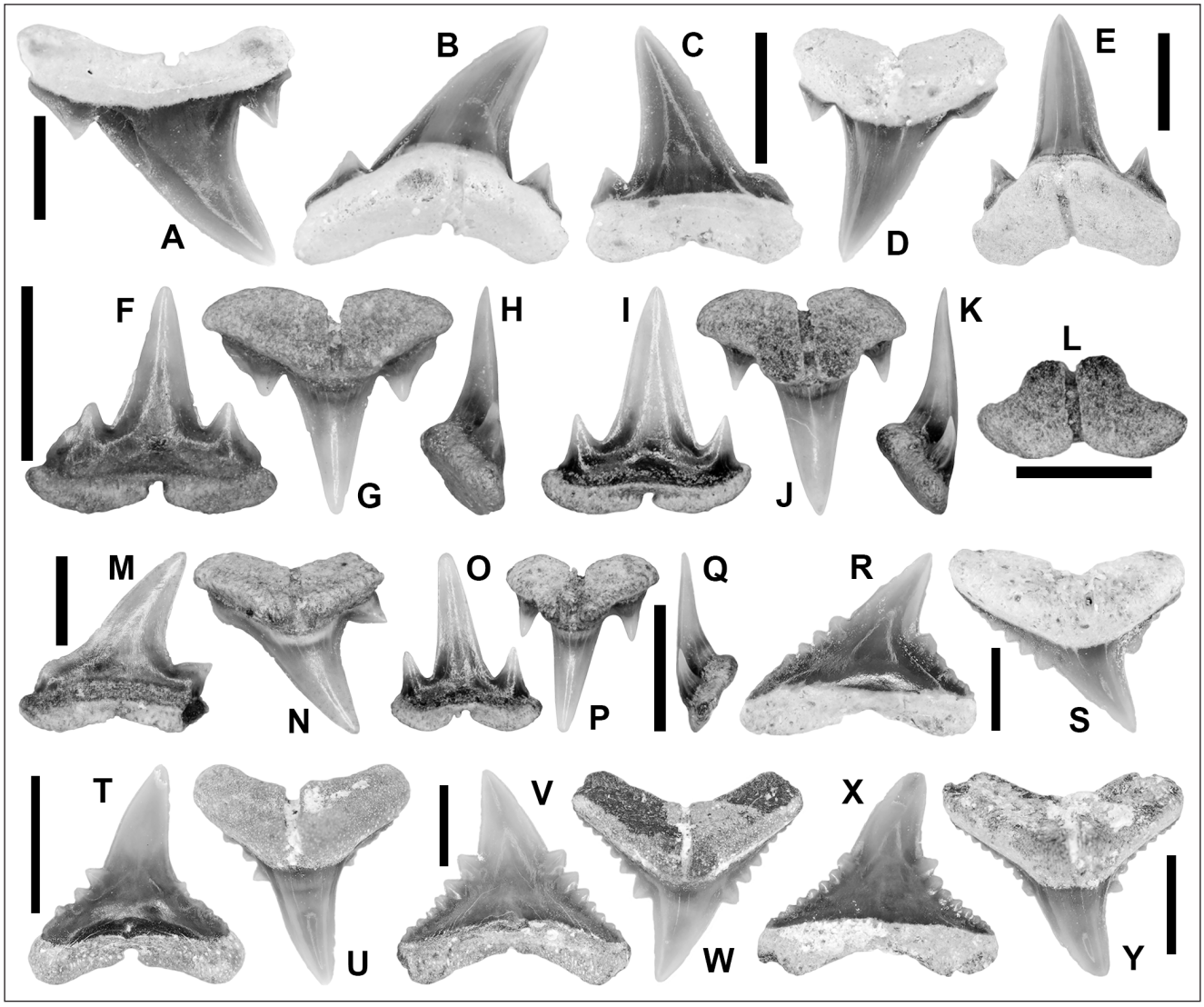

Fig. 14 - Carcharhiniform sharks from the Tupelo Bay Formation. A-E), *Abdounia enniskilleni*, upper left lateral tooth (A-B), SC2018.7.115, in labial (A) and lingual (B) views; lateral tooth (C-D), SC2018.7.114, in labial (C) and lingual (D) views; anterior tooth (E), SC2022.27.124, in lingual view. F-Q) *A. minutissima*, lower lateral tooth (F-H), SCSC2022.27.119, in labial (F), lingual (G), and mesial (H) views; upper(?) anterior tooth (I-L), SC2022.27.110, in labial (I), lingual (J), mesial (K), and basal (L)views; upper right posterolateral tooth (M-N), SC2022.27.114, in labial (M) and lingual (N) views; lower(?) anterior tooth (O-Q), SC2022.27.107, in labial (O), lingual (P), and mesial (Q) views. R-Y) *Pseudabdounia claibornensis*, posterolateral tooth (R-S), SC2022.27.139, in labial (R) and lingual (S) views; lower(?) anterior tooth (T-U), SC2022.27.130, in labial (T) and lingual (U) views; upper lateral tooth (V-W), SC2022.27.136, in labial (V) and lingual (W) views; lower(?) lateral tooth (X-Y), SC2022.27.133, in labial (X) and lingual (Y) views. Scale bars: 2 mm in F-Q, 5 mm in A-E & R-Y.

Material: 14 teeth, including: SC2022.27.107 (Fig. 14O–Q), SC2022.27.108, SC2022.27.109, SC2022.27.110 (Fig. 14I–L), SC2022.27.111, SC2022.27.112, SC2022.27.113, SC2022.27.114 (Fig. 14F–H), SC2022.27.115, SC2022.27.116 (2 specimens), SC2022.27.117, SC2022.27.118, SC2022.27.119 (Fig. 14M–N).

Description. Small teeth measuring less than 3 mm in height and up to 2.5 mm in width. The crown consists of a tall, narrow, triangular cusp flanked by a single pair of lateral cusplets. Most of the specimens have an erect and symmetrical cusp, but the main cusp is distally inclined on some teeth. The labial cusp face is flat, but the lingual face is convex. The labial crown foot is flat, and its basal margin is straight. The mesial and distal cutting edges are sharp, smooth, and continuous onto the lateral cusplets. The lateral cusplets are tall, narrow, slightly divergent, and located low on the crown. Most specimens exhibit a single cusplet on both sides of the main cusp, but the mesial cutting edge may be elongated and lack a cusplet. The crown enameloid is smooth. The root is bilobate with short and diverging lobes. In lingual view, a robust lingual boss is bisected by a long, narrow, and deep nutritive groove, and the root lobes have a reniform outline. In profile, the root is thick lingually, and the attach-

ment surface is wide, flat, and oblique to the height of the main cusp.

Remarks. There is some morphological variation among the teeth available to us that we attribute to heterodonty within a single taxon. Teeth that have a rather narrow and generally erect main cusp that is flanked by tall but narrow lateral cusplets are considered to represent anterior teeth (Fig. 14I–J). Specimens that are broader basally and have lower but more broad-based lateral cusplets (Fig. 14F–G) are believed to be lateral teeth (monognathic heterodonty). Additionally, teeth become more distally inclined/curved the closer to the commissure they were located, and more distal lateral teeth may lack a mesial cusplet (Fig. 14M–N). Upper anterior teeth have a wider main cusp compared to lower anterior teeth (compare Fig. 14I to 14O). Upper lateral teeth are distally inclined, whereas lower lateral teeth are more erect (dignathic heterodonty).

The teeth we identify as *Abdounia minutissima* can be distinguished from those of *A. enniskilleni* (see above) by their much smaller size, gracile stature, and lack of lingual ornamentation. Teeth of *A. minutissima* are comparable in size to *Pachyscyllium* sp. but differ from that taxon (see above) by having labio-lingually thinner lateral cusplets and a labial crown foot that is flat and straight at the crown/root juncture. Although superficially similar to some lamniform shark teeth, they can be distinguished by their lack of serrated cutting edges and/or very short root lobes that have a reniform appearance.

Abdounia minutissima was reported from lower-to-middle Eocene strata of Alabama (Ebersole et al. 2019) and is known from the middle Eocene of Belgium (Winkler 1974; Van den Eeckhaut & De Schutter 2009). The taxon has also been tentatively reported from middle Eocene deposits of France and Egypt (Adnet 2006b; Underwood et al. 2011; Zalmout et al. 2012; Asan et al. 2022).

Genus *Pseudabdounia* Ebersole, Cicimurri & Stringer, 2019

Pseudabdounia claibornensis (White, 1956)

Fig. 14R–Y

1956 *Galeorhinus recticona claibornensis* – White, p. 148.
1999 *Abdounia claibornensis* (White, 1956) – Müller, p. 48, pl. 5, figs. 10–12.
2000b *Abdounia recticona* (Winkler, 1874) – Case & Borodin, pl. 6, figs. 55–57.
2015 *Abdounia recticona* (Winkler, 1874) – Maisch et al., p. 166.
2019 *Pseudabdounia claibornensis* (White, 1956) – Ebersole et al., p. 88–90, fig. 32 A–R.

Material: 11 teeth, including: SC2015.59.15, SC2022.27.130 (Fig. 14T–U), SC2022.27.131, SC2022.27.132, SC2022.27.133 (Fig. 14X–Y), SC2022.27.134, SC2022.27.135, SC2022.27.136 (Fig. 14R–S), SC2022.27.137, SC2022.27.138, SC2022.27.139 (Fig. 14R–S).

Description. The teeth are small, measure less than 10 mm in apico-basal height, and have a broadly triangular crown that consists of a main cusp and multiple sets of lateral denticles. The main cusp is rather narrow and may be erect or distally inclined. The main cusp is flanked by four to eight lateral denticles, with the mesial side often having one or two more denticles than the distal side. The denticles are largest at the base of the cusp but decrease in size and coalesce into less conspicuous structures towards the crown foot. The cutting edge is smooth and continuous across the denticles and main cusp. The labial crown face is flat to weakly convex, but the lingual face is convex, and the crown enameloid is smooth on both faces. The labial crown foot is rather flat and does not bulge beyond the origin of the root. The root is bilobate with rather short, rectangular, widely diverging lobes. A long and narrow nutritive groove occurs on the lingual side of the root, and the interlobe area is V-shaped.

Remarks. This species was previously assigned to *Abdounia*, but Ebersole et al. (2019) moved this taxon, along with *A. recticona*, to *Pseudabdounia*. The *P. claibornensis* teeth in our sample exhibit morphological variation that we believe represents monognathic heterodonty. Teeth that are symmetrical with an erect main cusp and equal number of mesial and distal denticles are believed to be from anterior files. Teeth that are conspicuously wider, with distally inclined main cusps and a greater number of mesial denticles (i.e., the mesial edge is longer) are lateral teeth (Fig. 14W). Within the lateral files, crown height decreases but main cusp inclination increases towards the commissure (Fig. 14R). It is also possible that dignathic heterodonty is represented, as teeth with a relatively wide main cusp could be from the upper dentition (Fig. 14V) and specimens with a comparatively narrower main cusp (Fig. 14X) comprised the lower dentition.

The teeth of *P. claibornensis* are easily distinguished from those of *Abdounia minutissima* and *A. enniskilleni* that occur within the Tupelo Bay Formation (see above) by having four or more pairs of

lateral cusplets. The latter taxa typically have one but sometimes two pairs of cusplets. *Pseudabdounia claibornensis* teeth can be separated from superficially similar anterior teeth of *Galeorhinus* by their flat and smooth labial crown foot that does not overhang the root. The cusp of *P. claibornensis* teeth lacks serrated cutting edges as occur on *Galeocerdo* teeth.

Ebersole et al. (2019) documented *P. claibornensis* within the Bartonian (NP17) Gosport Sand of Alabama and it was reported in the slightly older (NP16) Cook Mountain Formation of Louisiana. Müller (1999) identified this species from Bed B of the Piney Point Formation of Virginia, which is also of Lutetian age (NP16). Case & Borodin (2000b) figured specimens (pl. 6) from the Lutetian Castle Hayne Formation of North Carolina that they identified as *Abdounia recticona*. Unfortunately, they did not provide descriptions of the material, but two of the specimens shown (figs. 55 and 57) possess four to five sets of lateral denticles, indicating a closer affinity to *P. claibornensis*. Maisch et al. (2015) also showed a single tooth (fig. 7U–V) identified as *A. recticona* from New Jersey, likely recovered from the middle Eocene Shark River Formation, that exhibits five pairs of cusplets and is therefore more like *P. claibornensis*. Interestingly, the species is apparently absent from the Clinchfield Formation of Georgia (i.e., Parmley & Cicimurri 2003)

Our comparison of a small sample (n = 8) of *P. claibornensis* teeth from the Piney Point Formation (SC2020.43.848 to SC2020.43.855) to those of the Tupelo Bay Formation revealed several minor differences. The Virginia specimens consistently differ by their smaller overall size, lower but wider main cusp, and lesser maximum number of denticles (up to six) but larger denticle size. Additionally, the denticles of the Virginia teeth are more clearly separated and remain distinctive to the crown foot. In contrast, the lateral denticles of the Tupelo Bay Formation *P. claibornensis* become inconspicuous distally and are more difficult to distinguish from one another. The features of the Castle Hayne specimens reported by Case & Borodin (2000b) more closely resemble the Piney Point Formation teeth rather than the Tupelo Bay Formation teeth.

The differences between the Piney Point/Castle Hayne and Gosport Sand/Tupelo Bay samples could be interpreted in several ways, one being that there was an increase in overall tooth size and number of denticles, but decrease in denticle size and cusp height within *P. claibornensis* from the Lutetian to the Priabonian. Alternatively, the older specimens could represent an additional species transitional between *P. recticona*, as occurs in the lower Lisbon Formation (NP15) of Alabama (Ebersole et al. 2019), and the younger fossils from the Gosport Sand and Tupelo Bay Formation. These possibilities require further investigation but are beyond the scope of this study.

Genus *Carcharhinus* Blainville, 1816

Carcharhinus sp.

Fig. 15

Material: 2 teeth, including: SC2022.27.245 (Fig. 15A–C), SC2024.17.5 (Fig. 15D–F).

Description. The two specimens are virtually identical to each other, with each consisting of a broadly triangular crown and broad-based root. The crown has an elongated and very slightly sinuous mesial cutting edge, whereas the distal margin can be roughly subdivided into an apical cutting edge and basal heel-like structure. The transition from apical edge to heel on SC2022.27.245 is contiguous through a concave arc, whereas the transition on SC2024.17.5 is more angular and disrupted by a weak medial notch. The mesial and distal cutting edges intersect apically to form a pointed cusp, with that of SC2022.27.245 being taller than on SC2024.17.5. The cutting edges on the latter specimen are serrated nearly to the apex, with those along the basal one-half of the mesial edge being the coarsest. The serrations of SC2022.27.245 are finer and difficult to discern along the apical one-half of the edges. The serrations of both specimens are simple. The labial crown faces are weakly convex, with the labial crown foot being slightly thickened and projecting beyond the root. The lingual crown face is very convex, and all crown enameloid is smooth. The root is massive, with a robust lingual boss bisected by a narrow and elongated nutritive groove (Fig. 15A & 15D). A large foramen is visible within the groove of SC2024.17.5. The root lobes are very short, highly divergent, and are separated by a shallow and broad V-shaped interlobe area.

Remarks. The two teeth described above are differentiated from those of Hemigaleidae and other Carcharhinidae within the Tupelo Bay For-

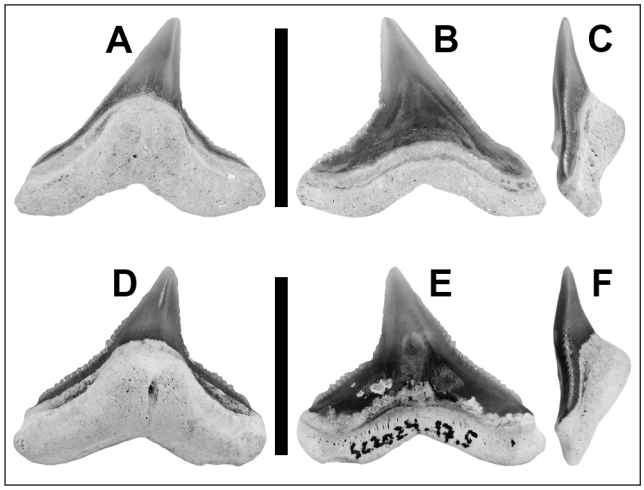

Fig. 15 - *Carcharhinus* sp. from the Tupelo Bay Formation. A-C) anterolateral tooth, SC2022.27.245, in lingual (A), labial (B), and mesial (C) views; anterolateral tooth (D-F), SC2024.17.5, in lingual (D), labial (E), and mesial (F) views. Scale bars: 1 cm.

mation by a combination of features that include cutting edges that are serrated nearly to the apex, a weakly differentiated distal heel, thickened labial crown foot, and the lack of lateral cusplets and distal heel denticles. Additionally, the cusp apices of the two *Carcharhinus* sp. teeth do not exhibit a "twisted" appearance along the mesial cutting edge (Fig. 15C & 15F) as seen on teeth of *Physogaleus* aff. *contortus* (Gibbes, 1849; see below).

The two *Carcharhinus* sp. teeth bear some resemblance to those of *Galeocerdo clarkensis* (see below), as both taxa have cutting edges that are serrated nearly to the cusp apex. Additionally, the *Galeocerdo* teeth have a thickened labial crown foot, compound (as opposed to simple) serrations, and some specimens possess a more finely serrated heel rather than a coarsely denticulated heel. However, the *Galeocerdo* teeth typically have a much more convex mesial edge, and the distal margin is very angular due to the intersection of the well-developed distal heel with the base of the cutting edge.

Two Eocene *Carcharhinus* species have been described from the Gulf Coastal Plain, including *C. mancinae* Ebersole et al., 2019 and *C. tingae* Cicimurri & Ebersole, 2021. The former taxon was described based on specimens from the Bartonian "upper" Lisbon Formation and Gosport Sand of Alabama, whereas the latter was recovered from the "upper" Lisbon Formation equivalent Cook Mountain Formation of Louisiana. The Gulf Coast taxa differ from the Tupelo Bay Formation *Carcharhinus* sp. by having coarse compound serrations as opposed to rather fine and simple serrations, and the distal heel is easily differentiated from the remainder of the crown.

Underwood & Gunter (2012) reported a *Carcharhinus* sp. upper tooth that was recovered from the Lutetian Guys Hill Formation of Jamaica. This specimen, preserved in labial view, differs from the two Tupelo Bay Formation *Carcharhinus* sp. teeth by having a shorter but broader crown, a well-developed and very coarsely denticulated distal heel, and angular transition from distal cutting edge to distal heel. Teeth of *C. underwoodi* Samonds et al., 2019 from middle-to-upper Eocene deposits of Madagascar exhibit a curved transition from distal cutting edge to distal heel like that occurring on the South Carolina *Carcharhinus* sp. teeth. However, the cusp of *C. underwoodi* is broader, the mesial cutting edge more coarsely serrated, and the distal heel has coarser denticulation compared to the Tupelo Bay Formation teeth.

Adnet et al. (2007) identified a new species, *Carcharhinus balochensis*, based on teeth recovered from the upper Eocene (Priabonian) Kirthar Formation of Pakistan. The upper anterior teeth of this species are very different from the Tupelo Bay Formation specimens, as the cusps are broader and the cutting edges are more heavily serrated. However, the upper lateral teeth of the Pakistan species are somewhat similar to the South Carolina material but appear to have a broader and more distally inclined cusp and more coarsely serrated mesial cutting edges. Additional Tupelo Bay Formation specimens are needed to elucidate the identity of the species represented by SC2022.27.245 and SC2024.17.5.

Genus *Negaprion* Whitley, 1940

Negaprion gilmorei (Leriche, 1942)

Fig. 16A–H

1942 *Sphyrna gilmorei* – Leriche, p. 45, pl. 4, fig. 1.
1956 *Negaprion gibbesi gilmorei* – White, p. 142, pl. 2 fig. 9.
1956 *Hypoprion greyegertoni* – White, p. 137, pl. 2 fig. 7.
1981 *Negaprion eurybathrodon* (Blake, 1862) – Case, p. 64, pl. 6, figs. 1–3.
1981 *Sphyrna zygaena* (Linnaeus, 1758) – Case, p. 66, pl. 8, fig. 4.
1981 *Scoliodon terraenovae* (Richardson, 1836) – Case, p. 64, pl. 5, fig. 5.
1999 *Carcharhinus gilmorei* (White, 1956) – Müller, p. 49, pl. 7, fig. 1.
2003 *N. eurybathrodon* (Blake, 1862) – Parmley & Cicimurri, p. 173, fig. 7 B.
2019 *Negaprion gilmorei* (White, 1956) – Ebersole et al., p. 73–77, fig. 27.

Material: 44 teeth, including: SC2001.109.3, SC2015.59.9, SC2015.59.10 (Fig. 16A–B), SC2015.59.11 (11 specimens), SC2018.7.12, SC2018.7.13, SC2018.7.14, SC2018.7.120 (Fig. 16G–H), SC2018.7.121, SC2018.7.122 (Fig. 16E–F), SC2018.7.123 (6 specimens), SC2018.7.124, SC2018.7.125 (4 specimens), SC2018.7.126 (4 specimens), SC2022.27.246, SC2022.27.247, SC2022.27.248, SC2022.27.249, SC2022.27.250, SC2022.27.251 (Fig. 16C–D), SC2022.27.252, SC2022.27.253, SC2022.27.254.

Description. Two tooth morphologies are assigned to this species, the first of which consists of teeth with a broadly triangular crown consisting of a large cusp separated from mesial and distal shoulders by a slight notch in the enameloid. The labial face of the crown is flat, whereas the lingual face is convex, and both faces bear smooth enameloid. The smooth cutting edges extend across the entirety of the cusp. The mesial and distal shoulders may be oblique or perpendicular to cusp height, and they vary in length. The shoulders are generally smooth but may be weakly crenulated on one or both sides of the crown. The root is bilobate, with short but widely diverging, rectangular lobes. The interlobe area ranges from V-shaped to U-shaped, and a thickened medial area on the lingual side of the root is bisected by a long nutritive groove. These teeth can attain widths of 1.3 cm and crown heights of just under 1 cm.

The second morphology includes teeth with a rather short and very narrow main cusp that is flanked by elongated mesial and distal shoulders. The cusp has a flat labial face but convex lingual face, and the enameloid is smooth on both faces. The smooth cutting edges extend along the cusp and onto the lateral shoulders and are generally not separated by a notch. The shoulders vary in length and are generally perpendicular to cusp height. Overall tooth width can reach 1 cm but crown height measures less than 7.0 mm.

Remarks. *Negaprion gilmorei* exhibits monognathic and dignathic heterodonty. Anterior teeth from the upper dentition are rather symmetrical and narrow (mesio-distally) and have a broad cusp with short and highly oblique lateral shoulders (Fig. 16G–H). Lateral teeth are comparatively wider and have more elongated and less oblique shoulders, and the cusp is distally directed (Fig. 16E–F). Teeth from the lower dentition have a simple crown consisting of a narrow cusp and elongated heels. Anterior teeth are rather narrow with an erect cusp (Fig. 16C–D), whereas lateral teeth have a distally inclined cusp and more elongated shoulders (Fig. 16A–B).

SC2001.109.3 was recovered from matrix surrounding the incomplete *Pristis* Link, 1790 rostrum (SC2001.209.1) described by Cicimurri (2007; this specimen is also discussed below). A tooth reported by Westgate (1984) from the middle Eocene Crow Creek local fauna is an upper antero-lateral tooth of *N. gilmorei*. This species was reported in lower-to-middle Eocene deposits of Alabama, where it was particularly common in the Bartonian Gosport Sand (Ebersole et al. 2019). In Louisiana, the species occurs in middle-to-upper Eocene strata of the Cook Mountain Formation, Yazoo Clay, and Danville Landing Formation (Manning & Standhardt 1986; McPherson and Manning 1986; Ebersole & Cicimurri 2025). Case (1981) and Cicimurri & Knight (2019) documented this species in the upper Eocene (Priabonian) Dry Branch Formation of Georgia and South Carolina, respectively. The species is also very common in the Clinchfield Formation of Georgia (Parmley & Cicimurri 2003).

Genus *Physogaleus* Cappetta, 1980

Physogaleus aff. ***contortus*** (Gibbes, 1849)

Fig. 16I–U

Material: 13 teeth, including: SC2015.59.4, SC2018.7.9 (Fig. 16I–L), SC2018.7.98, SC2018.7.99, SC2022.27.236 (Fig. 16M–O), SC2022.27.237, SC2022.27.238, SC2022.27.239, SC2022.27.240, SC2022.27.241 (Fig. 16P–R), SC2022.27.242, SC2022.27.243, SC2022.27.244 (Fig. 16S–U).

Description. The largest teeth in our sample measure up to 1.5 cm in apico-basal height but are generally less than 1.5 cm in mesio-distal width. The crown consists of a cusp and distinctive distal heel. The distally slanting mesial cutting edge is elongated and can be straight, uniformly convex, or sinuous. The distal cutting edge is much shorter, rather straight, and can be vertical or distally inclined. The mesial and distal cutting edges meet apically to form a very narrow (mesio-distally) and sharply pointed cusp. With respect to the mesial cutting edge, it is weakly crenulated to conspicuously denticulated up to one-half the crown height, whereas the remaining apical portion is smooth. The apical portion of the mesial cutting edge is also sinuous, which results in the cusp having a twisted appearance in mesial view. The distal cutting edge is smooth. The distal heel varies in length and is crenulated to conspicuously denticulated. Denticles can be of equal size or

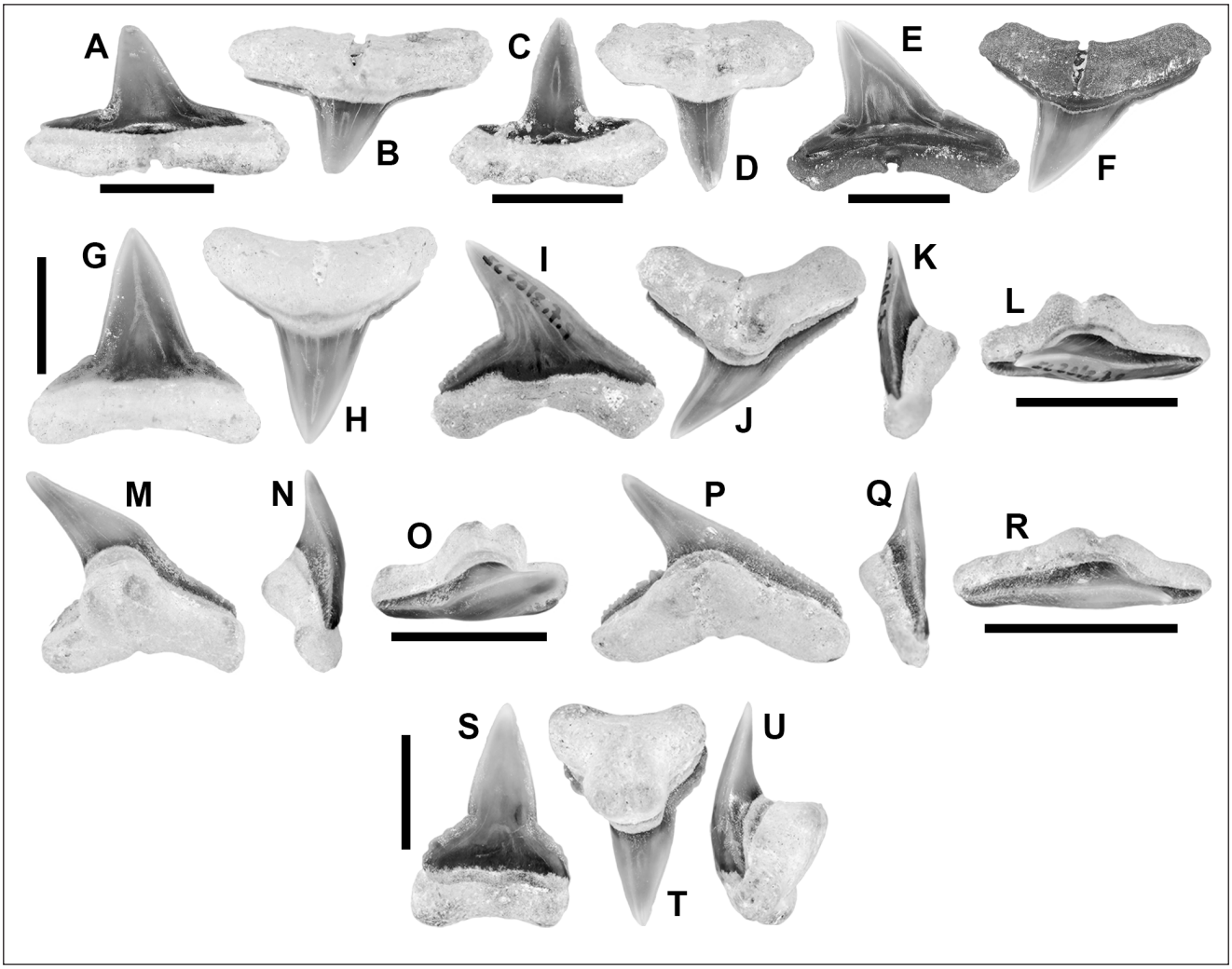

Fig. 16 - Carcharhinidae from the Tupelo Bay Formation. A-H) *Negaprion gilmorei*, lower right lateral tooth (A-B), SC2015.59.10, in labial (A) and lingual (B) views; lower anterior tooth (C-D), SC2022.27.251, in labial (C) and lingual (D) views; upper left lateral tooth (E-F), SC2018.7.122, in labial (E) and lingual (F) views; upper left anterior tooth (G-H), SC2018.7.120, in labial (G) and lingual (H) views. I-U) *Physogaleus* aff. *contortus*, anterolateral tooth (I-L), SC2018.7.9, in labial (I), lingual (J), mesial (K), and occlusal (L) views; anterior tooth (M-O), SC2022.27.236, in lingual (M), mesial (N), and occlusal (O) views; lateral tooth (P-R), SC2022.27.241, in lingual (P), mesial (Q), and occlusal R) views; symphyseal tooth (S-U), SC2022.27.244, in labial (S), lingual (T), and mesial (U) views. Scale bars: 5 mm in A-H & S-U, 1 cm in J-R.

decrease in size distally. The distal heel is separated from the distal cutting edge by a weak notch. The cutting edges are smooth. The bilobate root has robust but short, highly diverging lobes with rounded extremities. A massive lingual boss is bisected by a narrow and elongated nutritive groove. The labial crown face is flush with the transition to the root.

Remarks. Although or sample size is small, the specimens demonstrate that monognathic heterodonty was developed in this taxon. A symphyseal tooth in our sample (SC2022.27.244) is symmetrical with oblique crenulated mesial and distal heels (Fig. 16S–T). Specimens we identify as anterior teeth have a tall and somewhat erect cusp, with a highly sinuous mesial cutting edge (Fig. 16M–O). The mesial edge is straighter on lateral teeth, and the cusp is more distally inclined, with cusp height decreasing but inclination increasing towards the commissure (compare Fig. 16J to 16P).

The teeth described above are easily distinguished from those of *H. curvatus* lateral teeth by their flat labial crown face, lack of denticulation, having a much narrower cusp, a distal heel that is well-separated from the cusp, and massive lingual boss. Teeth of *Galeocerdo* (see below) have a wider cusp, serrated cutting edges, the cusp apex is not "twisted" in mesial view, and although the distal heel is distinguished from the distal cutting edge by a conspicuous notch, the angle formed by these two structures is obtuse (as opposed to 90° or less on *P.*

aff. *contortus*). *Galeorhinus* teeth are smaller and have an ornamented labial crown foot that overhangs the root. These *Physogaleus* teeth are morphologically like the two *Carcharhinus* sp. teeth described above but they differ by having teeth with a distinct notch separating the distal cutting edge from the heel, the cutting edges of the cusp are smooth, and the cusp apex is conspicuously twisted (compare Figs. 16I & 16K to 15B/E & 15C/F).

The features outlined above also serve to differentiate these *Physogaleus* teeth from those of Tupelo Bay Formation *P.* aff. *secundus* (see below). Teeth of the latter taxon are smaller, have well-developed distal heel denticulation, a straighter mesial cutting edge that is crenulated to strongly denticulated, and the root is more gracile in appearance (Fig. 17). With respect to the nature of the mesial cutting edge, Gibbes (1849) noted its "twisted" appearance and he ascribed the morphology to his new taxon, *Galeocerdo contortus* (= *Physogaleus* herein). *Physogaleus contortus* was recently documented form the lowermost Catahoula Formation (lower Chattian, Oligocene) of Mississippi by Cicimurri et al. (2025b), and these authors noted that Gibbes's (1849) specimens may have been derived from the Rupelian Ashley Formation (Oligocene, Rupelian, NP24) of South Carolina. Teeth like those from the Tupelo Bay Formation were also recently reported by Cicimurri et al. (2025a) from the Yazoo Clay of Alabama.

The Tupelo Bay Formation teeth are comparable to the Oligocene specimens from Mississippi and South Carolina in that the cusps of all specimens have a "twisted" appearance in mesial view. However, the Tupelo Bay Formation teeth differ by being smaller in overall size, having weakly developed mesial edge and distal heel denticles, and having smooth cutting edges on the cusp. It is possible that the Tupelo Bay Formation taxon represents a plesiomorphic ancestor of Oligo-Miocene *P. contortus* populations. Zouhri et al. (2021) reported an unspeciated *Physogaleus* morphology from the middle Eocene of Morocco that is very similar to the Tupelo Bay Formation specimens. Unfortunately, those authors did not describe the mesial cutting edge, nor did they provide images of teeth in mesial view (i.e., their fig. 4A–4C).

Physogaleus aff. ***secundus*** (Winkler, 1874)

Fig. 17

Material: 65 teeth, including: SC2015.59.3, SC2015.59.5, SC2018.7.11, SC2018.7.100, SC2018.7.101, SC2018.7.102 (Fig. 17S–T), SC2022.27.201, SC2022.27.202, SC2022.27.203, SC2022.27.204, SC2022.27.205, SC2022.27.206 (Fig. 17Y–Z), SC2022.27.207 (Fig. 17U–V), SC2022.27.208, SC2022.27.209 (Fig. 17AA–BB), SC2022.27.210 (Fig. 17CC–DD), SC2022.27.211 (2 specimens), SC2022.27.212, SC2022.27.213 (Fig. 17W–X), SC2022.27.214, SC2022.27.215 (11 specimens), SC2022.27.216 (Fig. 17A–B), SC2022.27.217 (Fig. 17M–N), SC2022.27.218 (Fig. 17Q–R), SC2022.27.219, SC2022.27.220, SC2022.27.221 (10 specimens), SC2022.27.222, SC2022.27.223, SC2022.27.224 (Fig. 17I–J), SC2022.27.225 (Fig. 17O–P), SC2022.27.226 (2 specimens), SC2022.27.227, SC2022.27.228, SC2022.27.229 (Fig. 17G–H), SC2022.27.230, SC2022.27.231 (Fig. 17K–L), SC2022.27.232, SC2022.27.233 (Fig. 17C–D), SC2022.27.234 (Fig. 17E–F), SC2022.27.235 (3 specimens).

Description. The teeth vary in apico-basal height and mesio-distal width but reach up to 8 mm and 9 mm in these dimensions, respectively. The crown consists of a well-developed cusp and a distal heel. The mesial cutting edge is elongated and may be concave, straight, sinuous, or weakly convex. The distal cutting edge is much shorter and may be straight or convex to varying degrees. The mesial and distal cutting edges intersect apically to form the cusp, which may be narrow or broad, and its apex is sharply pointed. The mesial edge may be completely smooth, or weakly crenulated to strongly denticulated along its basal half, whereas the distal edge is always smooth. The distal heel varies in length, is roughly perpendicular to cusp height, and separated from the cusp by a conspicuous notch. The heel typically bears two to three denticles that decrease in size distally. Some larger teeth bear four well-developed denticles and even a fifth diminutive one can occur. The labial crown face is weakly convex and does not have a distinctive labial convexity that overhangs the root. The lingual face is more convex, and both crown faces have smooth enameloid. The root is bilobate, with short subrectangular lobes that are highly diverging and separated by a very shallow U- or V-shaped interlobe area. The lingual root face is convex and bisected by a conspicuous nutritive groove.

Remarks. Although morphologically variable, we believe that the Tupelo Bay Formation teeth described above represent heterodonty within a single taxon. With respect to monognathic heterodonty, the anterior teeth have a narrow but fairly erect cusp and short distal heel (i.e., Fig. 17Y–Z & 17AA–BB). Teeth from lateral files are wider, with a broader and more distally inclined cusp and more

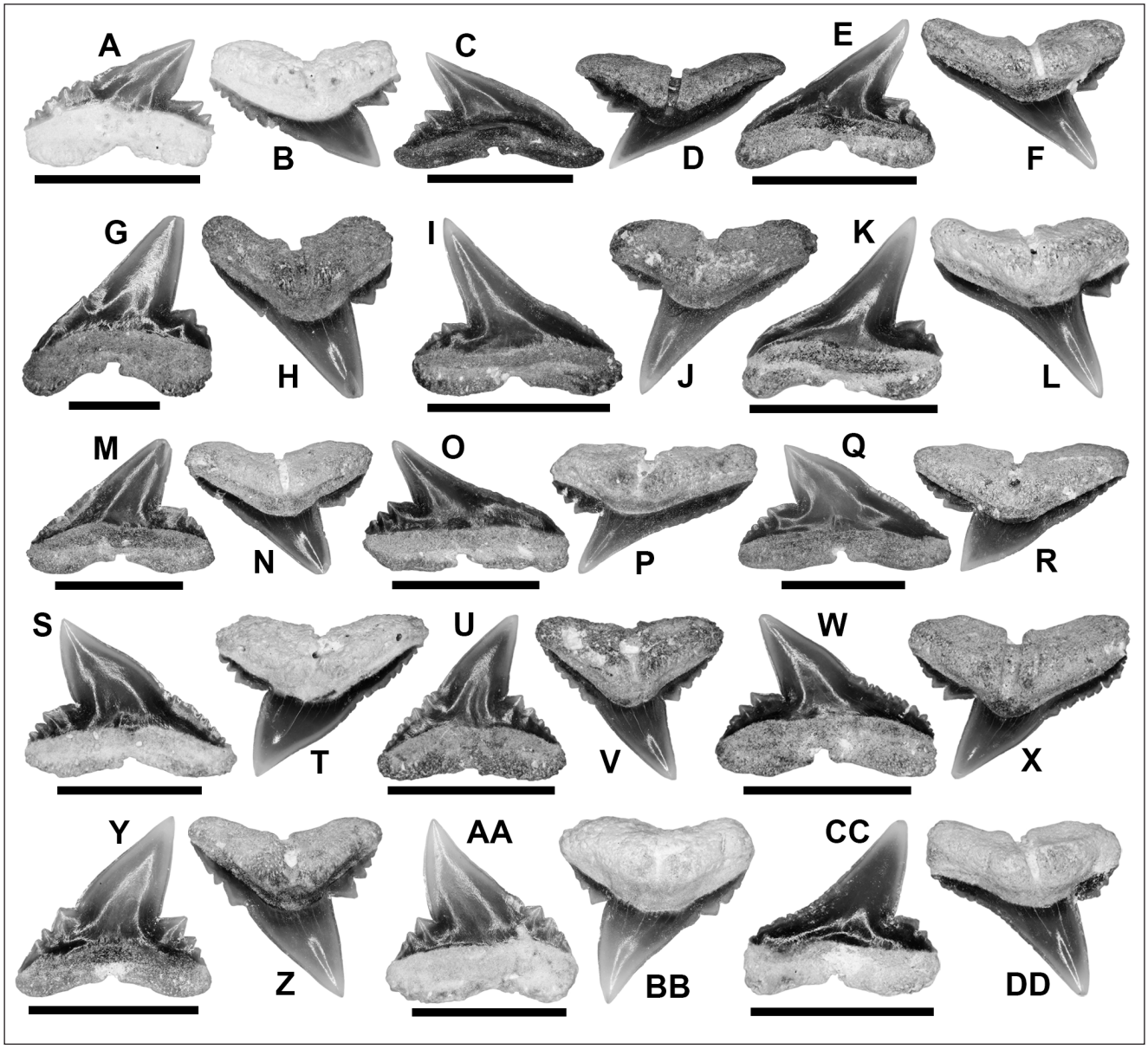

Fig. 17 - *Physogaleus* aff. *secundus* from the Tupelo Bay Formation. A-B) juvenile lateral tooth, SC2022.27.216, in labial (A) and lingual (B) views; juvenile lateral tooth (C-D), SC2022.27.233, in labial (C) and lingual (D) views; juvenile lower anterior tooth (E-F), SC2022.27.234, in labial (E) and lingual (F) views; upper right anterior tooth (G-H), SC2022.27.229, in labial (G) and lingual (H) views; juvenile lower anterior tooth (I-J), SC2022.27.224, in labial (I) and lingual (J) views; juvenile lower anterolateral tooth (K-L), SC2022.27.231, in labial (K) and lingual (L) views; upper lateral tooth (M-N), SC2022.27.217, in labial (M) and lingual (N) views; posterolateral tooth (O-P), SC2022.27.225, in labial (O) and lingual (P) views; upper lateral tooth (Q-R), SC2022.27.218, in labial (Q) and lingual (R) views; upper anterolateral tooth (S-T), SC2018.7.102, in labial (S) and lingual (T) views; lower(?) anterior tooth (U-V), SC2022.27.207, in labial (U) and lingual (V) views; lower(?) lateral tooth (W-X), SC2022.27.213, in labial (W) and lingual (X) views; upper anterior tooth (Y-Z), SC2022.27.206, in labial (Y) and lingual (Z) views; anterior tooth (AA-BB), SC2022.27.209, in labial (AA) and lingual (BB) views; lower lateral tooth (CC-DD), SC2022.27.210, in labial (CC) and lingual (DD) views. Scale bars: 5 mm.

elongated distal heel (i.e., Fig. 17S & 17C). The cusp height decreases but inclination increases towards the commissure (i.e., Fig. 17S, 17Q, 17A). Dignathic heterodonty is also evident with upper teeth having a wide cusp and a straight to convex mesial edge (i.e., Fig. 17Z, 17T, 17R). In contrast, lower teeth have a rather narrow cusp and conspicuously concave mesial edge (i.e., Fig. 17DD, 17L, 17P).

The teeth described above are superficially similar those of other carcharhiniform taxa co-occurring in the Tupelo Bay Formation. However, they can be separated from those of *Galeorhinus semiserratus* sp. nov. by their less thickened labial crown foot that is unornamented and does not overhang the root. The lack of serrations distinguishes these *Physogaleus* teeth from similarly sized specimens of

Galeocerdo. Upper teeth of *Negaprion gilmorei* never possess strong denticulation as occurs on the distal heel and often the lower part of the mesial edge of *P.* aff. *secundus*. Co-occurring *P.* aff. *contortus* (see above) teeth are larger and more robust, have finer and more numerous denticulation on the distal heel, and a conspicuously "twisted" cusp apex.

The taxon *P. secundus* was very widely distributed during the Eocene, having been reported from widely disparate locations in the USA (i.e., Case & Borodin 2000b; Ebersole et al. 2019; Ebersole & Cicimurri 2025), Europe (i.e., Van den Eekhaut & De Schutter 2009; Trif et al. 2019; Kovalchuck et al. 2023), Asia (Malyshkina et al. 2013; Malyshkina & Ward 2016; Popov et al. 2025), and Africa (i.e., Casier 1957; Dartevelle & Casier 1959; Boulemia & Adnet 2023).

Family Galeocerdonidae Poey, 1875
Genus *Galeocerdo* Müller & Henley, 1838

Galeocerdo clarkensis White, 1956

Fig. 18

2000a *Galeocerdo latidens* White, 1926 – Case & Borodin, p. 10, pl. 4, figs. 35–38.
2000b *Galeocerdo latidens* White, 1926 – Case & Borodin, p. 28 & 30, pl. 4, figs. 37–39.
2003 *G. alabamensis* Leriche, 1942 – Parmley & Cicimurri, p. 170–171, fig. 6 B.
2019 *G. clarkensis* White, 1956 – Ebersole et al., p. 103–105, fig. 104

Material: 18 teeth, including: SC2015.59.2, SC2018.7.12, SC2018.7.110, SC2018.7.111, SC2018.7.112, SC2022.27.266 (Fig. 18I–K), SC2022.27.267 (Fig. 18F–H), SC2022.27.268 (Fig. 18A–B), SC2022.27.269 (Fig. 17C–E), SC2022.27.270, SC2022.27.271, SC2022.27.272, SC2022.27.273 (Fig. 18R–T), SC2022.27.274, SC2022.27.27 (Fig. 17 O–Q), SC2024.17.6 (Fig. 18L–N), SC2024.17.7 (Fig. 18X–Z), SC2024.17.8 (Fig. 18U–W).

Description. The teeth are broad (up to 2 cm in mesio-distal width) and roughly triangular, although there is a distinctive angular distal crown margin. The crown has a long mesial cutting edge that intersects with a much shorter distal edge to form a sharply pointed cusp, which is rather high and narrow (mesio-distally). The mesial cutting edge is usually weakly sinuous with the medial portion varying in convexity (i.e., strongly or weakly convex), although some specimens have a uniformly convex edge. The mesial cutting edge is serrated, with the largest serrations occurring on the lower one half. However, serrations decrease in size both basally and apically, where they do not quite reach the cusp apex. The distal cutting edge ranges from vertical to inclined to varying degrees, is straight to moderately convex, and is serrated. The distal cutting edge serrations are of the same size as those on the basal or apical parts of the mesial cutting edge. The posterior one-third to one-half of the crown is comprised of a distal heel, and this forms a distinctive notch with the distal cutting edge. The cutting edge of the heel is sloping and very coarsely serrated, with serrations decreasing in size distally. All serrations are weakly compound (i.e., smaller serrations on the primary serrations). The labial crown face is flat to weakly convex, and the crown foot is rounded such that it overhangs the root, with a distinct furrow occurring at the crown/root juncture. The lingual face is strongly convex and the crown enameloid is smooth. There is a conspicuous transverse furrow at the crown/root juncture. The root is thick, with a robust transverse lingual swelling and medial boss. The boss is bisected by a wide, shallow, elongated nutritive groove that often bears a large foramen. Root lobes are short, rectangular, strongly divergent, and separated by a relatively shallow U- or V-shaped interlobe area.

Remarks. Numerous nominal fossil species have been assigned to *Galeocerdo*, but only six were recognized by Türtscher et al. (2021), including *G. aduncus* (Agassiz, 1835), *G. capellini* Lawley, 1876, *G. clarkensis* White, 1956, *G. eaglesomei*, White, 1955, *G. mayumbensis* Dartevelle & Casier, 1943, and extinct members of *G. cuvier* (Lesueur, 1822). In addition, Cicimurri et al. (2025b) recently named *G. platycuspidatum* based on Oligocene specimens from Mississippi, USA, and this taxon was later tentatively identified from the upper Eocene Yazoo Clay in Alabama (Cicimurri et al. 2025a). The Tupelo Bay Formation *Galeocerdo* teeth are identified as *G. clarkensis* because they are the same size, have the same gross morphology, and have weakly compound serrations. In contrast, teeth of middle Eocene *G. eaglesomei* have simple serrations (i.e., the primary serrations lack additional serrae) and the more convex mesial edge of Oligo-Pliocene *G. aduncus* is irregularly serrated (large and small serrations variously developed). Additionally, *G. eaglesomei* teeth generally lack a distinct notch marking the transition from distal cutting edge to distal heel. Teeth of Oligo-Miocene *G. mayumbensis* and Pliocene to modern-day *G. cuvier* attain larger overall sizes and have larger and

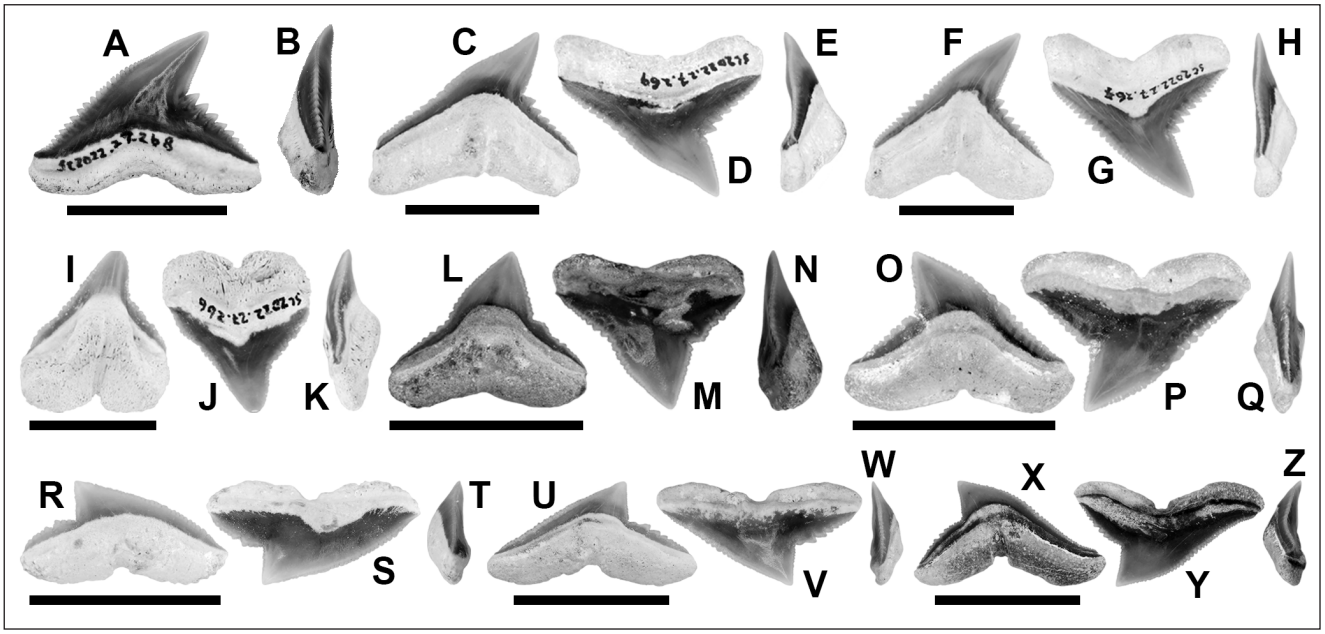

Fig. 18 - *Galeocerdo clarkensis* from the Tupelo Bay Formation.(A-B) lateral tooth, SC2022.27.268, in labial (A) and mesial (B) views; lateral tooth (C-E), SC2022.27.269, in lingual (C), labial (D), and mesial (E) views; anterolateral tooth (F-H), SC2022.27.267, in lingual (F), labial (G), and mesial (H) views; symphyseal tooth (I-K), SC2022.27.266, in lingual (I), labial (J), and mesial (K) views; juvenile anterior tooth (L-N), SC2024.17.6, in lingual (L), labial (M), and mesial (N) views; juvenile lateral tooth (O-Q), SC2022.27.275, in lingual (O), labial (P), and mesial (Q) views; posterior tooth (R-T), SC2022.27.273, in lingual R), labial (S), and mesial (T) views; posterolateral tooth (U-W), SC2024.17.8, in lingual (U), labial (V), and mesial (W) views; juvenile lateral tooth (X-Z), SC2024.17.7, in lingual (X), labial (Y), and mesial (Z) views. Scale bars: 1 cm.

more complexly serrated cutting edges compared to *Galeocerdo clarkensis*. Additionally, *G. mayumbensis* teeth have a relatively small cusp compared to tooth size, and the distal heel is strongly oblique to tooth height. Teeth of *G. platycuspidatum* differ from *G. clarkensis* by attaining much larger overall size, having a much wider but shorter cusp, and a distal heel that forms an obtuse angle with the distal cutting edge. Pliocene *G. capellini* is known by a single tooth that may be synonymous with *G. cuvier* (i.e., Applegate 1978; Türtscher et al. 2021), but in any case, teeth are apparently much larger than any specimen of *G. clarkensis* available to us. The Eocene taxon *G. aegyptiacus* Stromer, 1905 is difficult to interpret because a physical description is lacking, but the specimen originally illustrated (Stromer 1905: pl. XVI, fig. 4) has a more convex mesial cutting edge and narrower, more strongly inclined cusp compared to *G. clarkensis*.

We examined jaws of extant *G. cuvier* that represent three growth stages, with SC2000.120.10 representing the largest individual (approx. 45-cm gape), SC2020.53.18 the smallest (approx. 12-cm gape) and SC2020.53.4 of intermediate size (roughly 24-mm gape). Based on these jaws, the range of variation observed on Tupelo Bay Formation specimens represents, at least in part, monognathic heterodonty. A presumed symphyseal tooth is nearly symmetrical, with a slightly distally inclined cusp, and more angular distal margin (Fig. 18I–K). Within the remainder of the sample, tooth shape changes gradually towards the commissure, with overall tooth width increasing but height decreasing, and cusp inclination increasing (compare Figs. 18G, 18A, and 18S). With respect to dignathic heterodonty in *G. cuvier*, Cicimurri et al. (2025b) noted that cusp width was the same between the upper and lower dentitions, but the cusp length of upper teeth was slightly greater than that of lower teeth. Unfortunately, our sample size of *G. clarkensis* teeth is too small and variable for us to confidently distinguish upper from lower teeth.

Several small teeth in the sample are thought to be those of juvenile individuals (ontogenetic heterodonty) of *G. clarkensis*. These teeth measure 1 cm in width and have fewer distal heel denticles and less complex serrations compared to larger teeth, a phenomenon that Ebersole et al. (2019) and Cicimurri et al. (2025b) observed in the ontogenetic series of extant *G. cuvier* jaws at SC. It is interesting to note that, compared to the overall size of the tooth, the cusp of these smaller teeth is conspicuously shorter but wider than that of the larger teeth (compare

Figs. 18L, 18O, 18X to 18F & 18C). The small *Galeocerdo* teeth are easily differentiated from co-occurring *Galeorhinus semiserratus* sp. nov. and *Physogaleus* spp. by having mesial and distal serrations extending nearly to the cusp apex, and the serrations are compound. Additionally, the labial crown foot of *Galeocerdo* is thickened and overhangs the root, whereas that of *Physogaleus* is flat. Furthermore, the *Galeocerdo* teeth lack labial ornamentation as occurs on the crown foot of *Galeorhinus* teeth.

Galeocerdo clarkensis was based on teeth from the Priabonian Yazoo Clay of Alabama (White 1956), but the species was also confirmed from the Yazoo Clay of Louisiana (Ebersole & Cicimurri 2025), the Bartonian Gosport Sand of Alabama (Ebersole et al. 2019), and Moodys Branch Formation (Bartonian) of Alabama (MSC 43272) and Louisiana (Ebersole & Cicimurri 2025). A specimen reported by Westgate (1984) from the Crow Creek local fauna of Arkansas also appears to represent this species. Based on examination of *Galeocerdo* teeth included in accessions SC2004.34 and SC2013.43, teeth from Barnwell Group strata of Georgia (Clinchfield and overlying Dry Branch formations) reported by Case & Borodin (2000a) and Parmley & Cicimurri (2003) are *G. clarkensis*. Case & Borodin (2000b: pl. 4, figs. 37–39) identified *G. latidens* from the Lutetian Castle Hayne Formation of North Carolina, and these teeth are morphologically consistent with *G. clarkensis*, including development of compound serrations. The taxon may occur in the Dry Branch Formation (Priabonian) of South Carolina, but the material is too imperfectly preserved for specific identification (Cicimurri & Knight 2019). *Galeocerdo clarkensis* was recently identified in the Bartonian Bandah Formation of western India (Rana et al. 2021). *Galeocerdo clarkensis* differs from *Galeocerdo* sp. teeth occurring in the early Oligocene (NP23) Red Bluff Clay (overlying the Yazoo Clay) of Alabama (Ebersole et al. 2024) by its larger size, mesio-distally wider crown but smaller main cusp, and more numerous but smaller distal heel denticles.

Division BATOMORPHI Cappetta, 1980
Order **Rhinopristiformes** Naylor et al., 2012
Family Pristidae Bonaparte, 1838
Genus *Pristis* Linck, 1790

Pristis sp.
Fig. 19A–H

Material: partial rostrum and associated spines, SC2001.109.1 (Fig. 19A–D); two isolated spines, including SC2022.27.279, SC2022.27.280 (Fig. 19E–H).

Description. SC2001.109.1 is a partial rostrum that was described by Cicimurri (2007; formerly identified under the number SC2001.1) and assigned to *P. lathami* Galeotti, 1837. The isolated spines are elongated (roughly 12 cm) with approximately parallel anterior and posterior margins along some or nearly all of their length (Fig. 19C). Near the distal end, the anterior margin curves sharply a short distance to intersect with the posterior margin. Except for the distal tip, the anterior spine margin is convex, whereas the posterior margin is concave along the spine length (Fig. 19B & F). The dorsal and ventral surfaces are flat to weakly convex. In anterior/posterior view the spines can be straight or have a conspicuous ventral curvature (Fig. 16A). The distal tip of the spine is thin with a sharp anterior edge, and fine striations on the dorsal and ventral surfaces are oblique to spine length (Fig. 16G).

SC2022.27.279 and SC2022.27.280 are additional isolated rostral spines measuring up to 7.6 cm in length. These are comparable to the spines of SC2009.1.1, but they conspicuously differ in the degree of taper at the distal end. On these two spines, the anterior and posterior margins converge gradually to a sharp distal point, whereas on all the spines of SC2009.1.1, the anterior margin sharply curves posteriorly close to the distal tip. This morphology results in the spines having an abruptly truncated appearance. In contrast, the anterior margin of SC2022.27.279 and SC2022.27.280 tapers posteriorly (and is sharp) along a greater proportion of its length, resulting in a knife-like appearance. These latter spines also exhibit fine striations that are oriented oblique to spine length.

Remarks. In his description of SC2001.109.1, Cicimurri (2007) assigned the specimen to *Pristis lathami* based on the rostral spine morphology. However, Ebersole et al. (2019) noted the difficulty of speciating isolated *Pristis* spines based on their morphology, and we observed variation among the spines along the right and left sides of an extant *Pristis* rostrum (i.e., SC90.80.1). We therefore simply refer to SC2009.109.1 as *Pristis* sp. Although there are differences in spine morphology within our sample (compare Fig. 19A–D to 19E–H), this is within the range of variation exhibited by SC90.80.1 and the specimens are likely conspecific. As noted

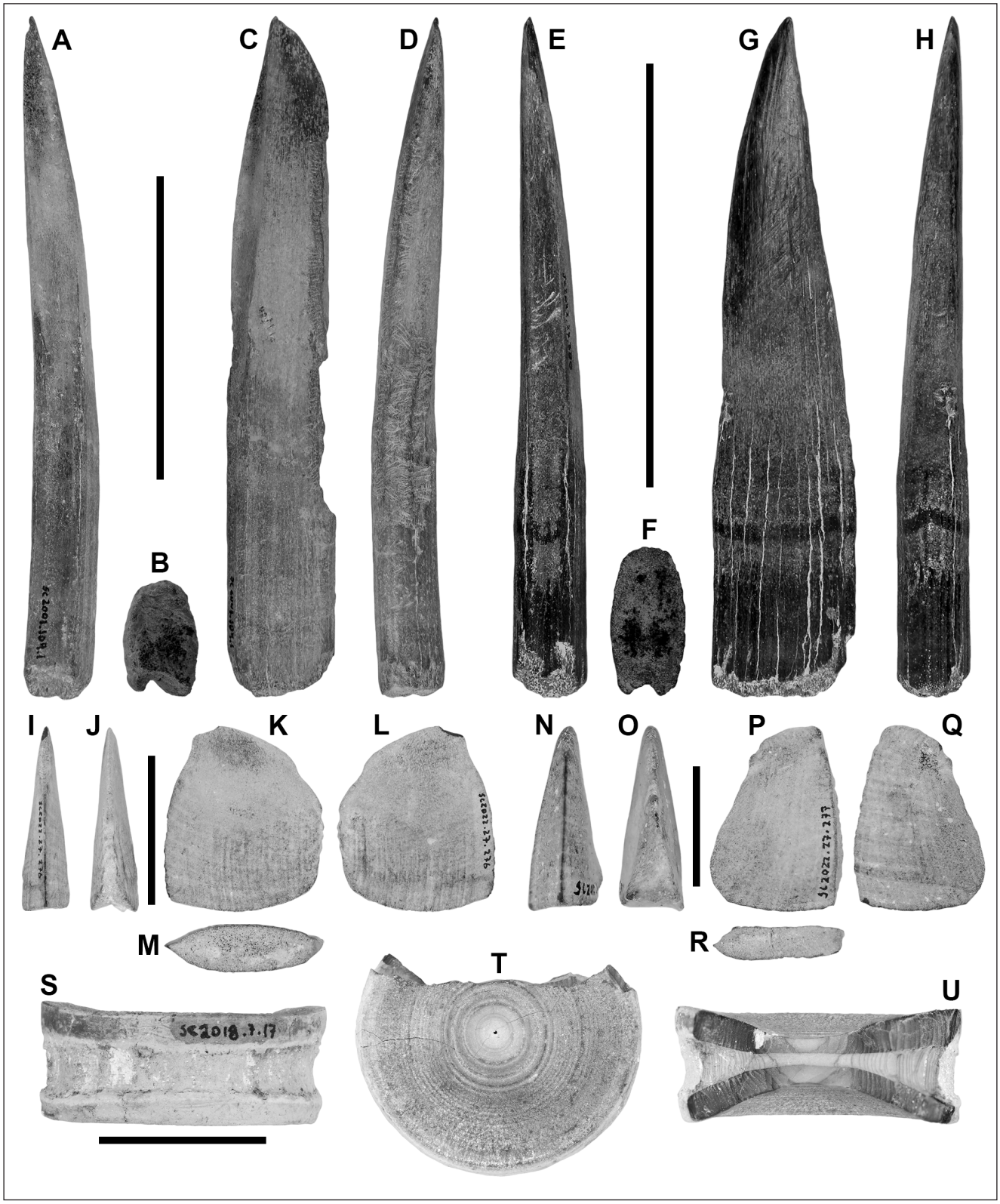

Fig. 19 - Pristidae from the Tupelo Bay Formation. A-H) *Pristis* sp., left rostral spine (A-D), SC2009.109.1, in posterior (A), basal (B), dorsal (C), and anterior (D) views; left rostral spine (E-H), SC2022.27.280, in posterior (E), basal (F), ventral (G), and anterior (H) views. I-R) *Propristis schweinfurthi*, right rostral spine (I-M), SC2022.27.276, in posterior (I), anterior (J), dorsal (K), ventral (L), and basal (M) views; right rostral spine (N-Q), SC2022.27.277, in posterior (N), anterior (O), ventral (P), dorsal (Q), and basal views (R). Pristidae indet. vertebral centrum (S-U), SC2018.7.17, in outer (S), articular (T), and cross-sectional (U) views. Scale bars: 1 cm in N-R, 2 cm in I-L & S-U, 5 cm in A-H.

by Cicimurri (2007), fine dorsal and ventral striations on the rostral spines (Fig. 19G) are probably related to their use in probing the coarse ocean bottom for prey. Several of the spines, particularly those of SC2009.109.1, exhibit multiple clusters of short, parallel grooves on parts of the anterior and/or posterior faces where significant dentine loss occurs (Fig. 19C–E). These ichnofossils are similar to marks identified as having been made by the radula of grazing chitons (i.e., De Gibert et al. 2007, Kázmér et al. 2015; Collareta et al. 2023).

The genus *Pristis* was widespread in the Atlantic and Gulf Coastal plains during the Eocene, and within the former, this taxon has been reported from the Castle Hayne Formation of North Carolina (Case & Borodin 2000b) and Ocala Limestone of Georgia (Case, 1981). Rostral spines also occur in the Clinchfield Formation of Georgia (i.e., SC2004.34.78). In the Gulf region, the genus is known from the Tallahatta and Lisbon formations and Gosport Sand of Alabama (Ebersole et al. 2019), the Gosport Sand/Moodys Branch Formation in Arkansas (Westgate 1984), Cane River (NP15), Cook Mountain (NP16), and Moodys Branch (NP17) formations and Yazoo Clay of Louisiana (Lancaster 1986; Manning & Standhard 1986; McPherson & Manning 1986; Ebersole & Cicimurri 2025), and Texas within the Lutetian Laredo Formation (Westgate 1989) and Lutetian-Bartonian Stone City Formation (Breard & Stringer 1999). We note that Case (1981) named *Pristis pickeringi* based on a single rostral spine from the Clinchfield Formation of Georgia. That specimen is difficult to evaluate based on the limited description and images provided (pl. 9, fig. 2), but it is similar to rostral spines of *Mesopristis osonensis* Farrés, 2003 (generically synonymized with *Anoxypristis* by Cappetta 2012) and *Anoxypristis mucrodens* (White, 1926; see also Asan et al. 2022). We did not observe comparable spines in the Clinchfield Formation collections at SC.

Genus *Propristis* Dames, 1883

Propristis schweinfurthi Dames, 1883

Fig. 19I–R

Material: three rostral spines, including: SC2022.27.276 (Fig. 19I–M), SC2022.27.277 (Fig. 19N–R), SC2022.27.278.

Description. The rostral spines are relatively short (up to 2.5 cm apico-basally), antero-posteriorly broad (slightly over 2 cm), and dorso-ventrally thin (about 7 mm). The anterior and posterior margins are roughly parallel for a short distance from the base, after which the anterior margin abruptly diverges towards the posterior margin. The posterior margin is sharp, and the distal end of the spine is developed into a thin, sharp blade. The basal one-third to one-half of the spine has a wrinkled texture that parallels the spine length, and very fine growth lines are also visible.

Remarks. *Propristis* rostral spines are easily separated from those of *Pristis* due to their shorter length, thinner profile, and sharper edges. Additionally, *Propristis* spines articulated to the rostrum via a shallow saddle-shaped depression (Fraas 1907), whereas *Pristis* spines were set in deep recesses (Cicimurri 2007). The apical edges of the spines are sharp, and oblique striations are visible on the dorsal and ventral surfaces of *Propristis* spines, indicating they were used in a similar manner as those of *Pristis* (i.e., for disturbing the sandy ocean floor for buried prey). Variable spine lengths (compare Fig. 19K to 19P) may reflect their location along the rostrum (i.e., shorter spines were likely located near the proximal end).

Propristis schweinfurthi was apparently uncommon in North America during the middle-to-upper Eocene, having only been reported from the Bartonian Gosport Sand in Alabama (Ebersole et al. 2019) and Moodys Branch Formation of Louisiana (Manning & Standhardt 1986; Ebersole & Cicimurri 2025), and the Priabonian Dry Branch Formation of Georgia (Case, 1981) and Yazoo Clay of Louisana (Breard & Stringer 1995). However, numerous specimens were recovered from the Riggins Mill Member of the Clinchfield Formation of Georgia (i.e., SC2004.34.82, SC2013.44.41). The taxon is well-documented in Egypt (i.e., Dames 1883; Asan et al. 2022) and has also been reported from Morocco (Adnet et al. 2010; Zouhri et al. 2021) and Tunisia. In Europe, rostral spines have been identified in Spain (Farrés & Fierstine 2009) and England (Kemp et al. 1990).

Pristidae gen. indet.

Fig. 19S–U

Material: two vertebral centra, including: SC2015.59.27, SC2018.7.17 (Fig. 19S–U).

Remarks. Although the centra are broken they appear to have maintained their original shape. Both have a circular anterior/posterior outline, and these surfaces are concave (Fig. 19 U). The anterior and posterior corpora calcarea form thick centrum rims, and the outer surfaces are ablated such that the specimens have a constricted appearance (Fig. 19S). There are no dorsal, lateral, or ventral fenestrae, nor lamellae within intermedialia. The anterior and posterior surfaces exhibit conspicuous concentric growth lines (Fig. 19T & 19U), and these suggest that the individuals represented by these specimens were approximately 26 years of age at death. Although we are unable to assign these two centra to *Pristis* or *Propristis*, we include them here for completeness.

Order **Myliobatiformes** Compagno, 1973
Suborder **Myliobatoidei** Compagno, 1973
Family Myliobatidae Bonaparte, 1838
Genus *Aetomylaeus* Garman, 1908

"Aetomylaeus" sp.
Fig. 20A–H

1981 *Myliobatis* sp. – Case, p. 72, pl. 9, fig. 10.
2000a *Myliobatis* sp. – Case & Borodin, p. 12, pl. 5, figs. 51–55.
.

Material: three dentitions, including SC2022.27.299 (Fig. 20A–D), SC2022.27.300, SC2022.27.301; four teeth including SC2022.27.302 (Fig. 20E–H), SC2022.27.303, SC2022.27.304, SC2022.27.305.

Description. The symphyseal teeth are much wider (mesio-distally) than long (labio-lingually), and largest specimens available to us measure approximately 2.8 cm and 1.0 cm in these dimensions. In occlusal view, labial and lingual crown margins are parallel and the crown ranges from straight to arcuate. The lateral angles (for articulation with lateral teeth) are oblique and medially located. In labial/lingual views, the crowns of unworn teeth are high, particularly medially, but taper laterally, and the occlusal surface can be straight or convex. In profile view the crown is roughly vertical, although the labial face is concave and the lingual face convex. The labial face is ornamented with a reticulated network of ridges that merge apically into anastomosing vertical ridges, whereas the lingual face is finely tuberculated. The labial and lingual crown foot can be straight or convex, and the lingual crown foot is marked by a very thin and sharp transverse ridge. The crown overhangs the root labially and laterally, with the labial and lingual root faces being strongly oblique in the lingual direction. There are numerous tiny labial and lingual foramina occurring immediately below the crown. The basal attachment surface is rather flat and subdivided into numerous closely spaced, parallel, narrow lamellae by nutritive grooves. The lingual side of the root projects distally well beyond the crown foot.

Lateral teeth are longer than wide (i.e., 6 mm and 2 mm, respectively), and although they appear to have a diamond-shaped occlusal outline, they are six-sided with very narrow labial and lingual faces. The roots are divided into two or three lamellae by one or two nutritive grooves.

Remarks. Upper and lower symphyseal teeth are represented in our sample, with the upper teeth having an arcuate occlusal outline, highly convex occlusal surface, and straight crown foot and basal root surface. In contrast, lower symphyseal teeth (Fig. 20E–H) have a straight occlusal outline and are thickest medially due to the very convex crown foot (resulting in a basally convex root). Three upper dentitions are available to us (Fig. 20A–D) all show that the overall occlusal surface is convex both labio-lingually (Fig. 20C) and mesio-distally (Fig. 20D). The anterior ends of the dentitions are marked by a flat surface that was the triturating area with the lower dentition. The individual teeth are very tightly connected to one another. The convex lingual crown face of a tooth crown is enveloped by the concave labial surface of the succeeding tooth, and the thin and protruding labial crown foot fits within a groove and overlaps the transverse ridge at the lingual crown foot of the preceding tooth. Additionally, the tubercles on the lingual crown face articulate with the pitted surface of the labial face of the succeeding tooth. A single file of lateral teeth is preserved on these specimens (Fig. 20B), but the distal margins of these teeth are not preserved well enough to determine if one or more additional distal files were present.

"*Aetomylaeus*" is common in the Lisbon Formation and Gosport Sand of Alabama (Ebersole et al. 2019), and Ebersole & Cicimurri (2025) reported numerous teeth from the Cook Mountain and Moodys Branch formations and Yazoo Clay of Louisiana. Additional specimens were identified in the Priabonian Dry Branch Formation of South

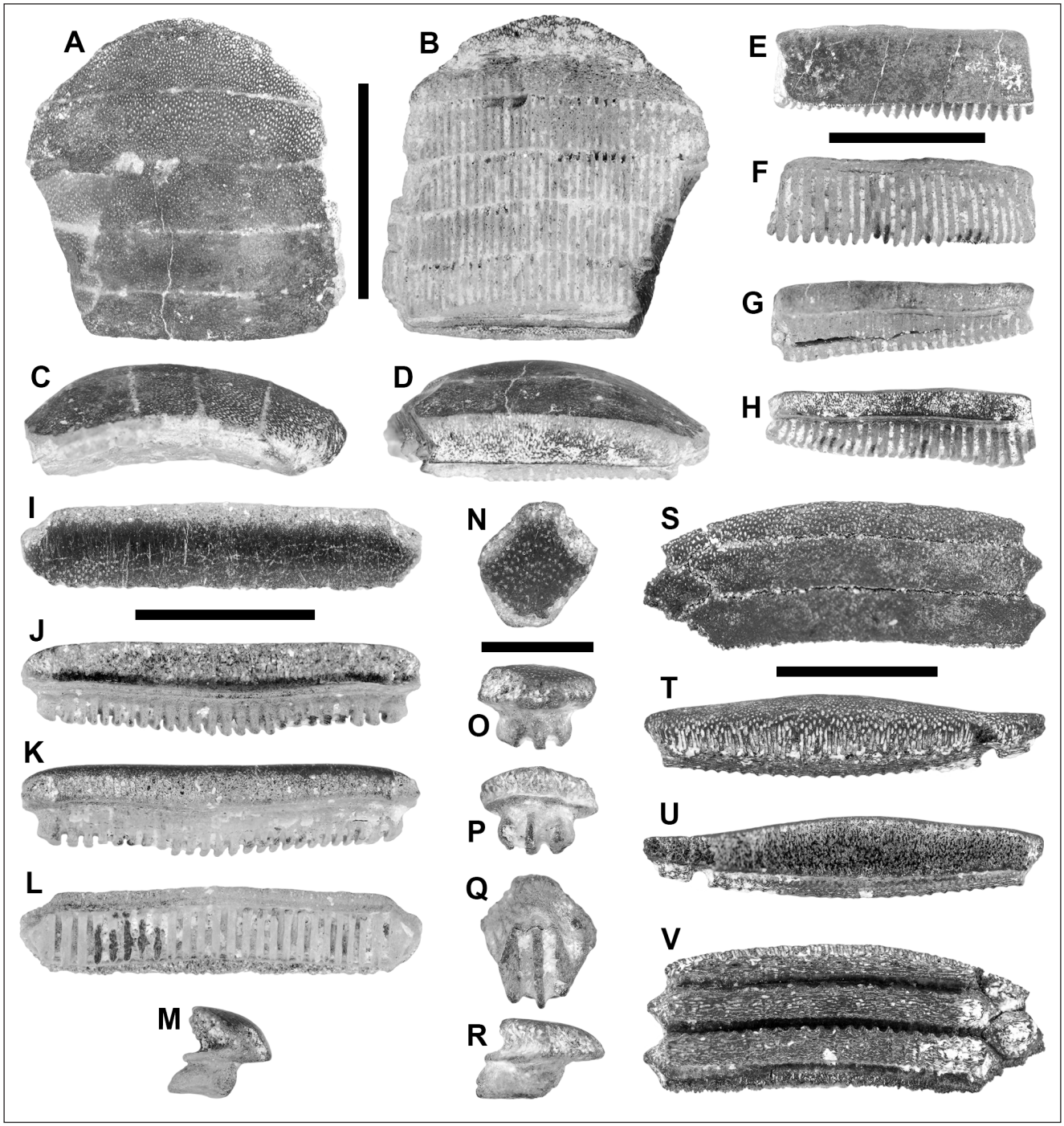

Fig. 20 - Myliobatidae from the Tupelo Bay Formation. A-H) "*Aetomylaeus*" sp., upper dentition (A-D), SC2022.27.299, in occlusal (A), basal (B), left lateral (C), and labial (D) views; lower symphyseal tooth (E-H), SC2022.27.302, in occlusal (E), basal (F), labial (G), and lingual (H) views. I-V) "*Myliobatis*" sp., lower symphyseal tooth (I-M), SC2022.27.284, in occlusal (I), lingual (J), labial (K), basal (L), and right lateral (M) views; lateral tooth (N-R), SC2022.27.287, in occlusal (N), labial (O), lingual (P), basal (Q), and profile (R) views; upper? dentition (S-V), SC2022.27.286, in occlusal (S), lingual (T), labial (U), and basal (V) views. Scale bars: 5 mm in N-R, 1 cm in I-M & S-V, 2 cm in A-H.

Carolina (Cicimurri & Knight 2019). The taxon was likely more widespread during the Eocene than is currently known, as we believe that the taxon has frequently been misidentified as *Rhinoptera* or *Myliobatis*. For example, a partial lower dentition purportedly from the Ocala Limestone of Georgia was identified by Case (1981) as *Myliobatis* sp. His description lacks detail, but the illustrated specimen (pl. 9, fig. 10) clearly shows characteristic ornament on the labial face and lateral teeth that are longer than wide, which is consistent with our "*Aetomylaeus*" sp. At least two of the dentitions identified as

Myliobatis sp. by Case & Borodin (2000a: pl. 5, fig. 51 & 53) that were purportedly recovered from the Dry Branch Formation (Irwinton Sand) of Georgia clearly show diamond-shaped lateral teeth and are therefore regarded by us to be "*Aetomylaeus*" sp. Specimens at SC demonstrate that the genus was quite common in the Clinchfield Formation of Georgia (i.e., SC2004.34.45 and SC2004.34.46).

Herein we follow Cicimurri et al. (2025b) by placing the generic name *Aetomylaeus* in quotations to signify that, although the specimens we examined are like those of extant *Aetomylaeus*, molecular divergence times indicate that the genus did not diverge from a common ancestor until sometime during the Miocene (i.e., Villalobos-Segura & Underwood 2020). Whichever taxon the Tupelo Bay Formation teeth represents, it was geographically widespread as teeth have been reported from middle Eocene strata of Russia (Popov et al. 2025).

Genus *Myliobatis* Cuvier, 1816

"Myliobatis" **sp.**

Fig. 20I–V

Material: partial dentition, including SC2022.27.286 (Fig. 20S–V); eight teeth, including SC2022.27.284 (Fig. 20I–M), SC2022.27.285, SC2022.27.287 (Fig. 20N–R), SC2022.27.288 (5 specimens).

Description. Symphyseal teeth are mesio-distally much wider than long, with the largest specimen in our sample measuring 2.3 cm in mesio-distal width. In occlusal view, the labial and lingual crown margins are parallel, and the crown is straight. The lateral angles are sharp and roughly 90º and medially located. In labial/lingual views the crown is thickest medially, and the occlusal surface is straight or convex. In profile view the crown may be vertical or appear lingually inclined due to oblique labial and lingual faces. The labial face may be flat or weakly concave, whereas the lingual face is flat or weakly convex. The labial and lingual faces have a highly tuberculated appearance. The labial and lingual crown foot can be straight or convex, and the lingual crown foot is marked by a shelf-like transverse ridge. The crown overhangs the root labially and laterally, with the labial and lingual root faces being slightly oblique in the distal direction. There are numerous tiny labial and lingual foramina occurring immediately below the crown. The basal attachment surface is rather flat and subdivided into numerous closely spaced, parallel, narrow lamellae by nutritive grooves. The lingual side of the root projects distally slightly beyond the transverse ridge.

The crowns of lateral teeth are approximately as wide mesio-distally as long and appear to be four-sided with a squared occlusal outline, but they are six-sided with narrow labial and lingual faces. The largest tooth in our sample measures 6 mm in mesio-distal width. All the teeth in our sample are worn to some degree, and the labial face is inclined whereas the lingual face is typically vertical. In profile view the crown is thin labially but increases in height lingually. The labial and lingual faces are highly crenulated. There is a distinctive shelf-like transverse ridge at the lingual crown foot. The roots can be divided into three or four basal lamellae by two or three nutritive grooves. The labial and lingual root faces are oblique, with the lingual face extending slightly beyond the transverse ridge.

Remarks. We utilized the dentition of an extant *Myliobatis californica* (Mitchill, 1815) (MSC 42594) to determine that upper and lower symphyseal teeth are represented in the Tupelo Bay Formation sample. Lower teeth have a nearly straight occlusal outline (Fig. 20I), flat occlusal surface (Fig. 20J), and medially convex crown foot and basal root surface (Fig. 20K). SC2022.27.286 is a partial upper dentition consisting of five articulated teeth. This specimen shows that individual teeth are convex mesio-distally (Fig. 20U) and that the overall occlusal surface is convex labio-lingually (Fig. 20V). Individual teeth are very tightly connected to one another, and in occlusal view the crown margins of each tooth are irregular (Fig. 20S). Teeth articulate such that the lingually inclined lingual crown face overlaps the labial face of a succeeding tooth, and the sharp labial crown foot of this succeeding tooth overlaps the shelf-like lingual transverse ridge and fits within the thin lingual furrow of the preceding tooth (Fig. 20J, 20K, 20M). Additionally, the tubercles on the labial and lingual crown faces interconnect via interstitial spaces of the preceding and succeeding teeth. A single lateral file is preserved on SC2022.27.286, but the angular distal margins of these teeth (Fig. 20N & 20S) indicate that at least one additional row was present.

"*Myliobatis*" sp. symphyseal teeth can be differentiated from those of "*Aetomylaeus*" sp. by their more irregular occlusal outline, sharp 90º lateral

angles, shelf-like lingual transverse ridge, and more vertical root faces with less elongated distal lobes. Lateral teeth of "*Myliobatis*" sp. have a rhomboidal outline in occlusal view and are about as long as they are wide, whereas those of "*Aetomylaeus*" sp. are much longer than wide and have a thin diamond-shaped outline.

Herein we utilize the term "*Myliobatis*" for the reason outlined above for "*Aetomylaeus*". The Tupelo Bay Formation "*Myliobatis*" sp. teeth compare well with those from the Bartonian Gosport Sand of Alabama that Ebersole et al. (2019) assigned to "*Myliobatis*" sp. 2. *Myliobatis* sp. teeth having highly irregular occlusal margins, like those of the Tupelo Bay Formation and Gosport Sand specimens, were recently reported from the Cook Mountain Formation of Louisiana (Ebersole & Cicimurri 2025) and middle Eocene deposits of Russia (Popov et al. 2025). It is difficult to establish the middle-to-late Eocene geographic range of the taxon, even within the southeastern/south-central USA, as specimens are often misidentified. For example, material that Westgate (1984, 1989) called *Myliobatis* appears to represent a *Rhinoptera*-type ray (see below). Additionally, teeth that Case (1981) identified as *Myliobatis* sp. are assigned by us to "*Aetomylaeus*" sp. and "*Rhinoptera*" sp. Case & Borodin (2000b) identified *Myliobatis* sp. from the Lutetian Castle Hayne Limestone of North Carolina, but the poorly preserved specimen is comparable to "*Rhinoptera*" sp. (see below). Additional pecimens at SC (i.e., SC2013.44.50) show that the taxon "*Myliobatis*" was an uncommon component in the Clinchfield Formation (Riggins Mill Member) paleofauna of Georgia.

Family Rhinopteridae Jordan & Evermann, 1896
Genus *Rhinoptera* Cuvier, 1829

"Rhinoptera" sp.

Fig. 21A-T

1981 *Myliobatis* sp. – Case, p. 72, pl. 9, fig. 8.
1981 *Rhinoptera daviesi* (Woodward, 1889) – Case, p. 71-72, pl. 9, fig. 7.

Material: 17 teeth, including SC2015.59.25, SC2015.59.26 (2 specimens), SC2018.7.16, SC2018.7.130, SC2018.7131, SC2018.7.132, SC2022.27.289, SC2022.27.290 (Fig. 21A-E), SC2022.27.291, SC2022.27.292, SC2022.27.293 (Fig. 21F-J), SC2022.27.294, SC2022.27.295, SC2022.27.296 (Fig. 21K-O), SC2022.27.297, SC2022.27.298 (Fig. 21P-T).

Description. Although the teeth are of variable width, with some specimens being three times wider than long and others of roughly equal proportions, they share several morphological features. In occlusal view, the labial and lingual crown margins are parallel, and the crown is straight, slightly convex, or sinuous. The lateral angles are sharp, range from acute to slightly obtuse, and medially located. In labial/lingual views, the crown of unworn teeth is of uniform thickness, and the occlusal surface is straight or convex. In profile view the crown has a square outline, but the outline of worn teeth is rectangular. The vertical labial face is flat but highly crenulated with robust vertical ridges. This ornamentation is overprinted by a much finer network of anastomosing ridges. The lingual face is also vertical and flat, and ornamentation is similar to that on the labial face but less developed. The labial and lingual crown foot can be straight or convex, and the lingual crown foot is marked by a thick and rounded transverse ridge. The crown overhangs the root labially and laterally, with the labial and lingual root faces being vertical to very slightly oblique in the distal direction. There are numerous tiny labial and lingual foramina occurring immediately below the crown. The basal attachment surface is rather flat, and nutritive grooves subdivide it into numerous closely spaced, parallel, narrow lamellae. The lingual side of the root does not project beyond the lingual transverse ridge. The largest symphyseal tooth in our sample measures 3.3 cm in mesio-distal width and 6.6 cm labio-lingually.

Remarks. Using extant *Rhinoptera bonasus* (Mitchill, 1815) (i.e., MSC 42598, SC88.120.1) as a model, we determined that very wide Tupelo Bay Formation "*Rhinoptera*" sp. teeth are from symphyseal files (Fig. 21A-E). Furthermore, those specimens having a convex labial appearance (both the crown and root) likely represent the upper dentition (Fig. 21B & 21E). Lateral teeth are distinguished by their higher mesial side compared to distal side (i.e., Fig. 21J, 21L, 21Q), and the root lamellae are oblique to crown width (Fig. 21 I). The wider, more proximally located lateral teeth, can be straight or convex in labial view, which may serve to separate these into upper (convex i.e., Fig. 21G) and lower (straight) files. The specimens in our sample show that the dentition of this extinct species also consisted of a row of wide symphyseal teeth that was flanked by multiple rows of lateral teeth, and the width of lateral files became progressively narrower

towards the commissure (compare Fig. 21G, 21O, 21Q). The distal-most lateral tooth (Fig. 21P-T) is five-sided, with the mesial side being angular (articulating with another tooth) and the distal side straight labio-lingually, marking the edge of the dentition (Fig. 21P). Although the teeth articulated with each in a similar way to those of "*Aetomylaeus*" sp. and "*Myliobatis*" sp., they must not have been as tightly connected with each other, as no fossil articulated dentitions from North America are known to us.

"*Rhinoptera*" sp. symphyseal teeth can be differentiated from those of Tupelo Bay Formation "*Aetomylaeus*" sp. and "*Myliobatis*" sp. by the combination of vertical crown faces with highly wrinkled surfaces, shorter, thicker and highly convex lingual transverse ridge, low root with vertical to near-vertical labial and lingual faces, and lingual root lobes that do not extend beyond the crown foot. Lateral teeth of "*Rhinoptera*" sp. are easily distinguished by their crown thickness, which is greater mesially than distally, and root lamellae that are oblique to crown width.

"*Rhinoptera*" sp. is very common in Claiborne Group strata of Alabama (Ebersole et al. 2019) and it occurs in the Cook Mountain (NP16) and Moodys Branch (NP17) formations and Yazoo Clay of Louisiana (Ebersole & Cicimurri 2025). Specimens housed at SC demonstrate that the taxon is common in the Riggins Mill Member of the Clinchfield Formation of Georgia (i.e., SC2013.44.53). The taxon was probably more widespread in the southern USA during the Eocene than is currently known, as at least some material has been misidentified as *Myliobatis* (Westgate 1984; 1989). Case (1981) identified *Myliobatis* sp. from the Dry Branch Formation of Georgia, but his illustrated specimen (pl. 9, fig. 8) is consistent with our concept of "*Rhinoptera*" sp. An additional specimen reported by Case (1981) is somewhat problematic based on his identification as *Rhinoptera daviesi* (Woodward, 1889), as this species has teeth with a characteristically concave enameloid-covered occlusal surface. However, the description provided by Case (1981: p. 72) and his illustration of the specimen (pl. 9, fig. 7) indicates it is a highly worn "*Rhinoptera*" sp. lateral tooth. Case & Borodin (2000b) identified a partial tooth from the Castle Hayne Limestone as *Myliobatis* sp., but its basal and occlusal outlines are also consistent with our concept of "*Rhinoptera*" sp. Numerous pecimens at SC demonstrate that "*Rhinoptera*" sp. was abundant in the Clinchfield Formation of Georgia (i.e., SC2004.34.90 and SC2013.44.53).

Myliobatiformes gen. et sp. indet.

Fig. 21U-W

Material: 7 caudal spines, including SC86.56.4, SC2015.59.39 (2 specimens), SC2018.7.22, SC2022.27.281, SC2022.27.282, SC2022.27.283 (Fig. 21U-W).

Description. Specimens consist of incomplete elongated caudal fin spines (i.e., stings) that are widest at the proximal end but taper distally to a point. Our reconstructed dimensions indicate lengths to at least 15 cm. In profile view, the spines are dorso-ventrally compressed, and in transverse section the dorsal and ventral surfaces are convex. The spines are thinnest (dorso-ventral) and widest (laterally) at the proximal end where the spine inserted into connective tissue. Nearly the entirety of the dorsal surface is covered with a thin layer of enameloid that is highly wrinkled parallel to spine length (Fig. 21U). Additionally, one to four longitudinal grooves extend along the surface, but their length is variable and they may not reach the distal tip. The ventral surface is very convex and lacks enameloid, and there can be a medial longitudinal furrow (Fig. 21W). The lateral margins of the spine are straight, and each bears a row of barbs along nearly the entire length (Fig. 21U & 21V). Although these barbs are smallest proximally, where they begin less than 2 cm from the tip of the spine, and they quickly enlarge to a size maintained to the distal end of the spine. Each barb is proximally directed, sharply pointed, and their distal edge exhibits a conspicuous angularity (Fig. 21W).

Remarks. Although extant *Aetomylaeus* spp. lack caudal spines (Compagno & Last 1998), the

Fig. 21 - Myliobatiformes from the Tupelo Bay Formation. A-T), "*Rhinoptera*" sp., symphyseal tooth (A-E), SC2022.27.290, in occlusal (A), labial (B), profile (C), basal (D), and lingual (E) views; proximal lateral tooth (F-J), SC2022.27.293, in occlusal (F), labial (G), mesial (H), basal (I), and lingual (J) views; distal lateral tooth (K-O), SC2022.27.296, in occlusal (K), labial (L), mesial (M), basal (N), and lingual (O) views; ultimate lateral tooth (P-T), SC2022.27.298, in occlusal (P), labial (Q), mesial (R), basal (S), and distal (T) views. Myliobatidae indet. caudal spine (U-W), SC2022.27.283, in dorsal (U), right lateral (V), and basal (W) views. Scale bars: 5 mm in K-T, 1 cm in A-J & U-W.

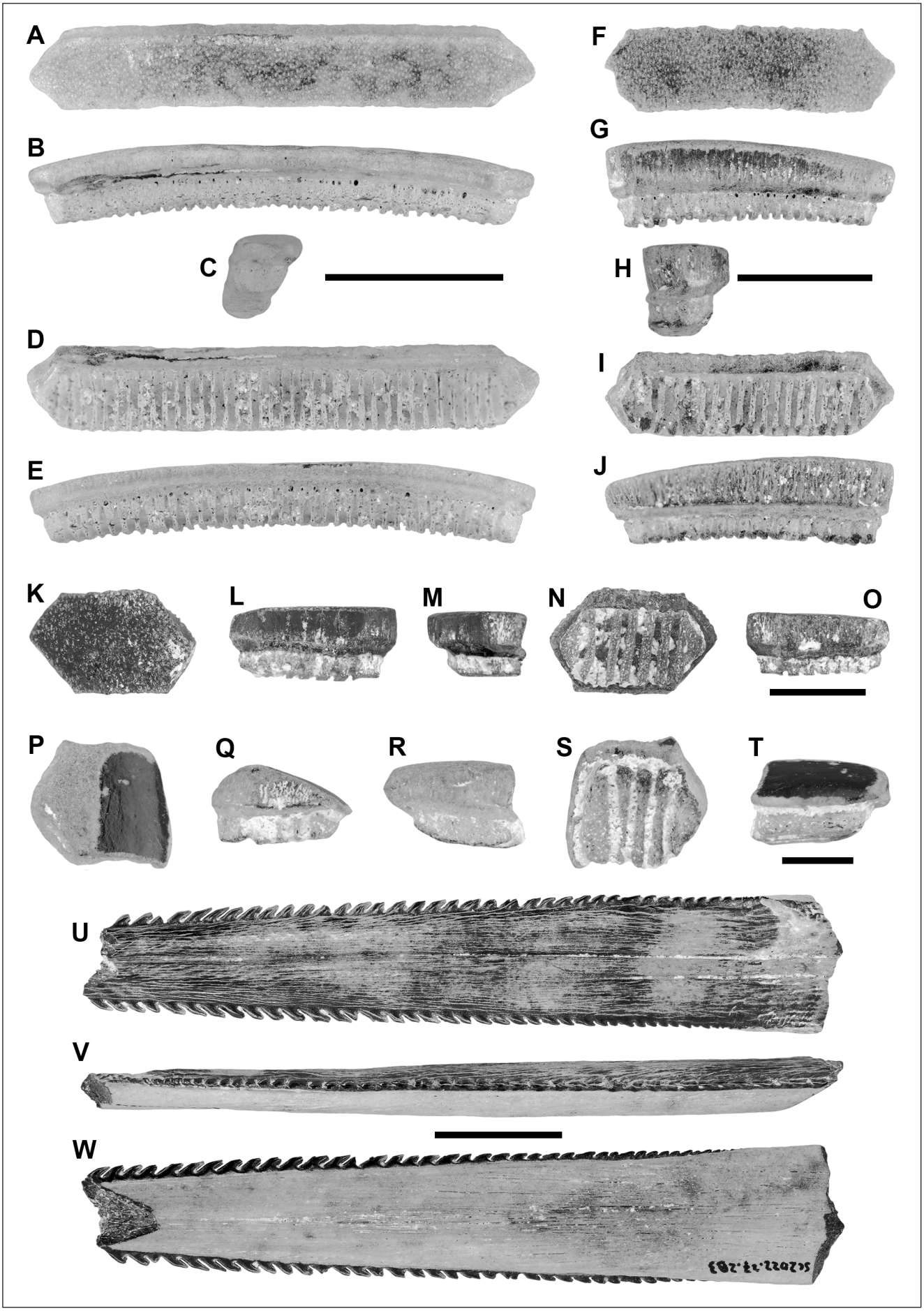

Fig. 21

Tupelo Bay Formation specimens cannot be assigned to a particular taxon with confidence, as living representatives of *Myliobatis* and *Rhinoptera* possess such structures (Hovestadt & Hovestadt-Euler 2013). However, all the spines available to us are similar with respect to the shape of the lateral denticles, and they may be congeneric.

Class **OSTEICHTHYES** Huxley, 1880
Subclass ACTINOPTERYGII *sensu* Goodrich, 1930
Subdivision TELEOSTEI Müller, 1846
Cohort ELOPOMORPHA Greenwood et al., 1966
Order Elopiformes Greenwood et al., 1966
Family Phyllodontidae Dartevelle & Casier, 1943
Genus *Egertonia* Cocchi, 1864

Egertonia isodonta Cocchi, 1864
Fig. 22A-C

Material: One tooth stack, including SC2022.27.321.

Description. The single specimen available to us consists of a column of three stacked teeth. The individual teeth are low with a slightly convex occlusal surface (Fig. 22A), the occlusal outline is roughly circular (Fig. 22B) and measures 4 mm across, and they consist only of a thick enameloid crown with open pulp cavity (Fig. 22C).

Remarks. The specimen is consistent with the individual stacks of teeth that comprise the pharyngeal plates of *Egertonia isodonta* and are therefore assigned to this taxon. Based on the wear that is evident, which is oblique to crown height (Fig. 22A & 22B), the stack of teeth may have been located near the margin of the tooth plate. This fish was common in the middle Eocene environments of the Lisbon Formation and Gosport Sand of Alabama (Ebersole et al. 2019), and it has also been reported from the Lutetian Laredo Formation of Texas (Westgate 1989) and Bartonian Moodys Branch Formation of Louisiana (Ebersole & Cicimurri 2025). The oldest record of the species in North America appears to be in the Paleocene of South Carolina (Weems 1998), but SC2022.27.321 currently represents the youngest occurrence.

Order **Albuliformes** Greenwood et al., 1966
Family Albulidae Bleeker, 1859
Genus *Albula* Gronow, 1763

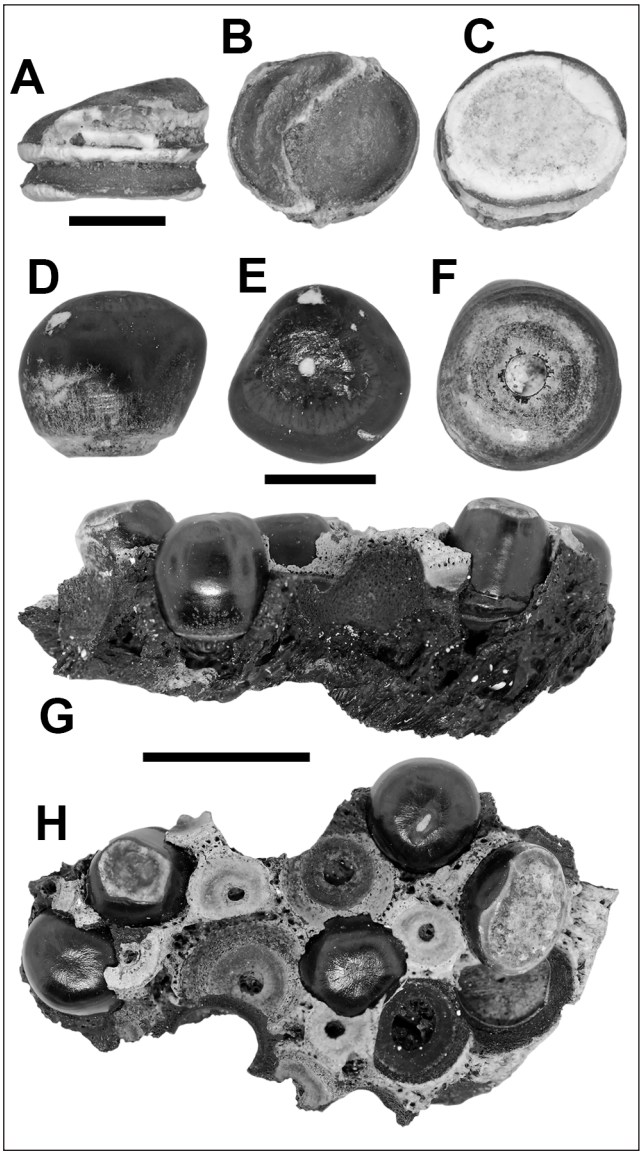

Fig. 22 - Teleost fishes from the Tupelo Bay Formation. A-C) *Egertonia isodonta*, partial tooth stack, SC2022.27.321, in profile (A), oral (B), and aboral (C) views. D-H) *Albula oweni*, tooth (D-F), SC2022.27.322, in profile (D), occlusal (E), and basal (F) views; pharyngeal bone (G-H), SC2009.28.1, in profile (G) and occlusal (H) views. Scale bars: 2 mm in A-C, 5 mm in D-E, 1 cm in G-H.

Albula oweni (Owen, 1845)
Fig. 22D-H

1845 *Pisodus oweni* – Owen, p. 138, pl. 47, fig. 3.
1901 *Albula oweni* (Owen, 1845) – Woodward, p. 108, pl. 3, figs. 3-5

Material: one jaw with teeth, including SC2009.28.1 (Fig. 22G-H); three teeth, including SC2022.27.322 (Fig. 22D-F), SC2022.27.323, SC2022.27.324.

Description. Specimen SC2009.28.1 consists of a partial jawbone containing multiple teeth. Sev-

eral teeth are fully formed, whereas others were still developing and are enclosed within the bone. These latter teeth consist of only a thick, highly convex enameloid cap with an open pulp cavity. Unworn, fully formed teeth are high, completely enameloid-covered, and have a convex occlusal surface (Fig. 22G). In contrast, teeth exhibiting slight *in vivo* wear have a window worn through the enameloid that reveals the internal dentine (Fig. 22H). Significantly worn teeth have a flat occlusal surface consisting of exposed dentine. The lateral faces of fully formed teeth taper basally, and alveoli within the jawbone indicate teeth have a circular basal pulp cavity framed by a thick wall of dentine (Fig. 22H).

SC2022.27.322 is a large and unworn isolated tooth that is comparable to teeth preserved with SC2009.28.1. The enameloid on the occlusal surface is highly convex and bears fine radiating wrinkles that do not meet the crown margins (Fig. 22E). In profile view the crown tapers basally (Fig. 22D). The crown is roughly circular in occlusal view and measures 9 mm in greatest dimension, and a deep pulp cavity is visible in basal view (Fig. 22F).

Remarks. The teeth in our sample are large and basally tapering, features that are consistent with teeth of *Albula oweni* reported from Eocene strata elsewhere (Weems 1999; Ebersole et al. 2019; Trif et al. 2021). The unerupted teeth of *A. oweni* differ from those of *Egertonia isodonta* (see above) by their more convex profile and thicker enameloid. Isolated *A. oweni* teeth are represented in the Clinchfield Formation collections at SC (i.e., SC2004.34.106 and SC2013.44.65).

Superorder **Acanthopterygii** Greenwood et al., 1966

Order **Istiophoriformes** Betancur-R et al., 2013

Family Sphyraenidae Berg, 1958

Genus *Sphyraena* Walbaum, 1792

Sphyraena sp.

Fig. 23

Material: six teeth, including: SC2015.59.30 (2 specimens), SC2015.59.31, SC2015.59.43 (Fig. 23A-E), SC2018.7.19, SC2018.7.133 (Fig. 23F-I).

Description. Two morphologies are represented, the first including teeth that are tall (at least 12 mm high) and highly laterally compressed. The anterior and posterior margins are formed into sharp, finely serrated carinae that extend from the base to the apex. The teeth are longest (antero-posterior) basally where the carinae are nearly vertical and parallel. The carinae are most convex medially, after which they quickly converge apically. The labial and lingual faces are weakly convex (Fig. 23D). Well-preserved specimens exhibit a thin layer of finely striated enameloid, with striations being more pronounced basally (Fig. 23A & 22C). In anterior/posterior view the crown is vertical to weakly medially curved (Fig. 23B). In basal view the attachment surface is concave, and the outline is elliptical (Fig. 22E).

The second morphology includes teeth that are tall (up to 18 mm high), erect, and have a sinuous profile. The anterior margin is formed into a sharp, very finely serrated carina that extends from the tooth base to the crown apex (Fig. 23H). This carina is most convex at its basal one-half, after which it is posteriorly directed and may or may not have a slight vertical rise to the apex. The posterior face is highly convex, thickest basally but thinning apically (Fig. 23G), and in profile the margin is straight to concave along the lower two-thirds, after which it can be straight to weakly convex and terminates with an inconspicuous posterior barb (Fig. 23F). Well-preserved teeth exhibit a thin layer of finely striated enameloid extending from the base to the apex (Fig. 23F), and the postero-basal part of the tooth may bear conspicuous wrinkling. In basal view the attachment surface is weakly concave and the outline ranges from oval to teardrop-shaped (Fig. 23I).

Remarks. Ebersole et al. (2019) and Ballen (2020) have suggested that tooth morphologies among extant Sphyraenidae can allow for some taxonomic distinction, but intraspecific variation is not well documented. Of the two morphologies in our sample, those that are tall with an anterior carina are consistent with the laniary (symphyseal) teeth of extant *Sphyraena barracuda* (Edwards, 1771) that we examined (SC2018.3.1). These teeth are located at the anterior end of the premaxilla and dentary. The laterally compressed and bicarinate specimens are comparable to teeth occurring in the palatine and dentary of *S. barracuda*. All the Tupelo Bay Formation teeth have finely serrated carinae and finely striated enameloid covering, indicating that the morphologies are likely conspecific.

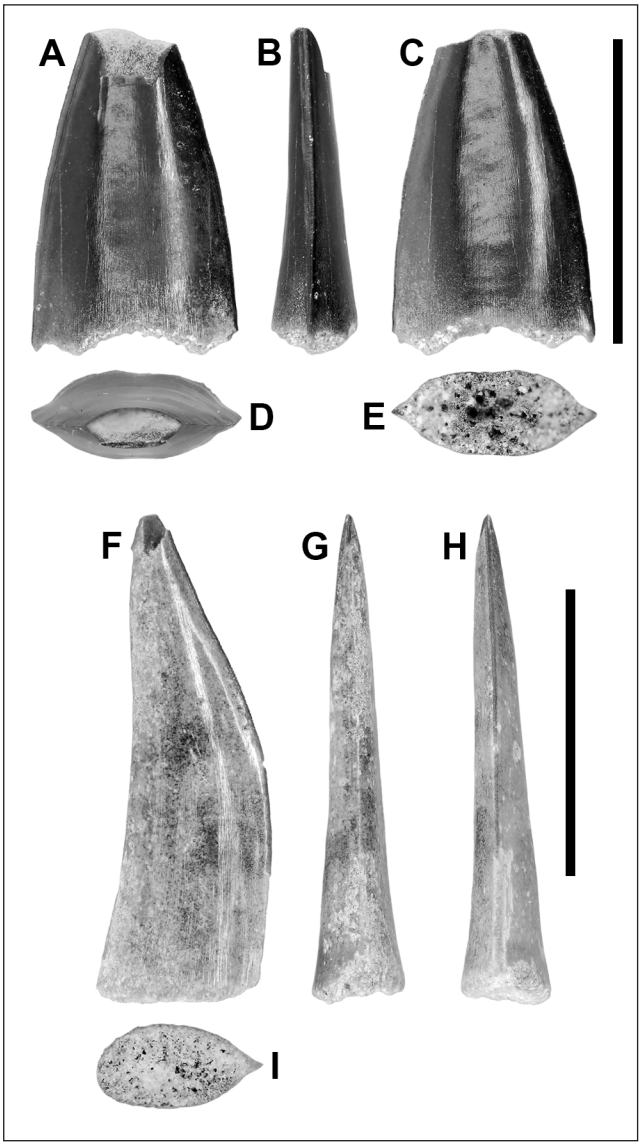

Fig. 23 - *Sphyraena* sp. from the Tupelo Bay Formation. A-E) tooth in labial (A), carinal (B), lingual (C), apical (D), and basal (E) views; SC2015.59; laniary tooth (F-I), SC2018.7.133, in profile (F), posterior (G), anterior (H), and basal (I) views. Scale bars: 1 cm.

Although the bicarinate teeth appear to be stable with respect to overall morphology, we observed some variation within the laniary teeth. Smaller teeth within this sample have the most sinuous outline in profile view, whereas the largest teeth have a more uniformly recurved appearance. However, in addition to finely striated enameloid, all laniary teeth have finely serrated anterior carinae and an inconspicuous posterior apical barb. These features lead us to consider the possibility that our sample reflects ontogenetic variation within a single taxon, rather than two or more taxa. Additionally, the anterior premaxillary laniary tooth of *S. barracuda* was observed to be more uniformly recurved compared to the more sinuous posterior laniary teeth.

Santini et al. (2015) demonstrated the existence of three *Sphyraena* lineages by the time of deposition of the Tupelo Bay Formation, and several Eocene species have been named based on isolated teeth (i.e., Casier 1966; Ballen 2020). We refrain from making a specific assignment without the aid of associated fossil skeletal material. It is of interest to note that features we observed on the Tupelo Bay Formations specimens, including posterior apical barb, finely serrated cutting edges, and finely striated enameloid, also occur on extant *S. barracuda* teeth that we examined. Ebersole et al. (2019) identified *Sphyraena* sp. in the Bartonian Gosport Sand of Alabama and Ebersole & Cicimurri (2025) documented teeth from numerous middle-to-upper Eocene units in Louisiana. Unreported specimens at SC show that the genus occurs in the Riggins Mill Member of the Clinchfield Formation of Georgia (i.e., SC2004.34.111 and SC2013.44.55). Comparable laniary and cheek teeth were documented in the Dry Branch Formation of South Carolina (Cicimurri & Knight 2019) and possibly Georgia (Cappetta & Borodin 2000a).

Family Xiphiorhynchidae Regan, 1909
Genus *Xiphiorhynchus* van Beneden, 1871

Xiphiorhynchus sp.
Fig. 24

Material: four rostra, including: SC2016.31.25 (Fig. 24A-H), SC2016.31.26 (Fig. 24I-L), SC2018.7.69 (Fig. 24M-R), SC2018.7.137.

Description. SC2016.31.26 is the most complete specimen, measuring 19.4 cm in greatest length. In profile view, the element is dorso-ventrally flattened (Fig. 24K) and in dorsal view, the lateral margins of the rostrum are very weakly convex and converge at the distal tip (Fig. 24J). The broken proximal end is laterally broad (3.8 cm as preserved) and the pointed distal tip measures only 3 mm in width (Fig. 24L). The angle of taper was measured at 10º. The element is bi-convex in proximal view (slightly more convex dorsally), where a large central canal (cc) measuring 7 mm in diameter is visible (Fig. 24I). The cc is flanked by a pair of dorsolateral nutrient canals (lcd) and a pair of ventrolateral nu-

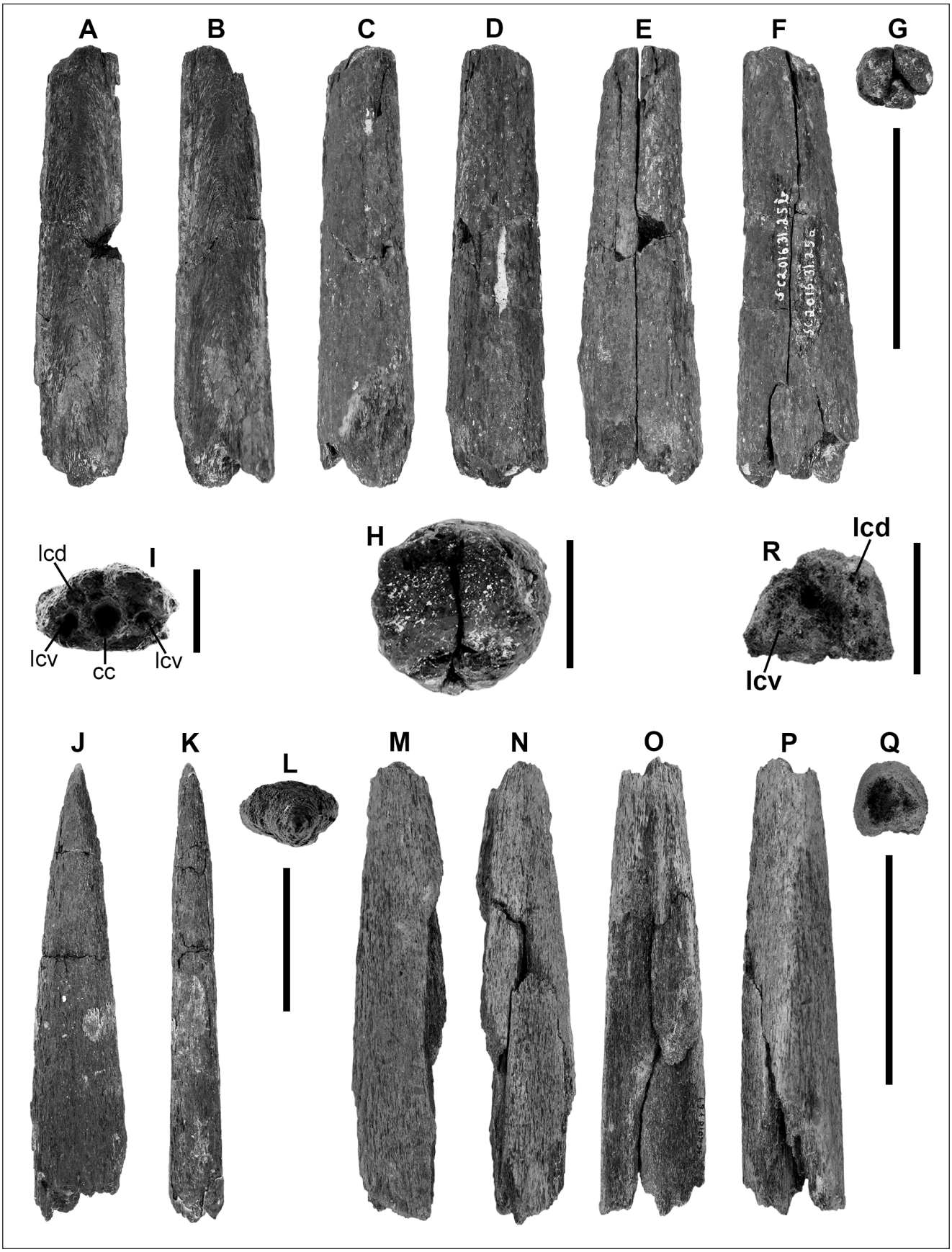

Fig. 24 - *Xiphiorhynchus* sp. from the Tupelo Bay Formation. A-H) rostrum, SC2016.31.25, in cross section (A of SC2016.31.25b), cross section (B of SC2016.31.25a), dorsal? (C), ventral? (D), right lateral? (E), left lateral? (F), distal (G), and proximal (H) views; I-L) rostrum, SC2016.31.26, in dorsal (I), left lateral (J), distal (K), and proximal (L) views; M-R) rostrum, SC2018.7.69, in right lateral (M), left lateral (N), ventral (O), dorsal (P), distal (Q), and proximal (R) views. Scale bars: 1 cm in H-I & R, 5 cm in A-G & J-Q.

trient canals (lcv). The lcd measure approximately 3 mm as exposed at the proximal end, but they appear to be filled with mineralized material. The lcv measure approximately 5 mm in diameter as exposed but they taper distally. The lcv are located closer to the lateral margins of the rostrum, whereas the lcd occur more medially. Dorsally, there is a shallow longitudinal furrow on each side of the rostrum, between the midline and lateral margin of the element (Fig. 24J).

Specimen SC2016.31.25 is a portion of rostrum broken at its proximal and distal ends. As preserved it measures 9.5 cm in length and 2.5 mm wide at the proximal end. The element tapers gently to a width of 1.5 cm at the broken distal end, with the angle of taper being approximately 6.5º as preserved. In profile views, the right and left sides of the rostrum possess a shallow, medially located longitudinal furrow along the anterior one-half (Fig. 24C & 24D). In proximal view, the rostrum has a circular outline (Fig. 24H), but distally, it is somewhat dorso-ventrally flattened and has an oval cross section (Fig. 24G). Mineral-filled lcd and lcv are visible at the distal end, the diameters of which measure approximately 2 mm, with the lcd located closer to the center of the rostrum. The furrows noted above are the exposed lcv, and mineralized material occurring in the right furrow can be traced back to the proximal end. In longitudinal cross-section, the rostrum is comprised of solid bony material generally having a cone-in-cone appearance, and although no cc is visible proximally or distally, the middle of the rostrum consists of dense material that is clearly delineated from the outer cone-in-cone structure (Fig. 24A-B). This dense material is thickest (4 mm) near the broken distal end but pinches out posteriorly to end roughly 5 mm from the broken proximal end. The concave nature of the broken proximal end appears to reflect the internal cone-in-cone structure. A portion of the mineral-filled left lcd is also visible in longitudinal cross section.

Specimen SC2018.7.69 is a portion of rostrum measuring 10.5 cm in length, although it is broken proximally and distally. The element tapers proximo-distally (Fig. 24P) but the angle of taper cannot be accurately measured. In distal view, the element is very convex dorsally but less so laterally, and the flat ventral surface results in a D-shaped cross-section (Fig. 24Q). A pair of lcv occur near the preserved outer margins of the element, with the left lcv measuring approximately 1 mm in diameter and exposed 4.0 cm from the preserved distal end, whereas the right lcv is exposed 8.8 cm from the distal end and measures roughly 2 mm in diameter. No cc is obvious proximally or at the broken distal end. The element exhibits a fibrous texture internally and externally that parallels its length (Fig. 24O-P).

Specimen SC2018.7.137 (not shown) consists of paired elements. Each element is elongated, with one measuring 11 cm in preserved length and the other 9.8 cm. Both are widest at the proximal end, measuring 2 to 2.6 cm, and taper towards the distal end. The dorsal surface of each specimen is weakly convex and has a texture similar to that of SC2018.7.69. The medial margin of each element is straight. Each element has a conspicuous lateral projection at the proximal end. In proximal view each element is dorso-ventrally thin, and in profile view their proximo-distal thickness is rather constant. In ventral view, each specimen possesses an elongated furrow along their preserved length (lateral nutrient canals?).

Remarks. Specimen SC2018.7.137 (not figured) was recovered from the lower part of the Tupelo Bay Formation. The overall shapes of the bones lead us to conclude that they are the proximal, unfused, ends of the right and left premaxillae, and that the straight medial margin is the contact surface between the two bones.

Based on its preservation, specimen SC2018.7.69 was derived from the phosphatized part of the Tupelo Bay Formation, or possibly from the immediately overlying Parkers Ferry Formation (Priabonian, NP19/20). Specimens SC2016.31.25 and SC2016.31.26 were recovered from the uppermost bedding surface of the Tupelo Bay Formation, which is the disconformable contact with the Parkers Ferry Formation. The fossils are included here due to their stratigraphic occurrence, but it is possible that the living animals inhabited the Parkers Ferry depositional environment, and their remains became incorporated into still soft Tupelo Bay Formation sediment.

Unfortunately, SC2016.31.25 and SC2016.31.26 are ablated and there are no traces of ventral tooth patches. SC2016.31.26 is dorso-ventrally flattened and bi-convex (in proximal view), whereas SC2016.31.25 has a thicker oval cross-section. However, the morphology of the latter

specimen likely does not reflect the original shape, as lateral furrows represent the exposed lcv, indicating a significant amount of bony material has been eroded from the specimen. The mineralized material filling the right lcv was examined under a microscope, and its greenish color weathering to red indicates it is glauconitic. Specimen SC2018.7.69 is also dorso-ventrally flattened, but the dorsal surface is very convex whereas the ventral surface is rather flat, resulting in a D-shaped cross-section in proximal view. This specimen preserves a pair of small lcv, but a central canal is not obvious.

Fierstine & Stringer (2007) listed seven Eocene *Xiphiorhynchus* species, including *X. aegyptiacus* Weiler, 1929, *X. elegans* van Beneden, 1871, *X. eocaenicus* (Woodward, 1901), *X. kimblaylocki* Fierstine & Applegate, 1974, *X. parvus* Casier, 1966, and *X. priscus* (Agassiz, 1844). An additional species, *X. rotundus* (Woodward, 1901), appears to have been derived from the upper Oligocene (Chattian, NP25) Chandler Bridge Formation of South Carolina (Monsch et al., 2005), a lithostratigraphic unit roughly 10 Ma younger than the Tupelo Bay Formation specimens.

Monsch (2005) illustrated the rostra of middle Eocene *Xiphiorhynchus eocaenicus* and lower Eocene (Ypresian) *X. priscus* and, although both have two pairs of lateral nutritive canals, the former has an oval cross-section and the latter has a circular cross-section. Specimens SC2016.31.25 and SC2016.31.26 both have oval proximal cross-sections, but they have a circular outline distally. Specimen SC2016.31.26 is comparable to the holotype of *X. kimblaylocki* (Fierstine & Applegate 1974), and SC2016.31.25 has a proximal cross-section like that of an *X. kimblaylocki* rostrum discussed by Monsch et al. (2005). Both of the *X. kimblaylocki* specimens noted here were recovered from the upper Eocene (Priabonian) Yazoo Clay of Louisiana and Mississippi. Specimen SC2018.7.69 has a cross-section like that of *X. aegyptiacus*, and it also appears to lack a central canal. Fierstine & Stringer (2007) described a similar rostrum from the Priabonian Yazoo Clay of Louisiana, but they refrained from assigning the specimen to *X. aegyptiacus* due to the preservation of their specimen and morphological differences with that taxon. The differing cross-sections of the specimens described herein could be taken as an indication that multiple species are represented, including one with a rostrum like *X. kimblaylocki* (and SC2016.31.26) and one apparently having a rostrum like *X. aegyptiacus* (SC2018.7.69). However, Monsch et al. (2005) noted there is inter- and intraspecific variation among *Xiphiorhynchus* rostra, and this phenomenon makes identification of broken and ablated specimens particularly difficult. We therefore refrain from making specific identifications until additional, more complete specimens are examined. It is interesting to note that SC2016.31.25 has an internal cone-in-cone appearance with a central mass of dense material, whereas the internal texture of SC2018.7.69 is fibrous. Although these differing textures could be an artifact of preservation, they also suggest that two different taxa are represented. The occurrence of *Xiphiorhynchus* in the Tupelo Bay Formation indicates a minimum early Priabonian age for this unit, as the earliest records of these billfish appear to be in NP18 deposits. Note that there has been variation in the familial placement of *Xiphiorhynchus*, with assignment to Xiphiidae (i.e., McCuen et al. 2020) and Xiphiorhynchidae, but we follow the most recent phylogenetic analysis by Rust et al. (2025) and place the genus in the latter family.

Order **Scombriformes** Bleeker, 1859
Suborder **Scombroidei** Bleeker, 1859
Family Trichiuridae Rafinesque, 1810
Genus *Trichiurides* Winkler, 1874

Trichiurides sagittidens Winkler, 1874

Fig. 25A-D

Material: eight teeth, including SC2015.59.32 (2 specimens), SC2018.7.134, SC2022.27.311 (Fig. 25A-D), SC2022.27.312, SC2022.27.313, SC2022.27.314, SC2022.27.315.

Description. Our sample is composed of elongated laniary (symphyseal) teeth, with the largest specimen available to us measuring 15 mm in apico-basal height. In profile view, the crown is uniformly curved such that the apex is posteriorly directed (Fig. 25B & 25C). The tooth is divided into nearly equal labial and lingual faces by sharp and smooth anterior and posterior cutting edges that do not reach the base (Fig. 25A). The crown faces are strongly convex, with the labial face being smooth but the lingual face (Fig. 25B) bearing numerous parallel longitudinal ridges at the base. The apical part of the tooth consists of a very laterally compressed and bicarinate enameloid cap. The carinae form smooth anterior and posterior cutting edges, and the postero-basal part produces a barb-like projection. In

basal view the tooth has a circular outline, and there is a circular pulp cavity framed by a thin dentine wall (Fig. 25D).

Remarks. *Trichiurides sagittidens* laniary teeth differ from those of Tupelo Bay Formation *Sphyraena* sp. by having a more gracile appearance, enameloid-covered apex with conspicuous posterior barb, strongly sinuous profile, and circular basal outline (as opposed to oval or teardrop-shaped).

Westgate (1984) documented this species from Eocene strata of Arkansas, with the specific unit potentially being the Bartonian to Priabonian (upper Eocene) Moodys Branch Formation. Ebersole et al. (2019) reported *T. sagittidens* from the Lutetian to Bartonian Lisbon Formation and Bartonian Gosport Sand of Alabama, and records of this fish from the Cook Mountain and Moodys Branch formations and Yazoo Clay were confirmed by Ebersole & Cicimurri (2025). The species was recovered from deposits in Georgia assigned to the Dry Branch Formation (Case & Borodin 2000a), and we document it in the Clinchfield Formation of Georgia (i.e., SC2004.34.124 and SC2013.44.58).

Family Scombridae Rafinesque, 1815
Subfamily Scombrinae Rafinesque, 1815
Genus *Scomberomorus* Lacepède, 1802

Scomberomorus sp.
Fig. 25E-T

Material: five teeth, including SC2022.27.316 (Fig. 25G-J), SC2022.27.317, SC2022.27.318, SC2022.27.319, SC2022.27.320 (Fig. 25K-N); left maxilla SC2016.47.3 (Fig. 25R-T); right dentary SC2009.2.1 (Fig. 25O-Q); vertebra SC2018.7.138 (Fig. 25E-F).

Description. Isolated tooth crowns are broad and triangular (Fig. 25I), measuring up to 10 mm in apico-basal height, and in carinal view there is little to no medial curvature (Fig. 25H). The crown is essentially differentiated into labial and lingual parts by smooth and convex anterior and posterior cutting edges. The edges meet apically to form a rounded to sub-angular apex. The labial and lingual crown faces are moderately to strongly convex, particularly at the lingual base. Specimen SC2022.27.319 demonstrates that the tooth crowns are covered by smooth enameloid, although on most specimens the enameloid is only preserved along the cutting edges (compare Fig. 25G to 25I).

Specimen SC2016.47.3 is a left maxilla measuring nearly 10 cm in length. The dorso-medial portion of the bone is slightly crushed and there is some bone loss, and the distal end exhibits some damage (Fig. 25S-T). The posterior two-thirds of the element is an elongated, blade-like, and medially curving ramus. The dorsal surface is convex, and the ventral surface is narrow and sharp. The medial curvature is sharp, but this is probably enhanced somewhat by the crushing and distortion of the ramus. Antero-ventrally, the maxilla is bifurcated into two mediolaterally thin processes, including a rather small and short lateral process and a much larger and more elongated medial process (Fig. 25R). A sulcus between these processes serves as the articular surface for the premaxilla. The ventral surface of the lateral process is formed into a sharp ridge that extends to the eminence of the ramus, whereas the ventral surface of the medial process is convex and there is a single large foramen on its lateral face. A massive reniform protuberance is located on the antero-dorsal surface, immediately above the ventral processes (Fig. 25S).

Specimens SC2009.2.1 and SC2022.27.320 are jaw sections with associated teeth. Specimen SC2009.2.1 is the anterior part of a right dentary with six articulated teeth. This fossil shows a single row (Fig. 25Q) of large teeth that are set into deep alveoli via an elongated root (Fig. 25O-P). Up to 11 mm of tooth crown is exposed. Teeth may become fused to the jawbone, as is seen on SC2022.27.320 (Fig. 25K-N), or remain loose in the alveolus. Both jaw sections exhibit resorption pits for replacement teeth, and some teeth of SC2009.2.1 also have associated notches at the crown base, where the cutting edges abruptly end at concave surfaces.

Fig. 25 - Scombriformes from the Tupelo Bay Formation. A-D) *Trichiurides sagittidens*, laniary tooth (A-D), SC2022.27.311, in anterior (A), lingual (B), labial (C), and basal (D) views. E-Q) *Scomberomorus* sp., caudal vertebra (E-F), SC2018.7.138, in anterior (E) and lateral (F) views; tooth (G-J), SC2022.27.316, in labial (G), carinal (H), lingual (I), and basal (J) views; jaw fragment with tooth (K-N), SC2022.27.320, in labial (K), carinal 1 (L), lingual (M), and carinal 2 (N) views; right dentary (O-Q), SC2009.2.1, in labial (O), lingual (P), and occlusal (Q) views; left maxilla (R-T), SC2016.47.3, in ventral (R), dorsal (S), and lateral (T) views. Scale bars: 1 cm in A-N, 5 cm in O-T.

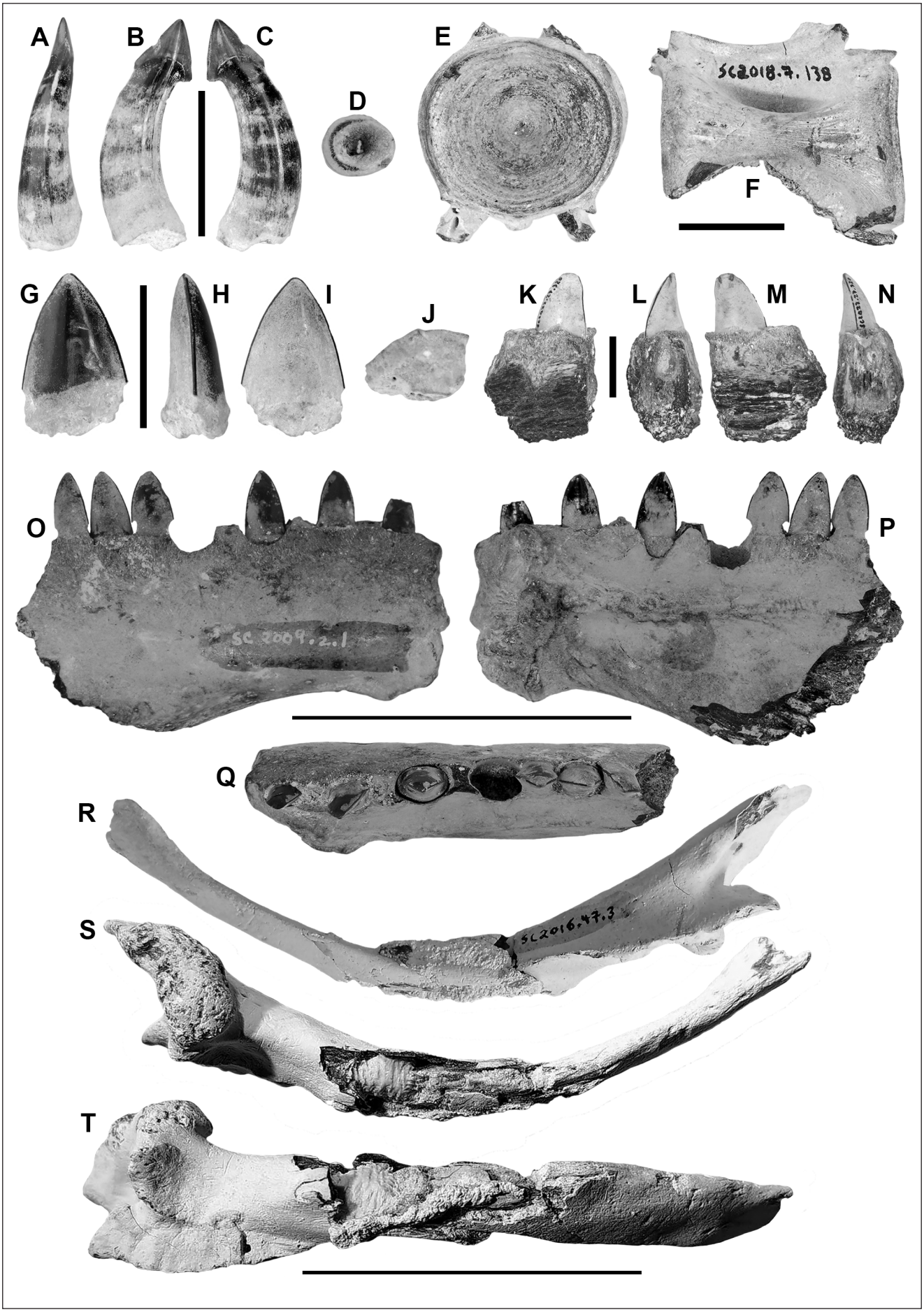

Fig. 25

SC2018.7.138 is a small incomplete centrum measuring 2.1 cm in length along the ventral surface. The antero-dorsal part of the centrum is not preserved. Posteriorly, the centrum rim is sub-circular in outline, being slightly wider than high (1.7 cm and 1.5 cm, respectively). The anterior and posterior surfaces are deeply concave and bear numerous concentric growth annuli (Fig. 25E). The lateral surfaces bear a large medial ridge that is framed dorsally and ventrally by deep oval fenestrae, and the anterior and posterior ends of the ridge have a fibrous texture (Fig. 25F). The ventral surface is slightly depressed nearly along the entire centrum length, and the surface is perforated by numerous tiny openings. The broken proximal ends of the haemal spine are preserved at the postero-ventral end of the centrum, and two shallow, triangular depressions occur between the spine bases and the centrum rim.

Remarks. *Scomberomorus* tooth crowns differ from palatine and dentary teeth of *Sphyraena* sp. by being labio-lingually thicker, with the lingual face being significantly more convex (compare Fig. 25J to 23E). *Scomberomorus* dentaries lack laniary teeth as occur in *Sphyraena* jaws (see above), and all the teeth in SC2009.2.1 are the same shape. All the isolated teeth and the one occurring on SC2022.27.320 are identical to those on SC2009.2.1, and we therefore consider the specimens conspecific. Specimen SC2016.47.3 is very similar to maxillae of extant *Scomberomorus cavalla* (Cuvier, 1829) that we examined (i.e., SC 2018.3.28) and is therefore regarded as congeneric. Similarly, specimen SC2018.7.138 is comparable to, albeit larger than, vertebrae of extant *S. cavalla* that we examined (SC2018.3.47).

Ebersole et al. (2019) documented two species of *Scomberomorus* in middle-to-upper Eocene (Claibornian) strata of Alabama, including *S. bleekeri* (Storms, 1892) and *S. stormsi* (Leriche, 1905). The teeth were differentiated by the nature of the overall crown outline in labial/lingual view, with those of *S. bleekeri* having a wider lanceolate appearance, whereas *S. stormsi* has roughly sub-parallel margins along the lower one-half of the tooth. Based on the tooth outline, the Tupelo Bay species may represent *S. bleekeri*.

Family indet.
Genus *Sphyraenodus* Agassiz, 1844

Sphyraenodus sp.
Fig. 26

Material: three teeth, including SC2022.27.332 (Fig. 26A-E), SC2022.27.333 (Fig. 26F-J), SC2022.27.334 (Fig. 26K-M).

Description. The teeth are roughly conical with slight labio-lingual compression and medial curvature (Fig. 26A, 26F, 26K). Cutting edges are absent, the enameloid (when preserved) is smooth (Fig. 26H & 26L), and the crown bases are very heavily crenulated (i.e., Fig. 26I). The crown apices are not very sharply pointed, although this may be an artifact of preservation. In apical view the crown base has a digitate appearance due to the heavy basal fluting (Fig. 26E, 26J, 26M). A small portion of bony tissue is preserved on the base of each specimen, particularly SC2022.27.332 (Fig.26A-D). The total apico-basal tooth height of the largest specimen, including preserved root, measures 14 mm.

Remarks. These teeth compare well to those of *Sphyraenodus priscus* Casier, 1966 from the lower Eocene (Ypresian) London Clay of England (also Monsch 2005) and to *S. chouberti* (Arambourg, 1952) from the late Paleocene (Thanetian) and Ypresian of Morocco. Unfortunately, teeth are the only remains available to us and for that reason we only refer them to *Sphyraenodus* sp. Monsch (2005) noted the only other North American occurrence of the genus in the Ypresian Nanjemoy Formation of Maryland. We note here that Maisch et al. (2016) reported a tooth from the Lutetian Tallahatta/Lisbon formational contact zone of Alabama, identified as *Scomberomorus* sp. (fig. 2, 27-29), that bears similarities to the Tupelo Bay Formation specimens shown in our Figure 26.

Specimen SC2022.27.333 is unusual in that there is a row of seven short, parallel scratch-like structures located on the lingual side of the crown (Fig. 26F-G). These structures are clearly secondary in origin and superficially similar to marks occurring on some *Pristis* sp. rostral spines in our sample (see above).

Order **Tetraodontiformes** Berg, 1940
Suborder **Ostracioidei** Tyler, 1980
Family Ostraciidae Rafinesque, 1810

Ostraciidae gen. et sp. indet.
Fig. 27A-F

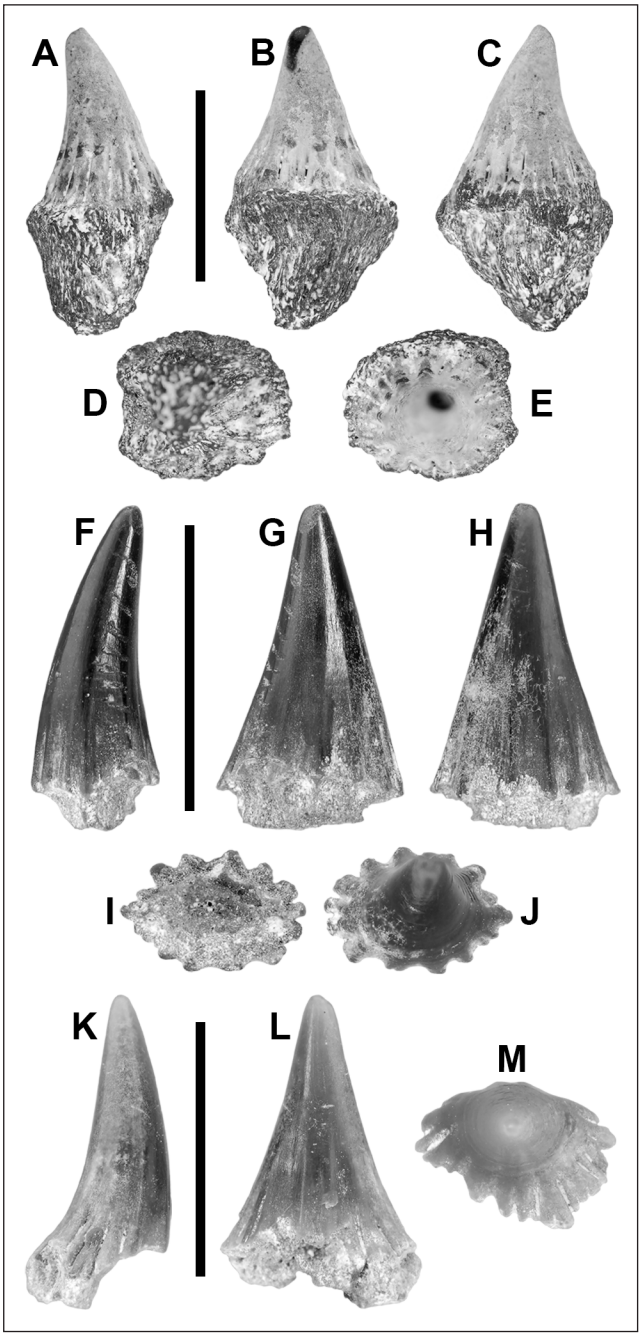

Fig. 26 - *Sphyraenodus* sp. from the Tupelo Bay Formation. A-E), tooth, SC2022.27.332, in profile 1 (A), posterior (B), profile 2 (C), basal (D), and apical (E) views; tooth (F-J), SC2022.27.333, in posterior (F), lingual (G), labial (H), basal (I), and apical (J) views; tooth (K-M), SC2022.27.334, in carinal (K), lingual (L), and apical (M) views. Scale bars: 1 cm.

2019 Ostraciidae gen. et. sp. indet. – Ebersole et al., p. 180, fig. 66M-U.

Material: five dermal plates, including SC2022.27.327 (Fig. 27A-C), SC2022.27.328 (Fig. 27D-E), SC2022.27.329, SC2022.27.330, SC2022.27.331 (Fig. 27F).

Description. The dermal plates are polygonal elements that are thinnest at the margins (Fig. 27B, 27E). The visceral surface is flat to concave and has a slightly roughened texture (Fig. 27C), whereas the external surface is convex and ornamented with numerous ovoid enameloid-covered tubercles. These tubercles are typically loosely arranged into circular patterns surrounding a central tubercle that is located on a slight prominence (Fig. 27A). The base of this prominence may bear numerous short radiating ridges (Fig. 27D-E).

Remarks. There is some morphological variation in the small sample available to us, with specimens ranging from elongated and ovate to subcircular to square in outline. Additionally, individual tubercles may occur at the corners of the element (Fig. 27F), arranged as a single ring (Fig. 27D), or occur within multiple loosely organized rings (Fig. 27A). We believe that the variation represents body location on a single boxfish taxon, as they all share the feature of radiating ridges on the medial prominence.

This dermal plate morphology is consistent with specimens of Ostraciidae that were reported from the Paleocene of South Carolina (Weems 1998), the lower Eocene Nanjemoy Formation of Virginia (Weems 1999), and from Claiborne Group strata (lower-to-middle Eocene) of Alabama (Ebersole et al. 2019). The authors of those various reports noted the limited taxonomic value of isolated dermal plates like those described above, nevertheless their morphology allows us to determine the familial placement of the elements.

Suborder **Balistoidei** Rafinesque, 1810
Family Balistidae Risso, 1810
Genus *Lobodus* Costa, 1866

Lobodus pedemontanus Costa, 1866

Fig. 27G-Z

2019 Balistidae – Ebersole et al., p. 180-181, fig. 67, fig. 67.
2025 Balistidae – Ebersole & Cicimurri, p. 184, fig. 6.40.
2025a *Lobodus pedemontanus* Costa, 1866 – Cicimurri et al., p. 30-31, fig. 24.

Material: five teeth, including SC2022.27.306 (Fig. 27G-J), SC2022.27.307 (Fig. 27K-N), SC2022.27.308 (Fig. 27S-V), SC2022.27.309 (Fig. 27W-Z), SC2022.27.310 (Fig. 27O-R).

Description. All teeth consist of an enameloid-covered crown that is laterally compressed and measuring no more than 2 mm in width (Fig. 27H, 27I, 27T, 27X). The total preserved

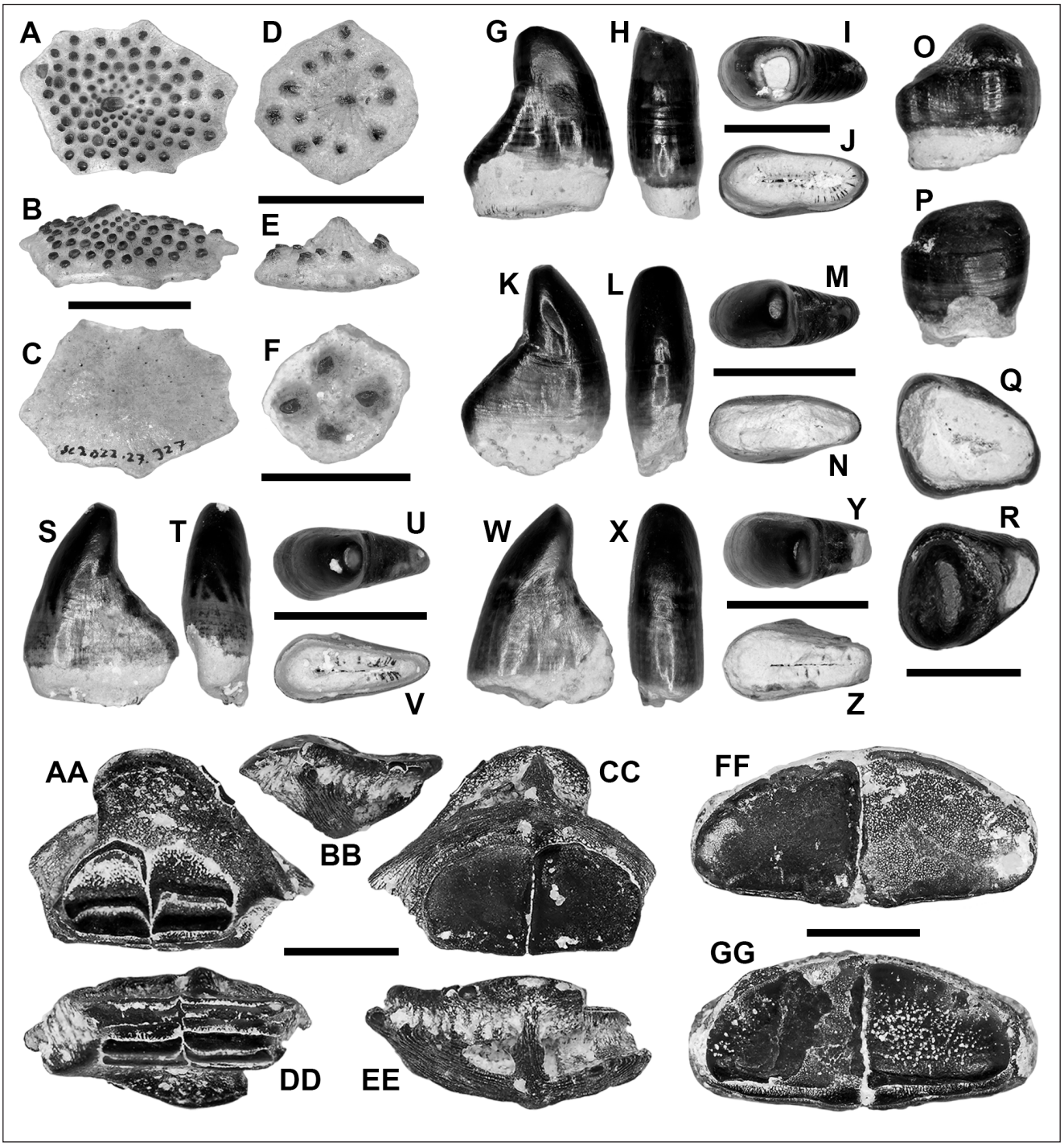

Fig. 27 - Tetraodontiformes from the Tupelo Bay Formation. A-F) Ostraciidae, dermal armor (A-C), SC2022.27.327, in apical (A), profile (B), and visceral (C) views; dermal armor (D-E), SC2022.27.328, in apical (D) and profile (E) views; dermal armor (F), SC2022.27.331, in apical view. G-V) *Lobodus pedemontanus*, tooth (G-J), SC2022.27.306, in lateral (G), anterior (H), occlusal (I), and basal (J) views; tooth (K-N), SC2022.27.307, in lateral (K), anterior (L), occlusal (M), and basal (N) views; tooth (O-R), SC2022.27.310, in lateral (O), anterior (P), basal (Q), and occlusal (R) views; tooth (S-V), SC2022.27.308, in lateral (S), anterior (T), occlusal (U), and basal (V) views; tooth (W-Z), SC2022.27.309, in lateral (W), anterior (X), occlusal (Y), and basal (Z) views. AA-GG) *Progymnodon hilgendorfi*, maxillary (AA-EE), SC2022.27.325, in oral (AA), left lateral (BB), aboral (CC), posterior (DD), and anterior (EE) views; dentary (FF-GG), SC2022.27.326, in aboral (FF) and oral (GG) views. Scale bars: 5 mm in F-GG, 1 cm in A-E.

height of the largest specimen is 10 mm. In profile view, the crown is labio-lingually elongated at the base, measuring up to 8 mm in this direction. However, the apical one-third to one-half of the crown is developed into a cusp that is located closer to the anterior margin (Fig. 27G, 27K, 27S, 27W). The cusp is roughly conical (i.e., Fig. 27M & 27U) and is lingually curved (i.e., Fig. 27S & 27W). In ante-

rior view, the crown is vertical and only very slightly medially curving (i.e., Fig. 27L, 27T), and the labial crown face is slightly more convex than the lingual face. In profile view, the labial crown margin is uniformly convex, but the lingual margin is sinuous (i.e., Fig. 27G & 27K). The thick crown enameloid exhibits fine growth lamellae on the basal one-half (i.e., Fig. 27O-P). The cusp apices are worn to varying degrees to expose the internal dentine (compare Fig. 27U to 27I), and the oblique portion of the lingual crown margin may exhibit a weak wear facet. The root is largely incomplete on each of the specimens, but the preserved portions demonstrate it lacks enameloid and is slightly smaller in area than the crown (i.e., Fig. 27J, 27N, 27Q, 27V).

Remarks. Four of the five specimens are morphologically similar to each other, varying only slightly with respect to cusp height, but SC2022.27.310 (Fig. 27O-R) differs from the others by having a much lower cusp and broader anterior region. Based on our examination of the jaws of an extant *Balistes capriscus* Gmelin, 1789 (MSC 49132), the variation in cusp development is likely related to location on the jaw, with cuspidate teeth like SC2022.27.308 (Fig. 27S-V) being from the medial to anterior part of the jaw, and those like SC2022.27.310 in the posterior part (see also Tyler 1980). The Tupelo Bay Formation specimens represent one of the few documented occurrences of fossil Balistidae in North America. Ebersole et al. (2019) were the first to report an Eocene triggerfish from the USA in their account of Claibornian fishes from Alabama, and Ebersole & Cicimurri (2025) recently reported a single specimen from the Moodys Branch Formation of Louisiana. Ebersole et al. (2021) also identified the first Oligocene record of the family in the Glendon Limestone Member of the Byram Formation (Rupelian) of southwestern Alabama. Based on additional specimens from Alabama, Cicimurri et al. (2025a) determined that this morphology belonged to *Lobodus pedemontanus*, a taxon named by Costa (1866) but with an uncertain familial affinity. Herein we concur with Ebersole et al. (2019) and Cicimurri et al. (2025a) that this taxon belongs to the Balistidae based on the morphological similarity to teeth of the various extant taxa. The shape and coloration of the teeth (dark brown with a lighter brown base or black with a green cusp apex) are distinctive, and the morphology is more widely distributed than is currently known. For example, a collection of fossils at SC contains several teeth that were recovered from the Clinchfield Formation of Georgia (i.e., SC2004.34.122 and SC2013.44.60).

Suborder **Tetraodontoidei** Nelson et al., 2016
Family Diodontidae Bonaparte, 1838
Genus *Progymnodon* Dames, 1883

Progymnodon hilgendorfi Dames, 1883

Fig. 27AA-GG

1981 ?*Diodon* sp. – Thurmond & Jones, p. 108, fig. 51.
2002 *Chilomycterus hilgendorfi* – Dica, p. 40, pl. 1, figs. 1-2.
2019 *Progymnodon hilgendorfi* – Ebersole et al., p. 182-183, fig. 68.
2025 *Progymnodon hilgendorfi* – Ebersole & Cicimurri, p. 185, fig. 6.41.

Material: two jaws, including SC2022.27.325 (Fig. 27AA-EE), SC2022.27.326 (Fig. 27FF-GG).

Description. The jaw elements are composed of a beak and two stacks of large triturating teeth. Unworn triturating teeth consist only of a thick but very low enameloid crown having a subtriangular outline (Fig. 27AA & 27GG). The tooth stacks become worn, through presumed *in vivo* use, such that portions of one or more replacement teeth are exposed at the posterior end of the jaw (Fig. 27AA & 27DD). The two tooth stacks articulate to one another along a medial symphysis but are separated from the beak by a large expanse of bone. The beak margin consists of small, closely spaced wedge-shaped teeth (Fig. 27BB).

Remarks. The jaws of *Progymnodon hilgendorfi* include the fused premaxillae and dentaries, and when complete the former can be distinguished from the latter by the angular (Fig. 27CC) versus uniformly convex (Fig. 27FF) labial margin. Ebersole et al. (2019) reported this taxon from the Gosport Sand (NP17) of Alabama, and the species was recently reported from the Cane River (NP15) and Moodys Branch (NP17) formations of Louisiana (Ebersole & Cicimurri 2025). Unpublished specimens at SC demonstrate the taxon occurs in the Clinchfield Formation of Georgia (i.e., SC2004.34.118 and SC2004.44.62) and the Priabonian Dry Branch Formation of South Carolina (SC96.97.3).

Order incertae sedis
Family incertae sedis
Genus *Cylindracanthus* Leidy, 1856

Cylindracanthus rectus (Agassiz, 1843)

Fig. 28A-B

Material: 9 rostra, including SC2015.59.29 (7 specimens), SC2018.7.136, SC2022.27.335 (Fig. 28A-B).

Description. All the specimens are portions of elongated, cylindrical rostra. More complete specimens demonstrate that the element tapers distally. The outer surface is subdivided by numerous deep, parallel grooves extending the length of the preserved specimens (Fig. 28A). Internally, one or two hollow tubes extend the length of the preserved elements (Fig. 28B). Although all our specimens are incomplete, the longest measures 5.7 cm in length as preserved.

Remarks. Three *Cylindracanthus* species have been identified from Eocene strata, including *C. acus* Cope, 1870, *C. ornatus* Leidy, 1856 and *C. rectus* (Agassiz, 1843). Ebersole et al. (2019) considered *C. acus* a junior synonym of *C. rectus*, which we follow herein. Of the two remaining species, both have a similar rostrum morphology, but the taxa differ by the presence (*C. ornatus*) or absence (*C. rectus*) of ventral rows of denticles. The specimens in our sample appear to lack ventral denticles we therefore assign them to *C. rectus*.

Cylindracanthus is rather widespread within the Eocene of the Gulf Coastal Plain of the USA, occurring in the Lisbon Formation and Gosport Sand of Alabama (Ebersole et al. 2019) and Moodys Branch Formation and Yazoo Clay of Louisiana (Ebersole & Cicimurri 2025). Previously unreported specimens at SC show that *Cylindracanthus* is found in the Riggins Mill Member of the Clinchfield Formation of Georgia (SC2013.44.70). This fish is only known from its rostra, and although previously thought to be related to sturgeon and paddlefish (Parris et al., 2001) and then allied with scombroid fishes (Monsch 2005), the most recent evaluation of the genus suggests that the taxon is a derived teleost of uncertain ordinal and familial affinities (Grandstaff et al. 2018). It must be noted that, unless a specimen is very well preserved, one may not be able to determine the presence or absence of ventral denticles and, therefore, accurately identify the species represented (see discussion in Ebersole et al. 2019).

Osteichthyes indet.

Fig. 28C–M

Material: isolated tooth, including SC2018.7.135 (Fig. 28N–O); four vertebrae, including SC2009.2.2 (Fig. 28C–E), SC2015.59.33, SC2016.47.2 (Fig. 28I–K), SC2018.7.139 (Fig. 28F–G); hypural SC2018.7.140 (Fig. 28L–M).

Description. SC2018.7.135 (Fig. 28N–O) is an isolated tooth measuring 8 mm in apico-basal height and 3 mm in maximum width. In profile view, the tooth is conical, but carinae divide the crown into a small and nearly flat labial face and much more expansive and convex lingual face. In labial view, the crown has a triangular appearance, and faint vertical ridges extend from the base towards the pointed apex. Vertical ridges occurring on the lingual face are more robust and extend nearly to the apex (Fig. 28N). Smooth lateral carinae extend from the apex towards the crown base. The basal portion of the tooth is ablated and lacks enameloid and ornamentation. In basal view, the tooth has a deep pulp cavity (Fig. 28O).

SC2009.2.2 (Fig. 28C–E) is a vertebral centrum measuring 2.4 cm in length, 2.1 cm in height, and 2.1 cm in maximum width. The anterior and posterior surfaces are deeply convex, have a nearly circular outline, and numerous growth annuli are visible (Fig. 28C). The base of the neural arch is preserved, and in dorsal view the neural canal has a fibrous texture. The neural arch base is flanked by a small but deep oval depression just anterior to the posterior margin. The lateral surfaces bear a high antero-medially located ridge that is framed dorsally and ventrally by deep conical fenestrae, and an additional but much smaller postero-ventral fenestra forms the posterior border of a short vertical ridge (Fig. 28D). A shallow postero-dorsal depression is located immediately posterior to the large dorsal fenestra. The bases of the haemal arch are preserved on the ventral margin. In ventral view, a narrow but deep depression between the haemal arch bases contains a row of five circular openings (Fig. 28E). Additionally, a large but shallow triangular depression occurs on each side of the centrum immediately anterior to the haemal arch bases, and a smaller oval fenestra occurs between each haemal arch base and the posterior rim. Specimen SC2015.59.33 is poorly preserved but identical to SC2009.2.2.

SC2016.47.2 is a large centrum measuring just over 5 cm in length. It is laterally compressed, with the anterior articular end measuring 4.0 cm high and 3.5 cm wide. The dimensions of the posterior end are slightly smaller, at 3.8 cm and 3.3 cm,

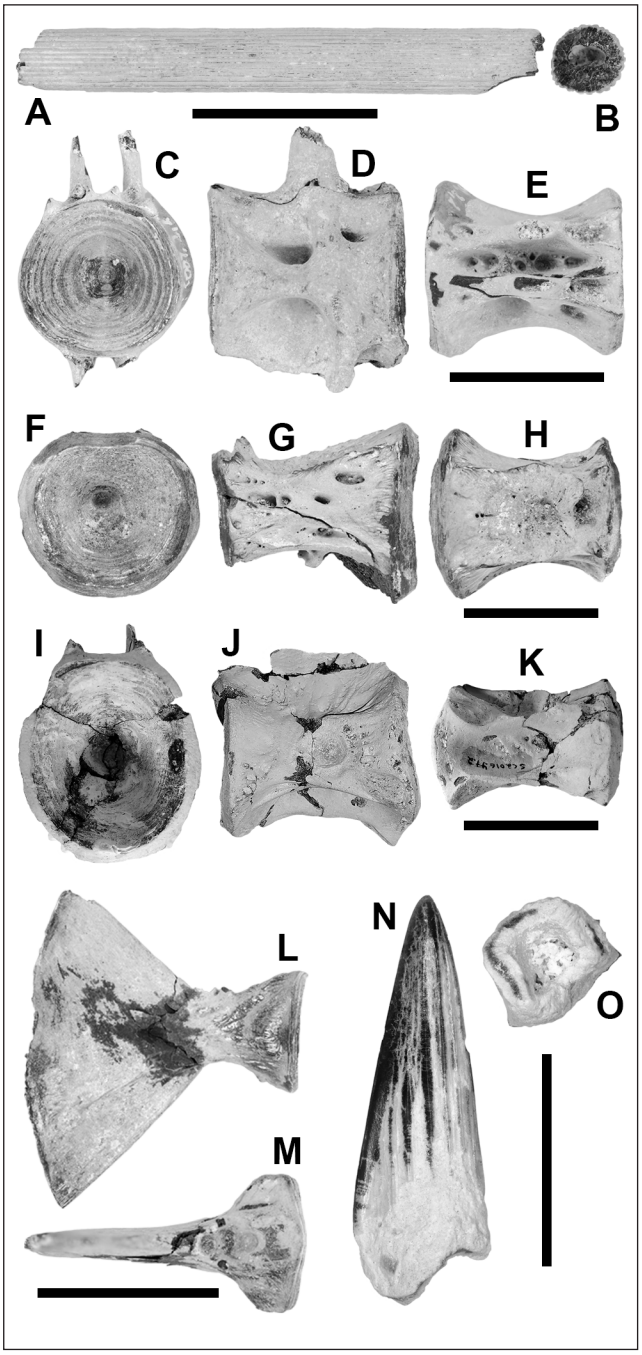

Fig. 28 - Teleostei from the Tupelo Bay Formation. A-B) *Cylindracanthus* sp., rostrum (A-B), SC2022.27.335, in profile view (A) and transverse cross-section (B). C-E) Teleostei indet. post-abdominal vertebra (C-E), SC2009.2.2, in anterior (C), right lateral (D), and dorsal (E) views; caudal vertebra (F-H), SC2018.7.139, in anterior (F), lateral (G), and dorsal (H) views; vertebra (I-K), SC2016.47.2, in posterior (I), right lateral (J), and dorsal (K) views; hypural, SC2018.7.140 (L-M), in right lateral (L) and dorsal (M) views; tooth (N-O), SC2018.7.135, in postero-lingual (N) and basal (O) views. Scale bars: 5 mm in N-O, 2 cm in A-H & L-M, 5 cm in I-K.

respectively. The anterior and posterior surfaces are therefore oval in outline, very deeply convex, and numerous concentric growth annuli are visible. The posterior surface is partly encrusted by serpulid worm tubes (Fig. 28I). Remnants of the neural arch are visible in dorsal view, as are three large serially arranged fenestrae along the dorsal surface. In lateral view, the centrum is medially constricted, has a large oval dorsal and ventral fossa, a distinctive medial circular depression, and scattered antero-medial and postero-ventral fenestration (Fig. 28J). The ventral surface is deeply depressed along centrum length, and several small circular openings are visible (Fig. 28K). Posteriorly, this depression is flanked by a short postero-ventrally directed projection just before the centrum rim.

SC2018.7.139 (Fig. 28F–H) is an incomplete centrum measuring 3.5 cm along the dorsal surface. The postero-dorsal part of the centrum is not preserved. Anteriorly, the articular rim is slightly wider than high, measuring a maximum width of 3.2 cm and height of 2.9 cm (Fig. 28F). At this end, the centrum outline is sub-circular, with a weakly concave dorso-medial portion and slight ventral taper. Although the posterior rim is broken, enough of its morphology is preserved to determine that its maximum width was only 2.7 cm. The anterior and posterior surfaces are deeply concave and numerous concentric growth annuli are visible. The lateral surfaces bear several shallow, elongated depressions that form two ridge-like structures which do not intersect with the articular margins. The depressions bear several small to moderately large oval fenestrae. Additionally, numerous short, very closely spaced striations occur at the anterior and posterior ends that do not intersect with the centrum rims (Fig. 28G). Dorsally there is a broad depression that is deepest closer to the posterior end (Fig. 28H). A deep fenestra occurs immediately posterior to this depression, and the fenestra is flanked by the bases of apparent spinous projections.

SC2018.7.140 (Fig. 28L–M) is a hypural complex consisting of anterior urostyle and hypural plate. The urostyle has the morphology of a typical vertebral centrum, which is slightly wider than high (1.7 cm and 1.5 cm, respectively) and deeply concave. The lateral faces of the urostyle are highly convex anteriorly and exhibit smooth to weakly fibrous texture, tapering posteriorly to the fused hypural plate (Fig. 28L). The dorsal and ventral surfaces of the urostyle are deeply depressed immediately anterior to the hypural plate (Fig. 28M). The plate itself is a very thin but tall paddle-like

structure, roughly triangular in outline, with the dorsal portion being somewhat larger than the ventral portion. The maximum height measures 4.8 cm (although there is slight damage at the ventral tip), the maximum width at the antero-dorsal surface is 4 mm, and the posterior width measures only 2 mm. In profile view, the antero-dorsal and antero-ventral margins are straight, and the surfaces are flat. The vertical posterior margin is moderately convex, but there is some damage to its medial portion. The dorsal and ventral portions of the lateral surfaces exhibit weak oblique ridges and grooves that represent the fused hypurals. The medial portion of the plate is smooth.

Remarks. The isolated tooth (SC2018.7.135) is easily distinguished from *Sphyraena* and *Scomberomorus* by its rather conical appearance and presence of coarse lingual ridges (compare Fig. 28N to Figs. 23B & 25H). The specimens of *Sphyraenodus* available to us are recurved, lack carinae (i.e., Fig. 26F), are fluted along the entire base of the crown (i.e., Fig. 26A), and lack a basal pulp cavity (i.e., Fig. 26D). The tooth lacks an apical barb as occurs on laniary teeth of *Trichiurides sagittidens* (compare Fig. 28N to Fig. 25C). Although it is superficially similar to teeth of *Eutrichiurides plicidens* (Arambourg, 1952) reported from the Bartonian Gosport Sand of Alabama (Ebersole et al. 2019), SC2018.7.135 does not have a sinuous profile, and its basal outline is D-shaped as opposed to circular.

Of the vertebral centra, specimens SC2009.2.2 (Fig. 28C–E) and SC2015.59.33 are morphologically identical and therefore considered by us to be conspecific. These vertebrae appear to have been from the post-abdominal region of the spinal column. The posterior surface of SC2016.49.2 is partially encrusted by worm tubes and bryozoan colonies (Fig. 28I), suggesting a period of exposure on the sea floor prior to burial. The ventral depression on SC2018.7.139 is likely an articulation for an autonomous haemal arch, indicating the specimen is from the ural region of the spine.

With respect to the hypural (SC2018.7.140), we evaluated the neontological skeletal marine fish collection at MSC to try and identify this fossil taxon. Our evaluation was by no means exhaustive, as less than 80 taxa were available to us, but we observed that a hypural complex is well-developed in a wide range of marine fishes, including *Opsanus pardus* (Goode & Bean, 1880) (Batrachoididae; MSC 39079), *Prionotus carolinus* (Linnaeus, 1771) (Triglidae; MSC 51171), and *Menticirrhus americanus* (Linnaeus, 1758) (Sciaenidae; MSC 51166). Due to the limited skeletal sample, we focused our comparative efforts on the hypural complexes of those teleost taxa represented in the Tupelo Bay Formation sample.

Although a specimen of Albulidae was not available to us, the caudal skeleton of *Pterothrissus gissu* Hilgendorf, 1877 illustrated by Forey (1973: fig. 68) shows that the hypurals are unfused elements. The hypurals of a juvenile *Trichiurus lepturus* Linnaeus, 1758 that we examined (MSC 42592) were similarly not fused to each other. The caudal skeleton of *Cylindracanthus* and *Sphyraenodus* is unknown. Of two *Sphyraena* (Sphyraenidae) hypural complexes we examined, one from a 39 cm total length *Sphyraena borealis* DeKay, 1842 (MSC 49480) and one of *S. barracuda* (Edwards, 1771) (SC2018.3.1) of unknown length, the parhypophysis is fused to hypurals 1 and 2, but this structure is not fused to the remainder of the complex (hypurals 3-4 are fused to each other and to the urostyle). Additionally, there is a deep notch separating the upper and lower halves of the hypural plate. Of two *Scomberomorus cavalla* (Cuvier, 1829) (Scombridae) hypurals that we examined (SC2018.3.49, SC2018.3.50), the hypural plate has a morphology similar to that of SC2018.7.140, but the urostyles of the former are significantly shorter, and the articular rims are more thickened compared to the fossil. Although an extant representative of Istiophoridae was not available to us, hypural plates of these fishes have been reported in the literature. Specimen SC2018.1.140 lacks a fused parhypural and the associated lateral keel of the parhypurapophysis as seen on istiophorid hypurals (Fierstine & Walters 1968; Potthoff & Kelley 1981; Purdy et al. 2001; Monsch 2005). The hypurals of *Chilomycterus reticulatus* (Linnaeus, 1758) and *Diodon histrix* Linnaeus, 1758 (Diodontidae) that we examined (MSC 51172 and MSC 49136, respectively) were not fused, but Tyler (1980) illustrated skeletons of both genera (figs. 288 and 281, respectively) that show the hypural plate has a rather rectangular outline and is largely conjoined with the urostyle. This was similarly true for the hypural complex of *Acanthostracion quadricornis* (Linnaeus, 1758) (Ostraciidae; MSC 49107), which also exhibits a deep medial posterior notch (see also Tyler 1980 for other members of this family). The hypural plate of both *Balistes capriscus* and

Canthidermis maculata (Bloch, 1786) (Balistidae; MSC 49484 and MSC 49305, respectively) is triangular in lateral view but has a very short urostyle with thickened articular rim and a large medial posterior notch (see Tyler, 1980 for other members of this family).

The hypural complex of several other fossil scombroid taxa has been documented, including those of Sardini and Thunnini. The parhypural may not be fused on some Sardini hypural plates, and the articular region can have a conspicuously embayed appearance. This feature is lacking on SC2018.7.140 but present on the hypural of an uncatalogued *Sarda sarda* (Bloch, 1793) we examined at SC (see also Uyeno & Fuji 1975; Monsch 2005; Oyanadel-Urbina et al. 2021). On *Acanthocybium* and *Neocybium*, the parhypophysis is fused to the urostyle and a parhypurapophysis is conspicuous (Purdy et al. 2001; Monsch 2005; Monsch & Bannikov 2011). Furthermore, the urostyle of thunniform fishes is similar to that of *Scomberomorus*, being short and with a thickened rim (i.e., MSC 51187; also Fierstine & Walters 1968; Purdy et al. 2001; Arratia & Schultze 2013), unlike the condition seen on SC2018.7.140.

Discussion

Our sample of nearly 600 teeth and skeletal remains from the Tupelo Bay Formation of Dorchester County, South Carolina, USA represents at least 41 fish taxa. Thirty of these are chondrichthyans and the remaining 11 are teleosts. Of the chondrichthyans, Carcharhinidae is the most diverse group and represented by 12 taxa, including a new species of *Galeorhinus*. The apparently depauperate teleost component and lack of microscopic taxa (i.e., Dasyatidae, Rajidae) at least partially reflects a collecting bias, since our field-collected sample consists of specimens visible to the naked eye (>2 mm in greatest dimension). Diversity may also have been affected by taphonomic processes, as several specimens are ablated (i.e., Fig. 28K), exhibit apparent bioerosion (Fig. 19C–D), or bear encrusting bryozoans and/or serpulid worm tubes (i.e., Fig. 28I), indicating that burial was not immediate (see Stringer 2016). The lack of microscopic remains in the 100 kg of processed matrix could reflect the general absence of species with such small skeletal elements or may indicate winnowing by bottom currents. Although otoliths representing a variety of teleost fishes have been reported from the middle and late Eocene of Alabama, Georgia, and Virginia (Ebersole et al. 2019; Stringer et al. 2022; Lin et al. 2024), none of these structures appear to have been preserved in the Tupelo Bay Formation and may be related to taphonomic processes like leaching.

As outlined above, many of the elasmobranch taxa in the Tupelo Bay Formation, like *Hexanchus agassizi*, *Otodus* (*Carcharocles*) *sokolowi*?, *Striatolamia macrota*, *Macrorhizodus praecursor*, and *Hemipristis curvatus* (among others), occur in Eocene strata of widely disparate global locations. *Physogaleus secundus* and *Premontreia* (*Oxyscyllium*) *gilberti* may be included in this group, but variations in the size and number of distal heel denticles, lateral cusplets, and ornamentation among the reported specimens indicate a broad interpretation of the taxa (i.e., multiple species may be represented). Interestingly, *Eostegostoma angustum* is now known to occur in the eastern and western global hemispheres but published accounts are very limited. In North America, *Heterodontus* was an apparently uncommon component of Eocene marine vertebrate assemblages, as relatively few specimens have been reported among thousands of teeth occurring in the Atlantic and Gulf coastal plains.

With respect to previously reported Eocene fish assemblages of the USA, that of the Tupelo Bay Formation most closely resembles those of the Gosport Sand of Alabama and Clinchfield Formation of Georgia. The latter units have been correlated with the Cross Member of the Tupelo Bay Formation (NP17), but the Pregnall Member (source of the fossils described herein) is slightly younger and within NP18, equivalent to the Cocoa Sand of the Yazoo Clay of Alabama and Mississippi in the Gulf Coastal Plain. Calcareous nannoplankton zone NP18 represents a relatively short, roughly 400 Ka time interval, and the difference in age among the Pregnall Member and NP17 units may not be appreciable.

Although there is general congruity among the various paleofaunas, notable exceptions include the absence of *H. agassizi*, *E. angustum*, *Isurolamna inflata*, and *Sphyraenodus* sp. from the Gosport Sand and Clinchfield Formation. This may not be surprising given that global occurrences of these taxa indicate they were uncommon. The absence of *Pseudabdounia claibornensis* from the Clinchfield Formation is notable considering the taxon occurs in Eocene deposits of North Carolina (Castle Hayne and Paint Hill formations) and likely as far north as

Taxon	Atlantic Coastal Plain		Gulf Coastal Plain
	Tupleo Bay Formation (NP18)	Clinchfield Formation (NP17)	Gosport Sand (NP17)
	n = 592	n = 7,049	n = 7,154
Hexanchus agassizi	X		
Heterodontus aff. *vincenti*	X	X	?
Squatina prima	X	X	X
Nebrius thielensi	X	X	X
Eostegostoma angustum	X		
Otodus (*Carcharocles*) *sokolowi*?	X	X	?
Anomotodon novus	X		?
Striatolamia macrota	X	X	X
Brachycarcharias twiggsensis	X	X	X
Macrorhizodus praecursor	X	X	X
Isurolamna inflata	X		
Alopias cf. *alabamensis*	X		
Galeorhinus semiserratus sp. nov.	X		
Pachyscyllium sp.	X		
Premontreia (*Oxyscyllium*) *gilberti*	X	X	
Hemipristis curvatus	X	X	X
Pseudabdounia claibornensis	X		X
Abdounia minutissima	X		X
Abdounia enniskilleni	X	X	X
Carcharhinus sp.	X		*C. mancinae*
Negaprion gilmorei	X	X	X
Physogaleus aff. *contortus*	X		
Physogaleus aff. *secundus*	X	X	X
Galeocerdo clarkensis	X	X	X
Pristis sp.	X	X	X
Propristis schweinfurthi	X	X	X
"*Aetomylaeus*" sp.	X	X	X
"*Myliobatis*" sp.	X	X	X
"*Rhinoptera*" sp.	X	X	X
Egertonia isodonta	X		X
Albula oweni	X	X	X
Sphyraena sp.	X	X	X
Xiphiorhynchus sp.	X		
Trichiurides sagittidens	X	X	X
Scomberomorus sp.	X		X
Sphyraenodus sp.	X		
Ostraciidae indet.	X		X
Lobodus pedemontanus	X	X	X
Progymnodon hilgendorfi	X	X	X
Cylindracanthus rectus	X	X	X

Tab. 1 - Comparison of the fish paleofaunas of the Tupelo Bay Formation (South Carolina), the Clinchfield Formation (Georgia), and Gosport Sand (Alabama). Tupelo Bay Formation records are based on this report. Records from the Clinchfield Formation are based on Parmley and Cicimurri (2003) and additional specimens housed at SC. Records from the Gosport Sand are based on Ebersole et al. (2019) and examination of the specimens at MSC. Fields marked with an "X" denote the occurrence of the taxon as identified in the far-left column, blank fields indicate their absence, and "?" indicates that the genus has been reported but the species is unknown. For example, *Anomotodon novus* occurs in the Tupelo Bay Formation, but unspeciated teeth were reported in the Gosport Sand and the genus is unknown in the Clinchfield Formation. Note that this table excludes Ginglymostomatidae indet. and Carchariidae indet. because the few teeth available could represent one of the species we identified based on other fossils (i.e., *Nebrius thielensi* and *Brachycarcharias twiggsensis*, respectively), rather than unique taxa (i.e., *Ginglymostoma* or *Mennerotodus*, respectively). However, Ostraciidae indet. is included because the remains are unique (dermal armor) among the other species represented by teeth and jaws. The total number of non-otolith fossils from each lithostratigraphic unit is indicated by "n".

New Jersey (Shark River Formation). Interestingly, there is a greater abundance of *Pristis* and *Propristis* rostral spines within the Clinchfield Formation compared to the Gosport Sand and Tupelo Bay Formation. It would appear that the taxonomic differences among the formations are more indicative of environmental conditions/depositional environment rather than a reflection of temporal variation. However, in the case of *Alopias* cf. *alabamensis*, the absence of the species from the Bartonian Gosport Sand and Clinchfield Formation is likely related to geologic age, as these units are older than the roughly contemporaneous records from the Priabonian Yazoo Clay (source of type specimens) and Tupelo Bay Formation.

Most of the specimens from the Tupelo Bay Formation were recovered from the lower 5 m of the exposed sections, and relatively few specimens were recovered from the uppermost 1 m of the formation. Unfortunately, most of the former specimens were recovered as float, and we cannot rule out the possibility that they originated from stratigraphically higher in the section (Parkers Ferry and Harleyville formations; see Fig. 2). Banks (1977) suggested that the lower limestone at the Giant Portland Cement quarry represents deposition within an outer neritic

environment where water depth was about 100 m. Such a depth could explain the presence in the Tupelo Bay Formation of *Hexanchus*, a genus regarded as a deepwater shark (>100 m) based on distributions of extant species (Compagno et al. 2005; Castro 2010). The Gosport Sand, in contrast, accumulated within a highly dynamic deltaic environment (Pietsch et al. 2016), and the Clinchfield Formation represents an inner shelf environment of normal to slightly reduced salinity with water depth of less than 20 m (Herrick 1972; Stringer et al. 2022). One of the few other Eocene records of hexanchid sharks in the Atlantic Coastal Plain, *Notorynchus*, was reported from nearshore marine sands of the Dry Branch Formation (Priabonian) of South Carolina (Cicimurri & Knight 2019). The extant species, *N. cepedianus* (Péron, 1807), is considered a nearshore (<100 m) taxon (Compagno et al. 2005).

Teeth of *O.* (*C.*) *sokolowi*? and *Brachycarcharias twiggsensis* were recovered from the lower and uppermost limestones of the Tupelo Bay Formation, indicating a broad environmental range. According to Banks (1977), the limestone comprising the upper part of the formation represents open-water deposition under normal salinity, sub-tropical to tropical conditions, below wave base in the subtidal zone. These records further demonstrate, as do specimens from the Gosport Sand (Ebersole et al. 2019) and Clinchfield Formation (Parmley & Cicimurri 2003), that these taxa could tolerate a variety of marine environments. If extant *Heterodontus francisci* (Girard, 1855) can be used as a model, the temperature at the depth at which *H.* aff. *vincenti* lived within the Tupelo Bay Formation environment was between 15° and 24° C (Meese & Lowe 2020). This temperature estimate might conflict with the occurrence of *Hexanchus agassizi*, but diel patterns of extant *H. griseus*, a deepwater taxon tolerating temperatures of <15° C (Rodríguez-Cabello et al. 2018), show that this shark migrates several hundred meters into shallower water each day (ca. 20° C), likely in search of food (Andrews et al. 2009; Coffey et al. 2020).

Conclusions

Forty-one unequivocal fish taxa have been identified in the Tupelo Bay Formation in South Carolina, USA. One new taxon, *Galeorhinus semiserratus* sp. nov., is recognized, and additional new records for the Eocene Atlantic Coastal Plain include the sharks *Eostegostoma angustum* and *Isurolamna inflata*, and the scombroid fish *Sphyraenodus* sp. The overall composition of the Tupelo Bay Formation fish assemblage is comparable to those of the Gosport Sand (Bartonian) of Alabama and Clinchfield Formation (Bartonian) of Georgia, USA. Our sample is likely size biased, as the taxa we identified are represented by elements collected as float that were visible to the naked eye. Future work within the Tupelo Bay Formation is warranted, as intensive bulk sampling could be conducted to recover microfossils like teeth of dasyatid rays and other bony fishes. However, recovery of only three shark teeth from approximately 100 kg of matrix associated with skeletal remains of larger taxa indicates it will be necessary to process a substantially large amount of material.

Acknowledgements: We wish to thank Sue Kelly for the many hours of her time volunteering at SC to help to organize, inventory, and catalogue the Tupelo Bay Formation specimens. Robyn Thiesbrummel (SC) arranged a loan of specimens and provided matrix samples for microfossil analyses. We are indebted to Chris Sagrera (SC) for his help during the final stages of manuscript preparation, which involved providing photographs and additional information for SC specimens. Our thanks are also extended to Emma Bernard, Peter Grugeon, and other NHMUK staff for their time and effort in tracking down, conserving, and photographing White's (1956) suite of *Alopias latidens alabamensis* teeth. Alberto Collareta (Università di Pisa, Italy) provided insight into the nature of the bioerosion occurring on *Pristis* sp. spines reported herein. We improved upon an earlier version of this manuscript thanks to the editorial comments received from Collareta, Gary Stringer (University of Louisiana, Monroe), and the editorial committee at the GSAfor their time and effort in reviewing the article content. The dedication and hard work of the RIPS staff is greatly appreciated.

References

Abd-Elhameed S. & Abd-Elhameed M. (2025) – Qualitative and quantitative analyses of middle Eocene odontaspidid shark (*Brachycarcharias*) from Wadi Garawi area, north Eastern Desert, Egypt. *Advances in Basic and Applied Sciences*, 5: 21-28. https://doi.org/10.21608/ABAS.2025.403624.1068

Adnet S. (2006a) – Biometric analysis of the teeth of fossil and Recent hexanchid sharks and its taxonomic implications. *Acta Palaeontologica Polonica*, 51(3): 477-488.

Adnet S. (2006b) – Nouvelles faunes de sélaciens (Elasmobranchii, Neoselachii) de l'Éocène des Landes (Sud-Ouest, France). Implication dans les connaissances des communautés deuax profondes. *Palaeo Ichthyologica*, 10, 128 p.

Adnet S. & Cappetta H. (2008) – New fossil triakid sharks from the early Eocene of Prémontré, France, and comments on fossil record of the family. *Acta Paleontologica Polonica*, 53(3): 433-448.

Adnet S., Cappetta H. & Reynders J. (2008) – Contribution of Eocene sharks and rays from southern France to the history of deep-sea selachians. *Acta Geologica Polonica*, 58(2): 261-264.

Adnet S., Antoine P.-O., Hassan Boqri S.R., Crochet J.-Y., Marivaux L., Welcomme J.-L. & Métais G. (2007) – New tropical carcharhinids (Chondrichthyes, Carcharhiniformes) from the late Eocene-early Oligocene of Balochistan, Pakistan: paleoenvironmental and paleogeographic implications. *Journal of Asian Earth Sciences*, 30(2): 303-323.

Adnet S., Cappetta H. & Tabuce R. (2010) – A middle-late Eocene vertebrate fauna (marine fish and mammals) from southwestern Morocco; preliminary report: age and palaeobiogeographical implications. *Geological Magazine*, 147(6): 860-870.

Adnet S., Marivaux L., Cappetta H., Charruault A.-L., Essid M., Jiquel S., Ammar H.K., Marandat B., Marzougui W., Merzeraud G., Temani R., Vianey-Liaud M. & Tabuce R. (2020) – Diversity and renewal of tropical elasmobranchs around the Middle Eocene Climatic Optimum (MECO) in North Africa: New data from the lagoonal deposits of Djebel el Kébar, Central Tunisia. *Palaeontologia Electronica*, 23(3): a38.

Adolfssen J.A. & Ward D.J. (2013) – Neoselachians from the Danian (Early Paleocene) of Denmark. *Acta Palaeontologica Polonica*, 60(2):313-338.

Agassiz J.L.R. (1833-1844) – *Recherches sur les Poissons fossiles*. Imprimerie de Petitpierre, Neuchâtel. https://doi.org/10.5962/bhl.title.4275

Albright L.B. (1996) – A protocetid cetacean from the Eocene of South Carolina. *Journal of Paleontology*, 70(3): 519-523.

Albright L.B. III, Sanders A.E., Weems R.E., Cicimurri D.J. & Knight J.L. (2019) – Cenozoic vertebrate biostratigraphy of South Carolina, U.S.A., and additions to the fauna. *Bulletin of the Florida Museum of Natural History*, 57(2) : 77-236.

Andrews K.S., Williams G.D., Farrer, D., Tolimieri N., Harvey C.J., Gargmann G. & Levin P.S. (2009) – Diel activity patterns of sixgill sharks, *Hexanchus griseus* : the ups and downs of an apex predator, *Animal Behaviour*, 78(2) : 525-536.

Applegate S.P. (1968) – A large Sand shark of the genus *Odontaspis* in Oregon. *The Ore Bin*, 30 (2) : 32-36.

Applegate S.P. (1972) – A revision of the higher taxa of orectolobids. *Journal of the Marine Biological Association of India*, 14(2) : 743-751.

Applegate S.P. (1978) – Phyletic studies. Part I. Tiger sharks. *Universidad Nacional Autonoma de Mexico, Instituto de Geologica, Revista*, 2(1) : 55-64.

Applegate S.P. & Espinosa-Arrubarenna L. (1996) – The fossil history of *Carcharodon* and its possible ancestor, *Cretolamna*: a study in tooth idnetification. Pp. 19-36 *in* Kimley A.P. & Ainley D.G. (eds.), Great white sharks. The biology of *Carcharodon carcharias*. Academic Press, San Diego, California.

Arambourg C. (1935) – Note preliminaire sur les vertébrés fossiles des phosphates du Maroc. *Bulletin de la Société géologique de France*, 5(5) : 413-439.

Arambourg C. (1952) – Les vertébrés fossiles des gisemens de phosphates (Maroc-Algérie-Tunisie). *Service Géologique du Maroc, Notes et Mémoires*, 92, 372 p.

Arratia G. & Schultze H.-P. (2013) – Outstanding features of a new Late Jurassic pachycormiform fish from the Kimmeridgian of Brunn, Germany and comments on current understanding of pachycormiforms. Pp. 87-120 in Arratia, G., H.-P. Schultze, and M.V.H. Wilson (eds.), *Mesozoic Fishes 5* – Global Diversity and Evolution.

Asan A., Salame I. & Strougo A. (2022) – Sharks and rays from the Mokattamian Stage (middle and late Eocene) of Egypt, including some species from the middle Eocene Midra Shale of Qatar. *Egyptian Journal of Geology*, 66:105-153.

Ballen G.A. (2020) – New records of the genus *Sphyraena* (Teleostei: Sphyraenidae) from the Caribbean with comments on dental characters in the genus. *Journal of Vertebrate Paleontology*, e1849246. https://doi.org/10.1080/02724634.2020.1849246

Banks R.S. (1977) – Stratigraphy of the Eocene Santee Limestone in three quarries in the Coastal Plain of South Carolina. *South Carolina Geological Survey Geological Notes*, 21(3): 85-149.

Baum G.R., Collins J.S., Jones R.M., Madfinger B.A. & Prowell R.J. (1980) - Correlation of the Eocene strata of the Carolinas. *South Carolina Geology*, 24(1): 19-27.

Berg L. (1940) – Classification of fishes both fossil and recent [in Russian]. *Proceedings of the Zoological Institute of Russa*, 5:87-517.

Berg L. (1958) – System der rezenten und fossilen Fischartigen und Fishe. Verlag der Wissenschaften, Berlin, 310 p.

Blainville H.M.D. (1816) – Podrome d'une nouvelle distribution systématique du règne animal. *Bulletin de la Société Philomathique de Paris*, 8: 105-112, 121-124.

Blainville H.M.D. (1818) – Sur les ichthyolites ou les poissons fossils. *Nouveau Dictionnaire d'Histoire Naturelle*, 27: 310-391.

Blake C.C. (1862) – Shark's teeth at Panama. *Geologist*, 5: 316.

Bleeker P. (1859) – Enumeratio specierum piscium hueusque in Archipelago Indico observatarum. *Verhandelingen der Wetenschappelijke Vereeniging in Nederlandsch Indië*, 6: 1-276.

Bloch M.E. (1786) – Naturgeschichte der ausländische Fische. Vol. 2. Berlin, Germany, 160 p.

Bloch M.E. (1793) – Naturgeschichte der ausländischen Fische. Vol. 7. Berlin, Germany

Bone D.A., Todd J.A. & Tracey S. (1991) – Fossils from the Bracklesham Group exposed in the M27 Motorway excavations, Southampton, Hampshire. *Tertiary Research* 12(3-4): 131-137.

Bonnaterre J.P. (1788) – Tableau encyclopédique et méthodique des trois règnes de la nature. Ichthyologie. Panckoucke, Paris: 215 p.

Bonaparte C.L. (1838) – Selachorum tabula analytica. *Nuovi Annali delle Scienze Naturali*, 1:195-214.

Bor T. (1985) – Elasmobranch teeth (Vertebrata, Pisces) from the Dongen Formation (Eocene) in the Netherlands. *Mededelingen Van De Werkgroep voor Tertiaire en Kwartaire Geologie*, 22(2) : 73-122.

Boulemia S. & Adnet S. (2023) – A new Paleogene elasmobranch fauna (Tebessa region, eastern Algeria) and the importance of Algerian-Tunisian phosphates for the North African fossil record. *Annales de Paleontologie*, 109(3): 102632. https://doi.org/10.1016/j.annpal.2023.102632

Breard S. & Stringer G. (1995) – Paleoenvironment of a diverse marine vertebrate fauna from the Yazoo Clay (Late Eocene) at Copenhagen, Caldwell Parish, Louisiana. *Gulf Coast Association of Geological Societies Transactions*, 45: 77-85.

Breard S. & Stringer G. (1999) – Integrated paleoecology and marine vertebrate fauna of the Stone City Formation (middle Eocene), Brazos River section, Texas. *Gulf Coast Association of Geological Societies Transactions*, 49: 132-142.

de Buen F. (1926) – Catálogo ictiológico del Mediterráneo español y de Marruecos recopilando lo publicado sobre peces de las costas mediterránea y próximas del Atlántico (Mar de España). Instituto Español de Oceanoografia. Resultado de las campañas realizadas por acuerdos internacionales bajo la dirección del Prof. O. de Buen, 2, 221 p.

Campbell D. (1995) – New molluscan faunas from the Eocene of South Carolina. *Tulane Studies in Geology and Paleontology*, 27(1-4): 119-152.

Cappetta H. (1976) – Sélaciens nouveaux du London Clay de l'Essex (Yprésien du Bassin de Londres). *Geobio*s, 9 :551-575.

Cappetta H. (1980) – Modification du statut générique de quelques espèces de sélaciens crétacés et tertiaires. *Palaeovertebrata*, 10(1): 29-42.

Cappetta H. (1981) – Additions a la faune de selaciens fossils du Maroc. 1: Sur la presence des genres *Heptranchias*, *Alopias* et *Odontorhytis* dans l'Ypresien des Ouled Abdoun. *Geobios*, 14(5): 563-575.

Cappetta H. (1987) – Chondrichthyes – Mesozoic and Cenozoic Elasmobranchii: Teeth. *Handbook of Paleoichthyology*, 3E, Friedrich Pfiel, Munich, Germany, 193 p.

Cappetta H. (1992) – Carcharhiniformes nouveaux (Chondrichthyes, Neoselachii) de l'Yprésien du Bassin de Paris. *Geobios*, 25(5): 6339-646.

Cappetta H. (2012) – Chondrichthyes – Mesozoic and Cenozoic Elasmobranchii: Teeth. *Handbook of Paleoichthyology*, 3E, Friedrich Pfiel, Munich, Germany, 512 p.

Cappetta H. & Case G.R. (1990) – The Eocene selachian fauna from the Fayum Depression in Egypt. *Palaeontographica Abteilung A*, 212(1-6): 1-30.

Cappetta H. & Case G.R. (2016) – A selachian fauna from the middle Eocene (Lutetian, Lisbon Formation) of Andalusia, Covington County, Alabama, USA. *Palaeontographica Abteilung A*, 307(1-6): 43-103.

Cappetta H. & Nolf D. (2005) – Révision quelques Odontaspididae (Neoselachii: Lamniformes) du Paléocène et de l'Eocène du Bassin de la Mer du Nord. *Bulletin de l'Institut Royal des Sciences Naturelles de Belgique*, Science de la Terre, 75: 237-266.

Carlsen A.W. & Cuny G. (2014) – A study of the sharks and rays from Lillebælt Clay (Early-Middle Eocene) of Denmark, and their paleoecology. *Bulletin of the Geological Society of Denmark*, 62: 39-88.

Case G.R. (1981) – Late Eocene selachians from south-central Georgia. *Palaeontographica Abteilung A*, 176: 52-79.

Case G.R. (1994) – Fossil fish remains from the Late Paleocene Tuscahoma and Early Eocene Bashi formations of Lauderdale County, Mississippi. Part 1. Selachians. *Palaeontographica Abteilung A*, 230(4-6): 97-138.

Case G.R. & Borodin P.D. (2000a) – Late Eocene selachians from the Irwinton Sand Member of the Barnwell Formation (Jacksonian), WKA mines, Gordon, Wilkinson County, Georgia. *Münchner Geowissenschafliche Abhandlungen Reihe A, Geologie und Paläontologie*, 39: 5-16.

Case G.R. & Borodin P.D. (2000b) – A middle Eocene selachian fauna from the Castle Hayne Limestone Formation of Duplin County, North Carolina. *Münchner Geowissenschaftliche Abhandlungen, A, Geologie und Paläontologie*, 39: 17-32.

Case G.R. & Cappetta H. (1990) – The Eocene selachian fauna from the Fayum Depression in Egypt. *Palaeontographica Abteilung A*, 212(1-6): 1-30.

Case G.R., Cook T.D. & Wilson, M.V.H. (2015) – A new elasmobranch assemblage from the early Eocene (Ypresian) Fishburne Formation of Berkeley County, South Carolina, USA. *Canadian Journal of earth Sciences*, 52(12): 1121-1136.

Case G.R., Udovichenko N.I., Nessov L.A., Averianov A.O. & Borodin P.D. (1996) – A middle Eocene selachian fauna from the White Mountain Formation of the Kizylkum Desert, Uzbekistan, CIS. *Palaeontographica Abteilung A*, 242(4-6): 99-126.

Casier E. (1946) – La faune ichthyologique de l'Yprésien de la Belgique. *Mémoire de l'Institut roal des Sciences naturelles de Belgique*, 104, 267 p.

Casier E. (1957) – Les faunes ichthyologiques du Crétacé et du Cénozoique de l'Angola et de l'Enclave de Cabinda. Leurs affinités paléobiogéographiques. *Comunicações dos Serviços Geológicos de Portugal*, 38(2): 269-290.

Casier E. (1966) – Faune ichthyologique du London Clay. British Museum (Natural History), London, 515p.

Castro J.I. (2010) – The sharks of North America. Oxford University Press, England, 640 .

Charnelli M., Gouiric-Cavalli S., Reguero M.A. & Cione A.I. (2023) - Middle Eocene chondricthyan fauna from Antarctic Peninsula housed in the Museo de La Plata, Argentina. *Advances in Polar Science*, 35(1): 14-47.

Cicimurri D.J. (2007) – A partial rostrum of the sawfish *Pristis lathami* Galeotti, 1837, from the Eocene of South Carolina. J*ournal of Paleontology*, 81(3): 597-601.

Cicimurri D.J. & Ebersole J.A. (2015) – Two new species of *Pseudaetobatus* Cappetta, 1986 (Batoidea: Myliobatidae) from the southeastern United States. *Palaeontologia Electronica*, 18(1)15A: 1-17. doi.org/10.26879/524

Cicimurri D.J. & Ebersole J.A. (2021) – New Paleogene elasmobranch (Chondrichthyes) records from the Gulf Coastal Plain of the United States, including a new species of *Carcharhinus* de Blainville, 1816. *Cainozoic Research*, 21(2):147-164.

Cicimurri D.J., Ebersole J.A. & Martin G. (2020) – Two new species of *Mennerotodus* Zhelezko, 1994 (Chondrichthyes: Lamniformes: Odontaspididae), from the Paleogene of the southeastern United States. *Fossil Record*, 23: 117-140.

Cicimurri D.J., Stringer G.L. & Ebersole J.E. (2025a) – Additional records of Paleogene fishes (Chondrichthyes and Osteichthyes) from Alabama, USA. *Acta Geologica Polonica*, 75(4-e60): 1-40.

Cicimurri D.J., Ebersole J.A., Stringer G.L., Starnes J.E. & Phillips G.E. (2025b) – Late Oligocene fishes (Chondrichthyes and Osteichthyes) from the Catahoula Formation in Wayne County, Mississippi, USA. *European Journal of Taxonomy*, 984: 1-131.

Cicimurri D.J. & Knight J.L. (2019) – Late Eocene (Priabonian) elasmobranchs from the Dry Branch Formation (Barnwell Group) of Aiken County, South Carolina, USA. *PaleoBios*, 36: 1-31.

Cicimurri D.J., Knight J.L., Self-Trial J.M., and Ebersole, S.M. (2016) – Late Paleocene glyptosaur (Reptilia: Anguidae) osteoderms from South Carolina, USA. *Journal of Paleontology* 90(1): 147-153.

Cigala-Fulgosi F. (1983) – First record of *Alopias superciliosus*

(Lowe, 1840) in the Mediterranean, with notes on some fossil species of the genus *Alopias*. *Estratto dagli Annali del Museo Civico di Storia Naturale di Genova*, 84: 211-229.

Cocchi I. (1864) – Monografia dei Pharyngodopilidae: Nuova famiglia di pesci Labroidi. Studi paleontologici. M. Cellini, Florence, Italy.

Coffey D.M., Royer M.A., Meyer C.G. & Holland K.N. (2020) – Diel patterns in swimming behavior of a vertically migrating deepwater shark, the bluntnose sixgill (*Hexanchus griseus*). *PLoS ONE* 15(1): e0228253.

Collareta A., Marella M., Casati S., Di Cencio A., Tinelli C. & Bianucci G. (2023) – Polyplacophoran feeding traces on Mediterranean Pliocene sirenian bones: Insights on the role of grazing bioeroders in shallow-marine vertebrate falls. *Life*, 13(327): 1-15. doi.org/10.3390/life1320327

Compagno L.J.V. (1973) – Interrelationships of living elasmobranchs. *Zoological Journal of the Linnaean Society*, 53(supplement 1): 15-61.

Compagno L.J.V. & Last P.R. (1998) – Batoid fishes. Pp. 1410-1529, *in* Carpenter K.E. & Niem V.H. (eds.), The living marine resources of the western central Pacific. Volume 2. Cephalopods, crustaceans, holothurians and sharks. *FAO*, Rome, Italy, p. 687-1396.

Compagno L.J.V., Dando, M. & Fowler S. (2005) – Sharks of the world. Princeton University Press, New Jersey, 368 p.

Cooke C.W. & MacNeil F.S. (1952) – Tertiary stratigraphy of South Carolina. *US Geological Survey Professional Paper* 243-B: 19-29.

Cope E.D. (1870) – Eocene marl of Farmingdale, Monmouth County, New Jersey. *Proceedings of the American Philosophical Society*, 12: 294.

Cope E.D. (1871) – Observations on the systematic relations of the fishes. The American Naturalist, 5: 579-593.

Costa O.G. (1866) – Nuove osservazioni intorno ai fossili di Gassino, ed illustrazione di alcune nouve specie, 41 pp. Antonio Cons tipografo, Napoli.

Cunningham S.B. (2000) – A comparison of isolated teeth of early Eocene *Striatolamia macrota* (Chondrichthyes, Lamniformes), with those of a recent sand shark, *Carcharias taurus*. *Tertiary Research*, 20(1-4): 17-31.

Cuvier G.L.C.F.D. (1816) – Le régne animal distsribué d'après son organization pour server de base à l'histoire naturelle des animaux et d'introduction à l'anatomie comparée. Les reptiles, les poissons, les mollusques et les annélides. Déterville, Paris, 532 p.

Cuvier G.L.C.F.D. (1829) – Le Règne Animal distribué, d'apres son organization, pour server de base à l'histoire naturelle des animaux et d'introduction à l'anatomie comparée. Déterville, Paris, 2nd edition, 406 p.

Dames W. (1883) – Uber eine tertiäre Wirbelthierfauna von der westlichen Insel der Birket-El-Qrûn im Fajum (Aegypten). *Stizungsberichte der Koniglich Preussischen Akademie der Wissenschaftenz zu Berlin*, 6: 129-153.

Dartevelle E. & Casier E. (1943) – Les poissons fossils du Bas-Congo et de regions voisines (part I). *Annales du Musée Congo Belge*, Serie A, 2(1): 1-200.

Dartevelle E. & Casier E. (1959) – Les poissons fossils du Bas-Congo et des regions voisines (part II). *Annales du Musée Congo Belge*, Serie A, 2(1): 257-568.

Deflandre G. & Fert C. (1954) – Observations sur les coccolithophidés actuels et fossils en microscopie ordinaire et électonique. *Annales de Paléontologie*, 40: 115-176.

De Gibert J.M., Domenech R. & Martinell J. (2007) – Bioerosion in shell beds from the Pliocene Roussilon Basin, France: Implications for the macro(bioerosion) ichnofacies model. *Acta Palaeontologica Polonica*, 52(4): 783-798.

DeKay J.E. (1842) – Zoology of New York, or the New York fauna: comprising detailed descriptions of all the animals hitherto observed within the state of New York, with brief notices of those occasionally found near its borders, and accompanied by appropriate illustrations. Part IV. Fishes. W. & A. White & J. Visscher, Albany, New York, 415 p.

Dica E.P. (2002) – A review of the Eocene diodontids and labrids from Transylvania. *Studia Universitatis Babes-Bolyai, Geologia* 47(2): 37-46.

Diedrich C.G. (2013) – Evolution of white and megatooth sharks, and evidence for early predation on seals, sirenians, and whales. *Natural Science*, 5(11): 1203-1218.

Dockery D.T. III & Manning E.M. (1986) – Teeth of the giant white shark *Carcharodon auriculatus* from the Eocene and Oligocene of Mississippi. *Mississippi Geology*, 7(1): 7-19.

Domning D.P., Morgan G.S. & Ray C.E. (1982) – North American Eocene sea cows (Mammalia: Sirenia). *Smithsonian Contributions to Paleobiology*, 52: 1-80.

Dumeril A.H.A. (1806) – Zoologie analytique ou mèthode naturelle de classification des animaux. Paris, France, 344 p.

Ebersole J.A. & Cicimurri D.J. (2025) – Fishes Part I – Chondrichthyes and Osteichthyes: Osteological remains. Pp. 147-191 *in* S. Ting, L.E. Smith, C.D. White, and I. Martí Gil (eds.), Vertebrate Fossils of Louisiana. *Special Publications of the Museum of Natural Science*, 5.

Ebersole J.A., Cicimurri D.J. & Stringer G.L. (2019) - Taxonomy and biostratigraphy of the elasmobranchs and bony fishes (Chondrichthyes and Osteichthyes) of the lower-to-middle Eocene (Ypreseian to Bartonian) Claiborne Group in Alabama, USA, including an analysis of otoliths. *European Journal of Taxonomy*, 585, 274 p.

Ebersole J.A., Cicimurri D.J. & Stringer G.L. (2021) – Marine fishes (Elasmobranchii, Teleostei) from the Glendon Limestone Member of the Byram Formation (Oligocene, Rupelian) at site Awa-9, Washington County, Alabama, USA, including a new species of gobiid (Gobiiformes: Gobiidae). *Acta Geologica Polonica,* 71(4): 481-518.

Ebersole J.E., Cicimurri D.J., Stallworth L.M. & Gentry D. (2024) – Preliminary report on the fishes (Chondrichthyes & Teleostei) from the lower Oligocene (Rupelian) Red Bluff Clay at site AMo-9, Monroe County, Alabama, USA. *Palaeovertebrata*, 47(2-e2): 1-24.

Edwards G. (1771) – A catalogue of the animals and plants represented in Catesby's Natural History of Carolina, with the Linnean names. 1771 revised edition of *The Natural History of Carolina, Florida and the Bahama Islands* by Catesby, M. 100p.

Edwards L.E., Bybell L.M., Gohn G.S. & Fredericksen N.O. (1997) – Paleontology and physical stratigraphy of the USGS – Pregnall No. 1 core (DOR-208), Dorchester County, South Carolina. *US Geological Survey Open-file Report* 97-145, 35 p.

Ehret D.J. & Ebersole J.A. (2014) – Occurrence of the megatoothed sharks (Lamniformes, Otodontidae) in Alabama, USA. *PeerJ* 2: e625. https://doi.org/10.7717/peerj.625.

Fanti F., Minelli D., Conte G.L. & Miyashita T. (2016) – An exceptionally preserved Eocene shark and the rise of modern predator-prey interactions in the coral reef

food web. *Zoological Letters*, 2(9): 1-18. https://doi.org/10.1186/s40851-016-0045-4

Farrés F. (2003) – *Mesopristis* nov. gen. *osonensis* nov. sp., nuevo genéro y especie de pez-sierra del Eoceno de Vic, (Catalunya, NE. de España). *Batalleria*, 11: 93-113.

Farrés F. & Fierstine H.L. (2009) – First record of the extinct sawfish *Propristis schweinfurthi* Dames, 1883 (Batoidea: Pristiformes: Pristidae) from the middle Eocene of Spain. *Palaontologische Zeitschrift*, 83(4): 459-466.

Fierstine H.L. & Applegate S.P. (1974) - *Xiphiorhynchus kimblaylocki*, a new billfish from the Eocene of Mississippi with remarks on the systematics of the xiphioid fishes. *Bulletin of the Southern California Academy of Sciences*, 73(1): 14-22.

Fierstine H.L. & Stringer G.L. (2007) – Specimens of the billfish *Xiphiorhynchus* van Beneden, 1871, from the Yazoo Clay Formation (late Eocene), Louisiana. *Journal of Vertebrate Paleontology*, 27(1): 226-231.

Fierstine H.L. & Walters V. (1968) – Studies in locomotion and anatomy of scombroid fishes. *Memoirs of the Southern California Academy of Sciences*, 6: 1-31.

Forey, P.L. (1973) – A revision of the elopiform fishes, fossil and recent. *Bulletin of the British Museum (Natural History)*, Supplement 10: 222 p.

Fraas E. (1907) – Säge von *Propristis schweinfurthi* Dames aus dem oberen Eocän von Ägypten. *Neues Jahrbuch für Mineralogie un Paläontologie*, 1907(1), 6 p.

Franţescu A.L., Feldmann R.M. & Schweitzer C.E. (2010) – A new genus and species of dromiid crab (Decapoda, Brachyura) from the Middle Eocene of South Carolina. Pp. 255-267 *in* Fransen C.H.J.M., DeGrave S. & Ng P.K.L. (eds.), Studies on Malcostrata: Lipke Bijdeley Holthuis Memorial Volume. *Crustaceana Monographs* 14.

Freile D., DeVore M.L. & Parmley D. (2001) – The first report of *Carcharocles auriculatus* from the Oligocene of Georgia in the context of previous Gulf Coast records. *Georgia Journal of Science*, 59(3): 128-136.

Galeotti H. (1837) – Mémoire sur la constitution géognostique de la province de Brabant. *Mémoire de la Academie Royal de Belgique*, 12(3), 193 p.

Ganis G.R., Willoughby R.H., Cicimurri D.J., Whittecar G.R. & Hageman S.J. (2025) – Evidence for distal bolide impact and tsunami deposits in the upper Atlantic Coastal Plain of Moore County (North Carolina, USA) generated by the Eocene Chesapeake Bay Bolide Impact. *Southeastern Geology*, 55(1): 47-67.

Garman (1908) – New Plagiostomia and Chismopnea. *Bulletin of the Museum of Comparative Zoology at Harvard College*, 51: 249-256.

Geisler J.H., Sanders A.E. & Luo Z.-X. (2005) – A new protocetid whale (Cetacea: Archaeoceti) from the late middle Eocene of South Carolina. *American Museum Novitates*, 3480, 65 p.

Gibbes R.W. (1849) - Monograph of the fossil Squalidae of the United States. *Journal of the Academy of Natural Sciences of Philadelphia,* 1(series 2): 191-206.

Gibson M.L., Mnieckowski J. & Geisler J.H. (2018) - *Tupelocetus palmeri*, a new species of protocetid whale (Mammalia, Cetacea) from the middle Eocene of South Carolina. *Journal of Vertebrate Paleontology*, 38(6): e1555165.

Gill T.N. (1862) – Analytical synopsis of the order of Squali, and revision of the nomenclature of the genera. *Annals of the Lyceum of Natural History of New York*, 7: 371-408.

Girard C.F. (1855) – Characteristics of some cartilaginous fishes of the Pacific coast of North America. *Proceedings of the Academy of Natural Sciences of Philadelphia*, 7(6): 196-197.

Glickman L.S. (1964) – Sharks of the Paleogene and their stratigraphic significance [in Russian]. *Nakua Press*: 229 p.

Glickman L.S. & Zhelezko V.I. (1985) – Paleogene sharks of the Mangyschlak Plateau and the Eocene-Oligocene boundary [in Russian]. *Byulleten' Moskovoskogo Obshchestva Ispytatelei Priody, Otdel Geologicheskii*, 60(5): 86-99.

Gmelin J.F. (1789) – Caroli a Linnaei Systema Naturae per Regna Tria Naturae. Tome 1. Pars III. Amphibia – Pisces. G.E. Beer, Leipzig, Germany: 1033-1516.

González Barba G. (2003) – Descripción de asociaciones faunísticas de elasmobranquios fósiles del Eoceno Superior (Priaboniano) de las formaciones Tepetate y Bateque de Baja California Sur, México. Unpublished Ms. Thesis, Instituto Politecnico Nacional Centro Interdisciplinario de Ciencias Marinas, La Paz, Baja California Sur, Mexico, 226 p.

Goode G.B. & Bean T.H. (1880) – Catalogue of a collection of fishes obtained in the Gulf of Mexico by Dr. J.W. Velie, with descriptions of seven new species. *Proceedings of the United States National Museum*, 2(98): 333-345.

Goodrich E.S. (1930) – Studies on the structure and development of vertebrates. Mamilland and Company, London, England.

Grandstaff B.S., Pellegrini R.A., Monsch K.A., Parris D.C. & Clements D. 2018. Over a century of thin-section microscopy of the fossil fish *Cylindracanthus*. *New Jersey State Museum Investigations*, 6: 11-27.

Gray J.E. (1831) – Description of three new species of fish, including two undescribed genera, discovered by John Reeves, Esq., in China. *Zoological Miscellany*, 1(6): 4-5.

Gray J.E. (1851) – List of the specimens of fish in the collection of the British Museum. Part 1. Chondropterygii. British Museum (Natural History), London, 160 p.

Greenwood P.H., Rosen D.E., Weitzman S.H. & Myers G.S. (1966) – Phyletic studies of teleostean fishes, with a provisional classification of living forms. *Bulletin of the American Museum of Natural History*, 131: 339-456.

Gronow L.T. (1763) – Zoophylacii Gronoviani fasciculus primus exhibens animalia quadrupeda, amphibia atque pisces, quae in museo suo adservat, rite examinavit, systematice disposuit,

Guitart, D.J. (1966) – Nuevo nombre para una especie de Tiburón del género *Isurus* (Elasmobranchii: Isuridae) de aguas Cubanas. *Poeyana, Instituto Biologia*, 15: 1-9.

Günther A. (1870) – Catalogue of the fishes in the British Museum. Vol. 8. British Museum, London: 549 p.

Hay O.P. (1902) – Bibliography and catalogue of the fossil Vertebrata of North America. *Bulletin of the United States Geological and Geographical Survey of the Territories*, 179, 868 p.

Hasse C. (1879) – Das natürliche System der Elasmobranchier auf Grundlage des Baues und der Entwicklung ihrer Wirbelsäule. Eine morphologische und paläontologische Studie. Gustav Fischer, Jena, Germany, 76 p.

Herman J. (1977) – Additions to the Eocene fish fauna of Belgium. 3. Revision of the Orectolobiforms. *Tertiary Research*, 1(4): 127-138.

Herman J., Hovestadt-Euler M & Hovestadt D.C. (1988) – Contributions to the study of the comparative morphology of teeth and other relevant ichthyodorulites in

living supraspecific taxa of Chondrichthyan fishes. Part A: Selachii. No. 2a: Order: Carcharhiniformes – Family Triakidae. *Bulletin de l'Institut Royal des Sciences Naturelles de Belgique*, 58: 99-126.

Herman J., Steurbaut E. & Vandenberghe N. (2000) – The boundary between the middle Eocene Brussel Sand and the Lede Sand formations in the Zaventem-Nederokkerzeel área (Northeast of Brussels, Belgium). *Geologica Belgica* 3(3-4): 231-255.

Herrick S.M. (1972) – Age and correlation of the Clinchfield Sand in Georgia. *US Geological Survey Bulletin* 1354-E: E1-E17.

Hilgendorf F.M. (1877) – *Pterothrissus*, eine neue Clupeidengattung. *Leopoldina, Amtliches Organ der Kaieserlich Leopoldinisch-Carolinisch-Deutschen Akademie der Natruforscher*, 13(15-16): 127-128.

Hovestadt D.C. (2018) – Reassessment and revision of the fossil Heterodontidae (Chondricthyes: Neoselachii) based on tooth morphology of extant taxa. *Palaeontos*, 20, 120 p.

Hovesadt D.C. & Hovestadt-Euler M. (2013) – Generic assessment and reallocation of Cenozoic Mylibatinae based on new information of tooth, tooth plate and caudal spine morphology of extant taxa. *Palaeontos*, 24:1-66.

Huddlestun P.F & Hetrick J.H. (1979) – The stratigraphy of the Barnwell Group of Georgia. *USGS Open File Report* 80-1, 96 p.

Huxley T.H. (1880) – On the application of the laws of evolution to the arrangement of the Vertebrata, and more particularly of the Mammalia. *Proceedings of the Zoological Society of London*, 43: 649-662.

Jaekel O. (1895) – Unter-tertiäre Selachier aus Sudrussland. Mémoirs du Comité géologique de St. Petersburg, 9(4): 19-35.

Jordan D.S. (1888) – Description of two new species of fishes from South America. *Proceedings of the Academy of Natural Sciences of Philadelphia*, 39: 387-388.

Jordan D.S. & Evermann B.W. (1896) – The fishes of North and Middle America, a descriptive catalogue of the species of fish-like vertebrates found in the waters of North America, north of the Isthmus of Panama. Part II. *Bulletin of the United States National Museum* 47: 1241-2183.

Kázmér M., Shafeea Leman M., Mohamed K.R., Aziz Ali C. & Taboroši D. (2015) – Features of intertidal bioerosion and bioconstruction on limestone coasts of Langkawi Islands, Malaysia. *Sains Malaysiana*, 44(7): 921-929.

Kemp D.J., Kemp L. & Ward D.J. (1990) – An illustrated guide to the British Middle Eocene vertebrates. Privately published, London, 59p.

Kent B.W. (1999) – Sharks from the Fisher/Sulivan site. *In*: Weems, R.E. (ed.) Fossil Vertebrates and Plants from the Fisher/Sullivan Site (Nanjemoy Formation) Stafford County, Virginia. *Virginia Division of Mineral Resources Publication* 152: 39-51.

Kite L.E. (1982) – Tertiary stratigraphy of the Oakwood quadrangle, Aiken County, South Carolina. *Carolina Geological Society Field Trip Guidebook 1982*: 65-78.

Klunzinger, C.B. (1871) – Synopsis der Fische des Rothen Meeres. II. Theil. *Verhandlungen der Kaiserlich-Königlichen Zoologisch-Botanischen Gesellschaft in Wein*, 21: 441-688.

Kovalchuk O., Kriwet J., Shimada K., Ryabokon T., Barkaszi Z., Dubikovska A., Anfimova G. & Davydenko D. (2023) - Middle Eocene cartilaginous fishes (Vertebrata: Chondrichthyes) of the Dnieper-Donets Basin, northern Ukraine. *Palaeontologia Electronica*, 26(2): a32.

Kozlov V.A. (2001) – Additions to the Paleogene elasmobranch fauna of western Kazakhstan. *Turania*, a new shark genus (Odontaspididae) and a new ray species (genus *Archaeomanta*, Mobulidae) [in Russian]. *Materialy po Stratigrafi i Paleontologii Urala*, 6: 83-86.

Lacepède B.G.E. (1802) – Histoire Naturelle des Poissons, 4. Paris, France.

Lancaster W.C. (1986) – The taphonomy of an archaeocete skeleton and its associated fauna. Pp. 119-131 in Schiebout J.A. & van den Bold W. (eds.), Montgomery Landing Site, Marine Eocene (Jackson) of Central Louisiana. Symposium Proceedings, *Gulf Coast Association of Geological Societies*, Baton Rouge.

Lawley R. (1876) – Nuovi studi sopra ai pesci ed altri vertebrati fossili delle Colline Toscana. Florence, Italy, 122 p.

Lea I. (1833) – Contributions to Geology. Carey, Lea and Blanchard, Philadelphia.

Leidy J. (1856) – Remarks on certain extinct species of fishes. *Proceedings of the Academy of Natural Sciences of Philadelphia*, 8: 301-302.

Leidy J. (1877) – Description of vertebrate remains, chiefly from the Phosphate Beds of South Carolina. *Journal of the Academy of Natural Sciences of Philadelphia*, 8(2): 209-261.

Leriche M. (1905) – Les poissons eocènes de la Belgique. *Mémoires du Musée royal d'Histoire naturelle de Belgique*, 2: 2-228.

Leriche M. (1942) – Contribution a l'étude des faunes ichthyologiques marines des terrains teriaires de la Plaine Côtière Atlantique et du centre des Etats-Unis. Les synchronismes des formations teriaires des deux côtès de l'Atlantique. *Memoires de la Société géologique de France* (new series), 20(45) : 5-110.

Lesueur C.A. (1822) – Description of a *Squalus*, of very large size, which was taken on the coast of New Jersey. *Journal of the Academy of Natural Sciences*, Philadelphia, 2 : 343-352.

Levin H.L. & Joerger A.P. (1967) – Calcareous nannoplankton from the Tertiary of Alabama. *Micropaleontology*, 13(2): 163-182.

Le Hon H. (1871) – Préliminaires d'un mémoire sur les poissons tertiaires de Belgique. C. Muquardt, Brussels, Belgium, 15 p.

Lin C.-H., Steurbaut E. & Nolf D. (2024) – Early Eocene fish otoliths from the eastern and southern USA. *European Journal of Taxonomy*, 935: 203-240. https://doi.org/10.5852/ejt.2024.935.2557

Linck H.F. (1790) – Versuch einer Eintheilung der Fische nach den Zähnen. *Magazin für das Neueste aus der Physik und Naturgeschichte*, 6(3): 28-38

Linnaeus C. (1758) – Systema Naturae per regna tria naturae, secundum classes, ordines, genera, species, cum characteribus, synonymis, locis. Tomus I. *Holmiae, Laurentii Salvii*: 824 p.

Linnaeus C. (1771) – Mantissa plantarum: altera Generum editionis VI & Specierum editionis II. *Holmiae, Laurentii Salvii*: 521-552.

Long D.J. (1992) – Sharks from the La Meseta Formation (Eocene), Seymour Island, Antarctic Peninsula. *Journal of Vertebrate Paleontology*, 12(1): 11-32.

Maisch H.M., Becker M.A. & Chamberlain J.A. (2015) – Chondrichthyans from a lag deposit between the Shark River Formation (middle Eocene) and Kirkwood Formation

(early Miocene), Monmouth County, New Jersey. *Paludicola*, 10(3): 149-183.

Maisch H.M., Becker M.A., Raines B.W. & Chamberlain J.A. (2014) – Chondrichthyans from the Lisbon-Tallahatta Formation contact (middle Eocene), Choctaw County, Silas, Alabama. *Paludicola*, 9(4): 183-209.

Maisch H.M., Becker M.A., Raines B.W. & Chamberlain J.A. (2016) – Osteichthyans from the Tallahatta-Lisbon Formation contact (middle Eocene – Lutetian) at Pigeon Creek, Conecuh-Covington counties, Alabama, with comments on Transatlantic occurrences in the Northern Atlantic Ocean basin. *PalArch's Journal of Vertebrate Paleontology*, 13(3): 1-22.

Malyshkina T. (2021) – *Striatolamia tchelkarnurensis* Glickman (Elasmobranchii: Lamniformes), the youngest valid Striatolamia species. *Paleontological Journal*, 55(2): 193-204.

Malyshkina T. & Ward D.J. (2016) – The Turanian Basin in the Eocene: the new data on the fossil sharks and rays from the Kyzylkum Desert (Uzbekistan). *Proceedings of the Zoological Institute, Russian Academy of Sciences*, 320(1): 50-65.

Malyshkina T., González-Barba G. & Bannikov A.F. (2013) – Records of elasmobranchian teeth in the Bartonian of the Northern Caucases (Russia) and Crimea (Ukraine). *Paleontological Journal*, 47(1): 98-103.

Manning E.M. & Standhardt B.R. (1986) – Late Eocene sharks and rays of Montgomery Landing, Louisiana. Pp. 133-161 *in* Schiebout J.A. & van den Bold W. (eds.), Montgomery Landing Site, Marine Eocene (Jackson) of Central Louisiana. Symposium Proceedings, *Gulf Coast Association of Geological Societies*, Baton Rouge.

McCuen W.N., Ishimori A.S. & Boessenecker R.W. (2020) – A new specimen of *Xiphiorhynchus* cf. *X. aegyptiacus* (Istiophoriformes, Xiphioidei, Xiphiidae) and billfish diversity in the Oligocene of South Carolina. *Vertebrate Anatomy Morphology Paleontology*, 8: 98-104. https://doi.org/10.18435/vamp29367

McPherson A.B. & Manning E.M. (1986) – New records of Eocene sea snakes (*Pterosphenus*) from Louisiana. Pp. 197-208 *in* Schiebout J.A. & van den Bold W. (eds.), Montgomery Landing Site, Marine Eocene (Jackson) of Central Louisiana. Symposium Proceedings, *Gulf Coast Association of Geological Societies*, Baton Rouge.

Meese E.N. & Lowe C.G. (2020) – Environmental effects on daytime sheltering behaviors of California horn sharks (*Heterodontus francisci*). *Environmental Biology of Fishes*, 103(6): 703-717.

Meyer F.A.A. (1793) – Systematisch-summarische Uebersicht der neuesten Zoologischen Entdeckungen in Neuholland un Afrika. Verlag Dykische Buchhandtung, Leipzig: 178 p.

Mitchill S.L. (1815) – The fishes of New York, described and arranged. *Transactions of the Literary and Philosophical Society of New York*, 1(5): 355-492.

Miyosi Y. (1939) – Description of three new species of elasmobranchiate fishes collected at Hyuga Nada, Japan. *Bulletin of the Biogeographical Society of Japan*, 9(5): 91-97.

Monsch K.A. (2005) – Revision of the scombroid fishes from the Cenozoic of England. *Transactions of the Royal Society of Edinburgh*, 95: 445-489.

Monsch K.A. & Bannikov A.F. (2011) – New taxonomic synopses and revision of the scombroid fishes (Scombroidei, Perciformes), including billfishes, from the Cenozoic of territories of the former USSR. T*ransactions of the Royal Society of Edinburgh*, 102: 253-300.

Monsch F.H., Fierstine H.L. & Weems R.E. (2005) – Taxonomic revision and stratigraphic provenance of '†*Histiophorus rotundus*' Woodward 1901 (Teleostei, Perciformes). *Journal of Vertebrate Paleontology*, 25(2): 274-279.

Müller A. (1999) – Ichthyofaunen aus dem atlantischen Tertiar der USA. *Leipziger Geowissenschaften*, 9/10, 360 p.

Müller J. (1846) – Über den Bau und die Grenzen der Ganoiden und über das natürliche System der Fische. Abhandlungen der Deutschen Akademie der Wissenschaften zu Berlin, 1844: 119-216.

Müller J. & Henle J. (1838) – Ueber die Gattungen der Plagiostomen. *Archiv für Naturgeshichte* 4: 83-85.

Müller J. & Henle J. (1839) – Systematische Beschreibung der Plagiostomen. Part 2: 29-102. Veit and Company, Berlin, Germany.

Mustafa H. & Zalmout I.S. (2002) – Elasmobranchs from the late Eocene Wadi Esh-Shallala Formation of Qa'Faydat ad Dahikiya, east Jordan. *Tertiary Research*, 21: 77-94

Naylor G.J.P., Caira J.N., Jensen K., Rosana K.A.M., Straube N. & Lakner C. (2012) – Elasmobranch phylogeny: A mitochondrial estimate based on 595 species. Pp. 31-56 in Carrier J.C., Musick J.A. & Heithaus M.R. (eds.), Biology of sharks and their relatives. CRC Press, Boca Raton, Florida.

Nelson J.S., Grande T.C. & Wilson M.V.H. (2016) – *Fishes of the World*, 5th Edition. J. Wiley and Sons, Hoboken, New Jersey.

Noubhani A. & Cappetta H. (1997) – Les Orectolobiformes, Carcharhiniformes et Myliobatiformes (Elasmobranchii, Neoselachii) des Bassins à phosphate du Maroc (Maastrichtien-Lutétien basal). Systématique, biostratigraphie, évolution et dynamique des faunes. *Palaeo Ichthyologica* 8: 1-327.

Owen R. (1845) – Odontography. *Annals and Magazine of Natural History* 6(11) :138.

Oyanadel-Urbina P., de Gracia C., Carrillo-Briceño J.D., Nielsen S.N., Flores H., Casteletto, V., Kriwet, J., Rivaneneira M.M. & Villafaña J.A. (2021) – Neogene bony fishes from the Bahia Inglesia Formation, northern Chile. *Ameghiniana*, 58(4): 345-368.

Parmley D. & Cicimurri D.J. (2003) – Late Eocene Sharks of the Hardie Mine local fauna of Wilkinson County, Georgia. *Georgia Journal of Science*, 61(3):153-179.

Parris D.C., Grandstaff B.S. & Bell, G.L., Jr. (2001) – Reassessment of the affinities of the extinct genus *Cylindracanthus* (Osteichthyes). *Proceedings of the South Dakota Academy of Science*, 80: 161-172.

Péron F. (1807) – Voyage de Découvertes aux Terres Australes, exécuté par ordre de sa majesté l'Empereur et Roi, sur les corvettes la Géographe, la Naturaliste et la Goulette la Casuarina, pendant les années 1800, 1801, 1803 et 1804. Voyage de Découvertes aux Terres Australes, 1: 496 p.

Pietsch C., Harrison H.C. & Allmon W.D. (2016) – Whence the Gosport Sand (upper Middle Eocene, Alabama)? The origin of glauconitic shell beds in the Paleogene of the U.S. Gulf Coastal Plain. *Journal of Sedimentary Research*, 86: 1249-1268. https://doi.org/10.2110/jsr.2016.72

Pledge N.S. (1967) – Fossil elasmobranch teeth of South Australia and their stratigraphic distribution. *Transactions of the Royal Society of South Australia*, 91: 135-160.

Poey F. (1875) – Enumeratio piscium cubensium. Parte III. *Anales de la Sociedad española de Historia natural* 5: 373-404.

Pooser W.K. (1965) – Biostratigraphy of Cenozoic ostracoda

from South Carolina*: The University of Kansas Paleontological Contributions*, Arthropoda Article 8, 80 p.

Popov E.V., Lopyrev V.A., Panteleev A.V., Biriukov A.V. & Timirchev F.K. (2025) – Chondrichthyan fishes from the Middle Eocene Osinovaya Formation of Rostov Region, Russia. *Historical Biology* 37(1): 126-152.

Potthoff T. & Kelley S. (1981) – Development of the vertebral column, fins and fin supports, branchiostegal rays, and squamation in the swordfish, *Xiphias gladius*. *Fishery Bulletin*, 80(2): 161-186.

Purdy R.W., Schneider V.P., Applegate S.P., McLellan J.H., Meyer R.L. & Slaughter B.H. (2001) – The Neogene sharks, rays and bony fishes from Lee Creek Mine, Aurora, North Carolina. Pp.71-202 *in* C.E. Ray and D.J. Bohaska (eds.), Geology and Paleontology of the Lee Creek Mine, North Carolina, III. *Smithsonian Contributions to Paleobiology*, 90.

Rafinesque C.S. (1810) – Caratteri di alcuni nuovi generi e nuove specie di animali e piante della sicilia, con varie osservazioni sopra i medisimi. Palermo, Italy: 3-69.

Rafinesque C.S. (1815) – Analyse de la nature ou Tableu de l'universe et des corps organisés. Self-published, Palermo, Italy, 224 p.

Rana R.S., Patel R., Cicimurri D.J. & Ebersole J.A. (2021) – Additions to the elasmobranch assemblage from the Bandah Formation (middle Eocene, Bartonian), Jaisalmer District, Rajasthan, India, and the palaeobiogeographic implications of the fauna. *Palaeovertebrata*, 44(2): e1. https://doi.org/10.18563/pv.44.2.e1

Regan C.T. (1906) – Descriptions of some new sharks in the British Museum collection. *Annals and Magazine of Natural History* (series 7), 18(108): 435-440.

Regan C.T. (1909) – On the anatomy and classification of the scombroid fishes. *Annals and Magazine of Natural History* 8: 66-75.

Reinecke T., Mohs H., Grant A. & Breitkreutz H. (2005) – Die Elasmobranchier des Norddeutschen Chattiums, insebesondere des Sternberger Gesteins (Eochattium, Oberes Oligozän). *Palaeontos*, 8: 134 p.

Richardson J. (1836) – Fauna Boerali-Americana: or the zoology of the northern parts of British America: containing descriptions of the objects of natural history collected on the late northern land expeditions, under the command of Sir Johan Franklin, R.N. The Fish. Bentley, London: 327 p.

Risso A. (1810) – Ichthyologie de Nice, ou, histoire naturelle des poissons du departement des Alpes Maritimes. F. Schoell, Paris, France.

Rodríguez D., Ward D.J. & Quezada J.A. (2023) – Paleontology and stratigraphic implications of a late Paleocene elasmobranch assemblage in Talcahuano, southcentral Chile. *Andean Geology*, 50(2):217-247.

Rodríguez-Cabello C., González-Pola C., Rodríguez A. & Sánchez F. (2018) – Insights about depth distribution, occurrence and swimming behavior of *Hexanchus griseus* in the Cantabrian Sea (NE Atlantic). *Regional Studies in Marine Science*, 23: 60-72. https://doi.org/10.1016/j.rsma.2017.10.015

Rüppell W.P.E. (1837) – Neue Wirbelthiere zu der Fauna von Abyssinien gehörig. Fische des Rothen Meeres. Siegmund Schmerber, Frankfurt, Germany, p. 53-80.

Rust S., Wium M., Otero R.A. & Terezow M. (2025) – Fossil billfish (Xiphioidei) from the Eocene of Hampden, North Otago, New Zealand. *Gondwana Research*, 150: 301-311. https://doi.org/10.1016/j.gr.2025.09.021

Samonds K.E., Andrianavalona T.S., Wallett L.W., Zalmout I.S. & Ward. D.J. (2019) – A middle-late Eocene neoselachian assemblage from nearshore marine deposits, Mahajanga Basin, northwestern Madagascar. *PLoS ONE*, 14(2): e0211789. https://doi.org/10.1371/journal.pone.o211789

Santini F., Carnevale G. & Sorenson L. (2015) – First time-tree of Sphyraenidae (Percomorpha) reveals a Middle Eocene crown age and an Oligo-Miocene radiation of barracudas. *Italian Journal of Zoology*, 2015:133-142.

Siverson M. (1995) – Revision of the Danian cow sharks, sand tiger sharks, and goblin sharks (Hexanchidae, Odontaspididae, Mitsukurinidae) from southern Sweden. *Journal of Vertebrate Paleontology*, 15(1): 1-12. https://doi.org/10.1080/02724634.1995.10011203

Siverson M. (1999) – A new large lamniform shark from the uppermost Gearle Siltstone (Cenomanian, Late Cretaceous) of Western Australia. *Transactions of the Royal Society of Edinburgh, Earth Sciences*, 90: 49-66. https://doi.org/10.1017/S0263593300002509

Slater T.S., Ashbrook K. & Kriwet J. (2020) – Evolutionary relationships among bullhead sharks (Chondrichthyes, Heterodontiformes). *Papers in Paleontology*, 2020: 1-13. https://doi.org/10.1002/spp2.1299

Stone N.R. & Shimada K. (2019) – Skeletal anatomy of the Bigeye Sand Tiger Shark, *Odontaspis noronhai* (Lamniformes: Odontaspididae), and its implications for lamniform phylogeny, taxonomy, and conservation biology. *Copeia*, 107(4): 632-652.

Storms R. (1892) – Sur le *Cybium* (*Enchodus*) *bleekeri* du terrain bruxellien. *Mémoires de la Société belge de Géologié, de Paléontologie et d'Hydrologie*, 6: 3-14.

Stringer G. (2016) – Evidence and implications of marine invertebrate settlement on Eocene otoliths from the Moodys Branch Formation of Montgomery Landing (Louisiana, USA). *Cainozoic Research*, 16 (1): 3-12

Stringer G., Parmley D. & Quinn A. (2022) – Eocene teleostean otoliths, including a new taxon, from the Clinchfield Formation (Bartonian) in Georgia, USA, with biostratigraphic, biogeographic, and paleoecologic implications. *Palaeovertebrata*, 45(1): e1.

Stromer E. (1905) – Die Fischreste des Mittleren und Oberen Eocäns von Ägypten. I. Teil: Selachii, B. Squaloidei und II. Teil: Teleostomi, A. Ganoidei. *Beiträge zur Paläontologie und Geologie Österreich-Ungarns*, 18: 163–185

Stromer E. (1910) – Reptilien und Fischreste aus dem marinen Alttertiär von Sudtogo (Westafrika). *Monastbericht der Deutschen Geologischen Gesellschaft*, 62(7): 478-505.

Swainson W. (1839) – The Natural History of Fishes, Amphibians, and Reptiles or monocardian animals II. Orme, Green, Longmans & Taylor, London, England, 448 p.

Tanaka T. & Kohno N. (2025) – Paleozoic, Mesozoic and Cenozoic Chondrichthyes from the Japanese islands. *National Museum of Nature and Science Monographs*, 56, 184 p.

Taverne L. & Nolf D. (1978) – Troiseme note sur les poissons des sables de Lede (Eocene belge): les fossils autres que les otolithes. *Bulletin de la Société Belge de Géologie*, 87(3): 125-152.

Thurmond J.T. & Jones D.E. (1981) – *Fossil Vertebrates of Alabama*. University of Alabama Press, Tuscaloosa, 256 p.

Treadwell R.C. (1954) – Moodys Branch-Cockfield contact in Sabine Parish, Louisiana, and adjacent areas. *AAPG Bulletin*, 38(11): 2302-2323.

Trif N., Codrea V. & Arghius V. (2019) – A fish fauna from the lowermost Bartonian of the Transylvanian Basin, Romania. *Palaeontogia Electronica*, 22(3): 1-29.

Trif N., Arghuiș V., Seitz J.C., Codrea V.A., Bălc R. & Bindiu-Haitonic R. (2021) – Integrated paleontological investigation of a new mid-late Bartonian fish fauna from Călata area, Transylvanian Basin, Romania. *Historical Biology*, 34(9): 1788-1816.

Türtscher J., López-Romero F.A., Jambura P.L., Kindlimann R., Ward D.J. & Kriwet J. (2021) – Evolution, diversity, and disparity of the tiger shark lineage *Galeocerdo* in deep time. *Paleobiology*, 47(4): 574-590.

Tyler J.C. (1980) – Osteology, phylogeny, and higher classification of the fishes of the order Plectognathi (Tetraodontiformes). *NOAA Technical Report NMFS Circular* 434, 422 p.

Uhen M.D. & Gingerich P.D. (2001) – New genus of dorudontine archaeocete (Cetacea) from the middle-to-late Eocene of South Carolina. *Marine Mammal Science*, 17(1): 1-34.

Underwood C.J. & Gunter G.C. (2012) – The shark *Carcharhinus* sp. From the Middle Eocene of Jamaica and the Eocene record of *Carcharhinus*. *Caribbean Journal of Earth Science*, 44: 25-30.

Underwoood C.J., Ward D.J., King C., Antar S.M., Zalmout I.S. & Gingerich P.D. (2011) – Shark and ray faunas in the middle and late Eocene of the Fayum area, Egypt. *Proceedings of the Geologist's Association*, 122(1): 47-66.

U.S. Geological Survey (2024) – Harleyville 1:24,000 topographic map, accessed June 4, 2026 at https://store.usgs.gov/product/825203.

U.S. Geological Survey (2024) – Holly Hill 1:24,000 topographic map, accessed June 4, 2026 at https://store.usgs.gov/product/8252015.

Uyeno T. & Fuji S. (1975) – A fossil fish of the family Scombridae from a Miocene bed in Toyama Prefecture, Japan. *Bulletin of the National Science Museum, Series C (Geology)*, 1(1): 11-16.

van Beneden P.J. (1871) – Reserches sur quelques poissons fossiles de Belgique. *Bulletin de l'Academie Royale des Sciences, des Lettres et des Beaux-Arts de Belgique*, 31: 493-518.

Van den Eeckhaut G. & De Schutter P. (2009) – The elasmobranch fauna of the Lede Sand Formation at Oosterzele (Lutetian, middle Eocene of Belgium). *Palaeofocus*, 1: 1-57.

Van der Laan R., Eschmeyer W. & Fricke R. (2024) – Eschmeyer's catalog of fishes: Family-Group names. www.calacademy.org/scientists/catalog-of-fishes-family-group-names (accessed 2/12/2025). doi.org/10.11646/zootaxa.3882.1.1

Villalobos-Segura E. & Underwood C.J. (2020) – Radiation and divergence times of Batoidea. *Journal of Vertebrate Paleontology*, 40(3): e1777147.

Walbaum J.J. (1792) – Genera piscium. In quibus systema totum ichthyologiae proponitur cum classibus, ordinibus, generum characteribus, specierum differentiis, observationibus plurimis. Redactis speciebus 242 ad genera 52. Ichthyologiae pars III. Impensis Ant. Ferdin. Röse, Grypeswald, Germany, p. 1-723.

Ward D.J. (1978) – Additions to the fish fauna of the English Paleogene. 1. Two new species of *Alopias* (Thresher Shark) from the English Eocene. *Tertiary Research*, 2(1): 23-28.

Ward D.J. (1979) – Additions to the fish fauna of the English Paleogene. 3. A review of the Hexanchid sharks with a description of four new species. *Tertiary Research*, 2(3): 111-129.

Ward D.J. (1980) - The distribution of sharks, rays and chimaeroids in the English Paleogene. *Tertiary Research*, 3(1): 13-19.

Weems R.E. (1998) – Actinopterygian remains from the Paleocene of South Carolina. Pp. 147-164 *in* A.E. Sanders (ed.), Paleobiology of the Williamsburg Formation (Black Mingo Group; Paleocene of South Carolina, U.S.A.). *Transactions of the American Philosophical Society*, 88(4).

Weems R.E. (1999) – Actinopterygian fish remains from the Fisher/Sullivan Site. P. 53-99 in Weems R.E. & Grimsley G.J. (eds.), Early Eocene vertebrates and plants from the Fisher/Sullivan Site (Nanjemoy Formation), Stafford County, Virginia. *Virginia Division of Mineral Resources Publication,* 152.

Weems R.E. & Brown K.M. (2017) – More-complete remains of *Procolpochelys charlestonensis* (Oligocene, South Carolina), an occurrence of *Euclastes* (upper Eocene, South Carolina), and their bearing on Cenozoic pancheloniid sea turtle distribution and phylogeny. *Journal of Paleontology*, 91(6): 1228-1243.

Weems R.E., Albright L.B. III, Bybell L.M., Cicimurri D.J., Edwards L.E., Harris W.B., Lewis W.C., Osborne J.E., Sanders A.E. & Self-Trail J.M. (2016) – Stratigraphic revision of the Cooper Group and the Chandler Bridge and Edisto Formations in the Coastal Plain of South Carolina. *South Carolina Geology*, 49: 1-24.

Weiler W. (1929) – Ergebnisse der Forschungsreisen Prof. E. Stromers in den Wüsten Ägyptens. V. Tertiare Wirbelteire. 3. Die Mittel und obereocane Fischfauna Ägyptens mid besonderer Berücksichtigung der Teleostomi. *Abhandlungen der Bayerischen Akademie der Wissenschaften Mathematisch-Naturwissensschaftliche Abteilung*. Neu Folge 1:1-57.

Welton B.J. & Zinsmeister W.J. (1980) – Eocene selachians from the La Meseta Formation, Seymour Island, Antarctic Peninsula. *Contributions to Science, Natural History Museum of Los Angeles County*, 329: 1-10.

Westgate J.W. (1984) – Lower vertebrates from the Late Eocene Crow Creek local fauna, St. Francis County, Arkansas. *Journal of Vertebrate Paleontology*, 4(4):536-546.

Westgate J.W. (1989) - Lower vertebrates from an estuarine facies of the middle Eocene Laredo Formation (Claiborne Group), Webb County, Texas. *Journal of Vertebrate Paleontology*, 9(3):282-294.

White E.I. (1926) – Eocene fishes from Nigeria. *Bulletin of the Geological Survey of Nigeria*, 10: 1-82.

White, E.I. (1955) – Notes on African Tertiary sharks. *Bulletin of the Geological Society of Nigeria*, 5(3): 319-325.

White E.I. (1956) – The Eocene fishes of Alabama. *Bulletins of American Paleontology*, 36(156):123-150.

Whitley G.P. (1940) – The fishes of Australia. Part I. The sharks, rays, devilfish, and other primitive fishes of Australia and New Zealand. Australian zoology handbooks, Royal Zoological Society of New South Whales, 280 p.

Wiley E. & Johnson G. (2010) – A teleost classification based on monophyletic groups. Pp. 123-182 *in* J. Nelson, H.-P. Schultze, and M.W.V. Wilson (eds.). *Origin and phylogenetic interrelationships of teleosts*. Friedrich Pfeil, Munich, Germany.

Winkler T.C. (1874) – Mémoire sur des dents de poissons du

terrain bruxellien. *Archives du Musée Teyler*, 3(4): 285-304.
Woodward A.S. (1889) – Catalogue of the fossil fishes in the British Museum, Part 1. *British Museum (Natural History)*, London, 474 p.
Woodward A.S. (1901) – Catalogue of the fossil fishes in the British Museum, Part 4. *British Musuem (Natural History)*, London, 636p.
Zalat A.A., Khalil H.M., Fathy M.S. & Tarek R.M. (2017) – Taxonomy and morphological study on the vertebrate remains of shark and rays fauna from the Middle and Late Eocene succession, Fayoum Depression, Egypt. *Delta Journal of Science*, 38:202-217.
Zalmout I.S., Antar M.M., Abd-El Shafy E., Metwally M.H., Hatab E-L.E. & Gingerich P.D. (2012) – Priabonian sharks and rays (Late Eocene: Neoselachii) from the Minqar Tabaghbagh in the western Qattara Depression, Egypt. *Contributions from the Museum of Paleontology* (University of Michigan), 32(6):71-90.
Zarkov M.P., Glikman L.S., Kaplan A.A. & Stelnykova N.I. (1976) – On the age of the Paleogene of Kaliningrad region [in Russian]. *Proceedings of the USSR Academy of Science, Geological Series*, 1: 132-134.
Zhelezko V.I. & Kozlov V.A. (1999) – Elasmobranchii and Palaeogene biostratigraphy of Trans Urals and Central Asia [in Russian]. *Materials on Stratigraphy and Paleontology of the Urals*, 3, Russian Academy of Sciences, 324 p.
Zouhri S., Gingerich P.D., Khalloufi B., Bourdon E., Adnet S., Jouve S., Elboudali N., Amane A., Rage J.-C. & Tabuce R. (2021) – Middle Eocene vertebrate fauna from the Aridal Formation, Sabkha of Gueran, southwestern Morocco. *Geodiversitas*, 43(5): 121-150.
Zullo V.A. & Harris W.B. (1987) – Sequence stratigraphy, biostratigraphy and correlation of Eocene through lower Miocene strata in North Carolina. *Cushman Foundation for Foraminiferal Research*, Special Publication 24: 197-214.
Zullo V.A. & Kite L.E. (1985) – Barnacles of the Jacksonian (upper Eocene) Griffins Landing Member, Dry Branch Formation in South Carolina and Georgia. *South Carolina Geology*, 28(1): 1-22.